ROMA TRE
UNIVERSITÀ DEGLI STUDI

DOCTORAL SCHOOL IN BIOLOGY

SECTION: Biology Applied to Human Health

XXIV DOCTORAL PROGRAM

Genetic and functional basis of *Acinetobacter baumannii* virulence

Luísa Cavaco Sobreda Antunes

Tutor
Prof. Paolo Visca

Co-tutors
Prof. Kevin Towner
Dr. Francesco Imperi

Thesis submitted for the
degree of Doctor of Philosophy
University Roma Tre
Department of Biology
October 2012

The work presented in this thesis was finantially supported by a doctoral degree grant (SFRH/BD/43420/2008) from Fundação para a Ciência e a Tecnologia (FCT).

Se eu não morresse, nunca! E eternamente
Buscasse e conseguisse a perfeição das cousas…
[Cesário Verde]

Abstract

Acinetobacter baumannii is an opportunistic nosocomial pathogen and many strains are multi- or pan-drug resistant. Although this bacterium has long been regarded as a low-grade pathogen, it can cause a broad range of severe infections, including pneumonia and bacteraemia, but also secondary meningitis, skin and soft-tissue, wound and urinary tract infections, and attributable mortality rates can reach 35%. However, the virulence traits and pathogenic potential of *A. baumannii* remain elusive.

The aim of this PhD thesis was to study the factors and mechanisms responsible for *A. baumannii* pathogenicity. The following main questions were asked:

1) is there a core set of conserved *A. baumannii* virulence factors?

2) did epidemic strains acquire new virulence determinants?

3) did a co-evolution between drug resistance and virulence occur?

4) is it possible to differentiate strains on the basis of their virulence factor profile?

5) is it possible to gain advantage from basic knowledge of *A. baumannii* metabolism to develop alternative therapeutic strategies against multidrug-resistant *A. baumannii*?

To address these questions, the genomes of epidemiologically diverse *A. baumannii* strains were compared, and genomic information was used as a guidance tool for phenotypic analyses (**Chapters 2 and 3**). As the second step, the distribution of a particular group of virulence determinants, i.e. iron uptake systems, was explored in more depth using a wide, representative collection of clinical, MDR *A. baumannii* strains (**Chapters 4 and 5**). Thirdly, the expression of putative *A. baumannii* virulence-associated traits identified in **Chapters 2 and 3** was studied in a collection of epidemic strains (**Chapter 6**). Lastly, a new antimicrobial strategy based on the disruption of iron metabolism was investigated (**Chapter 7**).

It was shown that *A. baumannii* has the potential to express a wide repertoire of putative virulence factors that are common to the genomes of most strains, but that these factors can be differentially expressed according to the strain. Additionally, it was found that epidemic strains had not acquired any new specific virulence determinants in addition to antibiotic resistance genes. Thirdly, a multiplicity of iron uptake capabilities was identified, consistent with the importance of iron for *A. baumannii* metabolism. This evidence ultimately prompted the assessment of a novel anti-*A. baumannii* strategy based on the disruption of iron metabolism by gallium, an iron-mimetic metal.

The results presented in this thesis revealed that *A. baumannii* is a very adaptable pathogen, possessing many diverse virulence attributes, and that it has an extraordinary ability to acquire new genetic material. Thus, although *A. baumannii* has long been considered a low-grade pathogen, in the future it could acquire new virulence genes in addition to antibiotic resistance genes, and become a more significant threat to human health. Hence, novel therapeutic strategies will continue to be needed to combat such a rapidly evolving pathogen, witch already has an uncertain clinical outcome.

Contents

Chapter 1

Introduction and aims

1.1 Species overview

Acinetobacter baumannii is an important opportunistic bacterial pathogen responsible for 2-10% of all Gram-negative hospital infections (Joly-Guillou, 2005). It is classified by the Infectious Diseases Society of America as one of the six most important multidrug resistant (MDR) microbes in hospitals worldwide (Talbot et al., 2006) and has been nicknamed the 'superbug' and the 'Gram-negative methicillin-resistant *Staphylococcus aureus*'.

A. baumannii belongs to the genus *Acinetobacter*, first described in 1954 (Brisou and Prevot, 1954). This genus has undergone a series of revisions, initially based on its morphological and metabolic characteristics, and followed, more recently, by detailed molecular and genomic analysis. At the moment, the genus comprises 27 officially named species and at least 9 other genomic species, as defined by DNA-DNA hybridisation (Table 1; http://www.bacterio.cict.fr). The most clinically successful species of the genus are *A. baumannii* (sp. 2), *A. pittii* (sp. 3) and *A. nosocomialis* (sp. 13TU). Strains belonging to these species and to *A. calcoaceticus* (sp. 1) are impossible to distinguish phenotypically and thus are often grouped under the umbrella name of '*A. calcoaceticus-A. baumannii* (Acb) complex', which confuses strain differentiation in the clinical practice. A more detailed review on the taxonomical history of *Acinetobacter* is found in Bergogne-Bérézin and Towner (1996). The genus *Acinetobacter* is currently defined as Gram-negative, immotile, oxidase-negative, non glucose-fermenting, strictly aerobic, catalase-positive bacteria with a G+C content of 39–47% (Bouvet and Grimont, 1986).

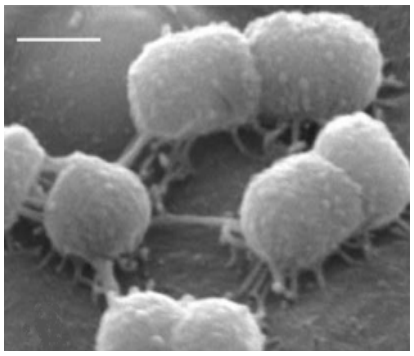

Fig. 1 Scanning electron micrograph of *A. baumannii* strain AYE (the white bar corresponds to 500 nm). Courtesy of Prof. Paolo Visca (Univ. Roma Tre, IT).

1.2 Taxonomy

The clinical relevance of *A. baumannii* has dramatically increased since the 1980s, with the emergence and spread of three predominant clones capable of causing hospital outbreaks worldwide ('international clones', ICs), of which IC-I and IC-II are MDR. However, more than 400 MLST sequence types (STs) are currently listed in the *A. baumannii* MLST database (http://pubmlst.org/abaumannii/), and a recent analysis has evidenced the existence of at least six major ICs distributed through continents (Karah et al., 2012). These six ICs include the previously identified three major outbreak clones, and demonstrate the worrisome emergence of new epidemic clones. It has been suggested that this species distribution is the result of the low phylogenetic diversity of *A. baumannii* and rapid spread following a severe population bottleneck (Diancourt et al., 2010).

1.3 Natural habitats

Contrary to other species of the *Acinetobacter* genus, which are frequently isolated from the soil, water and animals (Towner, 2009), *A. baumannii* is almost exclusively found in the hospital environment, in particular in intensive care units (ICUs). However, environmental occurrence has been reported in a few cases (Chen et al., 2001; Sengstock et al., 2010). The highest incidence of *A. baumannii* in non-clinical sources appears to be associated with lice (Bouvresse et al., 2011; Houhamdi and Raoult, 2006; Kempf et al., 2012a, La Scola and Raoult, 2004). Other non-human sources include animals, with several strains isolated from cases of infection of cats, dogs and horses (Endimiani et al., 2011; Zordan et al., 2011), and colonisation of fish, poultry and slaughterhouse meat (Ercolini, 2009; Hamouda et al., 2011; Houang et al., 2001). *A. baumannii* can also be found in vegetables (Berlau, 1999; Byrne-Bailey et al., 2009, Gennari and Lombardi, 1993), in milk (Nam et al., 2011) in aquaculture and in soils (Guardabassi et al., 1999; Hoa *et al*, 2011; Huys et al., 2007; Rokhbakhsh-Zamin et al., 2011), on human skin (Peleg et al., 2008; Zeana et al., 2003) and in human faeces (Dijkshoorn et al., 2005), which suggests the possibility of faecal-oral transmission. In remains to be assessed if these isolates, which are infrequent, are the result of hospital contamination or originate from natural reservoirs of this species.

1.4 Clinical importance and antibiotic resistance

In addition to asymptomatic colonisation and carriage on skin and in the respiratory tract, *A. baumannii* can cause a broad range of severe nosocomial infections, including skin and soft-tissue infections, wound infections, urinary tract infections and secondary meningitis. However, the most important infections, with the highest mortality rates, are ventilator-associated pneumonia and bloodstream infections (Dijkshoorn et al., 2007). The fact that *A. baumannii* is able to colonise the skin and respiratory tract without causing infection (Doughari et al., 2011), with skin carriage being 10-20% in healthy individuals, and as high as 50-75% in patients, is a factor to consider regarding its transmission within ICUs (Zeana et al., 2003). Infections are more common in patients suffering from an underlying disease or who have undergone intensive surgical procedures. *A. baumannii* can easily enter the body through open wounds, intravascular catheters and mechanical ventilators, and infections caused by *A. baumannii* are associated with long periods of hospitalisation (Peleg et al., 2008), the male gender, and older age (Wisplinghoff et al., 1999).

A. baumannii can also cause community-acquired infections. The most common is pneumonia (accounting for 85% of reports of community infections caused by *A. baumannii*), followed by bacteraemia. Other possible community-acquired infections include skin, soft-tissue and ocular infections, secondary meningitis and endocarditis (Chang et al., 2000, Falagas et al., 2007). These infections are more common in the male gender and are associated with old age, alcoholism, heavy smoking, diabetes mellitus, chronic obstructive pulmonary disease and renal disease. Pneumonia often occurs in the summer months in tropical and subtropical climates (Southeast Asia and North Australia). Community-acquired *A. baumannii* pneumonia is more serious than nosocomial pneumonia, is generally fulminant (death within eight days of diagnosis) and rates of mortality can be as high as 60% (Falagas et al., 2007).

The predominance of *A. baumannii* has also been reported to be rising in infections associated with injuries in war zones. Whereas no descriptions of this bacterium existed up to the Vietnam conflict (1955-75), in the last thirty years several studies have reported *A. baumannii* infections associated with the Iran-Iraq war (1980-88), the Gulf war (1990-91) and the Iraq war (2003-11). *A. baumannii* infections have also been associated with natural catastrophes such as the Turkey Marmara Earthquake (Centers for Disease Control and Prevention, 2004; Joly-Guillou, 2005; Murray et al., 2006).

The predominance and severity of *A. baumannii* infections seems to be related to the MDR phenotype of infecting strains (Diancourt et al., 2011). *A. baumannii* antimicrobial resistance has progressively increased. By 2007 up to 70% of isolates in certain settings (depending on country, hospital, medical department and clinical sample) were MDR, including resistance to carbapenems, which were once used as last resort against MDR-*A. baumannii* infections (Kempf and Rolain, 2012). Currently, colistin seems to be the most reliably effective drug against MDR *A. baumannii*, but it is nephrotoxic (Falagas and Rafailidis, 2009) and there are recent reports of resistance (Cai et al., 2012), resulting in the emergence of strains resistant to all known antibiotics (Al-Sweih et al., 2011). Worryingly, resistance appears to be spreading to the community, with reports of carbapenem-resistant *Acinetobacter* spp. in cattle (Poirel et al., 2012) and in the Seine river in Paris, France (Girlich et al., 2010). Detailed information on *A. baumannii* antimicrobial resistance mechanisms is provided in reviews by Peleg et al. (2008), Perez et al. (2007) and Poirel and Nordman (2006).

1.5 Virulence

1.5.1 Attributable mortality

There is some debate over the severity of *A. baumannii* infections, with attributable mortality rates varying, on average, from 8 to 35%, according to strain and type of infection (Falagas and Rafailidis, 2007). Accordingly, *A. baumannii* strains could be endowed with different pathogenicity potential, as suggested by two studies using the mouse model of pneumonia: an MDR strain isolated from the blood culture of a patient with nosocomial pneumonia showed 80% mortality to mice, in contrast to 13% for a strain causing meningitis (Eveillard et al., 2010), and an IC-I strain and a sporadic isolate were more virulent than a IC-III strain and the type strain (de Breij et al., 2012). Differences in mortality may be attributable to the expression of specific virulence factors and determinants. For example, two strains with the same PFGE profile, where one was a mucoid isolate from cerebrospinal fluid and the other was a non-mucoid isolate from a ventriculo-peritoneal catheter, showed mortality rates of 48% and 19%, respectively, in a mouse model of pneumonia (Eveillard et al., 2010).

1.5.2 Virulence factors and pathogenicity mechanisms

Although *A. baumannii* is able to cause a wide-range of infections, is increasingly resistant to antibiotics and may be associated with high mortality rates in ICU patients, its virulence factors and pathogenicity mechanisms were largely unknown in 2008, at the start of the work described in this thesis. The state of knowledge in 2008, as well as subsequent findings by other research groups, are described below and summarised in Table 2.

1.5.2.1 OmpA

The first *A. baumannii* virulence factor to be described and confirmed *in vivo* was the 38 kDa outer membrane protein OmpA. This is the most abundant *A. baumannii* outer membrane protein (Jyothisri et al., 1999) and is present in all strains (Hood et al., 2010). OmpA is important for abiotic attachment and contributes to biofilm formation (Gaddy et al., 2009). In addition, OmpA is important for initial attachment of *A. baumannii* epithelial cells to and its consequential invasion. Once inside the eukaryotic cell, OmpA is translocated to the nucleus (Choi et al., 2008a) and the mitochondria (Choi et al., 2005). In the nucleus, OmpA cleaves DNA with its intrinsic DNaseI-like activity and in the mitochondria it leads to the activation of caspase and cytochrome c (Choi et al., 2005), with both processes resulting in cell apoptosis. OmpA is essential for the bacteria to reach the bloodstream, since an OmpA knock-out mutant strain loses the ability to cause bacteraemia (Choi et al., 2008b). Once in the bloodstream, it is the main target of the humoral immune response (Luo et al., 2012a) where it can bind to the principal regulator of the alternative complement pathway, Factor H (Lee et al., 2010). As such, it is a major factor in *A. baumannii* serum resistance (Kim et al., 2009). However, OmpA does not seems to be essential for *A. baumannii* pathogenicity in the *Galleria mellonella* insect infection model (Wand et al., 2012).

1.5.2.2 Iron uptake systems

Other important virulence factors are iron uptake systems, in particular siderophores. Siderophores are high-affinity iron-chelating compounds essential for bacteria to survive in iron poor environments such as human body fluids.

A. baumannii contains a mixed (containing both catechol and hydroxamate groups) siderophore, structurally related to the siderophore anguibactin from *Vibrio anguillarum* (Yamamoto et al., 1994), which was thus called acinetobactin. The gene cluster of acinetobactin was characterised (Dorsey et al., 2004; Mihara et al., 2004) and biosynthetic and transport genes were identified. *A. baumannii* may also produce different siderophores: an early study reported that the type strain and several European clinical isolates produce acinetobactin and a 78 kDa iron-regulated outer membrane protein (IROMP) homologous to *V. anguillarum*, while American isolate 8399 produces a catechol siderophore and a 73 kDa IROMP (Dorsey et al., 2003; Echenique et al., 1992).

Genome sequencing of strain ATCC 17978 evidenced the existence of a second gene cluster that could code for an additional iron-acquisition system, as well as a cluster for haemin use (Smith et al., 2007). The acinetobactin system was disrupted by knock-out mutations and it was confirmed that *A. baumannii* could use haemin, but not haemoglobin in these conditions (Zimbler et al., 2009). Additional siderophore and haem systems were described during the course of the work described in this thesis (Eijkelkamp et al., 2011a; Zimbler et al., 2009). However, the catecholate siderophore synthesis and uptake system of strain 8399 was never characterised or studied in detail and, since so few *A. baumannii* strains have been studied for the presence of iron-acquisition systems, the distribution of these systems in this species has not been clarified. Moreover, no studies have demonstrated the importance of iron-acquisition systems, in particular siderophores, to *A. baumannii* virulence.

Lastly, in other species, the diversity in siderophore structure and the specificity of receptors have been used for strain and species typing, i.e. 'siderotyping'. In particular, fluorescent species of the *Pseudomonas* genus, which display over 50 different pyoverdine structures, can be differentiated according on the basis of the diversity of their peptide chain and receptor specificity (Fuchs et al., 2001). Since differentiation of *A. baumannii* isolates using phenotypic methods is complicated, the diversity of siderophore gene clusters in *A. baumannii* could be exploited for strain typing based on the genetic potential to produce siderophores or use exogenous iron sources.

1.5.2.3 Motility

Pili are filamentous structures of approximately 2-6 nm in diameter and over 20 nm in length that can be found in many bacteria. They are involved in a multiplicity of functions, including: biotic and abiotic adhesion, biofilm formation, motility, DNA transfer and phage transduction, all of which can be implicated in virulence (Proft and Baker, 2009). Pili can be divided into four types, which are assembled via diverse pathways and have different functions:

1) P and type I: assembled via the chaperone-usher pathway and involved in adherence,

2) curli: assembled via the extracellular nucleation/precipitation pathway and involved in adherence,
3) CS1: assembled via the alternative chaperone-usher pathway and involved in enterotoxicity in *Escherichia coli*,
4) type IV: assembled via the general secretion pathway and involved in twitching motility.

Two types of pili have been described in *Acinetobacter* spp., including *A. baumannii*:
1) type I or 'thin' pili: 2-3 mm diameter, short, peritrichous and involved in competence/transformation (Gohl et al., 2006),
2) type IV or 'thick' pili: 5-6 nm diameter, long, polar topology and involved in twitching motility (Henrichsen and Blom, 1975).

In *A. baumannii*, the 'thin' pili are called Csu pili and their biosynthetic cluster has been identified (Tomaras et al., 2003). They are involved in biofilm formation and adhesion to abiotic surfaces (Tomaras et al., 2003), as well as red blood cells (Gospodarek et al., 1998). However, they do not seem to be involved in adhesion to epithelial cells (de Breij et al., 2009). The *A. baumannii* 'thick' pili appear to be involved in twitching motility (Clemmer et al., 2011), since a *pilT* mutant is unable to twitch, but their role and structure has not been studied in detail. Twitching does not appear to be the sole type of motility of *A. baumannii*, as mutants in type IV pili are still able to show a sort of 'gliding' motility. Other factors involved in *A. baumannii* motility are: a two-component system (BfmRS), the OmpA protein, a lipopeptide that may act as surfactant, and a transglycosylase that may be involved in assembly of type IV pili (Clemmer et al., 2011).

1.5.2.4 Biofilm

Biofilm are complex, well-organised structures of microbial cells attached to a surface and surrounded by an extracellular matrix that is prevalently comprised of polysaccharides and proteins. In several species, including *A. baumannii*, this structure helps bacteria attach to solid surfaces and survive for longer periods in adverse conditions such as desiccation and during antimicrobial therapy.

A. baumannii can form biofilms on several abiotic surfaces, including polystyrene, polypropylene, polytetrafluoroethylene (Teflon) and glass (Tomaras et al., 2003, Vidal et al., 1996) and ca. 70% of strains are biofilm-formers (Cevahir et al., 2008, Rodríguez-Baño et al., 2008). When two strains isolated from the same patient were compared for virulence using a mouse model of pneumonia, the mucoid, biofilm-forming strain was more virulent than the non-mucoid, non biofilm-forming strain (Kempft et al., 2012b), indicating that biofilm formation may be associated with virulence. However, no correlation between biofilm formation and virulence was evident in a *G. mellonella* infection model (Wand et al., 2012). Secondly, no difference in biofilm formation was observed between outbreak and sporadic strains, although IC-II strains seemed to form larger biofilms than IC-I strains (de Breij et al., 2010). In agreement, respiratory and environmental strains seemed to be more adherent than wound and bacteremic strains (Kõljalg et al., 1996), whereas IC-II seemed to be more adherent than IC-I (Lee et al., 2006). Thirdly, clinically successful species *A. baumannii*, *A. pittii* and *A. nosocomialis* seemed to form larger biofilms on human skin than less clinically successful *A. calcoaceticus* (Peleg et al., 2012).

Biofilm formation appears to be positively correlated with multidrug resistance (Nucleo et al., 2009; Rao et al., 2008; Rodríguez-Baño et al., 2008), as well as resistance to desiccation (Gaddy and Actis, 2009) and to human serum (King et al., 2009). Several individual virulence factors have also been linked to *A. baumannii* biofilm formation. For example, Csu pili are essential for attachment to plastic surfaces, and expression of these pili is regulated by a two-component system, BfmRS, which also promotes biofilm formation (Tomaras et al., 2008). In addition, a high molecular mass adhesin homologous to the 'Biofilm-associated protein' (Bap) of *Staphylococcus* spp. is important in maintaining the structure of mature biofilms, possibly by allowing intercellular adhesions (Brossard and Campagnari, 2012; King et al., 2009; Loehfelm et al., 2008). The quorum sensing signal molecule is also involved in biofilm formation (Niu et al., 2008). The exopolysaccharide poly-β-1,6-N-acetylglucosamine (PNAG) is present in all *A. baumannii* strains and is essential for the biofilm structure (Choi et al., 2009). Lastly, the outer membrane protein OmpA is not essential for, but promotes biofilm formation (Gaddy et al., 2009).

1.5.2.5 Quorum sensing

A. baumannii produces a main signal molecule, *N*-(3-hydroxydodecanoyl)-L-homoserine lactone (AHL), and more than 60% strains also possess signal molecules of varying chain lengths, depending on the culture conditions (González et al., 2009). The IC-I representative strain RUH 875 produces two signal molecules and the IC-II representative strain RUH 134 produces three. Nevertheless, there does not appear to be a clear association between *Acinetobacter* species or strain and the number or kind of signal molecule produced (González et al., 2001). All these molecules are encoded by a single gene that is homologous to the *luxI* family of autoinducer genes (Niu et al., 2008; Smith et al., 2007). Besides its involvement in biofilm formation and motility, the role of quorum sensing in the regulation of other *A. baumannii* virulence factors has not been

elucidated and, in a *G. mellonella* infection model, a mutant in the signal molecule synthase gene was as virulent as the wild-type strain (Peleg et al., 2009).

1.5.2.6 Outer membrane structures

The lipopolysaccharide (LPS) is involved in virulence in many species (García et al., 1999). In *A. baumannii*, it has been shown to contribute to serum resistance (García et al., 2000) and the inflammatory response in mouse infection models (García et al., 1999). Moreover, colistin resistance is associated with the loss of LPS production. The *A. baumannii* LPS has a very conserved core (Luke et al., 2010), but an extremely diverse O-antigen composition (Pantophlet et al., 1998; Smith et al., 2007). Recently, a glycosylation system, which is involved in the synthesis of the O-antigen, was seen to be important for biofilm formation, as well as for virulence in amoeba, insect (*G. mellonella*) and mouse models of infection (Iwashkiw et al., 2012).

The capsule of *A. baumannii* has not been studied in depth. It is present in almost all *A. baumannii* isolates (Koeleman et al., 2001) and has been shown to increase growth in human ascites fluid and survival in a rat tissue infection model (Russo et al., 2008). However, there are conflicting reports regarding its involvement in serum resistance (García et al., 2000; Russo et al., 2010) and it does not seem to be associated with haemagglutination nor to be unequivocally associated with strain epidemicity (Koeleman et al., 2001).

Another component of the outer membrane of *A. baumannii* that is considered a putative virulence factor is the poly-β-1,6-N-acetylglucosamine (PNAG) surface polysaccharide, which has been seen to be involved in biofilm formation (Choi et al., 2009), as described above. In addition, a penicillin-binding protein (PBP 7/8) is required for survival in mouse models, but not in common laboratory media (Cayô et al., 2011; Russo et al., 2008). Its precise role in virulence remains unknown.

1.5.2.7 Exoenzymes

A. baumannii does not seem to produce a specific toxin, except for the gene-based prediction of an RTX toxin in strain ACICU (Iacono et al., 2008), homologous to the RTX toxin of *V. cholerae,* which in the latter acts in the depolymerisation of the actin cytoskeleton of eukaryotic cells (Sheahan et al., 2004). Instead, *A. baumannii* secretes several esterases, phospholipases and proteases. The *A. baumannii* phospholipase D was important for serum resistance, epithelial cell invasion and pathogenesis in a mouse pneumonia infection model (Jacobs et al., 2010). Gelatinase activity, which includes the capacity to hydrolyse gelatin, haemoglobin and collagen, was observed in 14% of clinical *A. baumannii* isolates, mostly in those associated with tracheal colonisation (Cevahir et al., 2008; Sechi et al., 2004). Urease activity was detected in *Acinetobacter* spp. (Rathinavelu et al., 2003) and urease genes were found in the genomes of different *A. baumannii* strains (Iacono et al., 2008; Smith et al., 2007; Vallenet et al., 2008), although no phenotypic studies with *A. baumannii* have been performed to date. Lipolytic activity has been demonstrated in several studies and appears to increase following exposure to antibiotics (Hostacká, 2000). Esterases were found in all *A. baumannii* strains analysed and their high diversity allows for typing of clinical isolates (Pouëdras et al., 1992). Haemagglutinating activity was detected with both 0 (0-25% isolates) and AB group erythrocytes (69-74% isolates) (Braun and Vidotto, 2004; Cevahir et al., 2008) and exopolysaccharide (slime) production was detected in 14% of isolates of *A. calcoaceticus* var. *anitratus*, which may be homologous to *A. baumannii* in modern taxonomy (Obana, 1986; Sechi et al., 2004).

1.5.2.8 Resistance to desiccation

Even if the attributable mortality and virulence potential of *A. baumannii* are still a matter of debate, no doubt exists concerning the exceptional ability of this species to persist in the hospital environment which, together with its antimicrobial resistance, constitutes a leading source of concern.

However, few studies have dealt with the resistance of *A. baumannii* to desiccation, and the factors and mechanisms behind this phenotype remain largely unknown. Clinical strains can survive on dry surfaces for several months (Wendt et al., 1997) although the average is 21-33 days (Jawad et al., 1998). There is no clear correlation between the ability to resist desiccation and strain epidemiology or isolation site. Nevertheless, there seems to be great strain-dependent variation in xerotolerance and strains collected from dry surfaces seem to survive longer than strains from wet sources (Wendt et al., 1997), indicating that the factors connected to desiccation might be intrinsic to individual strains. Biofilm-forming strains have been reported to resist desiccation for longer than non-biofilm-forming strains (36 vs 15 days) (Espinal et al., 2012).

1.5.2.9 Serum resistance

An important aspect of the pathogenesis of bacteria that can cause bacteraemia, such as *A. baumannii*, is serum resistance. About 60% of *A. baumannii* clinical isolates are serum resistant (Hostacká, 2002) and serum resistant isolates are endowed with higher mortality (Kim et al., 2009). The LPS of *A. baumannii* seems to be associated with serum resistance, since the treatment of bacterial cells with EDTA, which disrupts the LPS structure, decreases *A. baumannii* serum resistance (García et al., 2000). Nevertheless, LPS does not appear to be the sole

component responsible for serum resistance, since, when treated with EDTA, about half the isolates remain serum resistant (Kim et al., 2009). Other factors that possibly contribute to serum resistance are the OmpA (Kim et al., 2009) and PBP 7/8 (Russo et al., 2009) proteins, and treatment with imipenem seems to render strains more serum resistant (Hostacká, 1999). Oddly, there are conflicting results regarding the interaction of *A. baumannii* with complement factor H. Some authors reported no binding of any isolate to this regulatory protein (King et al., 2009), whereas other authors reported specific binding of OmpA to factor H (Kim et al., 2009).

1.5.3 Genomic analysis

Recent years have seen an acceleration in the number of sequenced and annotated *A. baumannii* genomes. As at October 2012, 10 chromosomal genomes have been fully sequenced, 40 are available as draft sequences (Fig. 2; Table 3) on the NCBI website and over 150 more genomes are currently being sequenced. This high number of available sequences has enabled comparative genomic analyses and the development of advanced knowledge on *A. baumannii* population structure and phylogenetic relationships, as well as on potential virulence and antimicrobial resistance determinants.

The first sequenced *A. baumannii* genome was that of ATCC 17978, a strain isolated in 1951 from a fatal case of meningitis and sensitive to the newest generation of antimicrobials (macrolides, glycopeptides, cephalosporins, and the latest beta-lactams) (Smith et al., 2007). Its genome is 3.9 Mb in size, with 39% G+C content and a total of 3758 predicted genes, of which 3670 are putative or confirmed protein-coding genes. Twenty-eight putative alien islands were identified in the genome of ATCC 17978, of which twelve contain genes predicted to be involved in pathogenicity, i.e., belonging to pathogenicity islands (PAIs). These genes encode functions involved in: 1) cell envelope biogenesis, 2) quorum sensing, 3) type IV pili, 4) drug resistance, and 5) iron transport.

The second genome sequence to be published was that of strain ACICU, an epidemic MDR strain isolated from the cerebrospinal fluid of a patient cared for in an Italian hospital and belonging to the IC-II (Iacono et al., 2008). Its genome has a comparable size to the genome of ATCC 17978 and a similar G+C content. Thirty-four PAIs were identified, 24 of which were homologous to PAIs identified in ATCC 17978 and 4 of which were unique to ACICU. The PAIs unique to ACICU coded for proteins involved in: 1) membrane transport, 2) antimicrobial resistance, 3) iron transport, 4) pilus biogenesis, and 5) haemagglutination/haemolysis. The profusion of genes coding for drug export proteins could explain why this strain is MDR and why strains belonging to the IC-II clone have high epidemic potential and often cause hospital outbreaks.

Contemporary to the sequencing of the ACICU genome, the genomes of MDR epidemic strain AYE, recovered from a patient suffering from bloodstream infection and belonging to IC-I, and SDF, a strain susceptible to most antibiotics and recovered from a body louse taken from a homeless patient, were sequenced (Vallenet et al., 2008). Similar to ACICU, the genome of outbreak MDR strain AYE contains genes coding for antibiotic and heavy metal resistance factors, but in this strain these genes are grouped in an 86 kb genomic island called AbaR1. This island contains 88 genes homologous to genes of *Pseudomonas* spp., *Salmonella* spp. and *E. coli* (Fournier et al., 2006) and thus the AYE strain likely acquired resistance genes by horizontal gene transfer, perhaps as a result of sharing its habitat with these other common pathogens.

In contrast to the genomes of the three clinical strains of *A. baumannii*, the genome of the body louse strain SDF is smaller, encompassing 3.2 Mb and containing 2913 putative genes, of which only 80% are predicted to encode proteins. Since the SDF strain was recovered from a separate habitat, the genes lacking in this strain could offer a clue concerning the virulence factors of *A. baumannii*. Alternatively, they could be a result of a regressive evolution of this strain following adaptation to a highly specialised habitat. In general, the three clinical strains contain genes encoding proteins involved in biofilm and quorum sensing, including Csu and type IV pili and an AHL, all of which were lacking in SDF. In addition, all three clinical strains encode several siderophore uptake systems, in contrast to the non-clinical strain SDF, which has haemagglutinin/haemolysin-related genes in common with strain ACICU, and thus might use haem instead of ferric iron. All genomes encode the *ompA* gene, as well as two copies of genes encoding phospholipase C and several copies of the genes encoding phospholipases A and D, and a higher number of two-component transport systems.

The important features of other sequenced genomes are summarised in Table 3. In particular, sequencing of additional MDR strains evidenced the existence of large resistance islands, homologous to that of AYE, in strains AB0057 and MDR-ZJ06 (Zhou et al., 2011) and significant strain variation at the level of the O-antigen gene cluster (Adams et al., 2008). Sequencing of strain MDR-ZJ06 evidenced that, although it forms strong biofilms, this strain does not encode for Csu pili, which have been demonstrated to be important for biofilm formation in *A. baumannii*. In addition, sequencing of the genome of strain 1656-2, an MDR clinical isolate with the property of forming strong biofilms, evidenced the existence of 13 genes putatively involved in biofilm

formation, including a gene for the synthesis of polyglutamic acid (PGA), and 34 cell adhesion protein-coding genes (Park et al., 2011). In comparison with the genomes of ATCC 17978, ACICU, AYE and SDF, the genome of this strain encodes more genes involved in cell adhesion, secretion and vesicular transport (Park et al., 2011), which could also be involved in biofilm formation.

1.5.4 Proteomic and transcriptomic analyses

Proteomic and transcriptomic analyses have higher informative power than analysis of individual virulence factors and genomic analysis. In the last years, several proteomic studies have investigated factors linked to *A. baumannii* antibiotic resistance and/or virulence, including biofilm formation, tetracycline and imipenem resistance, septic infection and metabolism (benzoate degradation, histidine metabolism).

Proteomic analysis allowed the confirmation of OmpA as the most abundant *A. baumannii* outer membrane protein (Martí et al., 2006), as well as a major vesicle and supernatant protein (Kim et al., 2008). In addition, several proteins were confirmed by proteomic and transcriptomic studies to be differentially regulated in response to iron-poor conditions: some outer-membrane proteins, several TonB-dependent receptors, three siderophore synthesis and uptake systems and antibiotic resistance genes were over-expressed under iron-limiting conditions, whereas type IV and Csu pili and iron storage proteins were over-expressed under iron-replete conditions (Eijkelkamp et al., 2011a; Nwugo et al., 2011).

In strains forming biofilm, TonB-dependent receptors, four siderophore synthesis and uptake systems, antibiotic resistance, the BfmRS two-component system, a lipase and several pili (Csu and two undescribed systems: P pili and type III), OmpA, LPS synthesis proteins and a putative phosphate transporter PstS were over-expressed (Cabral et al., 2011; Martí *et al*, 2011; Shin et al., 2009). Genes involved in biofilm formation were expressed in the exponential phase and genes involved in the maintenance of the biofilm structure, as well as resistance to desiccation, are mostly expressed during the stationary phase (Jacobs *et al*, 2012).

As a response to tetracycline and imipenem antibiotic stress, efflux pumps, the BfmRS two-component system and iron uptake system receptors were over-expressed, and the production of outer membrane proteins was down-regulated (Yun et al., 2011).

1.5.5 Models for the assessment of *A. baumannii* pathogenicity

1.5.5.1 Cellular models

Adherence to biotic surfaces is important as an *A. baumannii* virulence mechanism in the initial stages of infection (colonisation and invasion). Human bronchial epithelial cells have been used to test adherence of *A. baumannii* strains (Lee et al., 2006) and to test the involvement of specific virulence factors in adherence, namely acinetobactin (Gaddy et al., 2009), Csu pili (de Breij et al., 2009) and OmpA (Choi et al., 2008b). *A. baumannii* adhered to epithelial cells and IC-II isolates were more adherent than IC-I isolates. Csu pili and OmpA were shown to interact with epithelial cells, unlike acinetobactin. OmpA also promoted bacterial internalisation via a zipper-like mechanism (Choi et al., 2008b) and was implicated in the apoptosis of human laryngeal HEp-2 cells (Choi et al., 2005).

Lastly, the development of a 3D air-exposed skin equivalent model to study adherence of *A. baumannii* to epithelial cells demonstrated that type strain ATCC 19606 is able to colonise but not invade the stratum corneum (de Breij et al., 2012).

1.5.5.2 Animal models

Animal models are essential to the understanding of the pathogenesis of bacterial infections, since they allow the acquisition of knowledge on host-pathogen interactions, studies on the activity of virulence factors and the development of new antimicrobials without interfering and/or harming human patients. Nevertheless, it is clear that the models must be chosen on the basis of their accurate mimicry of human infection.

Two types of animal models have been employed to study *A. baumannii* virulence: mammalian and non-mammalian. Non-mammalian models do not fully mimic human infections, but are easier to handle, a higher number of animals can be used, which allow the screen of more robust statistical analysis, are more cost-constrained and often pose less ethical barriers. They are usually chosen for screening bacterial mutants and for initial antimicrobial testing. Mammalian models are more costly, more difficult to work with and may present ethical problems, but generate more directly relevant information, and are preferred for studies on host response and drug efficacy and toxicology.

1.5.5.2.1 Non-mammalian models

Virulence assays using the nematode *Caenorhabditis elegans* and the amoeba *Dictyostelium discoideum* resulted in the identification of 30 genes putatively required for the virulence of *A. baumannii* (Smith et al., 2007). Nevertheless, most of the genes were metabolism-related and the few known *A. baumannii* virulence factors were not identified by this approach, so the validity of these two systems remains questionable.

Conversely, the caterpillar *G. mellonella* model, which was used to test antimicrobial activity (Hornsey et al., 2011b, Peleg et al., 2009), to compare strain virulence (Wand et al., 2011) and to assess specific virulence factors (Gaddy et al., 2012), shows significant correlation in virulence (R = 0.56) with mouse models (Jander et al., 2000). *G. mellonella* has a more evolved immune system than *C. elegans* and *D. Discoideum* and a known immune gene repertoire (Brown *et al*, 2009; Vogel et al., 2011), is easy to manipulate, can be incubated at 37ºC and can be unambiguously scored for life/death status.

1.5.5.2.2 Mammalian models

For *A. baumannii*, the most common vertebrate infection model is the mouse model of pneumonia (de Breij et al., 2012; Eveillard et al., 2010; Knapp et al., 2006; Montero et al., 2002; Pachón-Ibáñez et al., 2011). Studies have been performed on the effects of one drug or comparison between drugs (Montero et al., 2002; Pachón-Ibáñez et al., 2011), to understand host-pathogen interactions (Knapp et al., 2006) or to compare the virulence of several *A. baumannii* strains (de Breij et al., 2012; Eveillard et al., 2010). The 50% lethal dose (LD_{50}) in the mouse pneumonia model varied between $0.5\text{-}5\times10^6$ CFU/g (de Breij et al., 2012; Eveillard et al., 2010), which is therefore comparable to other bacterial species such as *P. aeruginosa* and *S. enterica* (DiGiandomenico et al., 2004; Kintz et al., 2008). Secondly, the peritoneal sepsis mouse model has been employed to test the efficacy of antimicrobials (López-Rojas *et al*, 2011; Shankar et al., 1997) or vaccines (McConnell and Páchon, 2010; McConnell et al., 2011a; McConnell et al., 2011b), but animal sepsis models are difficult to extrapolate to human sepsis. Other mouse infection models include the thigh and lung model (Dudhani et al., 2010), the allergic asthma model (Qiu et al., 2011), the burn wound model (DeLeon et al., 2009; Han et al., 2009; Shankar et al., 2007), the diabetic pneumonia and the bacteraemia mice models (Luo et al., 2012b). Neutropenic mice have been used to avoid interaction with the immune system and thus favour the onset of infection (de Breij et al., 2012; Dudhani et al., 2010; Luo et al., 2012b).

The rat soft tissue model has been used to compare strain virulence, to identify specific virulence factors and to test the activity of new antimicrobials (Russo et al., 2008; Russo et al., 2010; Russo et al., 2011). It has the advantage of allowing samples to be taken from the same animal at multiple time points, but a relatively high inoculum is needed to cause disease. The rat thigh model has been used to test the effect of colistin (Pantopoulou et al., 2007), the sepsis model to test the effect of the combination of buforin II and rifampicin (Cirioni et al., 2009) and the osteomyelitis model to test *A. baumannii* virulence (Collinet-Adler et al., 2011).

Rabbits are preferred infection models in cases where external devices such as a pacemaker (Hansen et al., 2009) or a catheter (Rodríguez-Hernández et al., 2004) need to be used, due to their bigger size. An endocarditis model has been used to study the effect of colistin of *A. baumannii* on an infected ventricle (Rodríguez-Hernández et al., 2004).

1.6 Alternative antimicrobial strategies

A. baumannii has an incredible ability to continuously improve its ability to resist antibiotics, as seen by the recent emergence of pan-resistant strains (Al-Sweih et al., 2011), which calls for the development of alternative antimicrobial strategies for which resistance is less easily developed.

The oldest alternative antimicrobial strategy is phage therapy, which has been explored since the 1980s. It is cheap, very specific and one dosage suffices. However, bacteria might develop resistance to the phage, the phage might transfer bacterial toxins, many phages are strain-specific, and allergic reactions are possible (Matsuzaki et al., 2005). So far, there are no *in vivo* studies on *A. baumannii*, although the lysozyme of *A. baumannii* specific phage ΦAB2 is active *in vitro* against the peptidoglycan of *A. baumannii* (Lai et al., 2011).

Another possible solution is a 'Trojan-horse strategy', as involved in the administration of BAL30072, a siderophore-monosulfactam antibiotic that is already in phase-1 clinical trials. Alternatively, a few potential vaccines have been developed and have demonstrated some efficacy *in vivo*, including: an outer membrane complex vaccine (McConnell et al., 2010); inactivated whole-cell extracts (McConnell et al., 2011a), outer membrane vesicles (McConnell et al., 2011b), a Bap protein-directed vaccine (Fattahian et al., 2011), recombinant OmpA with an aluminium hydroxide adjuvant (Luo et al., 2012a) and a synthetic oligopeptide derived from PNAG (Bentancor et al., 2012).

In addition, the lactoferrin-derived antimicrobial peptide hLF(1-11) has been successful in a mouse thigh model, and several other antibacterial peptides have been successful *in vitro*, including: a synthetic cecropin A-melittin hybrid peptide (Alárcon et al., 2001), a diastereomer of K_6L_9 (Braunstein et al., 2004), a synthetic peptide from the brevinin-2 family (Al-Ghaferi et al., 2010), a synthetic human beta-defensin 2 (Routsias et al., 2010) and an [E4K] alyteserin analog peptide (Conlon et al., 2010). Antimicrobial peptides have limited resistance, are structurally diverse and have broad-spectrum activity (Jenssen et al., 2006), but can be inactivated by human serum, and therefore may need structural modifications in order to be effective (Gordon et al., 2005).

Lastly, other possible alternative therapies that have been validated *in vivo* include: photodynamic therapy (Dai et al., 2009), plasmid-encoded bactericidal gene transfer (Shankar et al., 2007), modified human skin tissue (Thomas-Virnig et al., 2009) and nitric oxide-releasing nanoparticles (Han et al., 2009). Overall, the foreseeable spread of pan-resistance among epidemic *A. baumannii* clones poses an urgent need to develop new therapeutic strategies that are complementary or an alternative to conventional antimicrobial therapy.

1.7 Aims of the thesis

Although several studies have focused on the problem of antimicrobial resistance in *A. baumannii*, little was known at the start of this work concerning the virulence factors and pathogenicity mechanisms of this species. In addition, it was not known whether *A. baumannii* has an homogenous population structure or whether some lineages/strains are more virulent than others or whether the acquisition of particular virulence factors is the reason behind the extraordinary fitness of *A. baumannii* in the nosocomial environment. In addition, with regard to the shortage of antimicrobial treatment options, although a few alternative antimicrobial drugs have been proposed, none has yet provided a dependable solution to treat patients infected with *A. baumannii*.

Accordingly, the studies presented in this thesis initially addressed the question of the nature of *A. baumannii* virulence and aimed to cover the following six main objectives:

1) to determine whether a core set of conserved *A. baumannii* virulence factors exists and is shared among different strains,
2) to determine whether epidemic strains have acquired new virulence determinants, in addition to antibiotic resistance genes,
3) to determine whether a co-evolution between drug resistance and virulence has occurred,
4) to determine whether strains can be differentiated on the basis of virulence factor conservation,
5) to assess the presence and the conservation of virulence factors in a collection of epidemic clinical isolates,
6) as a result of the above findings, to examine a viable alternative approach for the treatment of *A. baumannii* infections.

To achieve these aims, a strategy was proposed in which the genomes of four epidemiologically diverse *A. baumannii* strains were compared, and genomic information was used as a guidance tool for phenotypic analyses. Results obtained with these initial analyses are provided in **Chapters 2 and 3**. As a second step, the distribution of a particular group of virulence determinants, i.e. iron uptake systems, was explored in more depth using a wide, representative collection of clinical, MDR *A. baumannii* strains (**Chapters 4 and 5**). Thirdly, the expression of important *A. baumannii* virulence-associated traits identified in **Chapters 2 and 3** was studied in a clinically important collection of epidemic strains (**Chapter 6**). Lastly, a new antimicrobial approach, based on the disruption of iron metabolism, was investigated (**Chapter 7**). It is hoped that the results presented in this thesis will provide microbiologists and clinicians with a more robust platform of knowledge concerning the pathogenicity of *A. baumannii* and inspire future studies on innovative anti-*A. baumannii* therapies.

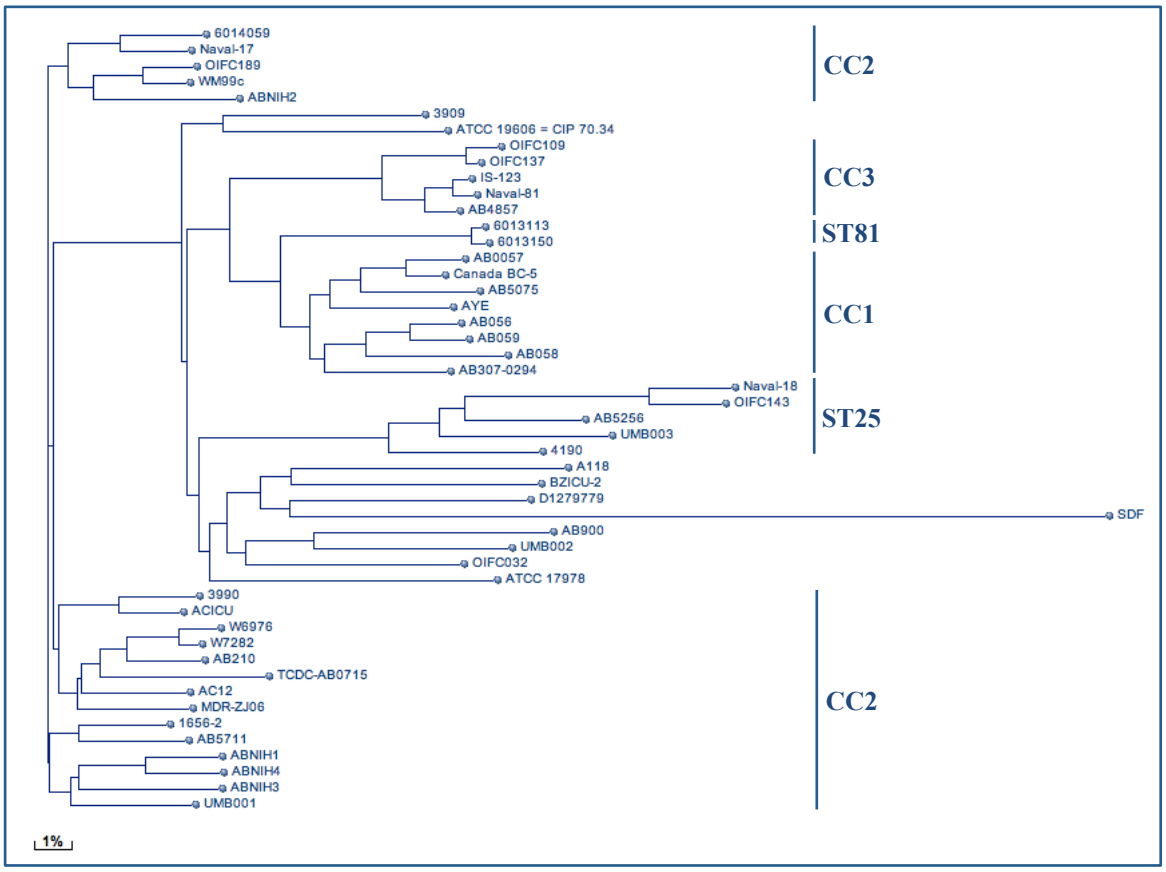

Fig. 2 Phylogenetic tree built on BLASTn whole-genome comparison of sequenced *A. baumannii* genomes (adapted from NCBI: http://www.ncbi.nl.nih.gov)

Table 1. Named *Acinetobacter* species and other recognised unnamed genomic species (October 2012)

Species name	Genomic species	Type or representative strain	Major habitat or source
A. calcoaceticus	1	ATCC 23055^T	soil, water
A. baumannii	2	ATCC 19606^T	clinical
A. pittii	3	ATCC 19004	clinical
A. haemolyticus	4	ATCC 17906^T	human
A. junii	5	ATCC 17908^T	human
	6	ATCC 17979	human
A. johnsonii	7	ATCC 17909^T	human skin, water, soil
A. lwoffii	8/9	ATCC 15309^T	human skin
A. bereziniae	10	ATCC 17924^T	human specimens, soil
A. guillouiae	11	ATCC 11171^T	human faeces, water, soil
A. radioresistens	12	IAM 13186^T	human, soil
A. nosocomialis	13TU	ATCC 17903	clinical
	13BJ, 14TU	ATCC 17905	human
	14BJ	CCUG 14816	human
	15TU	M 151a	human
	15 BJ	SEIP 23.78	human
	16	ATCC 17988	human
	17	SEIP Ac87.314	human, soil
	Between 1 and 3	10095	clinical
	Close to 13TU	10090	human clinical
A. baylyi		DSM 14961^T	activated sludge, soil
A. beijerinckii		NIPH 838^T	soil, water
A. bouvetii		DSM 14964^T	activated sludge
A. brisouii		DSM 18516	wetland
A. gerneri		DSM 14967^T	activated sludge
A. gyllenbergii		NIPH 2150^T	human
A. oleivorans		DR1	soil
A. parvus		NIPH384^T	human, animal
A. rudis		CCUG 57889	milk, wastewater
A. schindleri		NIPH1034^T	human
A. soli		KCTC 22184^T	soil
A. tandoii		DSM 14970^T	activated sludge, soil
A. tjernbergiae		DSM 14971^T	activated sludge
A. towneri		DSM 14962^T	activated sludge
A. ursingii		NIPH137^T	human
A. venetianus		RAG-1^T	marine water

Table 2. Summary of *A. baumannii* virulence-associated factors and methods for their assessment

Virulence factor	Method of assessment			Reference
	Phenotypic studies	Genomic/ proteomic analysis	*In vivo* studies	
Acinetobactin	✓	✓	✓	Dorsey et al., 2004; Gaddy et al., 2012; Yamamoto et al., 1994
Other siderophore systems	✓	✓	×	Echenique *et al*, 1992; Eijkelkamp et al., 2011a
Bap proteins	✓	✓	✓	Brossard et al., 2012; Fattahian et al., 2011; Loehfelm et al., 2008
BfmRS	✓	✓	×	Tomaras et al., 2008; Yun *et al*, 2011
Biofilm formation	✓	✓	✓	de Breij et al., 2010; Park et al., 2011; Wand et al., 2011
Capsule	✓	✓	✓	Russo et al., 2010; Shin *et al*, 2009
Esterase/Lipase	✓	✓	×	Hostacká, 2000; Iacono et al., 2008; Martí et al., 2011
Gelatinase	✓	×	×	Cevahir et al., 2008; Sechi et al., 2004
Haemagglutinins	✓	✓	×	Braun and Vidotto, 2004; Vallenet et al., 2008
Haemolysins	×	✓	×	Sechi et al., 2004; Vallenet et al., 2008
LPS	✓	✓	×	Kim et al., 2009; Luke et al., 2010
OmpA	✓	✓	✓	Cabral et al., 2011; Choi et al., 2005; Gaddy et al., 2009
Penicillin-binding protein 7/8	✓	✓	✓	Cayô et al. 2011; Russo et al., 2009
Phospholipase D	✓	✓	✓	Di Nocera et al., 2011; Jacobs et al., 2010; Martí et al., 2011
Phospholipase C	✓	✓	✓	Camarena, 2010; Vallenet et al., 2008
Csu pili	✓	✓	×	de Breij et al., 2009; Tomaras et al., 2008
Type IV pili	✓	✓	×	Clemmer et al., 2011; Iacono et al., 2008
PNAG	✓	✓	✓	Choi et al., 2009; Bentancor et al., 2012
Quorum sensing	✓	✓	✓	Iacono et al., 2008; Niu et al., 2008; Peleg et al., 2009
Resistance to desiccation	✓	×	×	Jawad et al., 1998; Wendt et al., 1997
Resistance to serum	✓	✓	×	Jacobs et al., 2012; Kim et al., 2009; King et al., 2009
RTX toxin	✓	×	×	Iacono et al., 2008
Exopolysaccharide (slime)	✓	×	×	Obana, 1986; Sechi et al., 2004
Urease	×	✓	✓	Iacono et al., 2008; Smith et al., 2007

Table 3. List of sequenced and annotated *A. baumannii* genomes (October 2012)

Strain	MLST profile[a]	Resistance profile	Source	Reference
Sequence fully available				
ATCC 17978	ST77[b]	susceptible	meningitis	Smith et al., 2007
ACICU	CC2[c]	MDR[d]	cerebrospinal fluid	Iacono et al., 2008
AYE	CC1	MDR	bloodstream infection	Vallenet et al., 2008
SDF	ST17	susceptible	insect gut	
AB0057	CC1	MDR	bloodstream infection	Adams et al., 2008
AB307-294	CC1	MDR	blood	
TCDC-AB0715	CC1	MDR	bacteraemia	Chen et al., 2011
MDR-TJ	CC2	MDR	ND[e]	Gao et al., 2011
MDR-ZJ06	CC2	MDR	bloodstream infection	Zhou et al., 2011
1656-2	CC2	MDR	ND	Park et al., 2011
Sequence available in scaffolds or contigs				
ATCC 19606^T	ST52	susceptible	urine	Bouvet and Grimont, 1986
3990	CC2	MDR	central venous catheter	Zarrilli et al., 2011
4190	ST25	MDR	bloodstream infection	
3909	ST78	MDR	pneumonia	
6013113	ST81	ND	skin	Human Microbiome Project
6013150	ST81	ND	skin	
6014059	CC2	ND	skin	
A118	ND	susceptible	bloodstream	Ramirez et al., 2011
AB056	CC1	MDR	bloodstream	Adams et al., 2010
AB058	ST20	MDR	bloodstream	
AB059	CC1	MDR	bloodstream	
AB210	CC2	MDR	intra-abdominal infection	Hornsey et al., 2011a
AB4857	CC3	MDR	osteomyelitis/sepsis	Zurawski et al., 2012
AB5075	CC1	MDR	osteomyelitis/sepsis	
AB5256	ST25	MDR	osteomyelitis/sepsis	
AB5711	CC2	MDR	osteomyelitis/sepsis	
AB900	ST49	MDR	peritoneum	Adams et al., 2008
ABNIH1	CC2	MDR	ND	Snitkin et al., 2011
ABNIH2	CC2	MDR	ND	
ABNIH3	CC2	MDR	ND	
ABNIH4	CC2	MDR	ND	
AC12	CC2	MDR	ND	Gan et al., 2012
BZICU-2	ND	ND	ND	Liu et al., 2012
Canada BC-5	CC1	ND	ND	Walter Reed Army Institute of Research, US
D1279779	ND	ND	ND	Eijkelkamp et al., 2011b
IS-123	CC3	MDR	wound	Walter Reed Army Institute of Research, US
Naval-17	CC2	ND	ND	
Naval-18	ST25	ND	ND	
Naval-81	CC3	ND	ND	
OIFC032	ST32	ND	ND	
OIFC109	CC3	ND	ND	
OIFC137	CC3	ND	ND	
OIFC143	ST25	ND	ND	
OIFC189	CC2	ND	ND	
UMB001	CC2	MDR	blood	Sahl et al., 2011

[a] Defined according to the Pasteur MLST scheme (http://www.pasteur.fr/recherche/genopole/PF8/mlst/Abaumannii.html)
[b] ST, sequence type
[c] CC, clonal complex
[d] MDR, multidrug resistant
[e] ND, no data or not determined

UMB002	ST16	MDR	perineum	
UMB003	ST25	MDR	wound	
W6976	CC2	ND	ND	University of Birmingham, UK
W7282	CC2	ND	ND	University of Birmingham, UK
WM99c	CC2	ND	ND	Eijkelkamp et al., 2011b

1.8 References

- **Adams MD, Goglin K, Molyneaux N, Hujer KM, Lavender H, Jamison JJ, MacDonald IJ, Martin KM, Russo T, Campagnari AA, Hujer AM, Bonomo RA, Gill SR.** Comparative genome sequence analysis of multidrug-resistant *Acinetobacter baumannii*. J Bacteriol. 2008 190(24):8053-64.
- **Al-Ghaferi N, Kolodziejek J, Nowotny N, Coquet L, Jouenne T, Leprince J, Vaudry H, King JD, Conlon JM.** Antimicrobial peptides from the skin secretions of the South-East Asian frog Hylarana erythraea (Ranidae). Peptides. 2010 31(4):548-54.
- **Al-Sweih NA, Al-Hubail MA, Rotimi VO.** Emergence of tigecycline and colistin resistance in *Acinetobacter* species isolated from patients in Kuwait hospitals. J Chemother. 2011 23(1):13-6.
- **Alarcón T, López-Hernández S, Andreu D, Saugar JM, Rivas L, López-Brea M.** *In vitro* activity of CA(1-8)M(1-18), a synthetic cecropin A-melittin hybrid peptide, against multiresistant *Acinetobacter baumannii* strains. Rev Esp Quimioter. 2001 14(2):184-90.
- **Bentancor LV, O'Malley JM, Bozkurt-Guzel C, Pier GB, Maira-Litrán T.** Poly-N-acetyl-β-(1-6)-glucosamine is a target for protective immunity against *Acinetobacter baumannii* infections. Infect Immun. 2012 80(2):651-6.
- **Bergogne-Bérézin E, Towner KJ.** *Acinetobacter* spp. as nosocomial pathogens: microbiological, clinical, and epidemiological features. Clin Microbiol Rev. 1996 9(2):148-65.
- **Berlau J, Aucken HM, Houang E, Pitt TL.** Isolation of *Acinetobacter* spp. including *A. baumannii* from vegetables: implications for hospital-acquired infections. J Hosp Infect. 1999 42(3):201-4.
- **Bouvet PJM and Grimont PAD.** Taxonomy of the genus *Acinetobacter* with the recognition of *Acinetobacter baumannii* sp. nov., *Acinetobacter haemolyticus* sp. nov., *Acinetobacter johnsonii* sp. nov., and *Acinetobacter junii* sp. nov. and emended descriptions of *Acinetobacter calcoaceticus* and *Acinetobacter lwoffii*. Int J Syst Bacteriol. 1986 36(2): 228-40.
- **Bouvresse S, Socolovshi C, Berdjane Z, Durand R, Izri A, Raoult D, Chosidow O, Brouqui P.** No evidence of *Bartonella quintana* but detection of *Acinetobacter baumannii* in head lice from elementary schoolchildren in Paris. Comp Immunol Microbiol Infect Dis. 2011 34(6):475-7.
- **Braun G, Vidotto MC.** Evaluation of adherence, hemagglutination, and presence of genes codifying for virulence factors of *Acinetobacter baumannii* causing urinary tract infection. Mem Inst Oswaldo Cruz. 2004 99(8):839-44.
- **Braunstein A, Papo N, Shai Y.** *In vitro* activity and potency of an intravenously injected antimicrobial peptide and its DL amino acid analog in mice infected with bacteria. Antimicrob Agents Chemother. 2004 48(8):3127-9.
- **Brisou J, Prevot AR.** [Studies on bacterial taxonomy. X. The revision of species under Acromobacter group]. Ann Inst Pasteur (Paris). 1954 86(6):722-8.
- **Brossard KA, Campagnari AA.** The *Acinetobacter baumannii* Biofilm-Associated Protein Plays a Role in Adherence to Human Epithelial Cells. Infect Immun. 2012 80(1): 228–233.
- **Brown SE, Howard A, Kasprzak AB, Gordon KH, East PD.** A peptidomics study reveals the impressive antimicrobial peptide arsenal of the wax moth *Galleria mellonella*. Insect Biochem Mol Biol. 2009 39(11):792-800.
- **Byrne-Bailey KG, Gaze WH, Kay P, Boxall AB, Hawkey PM, Wellington EM.** Prevalence of sulfonamide resistance genes in bacterial isolates from manured agricultural soils and pig slurry in the United Kingdom. Antimicrob Agents Chemother. 2009 53(2):696-702.
- **Cabral MP, Soares NC, Aranda J, Parreira JR, Rumbo C, Poza M, Valle J, Calamia V, Lasa I, Bou G.** Proteomic and functional analyses reveal a unique lifestyle for *Acinetobacter baumannii* biofilms and a key role for histidine metabolism. J Proteome Res. 2011 10(8):3399-417.
- **Cai Y, Chai D, Wang R, Liang B, Bai N.** Colistin resistance of *Acinetobacter baumannii*: clinical reports, mechanisms and antimicrobial strategies. J Antimicrob Chemother. 2012 67(7):1607-15.
- **Camarena L, Bruno V, Euskirchen G, Poggio S, Snyder M.** Molecular mechanisms of ethanol-induced pathogenesis revealed by RNA-sequencing. PLoS Pathog. 2010 6(4):e1000834.
- **Cayô R, Rodríguez MC, Espinal P, Fernández-Cuenca F, Ocampo-Sosa AA, Pascual A, Ayala JA, Vila J, Martínez-Martínez L.** Analysis of genes encoding penicillin-binding proteins in clinical isolates of *Acinetobacter baumannii*. Antimicrob Agents Chemother. 2011 55(12):5907-13.
- **Centers for Disease Control and Prevention.** *Acinetobacter baumannii* infections among patients at military medical facilities treating injured US service members, 2002–2004. MMWR 2004; 53: 1063–1066.
- **Cevahir N, Demir M, Kaleli I, Gurbuz M, Tikvesli S.** Evaluation of biofilm production, gelatinase activity, and mannose-resistant hemagglutination in *Acinetobacter baumannii* strains. J Microbiol Immunol

Infect. 2008 41(6):513-8.
- **Chang WN, Lu CH, Huang CR, Chuang YC.** Community-acquired *Acinetobacter* meningitis in adults. Infection. 2000 28(6):395-7.
- **Chen CC, Lin YC, Sheng WH, Chen YC, Chang SC, Hsia KC, Liao MH, Li SY.** Genome sequence of a dominant, multidrug-resistant *Acinetobacter baumannii* strain, TCDC-AB0715. J Bacteriol. 2011 193(9):2361-2.
- **Chen MZ, Hsueh PR, Lee LN, Yu CJ, Yang PC, Luh KT.** Severe community-acquired pneumonia due to *Acinetobacter baumannii*. Chest. 2001 120(4):1072-7.
- **Choi AH, Slamti L, Avci FY, Pier GB, Maira-Litrán T.** The *pgaABCD* locus of *Acinetobacter baumannii* encodes the production of poly-beta-1-6-N-acetylglucosamine, which is critical for biofilm formation. J Bacteriol. 2009 191(19):5953-63.
- **Choi CH, Hyun SH, Lee JY, Lee JS, Lee YS, Kim SA, Chae JP, Yoo SM, Lee JC.** *Acinetobacter baumannii* outer membrane protein A targets the nucleus and induces cytotoxicity. Cell Microbiol. 2008 10(2):309-19.
- **Choi CH, Lee EY, Lee YC, Park TI, Kim HJ, Hyun SH, Kim SA, Lee SK, Lee JC.** Outer membrane protein 38 of *Acinetobacter baumannii* localizes to the mitochondria and induces apoptosis of epithelial cells. Cell Microbiol. 2005 7(8):1127-38.
- **Choi CH, Lee JS, Lee YC, Park TI, Lee JC.** *Acinetobacter baumannii* invades epithelial cells and outer membrane protein A mediates interactions with epithelial cells. BMC Microbiol. 2008 8:216.
- **Cirioni O, Silvestri C, Ghiselli R, Orlando F, Riva A, Gabrielli E, Mocchegiani F, Cianforlini N, Trombettoni MM, Saba V, Scalise G, Giacometti A.** Therapeutic efficacy of buforin II and rifampin in a rat model of *Acinetobacter baumannii* sepsis. Crit Care Med. 2009 37(4):1403-7.
- **Clemmer KM, Bonomo RA, Rather PN.** Genetic analysis of surface motility in *Acinetobacter baumannii*. Microbiology. 2011 157(Pt 9):2534-44.
- **Collinet-Adler S, Castro CA, Ledonio CG, Bechtold JE, Tsukayama DT.** *Acinetobacter baumannii* is not associated with osteomyelitis in a rat model: a pilot study. Clin Orthop Relat Res. 2011 469(1):274-82.
- **Conlon JM, Ahmed E, Pal T, Sonnevend A.** Potent and rapid bactericidal action of alyteserin-1c and its [E4K] analog against multidrug-resistant strains of *Acinetobacter baumannii*. Peptides. 2010 31(10):1806-10.
- **Dai T, Tegos GP, Lu Z, Huang L, Zhiyentayev T, Franklin MJ, Baer DG, Hamblin MR.** Photodynamic therapy for *Acinetobacter baumannii* burn infections in mice. Antimicrob Agents Chemother. 2009 53(9):3929-34.
- **de Breij A, Dijkshoorn L, Lagendijk E, van der Meer J, Koster A, Bloemberg G, Wolterbeek R, van den Broek P, Nibbering P.** Do biofilm formation and interactions with human cells explain the clinical success of *Acinetobacter baumannii*? PLoS One. 2010 5(5):e10732.
- **de Breij A, Eveillard M, Dijkshoorn L, van den Broek PJ, Nibbering PH, Joly-Guillou ML.** Differences in *Acinetobacter baumannii* strains and host innate immune response determine morbidity and mortality in experimental pneumonia. PLoS One. 2012 7(2):e30673.
- **de Breij A, Gaddy J, van der Meer J, Koning R, Koster A, van den Broek P, Actis L, Nibbering P, Dijkshoorn L.** CsuA/BABCDE-dependent pili are not involved in the adherence of *Acinetobacter baumannii* ATCC19606(T) to human airway epithelial cells and their inflammatory response. Res Microbiol. 2009 160(3):213-8.
- **DeLeon K, Balldin F, Watters C, Hamood A, Griswold J, Sreedharan S, Rumbaugh KP.** Gallium maltolate treatment eradicates *Pseudomonas aeruginosa* infection in thermally injured mice. Antimicrob Agents Chemother. 2009 53(4):1331-7.
- **Diancourt L, Passet V, Nemec A, Dijkshoorn L, Brisse S.** The population structure of *Acinetobacter baumannii*: expanding multiresistant clones from an ancestral susceptible genetic pool. PLoS One. 2010 5(4):e10034.
- **DiGiandomenico A, Rao J, Goldberg JB.** Oral vaccination of BALB/c mice with *Salmonella enterica* serovar Typhimurium expressing *Pseudomonas aeruginosa* O antigen promotes increased survival in an acute fatal pneumonia model. Infect Immun. 2004 72(12):7012-21.
- **Dijkshoorn L, Nemec A, Seifert H.** An increasing threat in hospitals: multidrug-resistant *Acinetobacter baumannii*. Nat Rev Microbiol. 2007 5(12):939-51.
- **Dijkshoorn L, van Aken E, Shunburne L, van der Reijden TJ, Bernards AT, Nemec A, Towner KJ.** Prevalence of *Acinetobacter baumannii* and other *Acinetobacter* spp. in faecal samples from non-hospitalised individuals. Clin Microbiol Infect. 2005 11(4):329-32.
- **Di Nocera PP, Rocco F, Giannouli M, Triassi M, Zarrilli R.** Genome organization of epidemic *Acinetobacter baumannii* strains. BMC Microbiol. 2011 11:224.
- **Doughari HJ, Ndakidemi PA, Human IS, Benade S.** The ecology, biology and pathogenesis of

Acinetobacter spp.: an overview. Microbes Environ. 2011 26(2):101-12.

- **Dorsey CW, Tolmasky ME, Crosa JH, Actis LA.** Genetic organization of an *Acinetobacter baumannii* chromosomal region harbouring genes related to siderophore biosynthesis and transport. Microbiology. 2003 149(Pt 5):1227-38.
- **Dorsey CW, Tomaras AP, Connerly PL, Tolmasky ME, Crosa JH, Actis LA.** The siderophore-mediated iron acquisition systems of *Acinetobacter baumannii* ATCC 19606 and *Vibrio anguillarum* 775 are structurally and functionally related. Microbiology. 2004 150(Pt 11):3657-67.
- **Dudhani RV, Turnidge JD, Nation RL, Li J.** fAUC/MIC is the most predictive pharmacokinetic/pharmacodynamic index of colistin against *Acinetobacter baumannii* in murine thigh and lung infection models. J Antimicrob Chemother. 2010 65(9):1984-90.
- **Echenique JR, Arienti H, Tolmasky ME, Read RR, Staneloni RJ, Crosa JH, Actis LA.** Characterization of a high-affinity iron transport system in *Acinetobacter baumannii*. J Bacteriol. 1992 174(23):7670-9.
- **Eijkelkamp BA, Hassan KA, Paulsen IT, Brown MH.** Investigation of the human pathogen *Acinetobacter baumannii* under iron limiting conditions. BMC Genomics. 2011 12:126.
- **Eijkelkamp BA, Stroeher UH, Hassan KA, Papadimitrious MS, Paulsen IT, Brown MH.** Adherence and motility characteristics of clinical *Acinetobacter baumannii* isolates. FEMS Microbiol Lett. 2011 323(1):44-51.
- **Endimiani A, Hujer KM, Hujer AM, Bertschy I, Rossano A, Koch C, Gerber V, Francey T, Bonomo RA, Perreten V.** *Acinetobacter baumannii* isolates from pets and horses in Switzerland: molecular characterization and clinical data. J Antimicrob Chemother. 2011 66(10):2248-54.
- **Ercolini D, Russo F, Nasi A, Ferranti P, Villani F.** Mesophilic and psychrotrophic bacteria from meat and their spoilage potential *in vitro* and in beef. Appl Environ Microbiol. 2009 75(7):1990-2001.
- **Espinal P, Martí S, Vila J.** Effect of biofilm formation on the survival of *Acinetobacter baumannii* on dry surfaces. J Hosp Infect. 2012 80(1):56-60.
- **Eveillard M, Soltner C, Kempf M, Saint-André JP, Lemarié C, Randrianarivelo C, Seifert H, Wolff M, Joly-Guillou ML.** The virulence variability of different *Acinetobacter baumannii* strains in experimental pneumonia. J Infect. 2010 60(2):154-61.
- **Falagas ME, Karveli EA, Kelesidis I, Kelesidis T.** Community-acquired *Acinetobacter* infections. Eur J Clin Microbiol Infect Dis. 2007 26(12):857-68.
- **Falagas ME, Rafailidis PI.** Attributable mortality of *Acinetobacter baumannii*: no longer a controversial issue. Crit Care. 2007 11(3):134.
- **Falagas ME, Rafailidis PI.** Nephrotoxicity of colistin: new insight into an old antibiotic. Clin Infect Dis. 2009 48(12):1729-31.
- **Fattahian Y, Rasooli I, Mousavi Gargari SL, Rahbar MR, Darvish Alipour Astaneh S, Amani J.** Protection against *Acinetobacter baumannii* infection via its functional deprivation of biofilm associated protein (Bap). Microb Pathog. 2011 51(6):402-6.
- **Fournier PE, Vallenet D, Barbe V, Audic S, Ogata H, Poirel L, Richet H, Robert C, Mangenot S, Abergel C, Nordmann P, Weissenbach J, Raoult D, Claverie JM.** Comparative genomics of multidrug resistance in *Acinetobacter baumannii*. PLoS Genet. 2006 2(1):e7.
- **Fuchs R, Schäfer M, Geoffroy V, Meyer JM.** Siderotyping--a powerful tool for the characterization of pyoverdines. Curr Top Med Chem. 2001 1(1):31-57.
- **Gaddy JA, Actis LA.** Regulation of *Acinetobacter baumannii* biofilm formation. Future Microbiol. 2009 4(3):273-8.
- **Gaddy JA, Arivett BA, McConnell MJ, López-Rojas R, Pachón J, Actis LA.** Role of acinetobactin-mediated iron acquisition functions in the interaction of *Acinetobacter baumannii* strain ATCC 19606^T with human lung epithelial cells, *Galleria mellonella* caterpillars, and mice. Infect Immun. 2012 80(3):1015-24.
- **Gaddy JA, Tomaras AP, Actis LA.** The *Acinetobacter baumannii* 19606 OmpA protein plays a role in biofilm formation on abiotic surfaces and in the interaction of this pathogen with eukaryotic cells. Infect Immun. 2009 77(8):3150-60.
- **Gan HM, Lean SS, Suhaili Z, Thong KL, Yeo CC.** Genome Sequence of *Acinetobacter baumannii* AC12, a Polymyxin-Resistant Strain Isolated from Terengganu, Malaysia. J Bacteriol. 2012 194(21):5979-80.
- **Gao F, Wang Y, Liu YJ, Wu XM, Lv X, Gan YR, Song SD, Huang H.** Genome sequence of *Acinetobacter baumannii* MDR-TJ. J Bacteriol. 2011 193(9):2365-6.
- **García A, Salgado F, Solar H, González CL, Zemelman R, Oñate A.** Some immunological properties of lipopolysaccharide from *Acinetobacter baumannii*. J Med Microbiol. 1999 48(5):479-83.
- **García A, Solar H, González C, Zemelman R.** Effect of EDTA on the resistance of clinical isolates of *Acinetobacter baumannii* to the bactericidal activity of normal human serum. J Med Microbiol. 2000

49(11):1047-50.

- **Gennari M, Lombardi P.** Comparative characterization of *Acinetobacter* strains isolated from different foods and clinical sources. Zentralbl Bakteriol. 1993 279(4):553-64.
- **Girlich D, Poirel L, Nordmann P.** First isolation of the blaOXA-23 carbapenemase gene from an environmental *Acinetobacter baumannii* isolate. Antimicrob Agents Chemother. 2010 54(1):578-9.
- **Gohl O, Friedrich A, Hoppert M, Averhoff B.** The thin pili of *Acinetobacter* sp. strain BD413 mediate adhesion to biotic and abiotic surfaces. Appl Environ Microbiol. 2006 72(2):1394-401.
- **González RH, Dijkshoorn L, Van den Barselaar M, Nudel C.** Quorum sensing signal profile of *Acinetobacter* strains from nosocomial and environmental sources. Rev Argent Microbiol. 2009 41(2):73-8.
- **González RH, Nusblat A, Nudel BC.** Detection and characterization of quorum sensing signal molecules in *Acinetobacter* strains. Microbiol Res. 2001 155(4):271-7.
- **Gordon YJ, Romanowski EG, McDermott AM.** A review of antimicrobial peptides and their therapeutic potential as anti-infective drugs. Curr Eye Res. 2005 30(7):505-15.
- **Gospodarek E, Grzanka A, Dudziak Z, Domaniewski J.** Electron-microscopic observation of adherence of *Acinetobacter baumannii* to red blood cells. Acta Microbiol Pol. 1998;47(2):213-7.
- **Guardabassi L, Dalsgaard A, Olsen JE.** Phenotypic characterization and antibiotic resistance of *Acinetobacter* spp. isolated from aquatic sources. J Appl Microbiol. 1999 87(5):659-67.
- **Hamouda A, Findlay J, Al Hassan L, Amyes SG.** Epidemiology of *Acinetobacter baumannii* of animal origin. Int J Antimicrob Agents. 2011 38(4):314-8.
- **Han G, Martinez LR, Mihu MR, Friedman AJ, Friedman JM, Nosanchuk JD.** Nitric oxide releasing nanoparticles are therapeutic for *Staphylococcus aureus* abscesses in a murine model of infection. PLoS One. 2009 4(11):e7804.
- **Hansen LK, Brown M, Johnson D, Palme Ii DF, Love C, Darouiche R.** *In vivo* model of human pathogen infection and demonstration of efficacy by an antimicrobial pouch for pacing devices. Pacing Clin Electrophysiol. 2009 32(7):898-907.
- **Henrichsen J, Blom J.** Correlation between twitching motility and possession of polar fimbriae in *Acinetobacter calcoaceticus*. Acta Pathol Microbiol Scand B. 1975 83(2):103-15.
- **Hoa PT, Managaki S, Nakada N, Takada H, Shimizu A, Anh DH, Viet PH, Suzuki S.** Antibiotic contamination and occurrence of antibiotic-resistant bacteria in aquatic environments of northern Vietnam. Sci Total Environ. 2011 409(15):2894-901.
- **Hood MI, Jacobs AC, Sayood K, Dunman PM, Skaar EP.** *Acinetobacter baumannii* increases tolerance to antibiotics in response to monovalent cations. Antimicrob Agents Chemother. 2010 54(3):1029-41.
- **Hornsey M, Loman N, Wareham DW, Ellington MJ, Pallen MJ, Turton JF, Underwood A, Gaulton T, Thomas CP, Doumith M, Livermore DM, Woodford N.** Whole-genome comparison of two *Acinetobacter baumannii* isolates from a single patient, where resistance developed during tigecycline therapy. J Antimicrob Chemother. 2011 66(7):1499-503.
- **Hornsey M, Wareham DW.** *In vivo* efficacy of glycopeptide-colistin combination therapies in a *Galleria mellonella* model of *Acinetobacter baumannii* infection. Antimicrob Agents Chemother. 2011 55(7):3534-7.
- **Hostacká A.** Influence of some antibiotics on lipase and hydrophobicity of *Acinetobacter baumannii*. Cent Eur J Public Health. 2000 8(3):164-6.
- **Houang ET, Chu YW, Leung CM, Chu KY, Berlau J, Ng KC, Cheng AF.** Epidemiology and infection control implications of *Acinetobacter* spp. in Hong Kong. J Clin Microbiol. 2001 39(1):228-34.
- **Houhamdi L, Raoult D.** Experimental infection of human body lice with *Acinetobacter baumannii*. Am J Trop Med Hyg. 2006 74(4):526-31.
- **Huys G, Bartie K, Cnockaert M, Hoang Oanh DT, Phuong NT, Somsiri T, Chinabut S, Yusoff FM, Shariff M, Giacomini M, Teale A, Swings J.** Biodiversity of chloramphenicol-resistant mesophilic heterotrophs from Southeast Asian aquaculture environments. Res Microbiol. 2007 158(3):228-35.
- **Iacono M, Villa L, Fortini D, Bordoni R, Imperi F, Bonnal RJ, Sicheritz-Ponten T, De Bellis G, Visca P, Cassone A, Carattoli A.** Whole-genome pyrosequencing of an epidemic multidrug-resistant *Acinetobacter baumannii* strain belonging to the European clone II group. Antimicrob Agents Chemother. 2008 52(7):2616-25.
- **Iwashkiw JA, Seper A, Weber BS, Scott NE, Vinogradov E, Stratilo C, Reiz B, Cordwell SJ, Whittal R, Schild S, Feldman MF.** Identification of a general O-linked protein glycosylation system in *Acinetobacter baumannii* and its role in virulence and biofilm formation. PLoS Pathog. 2012 8(6):e1002758.
- **Jacobs AC, Hood I, Boyd KL, Olson PD, Morrison JM, Carson S, Sayood K, Iwen PC, Skaar EP, Dunman PM.** Inactivation of phospholipase D diminishes *Acinetobacter baumannii* pathogenesis. Infect Immun. 2010 78(5):1952-62.

- **Jacobs AC, Sayood K, Olmsted SB, Blanchard CE, Hinrichs S, Russell D, Dunman PM.** Characterization of the *Acinetobacter baumannii* growth phase-dependent and serum responsive transcriptomes. FEMS Immunol Med Microbiol. 2012 64(3):403-12.
- **Jander G, Rahme LG, Ausubel FM.** Positive correlation between virulence of *Pseudomonas aeruginosa* mutants in mice and insects. J Bacteriol. 2000 182(13):3843-45.
- **Jarrell KF, Kropinski AM.** The virulence of protease and cell surface mutants of *Pseudomonas aeruginosa* for the larvae of *Galleria mellonella*. J Invertebr Pathol. 1982 39(3):395-400.
- **Jawad A, Seifert H, Snelling AM, Heritage J, Hawkey PM.** Survival of *Acinetobacter baumannii* on dry surfaces: comparison of outbreak and sporadic isolates. J Clin Microbiol. 1998 36(7):1938-41.
- **Jenssen H, Hamill P, Hancock RE.** Peptide antimicrobial agents. Clin Microbiol Rev. 2006 19(3):491-511.
- **Joly-Guillou ML.** Clinical impact and pathogenicity of *Acinetobacter*. Clin Microbiol Infect. 2005 11(11):868-73.
- **Jyothisri K, Deepak V, Rajeswari MR.** Purification and characterization of a major 40 kDa outer membrane protein of *Acinetobacter baumannii*. FEBS Lett. 1999 22;443(1):57-60.
- **Karah N, Sundsfjord A, Towner K, Samuelsen O.** Insights into the global molecular epidemiology of carbapenem non-susceptible clones of *Acinetobacter baumannii*. Drug Resist Updat. 2012 Jul 26. [Epub ahead of print]
- **Kempf M, Abdissa A, Diatta G, Trape JF, Angelakis E, Mediannikov O, La Scola B, Raoult D.** Detection of *Acinetobacter baumannii* in human head and body lice from Ethiopia and identification of new genotypes. Int J Infect Dis. 2012 16(9):e680-3.
- **Kempf M, Eveillard M, Deshayes C, Ghamrawi S, Lefrançois C, Georgeault S, Bastiat G, Seifert H, Joly-Guillou ML.** Cell surface properties of two differently virulent strains of *Acinetobacter baumannii* isolated from a patient. Can J Microbiol. 2012 58(3):311-7.
- **Kempf M, Rolain JM.** Emergence of resistance to carbapenems in *Acinetobacter baumannii* in Europe: clinical impact and therapeutic options. Int J Antimicrob Agents. 2012 39(2):105-14.
- **Kim SA, Yoo SM, Hyun SH, Choi CH, Yang SY, Kim HJ, Jang BC, Suh SI, Lee JC.** Global gene expression patterns and induction of innate immune response in human laryngeal epithelial cells in response to *Acinetobacter baumannii* outer membrane protein A. FEMS Immunol Med Microbiol. 2008 54(1):45-52.
- **Kim SW, Choi CH, Moon DC, Jin JS, Lee JH, Shin JH, Kim JM, Lee YC, Seol SY, Cho DT, Lee JC.** Serum resistance of *Acinetobacter baumannii* through the binding of factor H to outer membrane proteins. FEMS Microbiol Lett. 2009 301(2):224-31.
- **King LB, Swiatlo E, Swiatlo A, McDaniel LS.** Serum resistance and biofilm formation in clinical isolates of *Acinetobacter baumannii*. FEMS Immunol Med Microbiol. 2009 55(3):414-21.
- **Kintz E, Scarff JM, DiGiandomenico A, Goldberg JB.** Lipopolysaccharide O-antigen chain length regulation in *Pseudomonas aeruginosa* serogroup O11 strain PA103. J Bacteriol. 2008 190(8):2709-16.
- **Knapp S, Wieland CW, Florquin S, Pantophlet R, Dijkshoorn L, Tshimbalanga N, Akira S, van der Poll T.** Differential roles of CD14 and toll-like receptors 4 and 2 in murine *Acinetobacter* pneumonia. Am J Respir Crit Care Med. 2006 173(1):122-9.
- **Koeleman JG, van der Bijl MW, Stoof J, Vandenbroucke-Grauls CM, Savelkoul PH.** Antibiotic resistance is a major risk factor for epidemic behavior of *Acinetobacter baumannii*. Infect Control Hosp Epidemiol. 2001 22(5):284-8.
- **Kõljalg S, Vuopio-Varkila J, Lyytikäinen O, Mikelsaar M, Wadström T.** Cell surface properties of *Acinetobacter baumannii*. APMIS. 1996 104(9):659-65.
- **La Scola, B and Raoult D.** *Acinetobacter baumannii* in human body louse. Emerg. Infect. Dis. 2004 10:1671–1673.
- **Lai MJ, Lin NT, Hu A, Soo PC, Chen LK, Chen LH, Chang KC.** Antibacterial activity of *Acinetobacter baumannii* phage ϕAB2 endolysin (LysAB2) against both gram-positive and gram-negative bacteria. Appl Microbiol Biotechnol. 2011 90(2):529-39.
- **Lee JC, Koerten H, van den Broek P, Beekhuizen H, Wolterbeek R, van den Barselaar M, van der Reijden T, van der Meer J, van de Gevel J, Dijkshoorn L.** Adherence of *Acinetobacter baumannii* strains to human bronchial epithelial cells. Res Microbiol. 2006 157(4):360-6.
- **Lee JS, Choi CH, Kim JW, Lee JC.** *Acinetobacter baumannii* outer membrane protein A induces dendritic cell death through mitochondrial targeting. J Microbiol. 2010 48(3):387-92.
- **Liu S, Wang Y, Xu J, Li Y, Guo J, Ke Y, Yuan X, Wang L, Du X, Wang Z, Huang L, Zhang N, Chen Z.** Genome Sequence of an OXA23-Producing, Carbapenem-Resistant *Acinetobacter baumannii* Strain of Sequence Type ST75. J Bacteriol. 2012 194(21):6000-1.
- **Loehfelm TW, Luke NR, Campagnari AA.** Identification and characterization of an *Acinetobacter baumannii* biofilm-associated protein. J Bacteriol. 2008 190(3):1036-44.

- **López-Rojas R, Docobo-Pérez F, Pachón-Ibáñez ME, de la Torre BG, Fernández-Reyes M, March C, Bengoechea JA, Andreu D, Rivas L, Pachón J.** Efficacy of cecropin A-melittin peptides on a sepsis model of infection by pan-resistant *Acinetobacter baumannii*. Eur J Clin Microbiol Infect Dis. 2011 30(11):1391-8.
- **Luke NR, Sauberan SL, Russo TA, Beanan JM, Olson R, Loehfelm TW, Cox AD, St Michael F, Vinogradov EV, Campagnari AA.** Identification and characterization of a glycosyltransferase involved in *Acinetobacter baumannii* lipopolysaccharide core biosynthesis. Infect Immun. 2010 78(5):2017-23.
- **Luo G, Lin L, Ibrahim AS, Baquir B, Pantapalangkoor P, Bonomo RA, Doi Y, Adams MD, Russo TA, Spellberg B.** Active and passive immunization protects against lethal, extreme drug resistant-*Acinetobacter baumannii* infection. PLoS One. 2012 7(1):e29446.
- **Luo G, Spellberg B, Gebremariam T, Bolaris M, Lee H, Fu Y, French SW, Ibrahim AS.** Diabetic murine models for *Acinetobacter baumannii* infection. J Antimicrob Chemother. 2012 67(6):1439-45.
- **Martí S, Nait Chabane Y, Alexandre S, Coquet L, Vila J, Jouenne T, Dé E.** Growth of *Acinetobacter baumannii* in pellicle enhanced the expression of potential virulence factors. PLoS One. 2011;6(10):e26030.
- **Martí S, Sánchez-Céspedes J, Oliveira E, Bellido D, Giralt E, Vila J.** Proteomic analysis of a fraction enriched in cell envelope proteins of *Acinetobacter baumannii*. Proteomics. 2006 6 Suppl 1:S82-7.
- **Matsuzaki S, Rashel M, Uchiyama J, Sakurai S, Ujihara T, Kuroda M, Ikeuchi M, Tani T, Fujieda M, Wakiguchi H, Imai S.** Bacteriophage therapy: a revitalized therapy against bacterial infectious diseases. J Infect Chemother. 2005 11(5):211-9.
- **McConnell MJ, Domínguez-Herrera J, Smani Y, López-Rojas R, Docobo-Pérez F, Pachón J.** Vaccination with outer membrane complexes elicits rapid protective immunity to multidrug-resistant *Acinetobacter baumannii*. Infect Immun. 2011 79(1):518-26.
- **McConnell MJ, Pachón J.** Active and passive immunization against *Acinetobacter baumannii* using an inactivated whole cell vaccine. Vaccine. 2010 29(1):1-5.
- **McConnell MJ, Rumbo C, Bou G, Pachón J.** Outer membrane vesicles as an acellular vaccine against *Acinetobacter baumannii*. Vaccine. 2011 29(34):5705-10.
- **Mihara K, Tanabe T, Yamakawa Y, Funahashi T, Nakao H, Narimatsu S, Yamamoto S.** Identification and transcriptional organization of a gene cluster involved in biosynthesis and transport of acinetobactin, a siderophore produced by *Acinetobacter baumannii* ATCC 19606^T. Microbiology. 2004 150(Pt 8):2587-97.
- **Montero A, Ariza J, Corbella X, Doménech A, Cabellos C, Ayats J, Tubau F, Ardanuy C, Gudiol F.** Efficacy of colistin versus beta-lactams, aminoglycosides, and rifampin as monotherapy in a mouse model of pneumonia caused by multiresistant *Acinetobacter baumannii*. Antimicrob Agents Chemother. 2002 46(6):1946-52.
- **Murray CK, Yun HC, Griffith ME, Hospenthal DR, Tong MJ.** *Acinetobacter* infection: what was the true impact during the Vietnam conflict? Clin Infect Dis. 2006 43(3):383-4.
- **Nam HM, Lim SK, Kim JM, Joo YS, Jang KC, Jung SC.** *In vitro* activities of antimicrobials against six important species of gram-negative bacteria isolated from raw milk samples in Korea. Foodborne Pathog Dis. 2010 7(2):221-4.
- **Niu C, Clemmer KM, Bonomo RA, Rather PN.** Isolation and characterization of an autoinducer synthase from *Acinetobacter baumannii*. J Bacteriol. 2008 190(9):3386-92.
- **Nucleo E, Steffanoni L, Fugazza G, Migliavacca R, Giacobone E, Navarra A, Pagani L, Landini P.** Growth in glucose-based medium and exposure to subinhibitory concentrations of imipenem induce biofilm formation in a multidrug-resistant clinical isolate of *Acinetobacter baumannii*. BMC Microbiol. 2009 22 9:270.
- **Nwugo CC, Gaddy JA, Zimbler DL, Actis LA.** Deciphering the iron response in *Acinetobacter baumannii*: A proteomics approach. J Proteomics. 2011 74(1):44-58.
- **Obana Y.** Pathogenic significance of *Acinetobacter calcoaceticus*: analysis of experimental infection in mice. Microbiol Immunol. 1986 30(7):645-57.
- **Pachón-Ibáñez ME, Docobo-Pérez F, Jiménez-Mejias ME, Ibáñez-Martínez J, García-Curiel A, Pichardo C, Pachón J.** Efficacy of rifampin, in monotherapy and in combinations, in an experimental murine pneumonia model caused by panresistant *Acinetobacter baumannii* strains. Eur J Clin Microbiol Infect Dis. 2011 30(7):895-901.
- **Pantophlet R, Brade L, Dijkshoorn L, Brade H.** Specificity of rabbit antisera against lipopolysaccharide of *Acinetobacter*. J Clin Microbiol. 1998 36(5):1245-50.
- **Pantopoulou A, Giamarellos-Bourboulis EJ, Raftogannis M, Tsaganos T, Dontas I, Koutoukas P, Baziaka F, Giamarellou H, Perrea D.** Colistin offers prolonged survival in experimental infection by multidrug-resistant *Acinetobacter baumannii*: the significance of co-administration of rifampicin. Int J Antimicrob Agents. 2007 29(1):51-5.

- **Park JY, Kim S, Kim SM, Cha SH, Lim SK, Kim J.** Complete genome sequence of multidrug-resistant *Acinetobacter baumannii* strain 1656-2, which forms sturdy biofilm. J Bacteriol. 2011 193(22):6393-4.
- **Peleg AY, de Breij A, Adams MD, Cerqueira GM, Mocali S, Galardini M, Nibbering PH, Earl AM, Ward DV, Paterson DL, Seifert H, Dijkshoorn L.** The success of acinetobacter species; genetic, metabolic and virulence attributes. PLoS One. 2012 7(10):e46984.
- **Peleg AY, Jara S, Monga D, Eliopoulos GM, Moellering RC Jr, Mylonakis E.** *Galleria mellonella* as a model system to study *Acinetobacter baumannii* pathogenesis and therapeutics. Antimicrob Agents Chemother. 2009 53(6):2605-9.
- **Peleg AY, Seifert H, Paterson DL.** *Acinetobacter baumannii*: emergence of a successful pathogen. Clin Microbiol Rev. 2008 21(3):538-82.
- **Perez F, Hujer AM, Hujer KM, Decker BK, Rather PN, Bonomo RA.** Global challenge of multidrug-resistant *Acinetobacter baumannii*. Antimicrob Agents Chemother. 2007 51(10):3471-84.
- **Poirel L, Berçot B, Millemann Y, Bonnin RA, Pannaux G, Nordmann P.** Carbapenemase-producing *Acinetobacter* spp. in Cattle, France. Emerg Infect Dis. 2012 18(3):523-5.
- **Poirel L, Nordmann P.** Carbapenem resistance in *Acinetobacter baumannii*: mechanisms and epidemiology. Clin Microbiol Infect. 2006 12(9):826-36.
- **Pouëdras P, Gras S, Sire JM, Mesnard R, Donnio PY, Picard B, Avril JL.** Esterase electrophoresis compared with biotyping for epidemiological typing of *Acinetobacter baumannii* strains. FEMS Microbiol Lett. 1992 75(2-3):125-8.
- **Proft T, Baker EN.** Pili in Gram-negative and Gram-positive bacteria - structure, assembly and their role in disease. Cell Mol Life Sci. 2009 66(4):613-35.
- **Qiu H, Kuolee R, Harris G, Zhou H, Miller H, Patel GB, Chen W.** *Acinetobacter baumannii* infection inhibits airway eosinophilia and lung pathology in a mouse model of allergic asthma. PLoS One. 2011 6(7):e22004.
- **Ramirez MS, Adams MD, Bonomo RA, Centrón D, Tolmasky ME.** Genomic analysis of *Acinetobacter baumannii* A118 by comparison of optical maps: identification of structures related to its susceptibility phenotype. Antimicrob Agents Chemother. 2011 55(4):1520-6.
- **Rao RS, Karthika RU, Singh SP, Shashikala P, Kanungo R, Jayachandran S, Prashanth K.** Correlation between biofilm production and multiple drug resistance in imipenem resistant clinical isolates of *Acinetobacter baumannii*. Indian J Med Microbiol. 2008 26(4):333-7.
- **Rathinavelu S, Zavros Y, Merchant JL.** *Acinetobacter lwoffii* infection and gastritis. Microbes Infect. 2003 5(7):651-7.
- **Rodríguez-Baño J, Martí S, Soto S, Fernández-Cuenca F, Cisneros JM, Pachón J, Pascual A, Martínez-Martínez L, McQueary C, Actis LA, Vila J; Spanish Group for the Study of Nosocomial Infections (GEIH).** Biofilm formation in *Acinetobacter baumannii*: associated features and clinical implications. Clin Microbiol Infect. 2008 14(3):276-8.
- **Rodríguez-Hernández MJ, Jiménez-Mejias ME, Pichardo C, Cuberos L, García-Curiel A, Pachón J.** Colistin efficacy in an experimental model of *Acinetobacter baumannii* endocarditis. Clin Microbiol Infect. 2004 10(6):581-4.
- **Rokhbakhsh-Zamin F, Sachdev D, Kazemi-Pour N, Engineer A, Pardesi KR, Zinjarde S, Dhakephalkar PK, Chopade BA.** Characterization of plant-growth-promoting traits of *Acinetobacter* species isolated from rhizosphere of *Pennisetum glaucum*. J Microbiol Biotechnol. 2011 21(6):556-66.
- **Routsias JG, Karagounis P, Parvulesku G, Legakis NJ, Tsakris A.** *In vitro* bactericidal activity of human beta-defensin 2 against nosocomial strains. Peptides. 2010 31(9):1654-60.
- **Russo TA, Beanan JM, Olson R, MacDonald U, Luke NR, Gill SR, Campagnari AA.** Rat pneumonia and soft-tissue infection models for the study of *Acinetobacter baumannii* biology. Infect Immun. 2008 76(8):3577-86.
- **Russo TA, Luke NR, Beanan JM, Olson R, Sauberan SL, MacDonald U, Schultz LW, Umland TC, Campagnari AA.** The K1 capsular polysaccharide of *Acinetobacter baumannii* strain 307-0294 is a major virulence factor. Infect Immun. 2010 78(9):3993-4000.
- **Russo TA, MacDonald U, Beanan JM, Olson R, MacDonald IJ, Sauberan SL, Luke NR, Schultz LW, Umland TC.** Penicillin-binding protein 7/8 contributes to the survival of *Acinetobacter baumannii in vitro* and *in vivo*. J Infect Dis. 2009 199(4):513-21.
- **Russo TA, Page MG, Beanan JM, Olson R, Hujer AM, Hujer KM, Jacobs M, Bajaksouzian S, Endimiani A, Bonomo RA.** *In vivo* and *in vitro* activity of the siderophore monosulfactam BAL30072 against *Acinetobacter baumannii*. J Antimicrob Chemother. 2011 66(4):867-73.
- **Sahl JW, Johnson JK, Harris AD, Phillippy AM, Hsiao WW, Thom KA, Rasko DA.** Genomic comparison of multi-drug resistant invasive and colonizing *Acinetobacter baumannii* isolated from diverse human body sites reveals genomic plasticity. BMC Genomics. 2011 12:291.

- **Sechi LA, Karadenizli A, Deriu A, Zanetti S, Kolayli F, Balikci E, Vahaboglu H.** PER-1 type beta-lactamase production in *Acinetobacter baumannii* is related to cell adhesion. Med Sci Monit. 2004 10(6):BR180-4.
- **Sengstock DM, Thyagarajan R, Apalara J, Mira A, Chopra T, Kaye KS.** Multidrug-resistant *Acinetobacter baumannii*: an emerging pathogen among older adults in community hospitals and nursing homes. Clin Infect Dis. 2010 50(12):1611-6.
- **Shankar R, He LK, Szilagyi A, Muthu K, Gamelli RL, Filutowicz M, Wendt JL, Suzuki H, Dominguez M.** A novel antibacterial gene transfer treatment for multidrug-resistant *Acinetobacter baumannii*-induced burn sepsis. J Burn Care Res. 2007 28(1):6-12.
- **Sheahan KL, Cordero CL, Satchell KJ.** Identification of a domain within the multifunctional *Vibrio cholerae* RTX toxin that covalently cross-links actin. Proc Natl Acad Sci U S A. 2004 101(26):9798-803.
- **Shin JH, Lee HW, Kim SM, Kim J.** Proteomic analysis of *Acinetobacter baumannii* in biofilm and planktonic growth mode. J Microbiol. 2009 47(6):728-35.
- **Smith MG, Gianoulis TA, Pukatzki S, Mekalanos JJ, Ornston LN, Gerstein M, Snyder M.** New insights into *Acinetobacter baumannii* pathogenesis revealed by high-density pyrosequencing and transposon mutagenesis. Genes Dev. 2007 21(5):601-14.
- **Snitkin ES, Zelazny AM, Montero CI, Stock F, Mijares L; NISC Comparative Sequence Program, Murray PR, Segre JA.** Genome-wide recombination drives diversification of epidemic strains of *Acinetobacter baumannii*. Proc Natl Acad Sci U S A. 2011 108(33):13758-63.
- **Talbot GH, Bradley J, Edwards JE Jr, Gilbert D, Scheld M, Bartlett JG; Antimicrobial Availability Task Force of the Infectious Diseases Society of America.** Bad bugs need drugs: an update on the development pipeline from the Antimicrobial Availability Task Force of the Infectious Diseases Society of America. Clin Infect Dis. 200642(5):657-68.
- **Thomas-Virnig CL, Centanni JM, Johnston CE, He LK, Schlosser SJ, Van Winkle KF, Chen R, Gibson AL, Szilagyi A, Li L, Shankar R, Allen-Hoffmann BL.** Inhibition of multidrug-resistant *Acinetobacter baumannii* by nonviral expression of hCAP-18 in a bioengineered human skin tissue. Mol Ther. 2009 17(3):562-9.
- **Tomaras AP, Dorsey CW, Edelmann RE, Actis LA.** Attachment to and biofilm formation on abiotic surfaces by *Acinetobacter baumannii*: involvement of a novel chaperone-usher pili assembly system. Microbiology. 2003 149(Pt 12):3473-84.
- **Tomaras AP, Flagler MJ, Dorsey CW, Gaddy JA, Actis LA.** Characterization of a two-component regulatory system from *Acinetobacter baumannii* that controls biofilm formation and cellular morphology. Microbiology. 2008 154(Pt11):3398-409.
- **Towner KJ.** Acinetobacter: an old friend, but a new enemy. J Hosp Infect. 2009 73(4):355-63.
- **Vallenet D, Nordmann P, Barbe V, Poirel L, Mangenot S, Bataille E, Dossat C, Gas S, Kreimeyer A, Lenoble P, Oztas S, Poulain J, Segurens B, Robert C, Abergel C, Claverie JM, Raoult D, Médigue C, Weissenbach J, Cruveiller S.** Comparative analysis of Acinetobacters: three genomes for three lifestyles. PLoS One. 2008 19;3(3):e1805.
- **Vidal R, Dominguez M, Urrutia H, Bello H, Gonzalez G, Garcia A, Zemelman R.** Biofilm formation by *Acinetobacter baumannii*. Microbios. 1996 86(346):49-58.
- **Vogel H, Altincicek B, Glöckner G, Vilcinskas A.** A comprehensive transcriptome and immune-gene repertoire of the lepidopteran model host *Galleria mellonella*. BMC Genomics. 2011 12:308.
- **Wand ME, Bock LJ, Turton JF, Nugent PG, Sutton JM.** *Acinetobacter baumannii* virulence is enhanced in *Galleria mellonella* following biofilm adaptation. J Med Microbiol. 2012 61(Pt 4):470-7.
- **Wendt C, Dietze B, Dietz E, Rüden H.** Survival of *Acinetobacter baumannii* on dry surfaces. J Clin Microbiol. 1997 35(6):1394-7.
- **Wisplinghoff H, Perbix W, Seifert H.** Risk factors for nosocomial bloodstream infections due to *Acinetobacter baumannii*: a case-control study of adult burn patients. Clin Infect Dis. 1999 28(1):59-66.
- **Yamamoto S, Okujo N, Sakakibara Y.** Isolation and structure elucidation of acinetobactin, a novel siderophore from *Acinetobacter baumannii*. Arch Microbiol. 1994 162(4):249-54.
- **Yun SH, Choi CW, Kwon SO, Park GW, Cho K, Kwon KH, Kim JY, Yoo JS, Lee JC, Choi JS, Kim S, Kim SI.** Quantitative proteomic analysis of cell wall and plasma membrane fractions from multidrug-resistant *Acinetobacter baumannii*. J Proteome Res. 2011 10(2):459-69.
- **Zarrilli R, Giannouli M, Rocco F, Loman NJ, Haines AS, Constantinidou C, Pallen MJ, Triassi M, Di Nocera PP.** Genome sequences of three *Acinetobacter baumannii* strains assigned to the multilocus sequence typing genotypes ST2, ST25, and ST78. J Bacteriol. 2011 193(9):2359-60.
- **Zeana C, Larson E, Sahni J, Bayuga SJ, Wu F, Della-Latta P.** The epidemiology of multidrug-resistant *Acinetobacter baumannii*: does the community represent a reservoir? Infect Control Hosp Epidemiol. 2003 4(4):275-9.

- **Zimbler DL, Penwell WF, Gaddy JA, Menke SM, Tomaras AP, Connerly PL, Actis LA.** Iron acquisition functions expressed by the human pathogen *Acinetobacter baumannii*. Biometals. 2009 22(1):23-32.
- **Zhou H, Zhang T, Yu D, Pi B, Yang Q, Zhou J, Hu S, Yu Y.** Genomic analysis of the multidrug-resistant *Acinetobacter baumannii* strain MDR-ZJ06 widely spread in China. Antimicrob Agents Chemother. 2011 55(10):4506-12.
- **Zordan S, Prenger-Berninghoff E, Weiss R, van der Reijden T, van den Broek P, Baljer G, Dijkshoorn L.** Multidrug-resistant *Acinetobacter baumannii* in veterinary clinics, Germany. Emerg Infect Dis. 2011 17(9):1751-4.
- **Zurawski DV, Thompson MG, McQueary CN, Matalka MN, Sahl JW, Craft DW, Rasko DA.** Genome sequences of four divergent multidrug-resistant *Acinetobacter baumannii* strains isolated from patients with sepsis or osteomyelitis. J Bacteriol. 2012 194(6):1619-20.

Chapter 2

The genomics of *Acinetobacter baumannii*: insights into genome plasticity, antimicrobial resistance and pathogenicity

Francesco Imperi[1], Luísa C. S. Antunes[2], Jochen Blom[3], Laura Villa[4], Michele Iacono[5], Paolo Visca[2] and Alessandra Carattoli[4]

[1]Department of Biology and Biotechnology Charles Darwin, Sapienza University of Rome, Rome, Italy
[2]Department of Biology, University Roma Tre, Rome, Italy
[3]Computational Genomics, Center for Biotechnology (CeBiTec), Bielefeld University, Bielefeld, Germany
[4]Department of Infectious, Parasitic and Immune-Mediated Diseases, Istituto Superiore di Sanità, Rome, Italy
[5]Applied Science Roche Diagnostics, Monza, Italy

IUBMB Life 63 (2011): 1068-74

Abstract

Acinetobacter baumannii is an opportunistic nosocomial pathogen and many strains are multi- or pan-drug resistant. Numerous studies have addressed the mechanisms behind multidrug resistance in *A. baumannii*, but very little is known regarding its virulence traits and pathogenetic potential.

The chromosomal genome sequences of 12 *A. baumannii* strains were compared, including members of the international clones I and II, responsible for the majority of hospital outbreaks, sporadic isolates and a non-human isolate. A particular focus was placed on the conservation and distribution of antimicrobial resistance genes and putative virulence factors. The calculated species pan-genome was impressively large, due to a wide contribution of dispensable genes, and the number of genes was predicted to be increasing. A large part of the dispensable genes were antimicrobial resistance genes, which were probably acquired by horizontal gene transfer by individual strains. In contrast, strains belonging to international clones I and II did not acquire additional virulence factors to which their predominance could be attributed and were found to be mostly common to all strains.

This study corroborates the view that antimicrobial resistance is a major selective advantage that drives the expansion of *A. baumannii* epidemic clones and that virulence is likely combinatorial and multifactorial in this species, with no unique virulence factor being identified that could individually account for its pathogenic success.

IUBMB *Life*, 63(12): 1068–1074, December 2011

Critical Review

The Genomics of *Acinetobacter baumannii*: Insights into Genome Plasticity, Antimicrobial Resistance and Pathogenicity

Francesco Imperi[1], Luísa C.S. Antunes[2], Jochen Blom[3], Laura Villa[4], Michele Iacono[5], Paolo Visca[2] and Alessandra Carattoli[4]

[1]*Department of Biology and Biotechnology Charles Darwin, Sapienza University of Rome, Rome, Italy*
[2]*Department of Biology, University Roma Tre, Rome, Italy*
[3]*Computational Genomics, Center for Biotechnology (CeBiTec), Bielefeld University, Bielefeld, Germany*
[4]*Department of Infectious, Parasitic and Immune-Mediated Diseases, Istituto Superiore di Sanità, Rome, Italy*
[5]*Applied Science Roche Diagnostics, Monza, Italy*

Summary

The genome sequences of a number of *Acinetobacter baumannii* strains, including representatives of the main epidemic international lineages, have now been determined, and several others are in progress. The study of *A. baumannii* genomics has provided an expanded view of the adaptation and virulence capacities of this bacterial species, whilst also presenting novel insights into its intraspecies diversity and genome evolution. Genomic analyses have revealed that the current *A. baumannii* clinical population consists of low-grade pathogens, whose pathogenicity relies mainly on an ability to persist in the hospital setting and survive antibiotic treatment. *A. baumannii* has a high capacity to acquire new genetic determinants and displays an open pan genome; this feature may have played a crucial role in the evolution of this human opportunistic pathogen towards clinical success.

IUBMB *Life*, 63(12): 1068–1074, 2011

Keywords clonal complexes; comparative genomics; core genome; pan genome; singletons; virulence.

INTRODUCTION

Acinetobacter baumannii has emerged as an important opportunistic pathogen worldwide (*1*) and is responsible for large outbreaks of nosocomial infection, particularly in intensive care units. Since the 1980s, three main epidemic *A. baumannii* lineages, hereafter referred to as clonal complexes I, II, and III (CC1, CC2, and CC3, respectively), have spread worldwide and are responsible for the majority of hospital outbreaks caused by *A. baumannii* (*2–4*). These lineages are characterized by multidrug resistance (MDR), a phenotype that has expanded alarmingly over the years, with reports of *A. baumannii* strains resistant to almost all clinically relevant antibiotics (*5, 6*). However, limited information is available concerning the virulence and pathogenicity traits of this bacterium. *A. baumannii* is historically regarded as an opportunistic pathogen of low virulence, whose ability to cause diseases is determined by major deficiencies in the infected patient rather than any intrinsic pathogenicity of the infecting strain (*7*). Nevertheless, some *A. baumannii* infections are more important clinically than others (*7, 8*). This review describes genomic analyses designed to investigate the genetic determinants that may have played a crucial role in the evolution of this human opportunistic pathogen toward clinical success.

A. baumannii GENOMICS: AN HISTORICAL OVERVIEW

Eight completed and annotated genome sequences of *A. baumannii* are now available, and about 60 others are in progress (http://www.genomesonline.org; http://www.ncbi.nlm.nih.gov/genomeprj?term=acinetobacter%20baumannii). The first *A. baumannii* strain to be sequenced was ATCC 17978 (*9*). Comparison of the ATCC 17978 genome with that of strain ADP1, a member of the nonpathogenic soil-living species *Acinetobacter baylyi* (*10*), led to the recognition of 28 putative alien islands (pAs) in ATCC 17978, defined as genomic regions >10 kb in size, possibly acquired by horizontal gene transfer.

Received 8 June 2011; accepted 9 June 2011

Address correspondence to: Alessandra Carattoli, Viale Regina Elena 299, Rome 00161, Italy. Tel: +39-06-49903128. Fax: +39-06-49387112. E-mail: alecara@iss.it

M.I. is an employee of Roche Diagnostics SpA, Italy. This does not affect the author's adherence to all the IUBMB Life policies on sharing data and materials.

ISSN 1521-6543 print/ISSN 1521-6551 online
DOI: 10.1002/iub.531

Twelve pAs possess genes sharing homology with well-known virulence genes of other pathogenic bacteria, such as genes involved in drug resistance, motility, protein secretion, quorum sensing, and iron uptake (*9*). Moreover, 35 genes putatively involved in virulence were identified using a transposon mutagenesis approach in conjunction with the *Caenorhabditis elegans* nematode and *Dictyostelium discoideum* amoeba models of infection. However, most of these genes were predicted to encode transcriptional factors, transport systems, or proteins involved in main or indispensable cellular functions (e.g., DNA repair and general metabolic functions) (*9, 11*), which questions their specific contribution to *A. baumannii* pathogenicity.

Five more *A. baumannii* strains were sequenced in 2008, with four being representatives of either CC1 (AYE, AB0057, and AB307-0294) or CC2 (ACICU), while the remaining strain (SDF) is a fully drug-susceptible strain isolated from a human body louse (*11–13*). By comparing the genomes of the CC1 strain AYE, the nonhuman isolate SDF and the soil bacterium *A. baylyi* ADP1, several functions were identified that may account for strain adaptation to diverse ecological niches (*11*). In particular, an 86-kb resistance island (AbaR) containing several mobile genetic elements and genes for antibiotic and heavy metal resistance was exclusively present in the MDR clinical isolate AYE (*14*), suggesting a role of AbaR in the MDR phenotype and, therefore, in the capacity of *A. baumannii* to spread in the hospital setting (*11*). Several AbaR variants have been described, differing mainly in the number and nature of resistance genes and mobile genetic elements (*12, 13, 15–18*), indicating that *A. baumannii* is prone to accumulate resistance genes in specific genetic regions. Notably, AbaR is absent from ATCC 17978, isolated before the development of new generation antimicrobials (*9*).

Additional interesting dissimilarities between the AYE, SDF and *A. baylyi* genomes are the higher coding potential for catabolic functions of the clinical strain AYE and the presence of a number of putative pathogenicity determinants in its genome, likely involved in biofilm formation, motility, iron uptake, quorum sensing, and virulence factor production (*11*). It has been proposed that the association of SDF with human body lice was the result of lice ingestion of contaminated blood from an individual with undiagnosed *A. baumannii* bacteremia (*19*); however, the lack of so many virulence-related determinants in its genome, possibly caused by an impressively high number of insertion sequence elements (*11*), calls into question its status as a human pathogen.

Analysis of the CC2 representative strain ACICU, and its comparison with ATCC 17978 and *A. baylyi* ADP1, allowed the identification of additional horizontally acquired pAs, eight of them exclusive to ACICU (*12*). Some of these pAs are predicted to encode drug resistance functions, iron uptake systems, and virulence factors, suggesting a contribution of these regions to the clinical success of ACICU (*12*). Although an antibiotic resistance island has been identified in ACICU, this region lacks several of the resistance genes found in the AbaR region of AYE, and thus seems to be less important in conferring resistance to clinically important classes of antibiotics. However, the genome of ACICU harbored a higher number of predicted drug efflux systems per Mb of genome with respect to the antibiotic-susceptible ATCC 17978 and *A. baylyi* ADP1 (*12*), with carbapenem resistance being encoded by an OXA-58 class D β-lactamase (CHDL) located on the pACICU1 plasmid (*12*).

Subsequently, the whole genome sequences of *A. baumannii* MDR isolate AB0057 and the drug-susceptible isolate AB307-294, both belonging to CC1, as well as the partial genome sequence of the antibiotic-susceptible strain AB900 were determined (*13*). By comparing three MDR (AYE, ACICU, and AB0057) and three drug-susceptible *A. baumannii* isolates (ATCC 17978, AB307-294 and AB900), it was concluded that, although *A. baumannii* can use several strategies to evade antibiotic toxicity, inactivating enzymes rather than drug efflux systems play a crucial role in antibiotic resistance (*13*). In addition, 475 genes were identified that were common to all *A. baumannii* clinical strains but missing from the soil-living relative bacterium *A. baylyi* ADP1; of these, 279 (59%) had been lost by the nonhuman isolate SDF and may form part of the *A. baumannii* subgenome contributing to colonization of the human host (*13*). However, most of these genes encode functions related to transport, transcriptional regulation, metabolism, and general cellular processes, with the only exceptions being genes for an acyl homoserine lactone-based quorum sensing system (*20*), which however, does not affect *A. baumannii* pathogenicity in the *Galleria mellonella* insect model of infection (*21*), and a chaperone/usher pilus assembly apparatus that is involved in attachment to plastic surfaces and biofilm formation (*22*).

Two other complete genome sequences recently became available for MDR *A. baumannii* strains isolated from a case of bacteremia in Taiwan (*23*) and from a sputum specimen in Korea (*24*), plus four draft genome sequences for three MDR strains isolated in Italy (*25*) and a MDR strain isolated in China (*26*). To date, the specific features of these genomes have not been described in the literature.

GENERAL FEATURES OF THE *A. baumannii* GENOME: THE OPEN PAN GENOME

Twelve available *A. baumannii* chromosomal genome sequences were compared using the EDGAR software, available at http://edgar.cebitec.uni-bielefeld.de/ (*27*). Phylogenetic relationships were assessed on a genomic scale by comparing concatenated DNA sequences of orthologous protein coding sequences (CDSs) common to all sequenced chromosomal genomes (Fig. 1). The resulting phylogenetic tree had two main clusters, corresponding to CC1 (AYE, AB0057 and AB307-294) and CC2 (ACICU, 3990 and TCDC-AB0715), respectively. Notably, strains 1656-2 and MDR-TJ clustered with CC2 isolates, suggesting that these strains also belong to CC2, and this has been corroborated by the *in silico* determination of their MLST profiles (data not shown). The other genomes cluster in

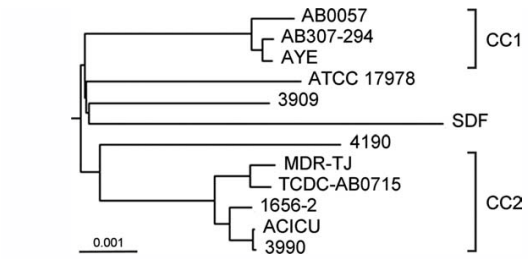

Figure 1. Phylogenetic relationship among *A. baumannii* isolates determined by aligning the concatenated CDSs common to all genomes by means of the comparative genomics tool EDGAR (*27*). The bar corresponds to the scale of sequence divergence. The tree has been generated using *Acinetobacter* sp. DR1 as an outgroup (not shown in the figure). Strains belonging to CC1 and CC2 are indicated on the right.

separate branches of the tree (Fig. 1), indicating that they are phylogenetically distant from clonal strains, in agreement with their assignment to distinct MLST types (*4, 25*).

The pan genome of a particular species represents its whole gene repertoire and corresponds to the sum of the core and dispensable genomes (*28–30*). The core genome includes genes that are present in all strains of a given species, while the dispensable genome includes genes that are absent in at least one strain, thus including functions that are not essential for bacterial growth, but which may confer selective advantages, such as adaptation to specific niches, stress resistance, and pathogenicity (*29, 31*). The analysis of the *A. baumannii* pan genome using the EDGAR comparative genomics tool (*27*) identified 8,818 CDSs, of which 1,455 are core genes while 7,363 are dispensable genes (Fig. 2A). Thus, the pan genome appears to be impressively large because of the contribution of a wide pool of dispensable genes. A high proportion of these dispensable genes (about 25%, corresponding to 1,860 CDSs) is unique to each strain, having no counterpart in any other *A. baumannii* genome, and is defined hereafter as singletons (Fig. 2B). As anticipated, the number of singletons is inversely correlated to the phylogenetic relatedness among the strains analyzed, being lower in strains sharing the same MLST type (Fig. 2B). In particular, strains 4190 and SDF contribute to the *A. baumannii* dispensable genome with the highest number of singletons (425 and 403 CDSs, respectively). While the singletons of SDF are mainly predicted to encode transposases or hypothetical proteins, mostly of phage origin, almost half (200 CDSs) of the strain 4190 singletons encode functionally categorized proteins (Fig. 2B). Strains ATCC 17978 and 3909 are also endowed with a significant number of functionally categorized singletons (93 and 58, respectively), whereas most singletons of the remaining strains correspond to hypothetical or phage-related proteins and strain-specific transposases (Fig. 2B).

Interestingly, the *A. baumannii* core genome appears to be relatively small, including on average <40% of the CDSs of each genome. However, if the 50-year-old isolate ATCC 17978 and the nonhuman isolate SDF are omitted, the size of the predicted core genome rises significantly to 2,406 CDSs (corresponding to about 65% of the average genome content; Fig. 2A). This is consistent with an analysis of the core genome and singleton development plots, which represent decay functions predicting the development of the number of core genes and singletons with an increasing number of genomes (*28*). Based on the 12 *A. baumannii* chromosomal genomes analyzed, the predicted number of core genes converges to 737 for an infinite number of sequenced genomes (Fig. 3A, left panel), while it converges to 2,201 if the same prediction is made on the basis of the 10 recent clinical strains, that is, excluding ATCC 17978 and SDF (Fig. 3A, right panel). Thus, for recent clinical isolates, the size of the predicted and calculated core genomes is similar (2,201 vs. 2,406).

In contrast, the singleton development plots predict a comparable number of additional singletons (142 or 164) putatively retrieved by future genome sequencing of other *A. baumannii*

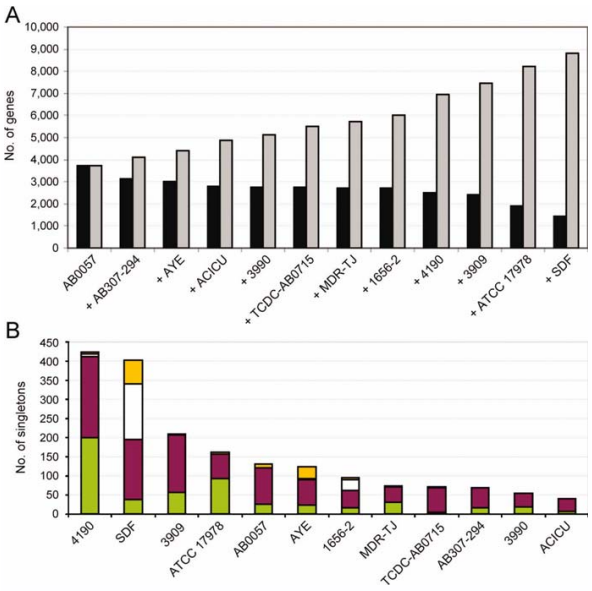

Figure 2. Estimates of the *A. baumannii* core genome, pan genome and singletons. (A) *A. baumannii* core and pan genomes (black and grey histograms, respectively) sequentially calculated from left to right on the basis of the 12 available genomes. (B) Number of singletons present in each genome. Singletons are classified according to the predicted function of the encoded protein: hypothetical proteins, purple; phage-related proteins, yellow; strain-specific transposases, white; other functionally-categorized proteins, green. [Color figure can be viewed in the online issue, which is available at wileyonlinelibrary.com.]

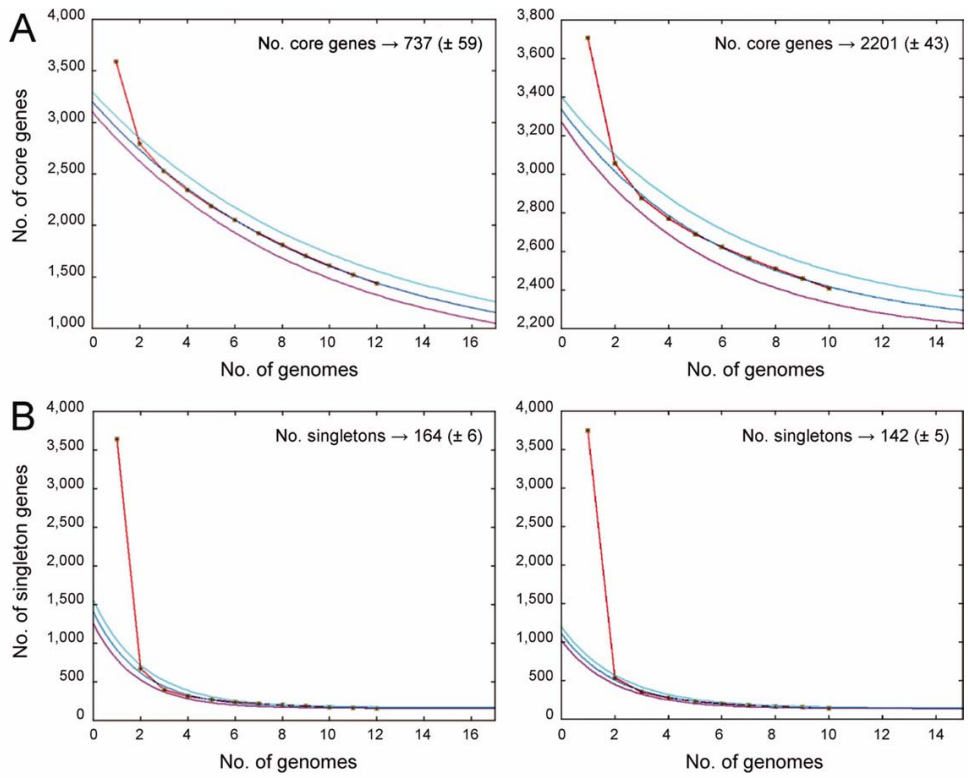

Figure 3. Development plots predicting (A) the size of the core genome and (B) the number of singletons with an increasing number of *A. baumannii* genomes. Predictions have been made considering either the 12 available genomes (left panels) or only the genomes of 10 clinical strains excluding ATCC 17978 and SDF (right panels). The red line shows the number of core/singleton genes as a function of the number of compared genomes. The mean values for all possible strain combinations of each respective genome count are taken. The dark-blue line shows a non-linear least squares curve fit of a exponential decay function to the data (*28*). The light-blue and purple lines show the upper and lower limit of a 95% confidence interval of the curve fit. The fitted models converge to the predicted number of core/singleton genes, which is shown into each panel. [Color figure can be viewed in the online issue, which is available at wileyonlinelibrary.com.]

strains, irrespective of the subset of available genomes used as template for the prediction (Fig. 3B). Such a high number of singletons reflect the propensity of *A. baumannii* to acquire exogenous genetic material and expand its dispensable genome, suggesting that the *A. baumannii* pan genome will increase rapidly in size as novel genome sequences become available. Such a genomic structure can be defined as an open pan genome, which is typical of bacterial species, such as streptococci and meningococci, which are able to colonize multiple environments and have multiple ways of exchanging genetic material (*29, 30, 31*). In species with an open pan genome, gene gain and loss can play a prominent role in the process of environmental niche and host adaptation, as well as in lifestyle changes (*29*). *A. baumannii* is generally described as a low-grade human pathogen. However, considering the propensity of the *A. baumannii* genome to exchange genetic material, and the persistence of this bacterium in the hospital setting where it could easily acquire virulence determinants from more pathogenic bacteria, it can reasonably be expected that *A. baumannii* could evolve toward enhanced pathogenicity. Indeed, cases of fulminant community-acquired *A. baumannii* pneumonia have been reported, suggesting that some *A. baumannii* strains may be of higher virulence than others (*7*), and this has also been observed in laboratory models of infection (*21, 32*).

THE CORE AND DISPOSABLE GENOMES OF *A. baumannii*: POSSIBLE ROLE IN ADAPTATION, DRUG RESISTANCE, AND VIRULENCE

The core genome of the current nosocomial population of *A. baumannii* is predicted to include about 2,200 CDSs, corresponding to 91.5% of the core genes retrieved by the analysis of the available genomes from current clinical strains (Figs. 2 and 3). Most (>65%) of the core genome of *A. baumannii* clinical isolates is responsible for metabolic and general cellular

processes, while a significant fraction (about 22%) encodes hypothetical proteins whose function cannot be inferred based on the predicted amino acid sequence. Other relevant functions putatively encoded by core genes are (i) adhesion and motility, (ii) cell–cell and environmental sensing, and (iii) iron metabolism, and (iv) drug resistance, together accounting for about 8% of the calculated core genome. Putative drug-resistance determinants include several drug-modification enzymes and a number of efflux systems predicted to be involved in xenobiotic and heavy metal extrusion. This gene repertoire is plausibly involved in the intrinsic level of *A. baumannii* drug resistance, while the specific drug resistance accessory genes differentially distributed among strains account for acquired resistance to particular antimicrobial classes (*13*). However, as antibiotic resistance is often associated with overexpression of intrinsic efflux pumps rather than acquisition of new transporters (*33*), it is possible that core efflux systems may contribute to the acquired multidrug resistance of *A. baumannii*.

With regard to iron uptake, the *A. baumannii* core genome potentially encodes two endogenous siderophores, a ferrous iron importer, and a system for heme acquisition (*34*). Interestingly, the outer membrane receptor genes of these clusters are highly divergent among strains, suggesting that these loci may be subject to strong selective pressure, as previously reported for other outer membrane receptors involved in iron uptake (*35*). The contribution of the disposable genome to iron uptake seems to be limited to a second heme uptake cluster shared by six of 12 sequenced genomes (*34*), a siderophore cluster unique to ATCC 17978 (*34, 36*), and a plethora of outer membrane receptor genes for the acquisition of exogenous iron chelators, which are distributed differentially among strains.

The core genome of *A. baumannii* clinical strains also encodes cell surface structures involved in adhesion and motility, such as two different kinds of fimbriae (σ and γ_4) and a type IV pilus apparatus. In *A. baumannii*, σ fimbriae play a role in attachment to abiotic surfaces and biofilm formation (*22*), while type IV pili are responsible for twitching motility (*37*). The quorum sensing system described previously is also shared by all clinical strains analyzed and is important for biofilm formation (*20*) and perhaps the regulation of other virulence factors. In addition, clinical *A. baumannii* strains potentially code for a urease and several secreted phospholipase- and hemolysin-like proteins, with phospolipase and hemolytic activities having been detected in culture supernatants of different *A. baumannii* strains (P. Visca, unpublished results). Notably, almost all the putative pathogenic factors encoded by the core genome of current clinical strains are also present in the ATCC 17978 genome, suggesting that the core genome of *A. baumannii* has not increased its virulence potential significantly over the past 50 years.

In an attempt to assess the contribution of the dispensable genome to the spread and success of the two major epidemic lineages of *A. baumannii*, the subsets of genes common to either the CC1 or CC2 core genomes were compared to the gene content of two clinical isolates (3909 and 4190) which do not belong to an epidemic lineage. This analysis identified 115 presumptive unique CDSs in CC1 and 105 presumptive unique CDSs in CC2, with 21 CDSs common to both epidemic lineages, but absent in nonepidemic isolates (Fig. 4). About 50% of these CDSs encode hypothetical proteins, with the remaining singletons mainly encoding functions related to metabolism, transcriptional regulation, environmental sensing, adhesion, and nutrient transport. No functions directly related to pathogenicity are present among either CC1 and CC2 singletons or CDSs common to both the CC1 and CC2 lineages.

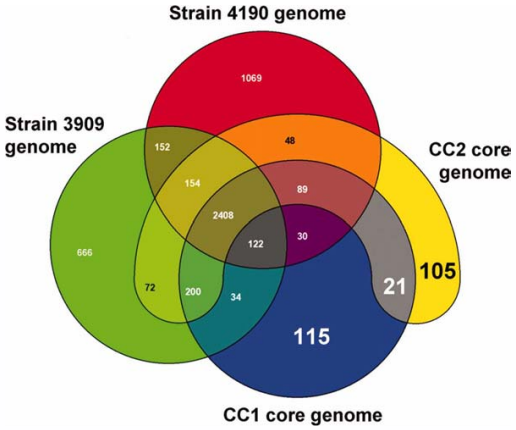

Figure 4. Calculation of putative genes unique to *A. baumannii* strains belonging to the CC1 or CC2. The Venn diagram, generated by EDGAR, shows the number of orthologous genes between the *A. baumannii* strains 3909 and 4190, and two core genomes calculated for either the CC1 strains (AB0057, AB307-294, AYE) or the CC2 strains (ACICU, 3990, TCDC-AB0715, MDR-TJ, 1656-2). Numbers of CDSs unique to the CC1 and CC2 core genomes, or exclusively present in both CC1 and CC2 are in a larger font size. [Color figure can be viewed in the online issue, which is available at wileyonlinelibrary.com.]

CONCLUDING REMARKS

A. baumannii has developed three basic properties to perfectly adapt to current healthcare settings: (i) widespread resistance to antimicrobial agents; (ii) ability to colonize skin, plastic intravascular devices and mucous membranes and to survive in the hospital environment; and (iii) survival in and on the human host. Circumstantial evidence has suggested that antimicrobial resistance is the major selective advantage that drives the ongoing rapid expansion of particular highly problematic clonal lineages (*4*). Genomic analysis has confirmed this hypothesis, highlighting the fact that drug resistance determinants can account for the increased pathogenicity of outbreak and epidemic lineages, while the importance of other genetic elements possibly related to pathogenicity is unclear (*9, 11–13*). Many putative virulence factors are shared by the majority of strains,

thus representing intrinsic pathogenicity determinants, but their specific contribution to the success of *A. baumannii* as a nosocomial human pathogen remains to be determined. Overall, genomic analysis confirms the multifactorial and combinatorial nature of *A. baumannii* virulence, with no unique virulence factor being identified which could individually account for the pathogenic success of this bacterium. However, it is important to emphasize that *A. baumannii* is endowed with an open pan genome, which appears to be prone to easily acquire new functions. The persistence of *A. baumannii* in the hospital setting, together with the strong selection pressure imposed by the use of antimicrobials in clinical practice, has promoted the evolution of the *A. baumannii* pan genome toward drug resistance, but the high plasticity of the *A. baumannii* genome also represents a favorable prerequisite for the acquisition of novel virulence traits, potentially transforming this opportunistic pathogen into an even greater threat to human health. Current *A. baumannii* clinical isolates probably represent a relatively homogenous population of strains that share a significant portion of their genome, while subpopulations of highly genotypically diverse strains exist both inside and outside the hospital environment. Deciphering the relevance and distribution of such atypical strains could potentially help to reconstruct the evolution of *A. baumannii* toward human pathogenicity.

ACKNOWLEDGEMENTS

L.C.S.A. was supported by a Ph.D. fellowship from the Portuguese Fundação para a Ciência e a Tecnologia (FCT; grant SFRH/BD/43420/2008). J.B. was supported by the German Federal Ministry of Education and Research (grant 0315599B "GenoMik-Transfer"). This study was partially supported by funds of the Italian Minister of Health to A.C.

REFERENCES

1. Dijkshoorn, L., Nemec, A., and Seifert, H. (2007) An increasing threat in hospitals: multidrug-resistant *Acinetobacter baumannii*. *Nat. Rev. Microbiol.* **5**, 939–951.
2. Nemec, A., Dijkshoorn, L., and van der Reijden, T. J. (2004) Long-term predominance of two pan-European clones among multi-resistant *Acinetobacter baumannii* strains in the Czech Republic. *J. Med. Microbiol.* **53**, 147–153.
3. van Dessel, H., Dijkshoorn, L., van der Reijden, T., Bakker, N., Paauw, A., et al. (2004) Identification of a new geographically widespread multiresistant *Acinetobacter baumannii* clone from European hospitals. *Res. Microbiol.* **155**, 105–112.
4. Diancourt, L., Passet, V., Nemec, A., Dijkshoorn, L., and Brisse, S. (2010) The population structure of *Acinetobacter baumannii*: expanding multiresistant clones from an ancestral susceptible genetic pool. *PLoS One* **7**, e10034.
5. Peleg, A. Y., Seifert, H., and Paterson, D. L. (2008) *Acinetobacter baumannii*: emergence of a successful pathogen. *Clin. Microbiol. Rev.* **21**, 538–582.
6. Towner, K. J. (2009) *Acinetobacter*: an old friend, but a new enemy. *J. Hosp. Infect.* **73**, 355–363.
7. Joly-Guillou, M. L. (2005) Clinical impact and pathogenicity of *Acinetobacter*. *Clin. Microbiol. Infect.* **11**, 868–873.
8. Perez, F., Endimiani, A., and Bonomo, R. A. (2008) Why are we afraid of *Acinetobacter baumannii? Expert Rev. Anti-Infect. Ther.* **6**, 269–271.
9. Smith, M. G., Gianoulis, T. A., Pukatzki, S., Mekalanos, J. J., Ornston, L. N., et al. (2007) New insights into *Acinetobacter baumannii* pathogenesis revealed by high-density pyrosequencing and transposon mutagenesis. *Gene Devel.* **21**, 601–614.
10. Barbe, V., Vallenet, D., Fonknechten, N., Kreimeyer, A., Oztas, S., et al. (2004) Unique features revealed by the genome sequence of *Acinetobacter* sp. ADP1, a versatile and naturally transformation competent bacterium. *Nucleic Acids Res.* **32**, 5766–5779.
11. Vallenet, D., Nordmann, P., Barbe, V., Poirel, L., Mangenot, S., et al. (2008) Comparative analysis of Acinetobacters: three genomes for three lifestyles. *PLoS One* **3**, e1805.
12. Iacono, M., Villa, L., Fortini, D., Bordoni, R., Imperi, F., et al. (2008) Whole-genome pyrosequencing of an epidemic multidrug-resistant *Acinetobacter baumannii* strain belonging to the European clone II group. *Antimicrob. Agents Chemother.* **52**, 2616–2625.
13. Adams, M. D., Goglin, K., Molyneaux, N., Hujer, K. M., Lavender, H., et al. (2008) Comparative genome sequence analysis of multidrug-resistant *Acinetobacter baumannii*. *J. Bacteriol.* **190**, 8053–8064.
14. Fournier, P. E., Vallenet, D., Barbe, V., Audic, S., Ogata, H., et al. (2006) Comparative genomics of multidrug resistance in *Acinetobacter baumannii*. *PLoS Genet.* **2**,e7.
15. Post, V., Hall, R. M. (2009) AbaR5, a large multiple-antibiotic resistance region found in *Acinetobacter baumannii*. *Antimicrob. Agents Chemother.* **53**, 2667–2671.
16. Adams, M. D., Chan, E. R., Molyneaux, N. D., and Bonomo, R. A. (2010) Genomewide analysis of divergence of antibiotic resistance determinants in closely related isolates of *Acinetobacter baumannii*. *Antimicrob. Agents Chemother.* **54**, 3569–3577.
17. Post, V., White, P. A., and Hall, R. M. (2010) Evolution of AbaR-type genomic resistance islands in multiply antibiotic-resistant *Acinetobacter baumannii*. *J. Antimicrob. Chemother.* **65**, 1162–1170.
18. Krizova, L. and Nemec, A. (2010) A 63 kb genomic resistance island found in a multidrug-resistant *Acinetobacter baumannii* isolate of European clone I from 1977. *J. Antimicrob. Chemother.* **65**, 1915–1918.
19. La Scola, B. and Raoult, D. (2004) *Acinetobacter baumannii* in human body louse. *Emerg. Infect. Dis.* **10**, 1671–1673.
20. Niu, C., Clemmer, K. M., Bonomo, R. A., and Rather, P. N. (2008) Isolation and characterization of an autoinducer synthase from *Acinetobacter baumannii*. *J. Bacteriol.* **190**, 3386–3392.
21. Peleg, A. Y., Jara, S., Monga, D., Eliopoulos, G. M., Moellering, R. C., et al. (2009) *Galleria mellonella* as a model system to study *Acinetobacter baumannii* pathogenesis and therapeutics. *Antimicrob. Agents Chemother.* **53**, 2605–2609.
22. Tomaras, A. P., Dorsey, C. W., Edelmann, R. E., and Actis, L. A. (2003) Attachment to and biofilm formation on abiotic surfaces by *Acinetobacter baumannii*: involvement of a novel chaperone-usher pili assembly system. *Microbiology* **149**, 3473–3484.
23. Chen, C. C., Lin, Y. C., Sheng, W. H., Chen, Y. C., Chang, S. C., et al. (2011) Genome sequence of a dominant multidrug-resistant *Acinetobacter baumannii* strain TCDC-AB0715. *J. Bacteriol.* **193,** 2361–2362.
24. Lee, H. W., Koh, Y. M., Kim, J., Lee, J. C., Lee, Y. C., et al. (2008) Capacity of multidrug-resistant clinical isolates of *Acinetobacter baumannii* to form biofilm and adhere to epithelial cell surfaces. *Clin. Microbiol. Infect.* **14**, 49–54.
25. Zarrilli, R., Giannouli, M., Rocco, F., Loman, N. J., Haines, A. S., et al. (2011) Genome sequences of three *Acinetobacter baumannii* strains assigned to ST2, ST25 and ST78 multilocus sequencing typing genotypes. *J. Bacteriol*., **193,** 2359–2360.
26. Gao, F., Wang, Y., Liu, Y. J., Wu, X. M., Lu, X., et al. (2011) Genome sequence of *Acinetobacter baumannii* MDR-TJ. *J. Bacteriol*., **193**, 2365–2366.

27. Blom, J., Albaum, S. P., Doppmeier, D., Puhler, A., Vorholter, F. J., et al. (2009) EDGAR: a software framework for the comparative analysis of prokaryotic genomes. *BMC Bioinformatics* **10**, 154.
28. Tettelin, H., Masignani, V., Cieslewicz, M. J., Donati, C., Medini, D., et al. (2005) Genome analysis of multiple pathogenic isolates of *Streptococcus agalactiae*: implications for the microbial "pan-genome". *Proc. Natl. Acad. Sci. USA* **102**, 13950–13955.
29. Medini, D., Donati, C., Tettelin, H., Masignani, V., and Rappuoli, R. (2005) The microbial pan-genome. *Curr. Opin. Genet. Dev.* **15**, 589–594.
30. Field, D., Wilson, G., and van der Gast, C. (2006) How do we compare hundreds of bacterial genomes? *Curr. Opin. Microbiol.* **9**, 499–504.
31. Schoen, C., Blom, J., Claus, H., Schramm-Glück, A., Brandt, P., et al. (2008) Whole-genome comparison of disease and carriage strains provides insights into virulence evolution in *Neisseria meningitidis*. *Proc. Natl. Acad. Sci. USA* **105**, 3473–3478.
32. Eveillard, M., Soltner, C., Kempf, M., Saint-Andre, J. P., Lemarie, C., et al. (2010) The virulence variability of different *Acinetobacter baumannii* strains in experimental pneumonia. *J. Infect.* **60**, 154–161.
33. Vila, J., Marti, S., and Sanchez-Cespedes, J. (2007) Porins, efflux pumps and multidrug resistance in *Acinetobacter baumannii*. *J. Antimicrob. Chemother.* **59**, 1210–1215.
34. Antunes, L. C. S., Imperi, F., Towner, K. J., and Visca, P. (2011) Genome-assisted identification of putative iron-utilization genes in *Acinetobacter baumannii* and their distribution among a genotypically diverse collection of clinical isolates. *Res. Microbiol.* **162**, 279–284.
35. Tümmler, B. and Cornelis, P. (2005) Pyoverdine receptor: a case of positive Darwinian selection in *Pseudomonas aeruginosa*. *J. Bacteriol.* **187**, 3289–3292.
36. Zimbler, D. L., Penwell, W. F., Gaddy, J. A., Menke, S. M., Tomaras, A. P., et al. (2009) Iron acquisition functions expressed by the human pathogen *Acinetobacter baumannii*. *Biometals* **22**, 23–32.
37. Jarrell, K. F. and McBride, M. J. (2008) The surprisingly diverse ways that prokaryotes move. *Nat. Rev. Microbiol.* **6**, 466–476.

Chapter 3

Deciphering the multifactorial nature of *Acinetobacter baumannii* pathogenicity

Luísa C. S. Antunes[1], Francesco Imperi[1], Alessandra Carattoli[2], and Paolo Visca[1]

[1]Department of Biology, University Roma Tre, Rome, Italy

[2]Department of Infectious, Parasitic and Immune-Mediated Diseases, Istituto Superiore di Sanità, Rome, Italy

PLoS One 6 (2011): e22674

Abstract

Acinetobacter baumannii is an opportunistic nosocomial pathogen involved in a broad range of severe infections and two multidrug-resistant clones are responsible for a large number of outbreaks worldwide. However, very little is known regarding the virulence factors and mechanisms behind *A. baumannii* infection.

In this chapter, four *A. baumannii* strains of different origin and pathogenic potential were compared for the presence of putative virulence genes and production of virulence factors, using a combinatorial approach of genomic and phenotypic analyses. All strains had the genomic potential for several putative virulence factors and each clinical strain expressed, to different levels, a combination of virulence-associated factors and pathogenicity mechanisms, including exoproducts with haemolytic, phospholipase, protease and iron-chelating activity, biofilm formation, surface motility, resistance to desiccation and ability to grow in human serum. Nevertheless, all clinical strains showed similar virulence in the *Galleria mellonella* insect model of infection.

Therefore, virulence of *A. baumannii* appears to be multifactorial, depending on the expression of a multiplicity of virulence factors that are expressed in different combinations between strains, but that result in apparently similar pathogenic potential. Differences in nosocomial predominance between strains are probably not related to differential expression of virulence factors, but rather to the resistance phenotype of individual strains.

OPEN ACCESS Freely available online

PLoS one

Deciphering the Multifactorial Nature of *Acinetobacter baumannii* Pathogenicity

Luísa C. S. Antunes[1], Francesco Imperi[1¤], Alessandra Carattoli[2], Paolo Visca[1]*

1 Department of Biology, University Roma Tre, Rome, Italy, **2** Department of Infectious, Parasitic and Immune-Mediated Diseases, Istituto Superiore di Sanità, Rome, Italy

Abstract

Background: *Acinetobacter baumannii* is an emerging bacterial pathogen that causes a broad array of infections, particularly in hospitalized patients. Many studies have focused on the epidemiology and antibiotic resistance of *A. baumannii*, but little is currently known with respect to its virulence potential.

Methodology/Principal Findings: The aim of this work was to analyze a number of virulence-related traits of four *A. baumannii* strains of different origin and clinical impact for which complete genome sequences were available, in order to tentatively identify novel determinants of *A. baumannii* pathogenicity. Clinical strains showed comparable virulence in the *Galleria mellonella* model of infection, irrespective of their status as outbreak or sporadic strains, whereas a non-human isolate was avirulent. A combined approach of genomic and phenotypic analyses led to the identification of several virulence factors, including exoproducts with hemolytic, phospholipase, protease and iron-chelating activities, as well as a number of multifactorial phenotypes, such as biofilm formation, surface motility and stress resistance, which were differentially expressed and could play a role in *A. baumannii* pathogenicity.

Conclusion/Significance: This work provides evidence of the multifactorial nature of *A. baumannii* virulence. While *A. baumannii* clinical isolates could represent a selected population of strains adapted to infect the human host, subpopulations of highly genotypically and phenotypically diverse *A. baumannii* strains may exist outside the hospital environment, whose relevance and distribution deserve further investigation.

Citation: Antunes LCS, Imperi F, Carattoli A, Visca P (2011) Deciphering the Multifactorial Nature of *Acinetobacter baumannii* Pathogenicity. PLoS ONE 6(8): e22674. doi:10.1371/journal.pone.0022674

Editor: Ben Adler, Monash University, Australia

Received February 8, 2011; **Accepted** June 29, 2011; **Published** August 1, 2011

Funding: The study was supported by a PhD fellowship to L.C.S.A. from the Portuguese Fundação para a Ciência e a Tecnologia (FCT) (grant SFRH/BD/43420/2008). The funders had no role in study design, data collection and analysis, decision to publish, or preparation of the manuscript.

Competing Interests: The authors have declared that no competing interests exist.

* E-mail: visca@uniroma3.it

¤ Current address: Department of Biology and Biotechnology Charles Darwin, Sapienza University of Rome, Rome, Italy

Introduction

Acinetobacter baumannii is an emerging human pathogen which causes a broad array of infections (e.g. pneumonia, urinary tract, bloodstream and skin infections) that account for about 10% of all nosocomial infections [1,2,3]. Since the 1980s, three main epidemic *A. baumannii* lineages, hereafter referred to as clonal complexes I, II and III (CC1, CC2 and CC3, respectively) have emerged and spread internationally throughout many geographical areas [4]. Both multi-locus sequence typing and comparative genomics analysis revealed that isolates belonging to the same CC are highly homogenous, suggestive of a recent clonal expansion [4,5]. These three lineages are characterized by multidrug resistance (MDR), a phenotype that has been expanding alarmingly over the years, with frequent reports of *A. baumannii* strains resistant to almost all clinically relevant antibiotics [6,7].

While the epidemiology and antibiotic resistance of *A. baumannii* strains has been extensively studied, limited information is so far available concerning the virulence and pathogenicity traits of this bacterium. Cohort and case-control clinical studies have shown that *A. baumannii* infections can be severe, and clinical observations have posed the question of the existence of a strain-dependent pathogenicity [8]. However, the molecular and genetic basis of *A. baumannii* virulence remains poorly understood, and only a few determinants have been demonstrated to be important for *A. baumannii* virulence *in vivo*. One of these is OmpA, an outer membrane protein which adheres to and is taken up by epithelial cells, where it can induce apoptosis [9]. OmpA is also implicated in resistance to complement and biofilm formation [10,11]. Recently, other proteins have also been proposed to contribute to *A. baumannii* virulence. A phospholipase D has been demonstrated to be important for resistance to human serum, epithelial cell invasion and pathogenesis in a murine model of pneumonia [12], while a phospholipase C has been shown to enhance toxicity to epithelial cells [13]. Moreover, a transposon mutant in a gene for penicillin binding protein 7/8 showed reduced virulence in rat pneumonia and soft-tissue models, as well as reduced serum resistance [14].

Several other factors have been investigated as potential determinants of *A. baumannii* pathogenicity, but their role has not yet been definitively ascertained. Capsular polysaccharide has been implicated in serum resistance since mutants in its biosynthetic pathway fail to survive in human serum [15]. The extracellular polysaccharide poly-β-(1–6)-N-acetyl glucosamine

(PNAG), synthesized by the *pgaABCD* locus, and the Csu pili play a role in biofilm formation [16,17], while a homologue of the staphylococcal biofilm-associated protein (Bap) is required for the development of mature biofilm structures [18]. Quorum sensing has been also shown to contribute to biofilm formation [19], but did not affect virulence in the *Galleria mellonella* insect model of infection [20]. In addition, some but not all *A. baumannii* isolates show gelatinase activity and cause mannose-resistance hemagglutination [21]. Moreover, different *A. baumannii* isolates display diverse resistance to desiccation [22], a feature that can influence persistence in the hospital environment.

Finally, bacterial pathogenicity is intimately linked to the ability to use specific iron acquisition strategies, which are essential for pathogen survival and growth in the low-iron environment of the human host [23]. In addition to the well-characterized siderophore acinetobactin [24], genome investigations have recently shown that *A. baumannii* has the potential to express several iron-acquisition systems, including two other siderophores, one shared by all *A. baumannii* strains sequenced to date, with the exception of SDF, while the other is so far unique to ATCC 17978, two heme-uptake systems and a ferrous iron acquisition [25,26].

The aim of the present work was to identify specific virulence determinant(s) that could contribute to the success of *A. baumannii* as a human pathogen, and to investigate whether the occurrence of such virulence determinants in representative strains of the two main clonal lineages, CC1 and CC2, could explain the increased ability of these lineages to cause infection and persist in the hospital setting. In this context, four *A. baumannii* strains of different origin (three clinical isolates and one isolate from a human body louse), belonging to diverse clonal complexes, whose genomes were completely sequenced and annotated, were comparatively analyzed by a combination of genome- and phenotype-based strategies. This led to the identification of a number of virulence factors that could contribute to the pathogenic potential of *A. baumannii*.

Materials and Methods

Ethics Statement

Serum was obtained from five healthy volunteers who gave their written informed consent to the study, which was approved by the Review Board of the Department of Biology of the University Roma Tre.

Bacterial strains and culture conditions

Bacterial strains used in this study were *A. baumannii* AYE, ACICU, ATCC 17978 and SDF, and *Pseudomonas aeruginosa* PAO1 (ATCC 15692). AYE strain is an epidemic multidrug-resistant clinical isolate responsible for a nationwide outbreak in France in 2001 [27]; ACICU is an epidemic multidrug-resistant clinical isolate responsible for an outbreak in Rome (Italy) in 2005 [28]; ATCC 17978 was isolated in 1951 from a 4-month-old infant with fatal meningitis, and differs from AYE and ACICU in being susceptible to most common antibiotics [29]; SDF is a fully antibiotic-susceptible strain isolated from a human body louse [27]. Since *A. baumannii* is rarely found on the human skin, it has been proposed that the association of SDF with a non-human host is the result of the louse's ingestion of contaminated blood from an individual with undiagnosed *A. baumannii* bacteremia [30]. Strains AYE and ACICU are phylogenetically grouped inside CC1 and CC2, respectively, whereas ATCC 17978 and SDF represent two discrete and less common lineages within the *A. baumannii* population [4]. No isolates belonging to the CC3 have been completely sequenced to date, and thus representatives of this clonal lineage were not included in this study.

Bacteria were cultured in Luria-Bertani broth (LB), minimal broth M9 with succinate as carbon source [31], Chelex 100-treated trypticase soy broth dialysate (TSBD) [32] and casamino acid medium supplemented with 0.4 mM $MgCl_2$ (CAA) [33]. When required, media were supplemented with either 50 μM 2,2′-dipyridyl or 50 μM $FeCl_3$ to generate low- and high-iron growth conditions, respectively.

G. mellonella killing assay

The *G. mellonella* virulence assay was performed as described previously [34], with minor modifications. *G. mellonella* caterpillars in the final instar larval stage (average weight 500±60 mg) were injected with 10 μl of serial ten-fold dilutions in saline solution of *A. baumannii* cells grown for 14 h at 37°C in TSBD. Bacterial colony counts on LB agar plates were used to estimate the number of viable cells in each inoculum. At least 20 larvae were inoculated per experiment, with a total of at least three dependent and three independent experiments per strain. Ten larvae per experiment were injected with 10 μl of sterile saline solution as a negative control. Larvae were incubated at 37°C in Petri dishes (five larvae per dish) and monitored for a three-day time period. Larvae were considered dead when they did not respond to gentle prodding [34]. When required, bacterial cells were heat-killed by incubation at 80°C for 60 min. Lethal dose 50% (LD_{50}) values were calculated using GraphPad Prism and the following equation: $Y = A+(1 - A)/[1+\exp(B - G\times\ln X)]$, where X is the number of viable bacterial cells injected, Y the fraction of larvae killed by the bacterial solution, A is the fraction of larvae killed by the control solution, and B and G are curve-fitting constants automatically calculated by GraphPad Prism [34]. LD_{50} was calculated as the value of X that corresponds to $Y = 0.5$.

Growth assays

Cells from overnight cultures in a given medium were normalized to an OD_{600} of 0.01 in the same medium and grown at 4, 25, 30, 37, 42, 45 or 50°C for 24 h with vigorous aeration (250 rpm). The culture cell density was determined every hour by measuring the OD_{600}. Maximum specific growth rates (μ_{max}) were determined by fitting growth data to a logistic growth curve using GraphPad Prism and the following equation: $Y = Y_M\times Y_0/((Y_M-Y_0)\times e^{-xk}+Y_0)$, where Y_0 and Y_M represent OD_{600} values at time points 0 and M, respectively, k is a constant calculated automatically by the program and x represents the time of growth (in hours). Each μ_{max} was calculated as the derivative of the equation for the time point of maximum growth. The coefficient of determination (R^2) was used to verify the goodness of fit of the data to the equation.

Resistance to iron starvation and production of iron-chelating compounds

Resistance to iron starvation was assessed on TSBD agar plates containing a linear gradient of the iron chelator 2,2′-dipyridyl, ranging from 0 to 500 μM, generated according to the agar gradient-plate technique [35]. *A. baumannii* strains were grown in TSBD at 37°C for 14 h and then inoculated with a sterile loop handle onto the plates, starting from the side with the highest concentration of the iron chelator. Plates were incubated at 37°C for 24 h.

Total iron-chelating activity and the amount of hydroxamate- and catechol-type groups were measured in filter-sterilized culture supernatants by the chrome azurol S (CAS) liquid assay [36], the Csàky assay as modified by Gillam [37] and the Arnow test [38], respectively.

Hemolytic activity assays

Hemolytic activity was assessed using both agar plate and liquid assays. For plate assays, bacterial cells were grown in TSBD at 37°C for 14 h, normalized to an OD_{600} of 1 in sterile saline, and 5 µl aliquots were spotted on Columbia agar plates (Biokar Diagnostics) supplemented with 5% sheep or horse defibrinated blood (OXOID). Plates were incubated at 37°C for 48 h.

Hemolytic activity in culture supernatants was determined by incubating filter-sterilized supernatants from bacterial cultures grown in TSBD for 14 h in the presence of 10% (final concentration) sheep or horse defibrinated blood, previously washed several times with sterile ice-cold phosphate-buffered saline (PBS), pH 7.4. After 3 h incubation at 37°C with gentle agitation, intact erythrocytes were harvested by centrifugation at 1000 g and 4°C for 20 min. The amount of hemoglobin released in supernatants was evaluated by measuring the OD_{545}. The percentage of hemolysis (P) was calculated using the equation $P = (X-B)/(T-B)\times 100$, and then normalized to the cell density (OD_{600}) of the bacterial culture. X is the OD_{545} of the sample analyzed, while B and T represent the baseline and total hemolysis, i.e. the OD_{545} obtained with sterile TSBD and deionized water instead of culture supernatant, respectively [39].

Phospholipase C activity assay

Extracellular phospholipase C activity was determined using the chromogenic substrate *p*-nitrophenylphosphorylcholine (PNPC) as described [40]. Briefly, 900 µl of a solution of 10 mM PNPC in 250 mM Tris-HCl, pH 7.2, 1 µM $ZnCl_2$, 60% glycerol was added to 100 µl of filter-sterilized supernatants from cultures grown for 14 h in TSBD. The reaction mixture was incubated at 37°C for 24 h and the OD_{405} was measured.

Proteolytic activity assay

Extracellular proteolytic activity was determined using the azoalbumin assay as previously described [41]. Briefly, 500 µl of a 1 mg/ml azoalbumin solution in Tris-HCl, pH 7.7, were added to 500 µl filter-sterilized supernatants from cultures grown in TSBD for 14 h, and then incubated at 37°C for 24 h. Trichloroacetic acid was added at 13% final concentration to precipitate the non-degraded protein. Samples were incubated at −20°C for 20 min, centrifuged at 15000 g for 10 min, and the OD_{440} of the resulting supernatants was measured.

Biofilm assay

Biofilm formation was measured according to the microtiter plate assay [42]. Bacterial cells were grown in TSBD for 14 h and normalized to an OD_{600} of 1.0. Aliquots of 100 µl were transferred to a sterile 96-well polystyrene microtiter plate (12 wells per strain) and incubated at 37°C for 24 h. Planktonic cells were removed and the attached cells were gently washed three times with sterile PBS, air dried, and stained with 0.1% crystal violet solution for 15 min. After washing the wells four times with distilled water, the surface-associated dye was solubilized by adding 200 µl of 95% ethanol to each well. The dye solutions from three wells were pooled and the OD_{540} was measured.

Surface motility assay

LB, CAA and TSBD plates containing 0.5% agarose were prepared and strains were stab-inoculated with a pipette tip to the bottom of the polystyrene Petri dish from bacterial colonies grown overnight in LB agar (1.5%) plates. The plates were closed tightly with parafilm to prevent drying and incubated at 37°C for 24 h. Swarming motility was observed at the air-agarose interface. Twitching motility was assessed by removing the agarose layer, staining the plates with a 0.1% crystal violet solution for 30 min, and measuring the diameter of the motility disk. A minimum of three independent experiments was performed.

Assay for resistance to human serum

Resistance to human serum was measured according to the protocol of Kim *et al.* [11]. In brief, bacterial cells grown in TSBD for 14 h were washed and resuspended in PBS to an OD_{600} of 1.0. Human serum from five healthy individuals was pooled together and diluted in PBS to a 40% final dilution. Heat-inactivated serum was prepared by incubating the same serum at 56°C for 30 min. Bacterial suspensions were then added to human serum or heat-inactivated serum to obtain a bacterial cell concentration of ca. 1×10^7 CFU/ml and samples were incubated at 37°C for 2 h. Viable counts were determined at 0 and 2 h time points, and three independent experiments were performed.

Assay for resistance to desiccation

Resistance to desiccation was measured according to the protocol of Jawad *et al.* [22]. Bacterial cells were grown in TSBD for 14 h, washed twice with PBS and resuspended in distilled water to an OD_{600} of 1. Twenty µl of each suspension (ca. 2×10^7 CFU) were deposited onto sterile 13 mm diameter rounded glass coverslips and placed in an uncovered petri dish in an airtight transparent plastic box (17 by 11 by 5.5 cm). The relative humidity inside the plastic boxes was maintained at 31% by the presence of a saturated salt solution of $CaCl_2$ in an open 5 ml beaker [22]. For viable cell determination, at each sampling time point the glass coverslips were vortexed vigorously for 15 s in 2 ml of sterile distilled water, the cells were harvested by centrifugation (2,000×g for 10 min), resuspended in 200 µl of saline solution and 100-µl aliquots of these suspensions (or of appropriate dilutions) were plated onto LB agar plates by the spread plate method. Three glass coverslips were analyzed for each sample. In case of samples containing <10 CFU/coverslip, the absence of viable cells attached to the coverslip was confirmed by placing the coverslip in 2 ml of LB medium. Bacterial growth was never observed after 48 h at 37°C and 250 rpm.

Statistical analysis

Statistical analysis was performed with the software GraphPad Instat, using One-Way Analysis of Variance (ANOVA) followed by Tukey-Kramer multiple comparison tests. Survival plots were generated by the Kaplan-Meier method and analyzed by the log-rank test. Differences having a P value <0.05 were considered to be statistically significant.

Results

Virulence in the *G. mellonella* model of infection

G. mellonella has recently been proposed as a simple and useful *in vivo* model to assess *A. baumannii* pathogenicity [20]. Accordingly, the *G. mellonella* model of infection was used to compare the virulence of *A. baumannii* strains AYE, ACICU, ATCC 17978 and SDF. A representative time-kill experiment is illustrated in Supporting Information (Fig. S1). The LD_{50} values were calculated for each strain at 24, 48 and 72 h post-infection (Table 1). For all strains, the LD_{50} values decreased with time of incubation, attaining the final value at 48 h. No killing was observed with heat-inactivated *A. baumannii* cells. No significant differences in virulence were observed between the epidemic strains AYE and ACICU and the non-epidemic strain ATCC 17978 ($P>0.05$), all three of which showed similar LD_{50} values

Table 1. *G. mellonella* killing by *A. baumannii* strains.

Strain	LD_{50} (± SEM) [a]		
	24 h	48 h	72 h
AYE	7.51 (±0.68)×10^5	2.01 (±0.05)×10^5	1.98 (±0.04)×10^5
ACICU	6.64 (±0.26)×10^5	5.58 (±0.09)×10^5	5.54 (±0.11)×10^5
ATCC 17978	3.92 (±0.10)×10^5	2.42 (±0.13)×10^5	2.38 (±0.12)×10^5
SDF [bc]	4.99 (±0.31)×10^7	4.84 (±0.06)×10^7	4.84 (±0.06)×10^7

[a]The LD_{50} values are expressed in CFU and were calculated as described in Materials and Methods after 24, 48 and 72 h of infection with *A. baumannii* cells. Values are the mean (± SEM) of at least three independent experiments and were inferred from a regression curve calculated from at least six different infecting inocula for each experiments.

[b]Since SDF causes insufficient killing of larvae for experimental determination of the LD_{50} even at the highest infecting dose (i.e. 4×10^7 CFU/larva), the reported LD_{50} is a theoretical estimate generated by GraphPad Prism.

[c]The difference between the LD_{50} values of SDF and those of clinical strains is statistically significant ($P<0.001$) at every time point.

doi:10.1371/journal.pone.0022674.t001

($2.0-5.5\times10^5$ CFU). These results are comparable to those obtained by Peleg *et al.* [20] for other clinical *A. baumannii* strains. In contrast, the non-clinical strain SDF showed insufficient larval killing to calculate the LD_{50}, even at the highest inoculum size. Thus, the estimated LD_{50} for SDF represents a theoretical approximation to the actual LD_{50} value, and can confidently be considered to be at least 100-fold higher than the LD_{50} values for the three clinical strains.

Growth kinetics

In order to establish the optimal conditions for *in vitro* growth of the different *A. baumannii* strains, the growth kinetics were determined for each strain at temperatures ranging between 4 and 50°C in different minimal and complex growth media, namely LB, M9 minimal medium, CAA and TSBD.

SDF grew slower than the other strains in all the media tested, with TSBD being the only medium supporting the growth of SDF to levels almost comparable to those of the other strains (Fig. 1; data not shown). In general, TSBD and LB were found to be the preferential media for growth of *A. baumannii*, with maximum growth rates (μ_{max}) of the clinical strains being slightly higher in TSBD (average of 2.8 h^{-1} at 37°C) than in LB (average of 2.5 h^{-1} at 37°C). When grown at 37°C in TSBD, strains entered stationary growth phase after ca. 10–12 h, with a doubling time of ca. 40 min for clinical strains and 100 min for SDF.

All *A. baumannii* strains of clinical origin grew at temperatures ranging between 25 and 45°C, with maximum growth rates at 37°C. In contrast, growth of the non-human SDF strain was impaired at temperatures higher than 37°C (Fig. 1), a feature that would hamper growth in humans during pyrexia.

Iron-uptake capability

The capability of the different *A. baumannii* strains to resist iron starvation was compared by growing the strains on TSBD agar plates in the presence of a gradient of the iron chelator 2,2′-dipyridyl (0–500 μM) (Fig. 2A). Considerable differences in resistance to iron starvation were found between strains, with clinical strains showing significantly higher capability to overcome iron starvation than the non-human isolate SDF (Fig. 2A; $P<0.01$).

In order to correlate the observed iron starvation resistance profiles to the production of iron-chelating compounds, the

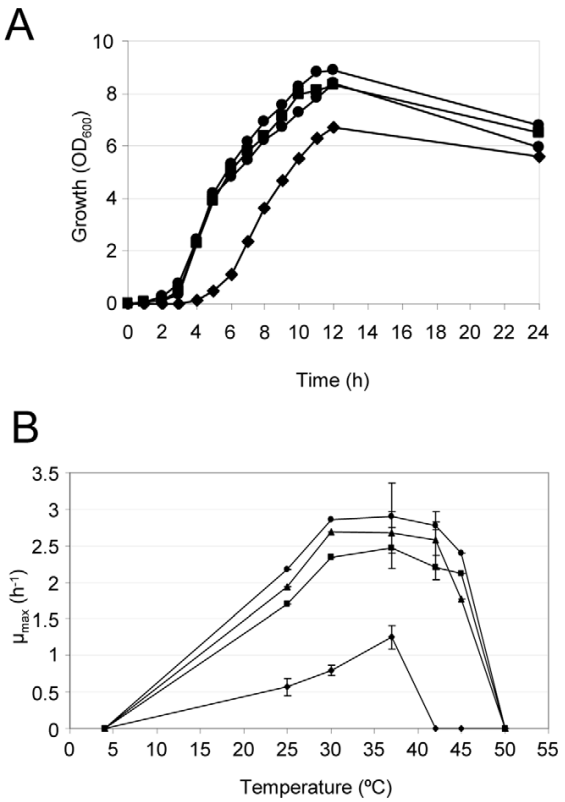

Figure 1. *A. baumannii* growth kinetics. (A) Growth (OD_{600}) of *A. baumannii* strains at 37°C in TSBD medium. (B) Temperature-dependent growth kinetics, defined as maximum growth rates (μ_{max}) of *A. baumannii* strains grown in TSBD medium at the different temperatures. Values represent the mean (± standard deviation, SD) of three independent experiments. Symbols: AYE, squares; ACICU, circles; ATCC 17978, triangles; SDF, diamonds.

doi:10.1371/journal.pone.0022674.g001

different *A. baumannii* strains were compared for total iron-chelating activity released in culture supernatants, as well as for production of iron-regulated molecules containing chemical groups involved in iron chelation, namely hydroxamates and catechols. To this aim, *A. baumannii* strains were grown in poor (CAA) or rich (TSBD) medium supplemented with either 50 μM 2,2′-dipyridyl or 50 μM $FeCl_3$, as iron-depleted and iron-replete growth conditions, respectively. While CAA is one of the reference media used for iron-uptake studies, TSBD was chosen since it supports growth of SDF to levels comparable to the other strains (Fig. 1).

With the exception of SDF, all strains showed iron-chelating activity in the supernatant of cultures grown under iron-depleted growth conditions (Fig. 2B), consistent with the genomic predictions. With regard to the chemical nature of the iron-chelating groups, all the siderophore-producing strains secreted comparable amounts of hydroxamate groups, while AYE showed only marginal catechol production with respect to ACICU and ATCC 17978 (Figs. 2C and D). Notably, the ratios between hydroxamate and catechol groups released by strains ACICU and ATCC 17978 were significantly different for the two growth media ($P<0.001$). While both strains produced higher amounts of

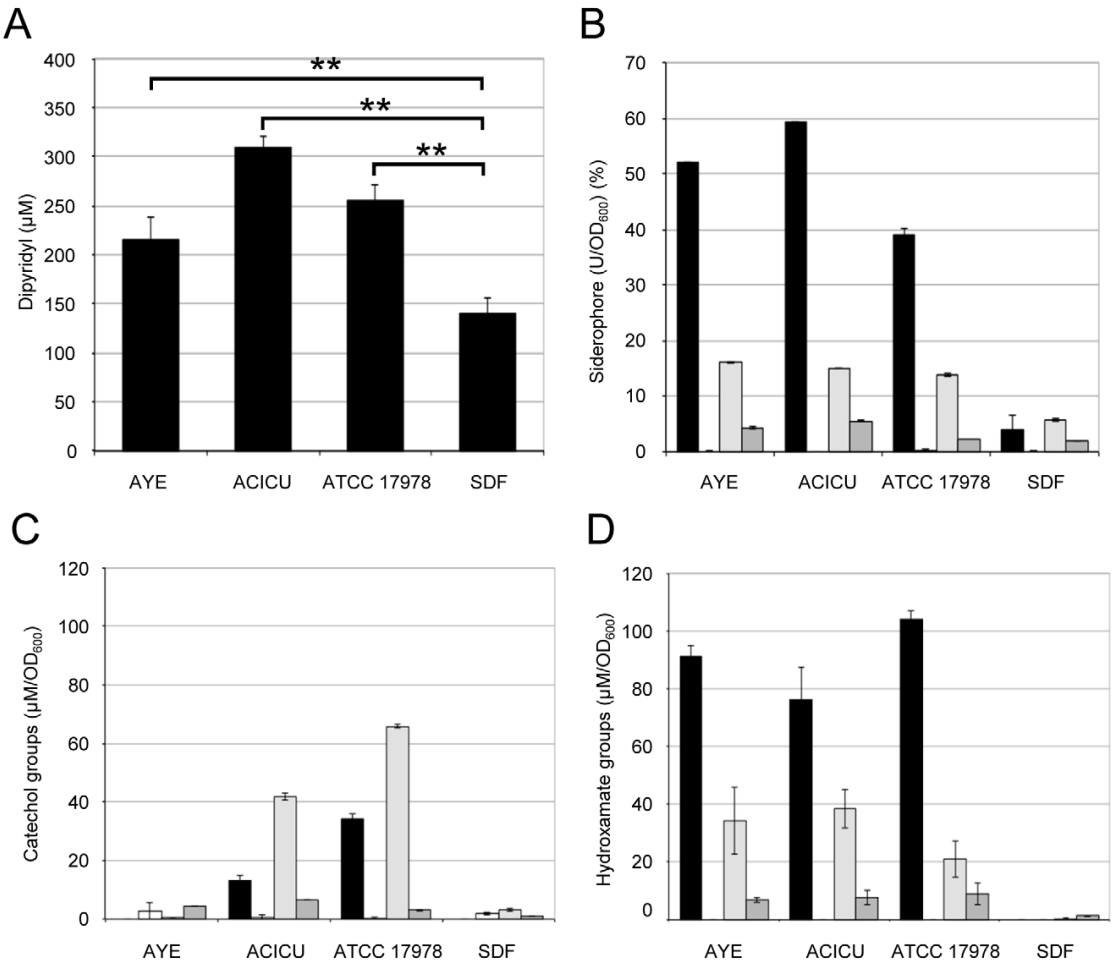

Figure 2. Iron-uptake capability. (A) Growth of *A. baumannii* strains on 2,2′-dipyridyl gradient (0–500 μM) TSBD agar plates. The ordinate shows the minimal inhibitory concentration of the iron chelator 2,2′-dipyridyl. (B) Iron-chelating activity in culture supernatants of *A. baumannii* strains grown in CAA supplemented with either 50 μM 2,2′-dipyridyl or 50 μM $FeCl_3$ (black and white bars, respectively) and TSBD supplemented with 50 μM 2,2′-dipyridyl or 50 μM $FeCl_3$ (light and dark gray bars, respectively). Values are expressed as percentage of siderophore units (U) normalized to the cell density (OD_{600}) of the bacterial culture. Amount of catechol (C) and hydroxamate (D) groups in the supernatants of *A. baumannii* cultures. Values are expressed as concentration (μM) of hydroxamate or catechol groups normalized to the OD_{600} of the bacterial culture. Growth conditions and symbols correspond to those described in the legend to panel B. Values represent the mean (±SD) of two independent experiments, each including three biological replicates. ** $P<0.01$ (ANOVA).
doi:10.1371/journal.pone.0022674.g002

hydroxamates than catechols in CAA, the opposite occurred in TSBD (Figs. 2C and D), indicating that the composition of the growth medium may affect the production of the different iron-chelating compounds.

Hemolytic activity

Although *A. baumannii* is generally considered to be a non-hemolytic species [43], genomic analysis revealed the presence of two phospholipase C genes and a number of hemolysin-related genes in all the *A. baumannii* strains sequenced to date (Table S1 and ref. 19).

In order to assay the hemolytic activity, *A. baumannii* strains were grown on 5% sheep or horse blood agar plates. Intriguingly, all strains caused appreciable hemolysis of horse but not sheep erythrocytes (Fig. 3A; data not shown). To quantify extracellular hemolytic activity, filter-sterilized bacterial supernatants from TSBD cultures were incubated with horse and sheep defibrinated blood. Whereas no hemolysis was detected in the presence of sheep blood, all strains caused hemolysis of horse erythrocytes to levels comparable to that of *P. aeruginosa* PAO1, which was used as a positive control (Fig. 3B).

Phospholipase C and exoprotease production

The genomes of the sequenced *A. baumannii* strains contain two genes putatively coding for a phospholipase C and several genes encoding putative secreted proteolytic enzymes (Table S1). Therefore, phospholipase C and exoprotease activities were compared in culture supernatants of the different *A. baumannii* strains. All strains showed phospholipase C and protease activities (Fig. 4). Whereas no statistically significant differences in

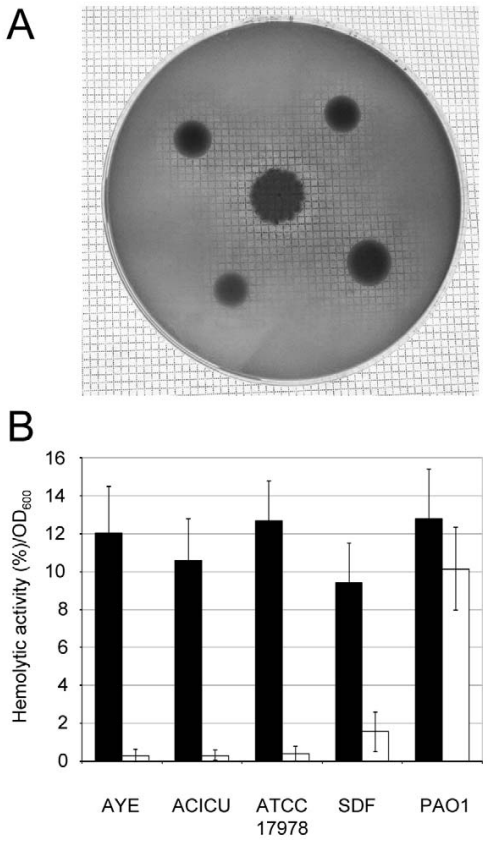

Figure 3. Hemolytic activity. (A) Hemolysis on 5% horse blood Columbia agar plates. *A. baumannii* strains are, from top left in clockwise order: AYE, ACICU, ATCC 17978 and SDF. *P. aeruginosa* PAO1 was spotted on the center of the plate as positive control for hemolysis. Hemolysis is evidenced by the transparent halo around the colony. (B) Hemolytic activity on horse and sheep erythrocytes (black and white bars, respectively) of cell-free supernatants from *A. baumannii* cultures grown in TSBD medium. Hemolytic activity was normalized to the OD_{600} of the bacterial culture. Values represent the mean (± SD) of two independent experiments, each including three biological replicates.
doi:10.1371/journal.pone.0022674.g003

phospholipase C levels were observed among isolates ($P>0.05$), ACICU and ATCC 17978 showed higher protease activities than AYE and SDF ($P<0.01$; Fig. 4B).

Biofilm formation

Analysis of the *A. baumannii* genomes indicated that several genes predicted to encode factors responsible for promoting and regulating biofilm formation, e.g. pili and quorum sensing, were differently distributed among *A. baumannii* strains [5,27,28]. Biofilm formation was compared among the different *A. baumannii* strains by measuring cell adhesion to the surface of polystyrene microtiter plate wells after static incubation at 37°C for 24 h. Under these conditions, the non-clinical strain SDF showed ≥10-fold higher ability to adhere to the surface and form biofilms with respect to the clinical strains ($P<0.001$; Fig. 5). Among these, the ACICU strain, representative of CC2, exhibited significantly higher biofilm formation than the AYE strain, representative of CC1, and the non-epidemic strain ATCC 17978 ($P<0.05$; Fig. 5), in line with the recent observation that biofilm formation capability is higher in isolates belonging to CC2 compared with CC1 isolates [44].

Surface motility

The *A. baumannii* genomes contain several genes and gene clusters putatively responsible for type IV pilus-mediated twitching motility. Compared with the epidemic strains AYE and ACICU, strain ATCC 17978 lacks three genes predicted to be involved in pilus adhesion, whilst SDF lacks most genes essential for pilus biogenesis and functioning (Table S2).

Surface motility was assessed on LB, CAA and TSBD plates containing 0.5% agarose. After incubation at 37°C for 24 h, twitching motility was measured in terms of the bacterial spread at the agarose/petri plate interface [45]. Twitching was observed for AYE in LB and TSBD, but not in CAA plates, while the other strains did not twitch in any of the tested media (Fig. 6 and data not shown). Moreover, different forms of swarming were detected at the air/agarose interface for ATCC 17978 in CAA and for AYE in TSBD medium (Fig. S2).

Resistance to human serum and desiccation

The different *A. baumannii* strains were compared for the ability to survive for long periods on dry surfaces and the ability to avoid the bactericidal activity of human serum. Overall, ACICU, AYE and SDF displayed a comparable resistance to human serum, while ATCC 17978 showed lower survival in the presence of human serum, a difference which was statistically significant only with respect to ACICU ($P<0.01$; Fig. 7A). On the other hand, the *A. baumannii* strains showed a considerably different ability to survive on dry surfaces (Fig. 7B). The louse strain SDF was strongly impaired in its ability to resist desiccation (survival time less than 10 days). The non-epidemic strain ATCC 17978 and the representative CC2 strain ACICU showed comparable trends of survival (survival time of 40–70 days). Notably, the representative CC1 strain AYE showed extremely high resistance to desiccation, surviving on dry surfaces for more than 100 days (Fig. 7B).

Discussion

A. baumannii is an emerging human pathogen responsible for a broad array of nosocomial infections. Its ability to persist in the hospital setting and to steadfastly acquire antibiotic resistance has become a global concern for the medical community [1,3]. Most studies have focused on the epidemiology and evolution of antibiotic resistance of *A. baumannii*; however, the basis of its virulence remains ill-defined.

Recently, Peleg and coworkers demonstrated the suitability of *G. mellonella* as a model to study *A. baumannii*-host interactions [20]. This simple animal model of infection was used in the present study to compare the pathogenicity of four *A. baumannii* strains with completely sequenced genomes. Three of these strains were isolated from clinical specimens of infected patients, including two MDR representatives of CC1 and CC2 and the sporadic isolate ATCC 17978. The fourth strain, SDF, has a non-human origin, although it has been suggested that its isolation from a body louse could result from the ingestion of contaminated blood from a bacteremic patient. While no significant differences in virulence were observed among the clinical strains, irrespective of their resistance phenotype or their classification as epidemic (AYE and ACICU) or sporadic (ATCC 17978), the body louse strain SDF was practically avirulent in this model of infection, suggesting that this strain could be used as a pathogenicity-defective benchmark in the search for novel *A. baumannii* virulence determinants.

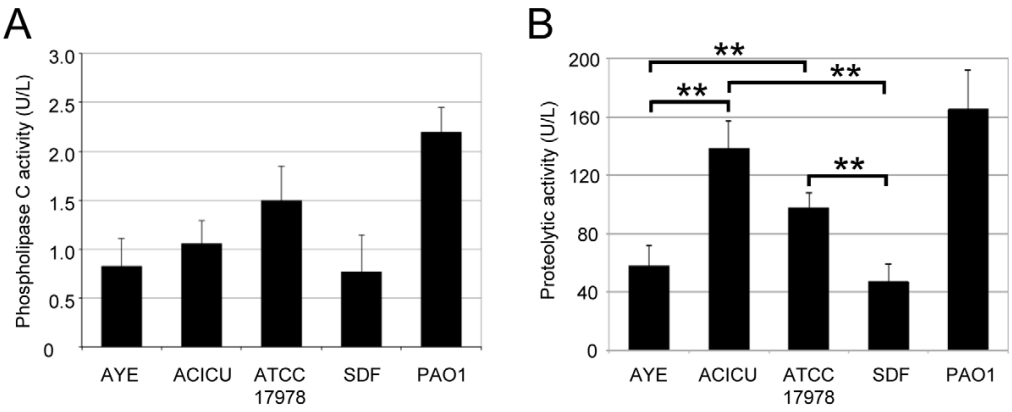

Figure 4. Production of virulence-related exoproteins. Phospholipase C (A) and total proteolytic (B) activities in filter-sterilized supernatants of the different *A. baumannii* strains grown for 14 h in TSBD at 37°C. Activities are expressed in U/L of culture supernatants and normalized to the OD_{600} of the bacterial cultures. *P. aeruginosa* PAO1 was used as positive control for phospholipase C and proteolytic activities. Values represent the mean (± SD) of three independent experiments. ** $P<0.01$ (ANOVA).
doi:10.1371/journal.pone.0022674.g004

In order to tentatively link the reduced virulence of SDF to the lack of specific virulence trait(s), the presence and expression of several virulence factors, namely hemolysins, phospholipase C, exoproteases and iron acquisition systems, were investigated by a combined approach of genomic and phenotypic analysis. In addition, several multifactorial phenotypes, such as growth capability, motility, biofilm formation and resistance to serum, iron deficiency and desiccation, were analyzed, as all these phenotypes are known to contribute to the pathogenicity and ecological fitness of other opportunistic bacterial pathogens.

On the whole, the *A. baumannii* clinical isolates displayed the ability to express a number of virulence determinants, including exoproducts with hemolytic, phospholipase and protease activities, and siderophore-based iron uptake mechanisms. This is in full agreement with the presence in their genomes of specific genes for the synthesis of such potential virulence factors [25,27,28,29]. Notably, the hemolytic activity of *A. baumannii* strains is much more evident in liquid assay than on agar plates, and can be detected using horse, but not sheep, erythrocytes (Fig. 3). This intriguing result could explain why *A. baumannii* has historically been regarded as a non-hemolytic bacterium [43].

Differences were observed in the production of specific virulence factors between the non-human isolate SDF and the clinical strains, with the most noteworthy being the inability of SDF to use siderophores as an iron-uptake strategy, which affects its ability to grow under iron-depleted conditions (Fig. 2). On the

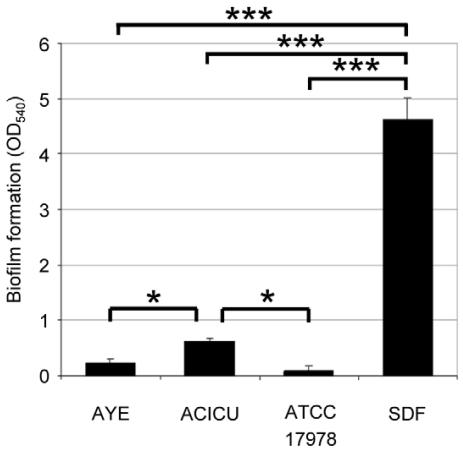

Figure 5. Biofilm formation. Biofilm formation on 96-well polystyrene microtiter plates by *A. baumannii* strains grown statically in LB medium for 24 h. Values represent the mean (± SD) of five independent experiments performed in quadruplicate. * $P<0.05$, *** $P<0.001$ (ANOVA).
doi:10.1371/journal.pone.0022674.g005

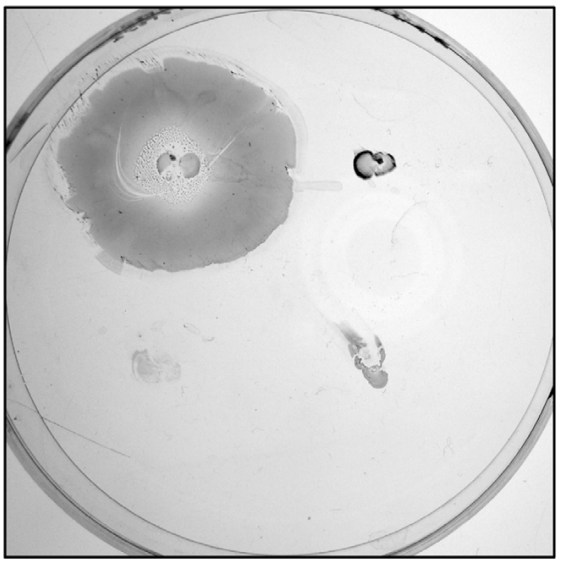

Figure 6. Twitching motility. *A. baumannii* twitching motility after 24 h of growth at 37°C in TSBD medium. *A. baumannii* strains are, from top-left in clockwise order: AYE, ACICU, SDF and ATCC 17978. The plate shown in the figure is representative of three independent experiments giving similar results.
doi:10.1371/journal.pone.0022674.g006

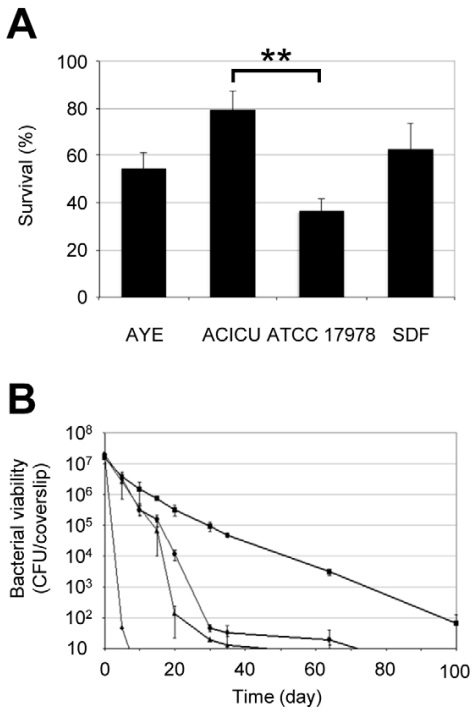

Figure 7. Resistance to human serum and desiccation. (A) Serum resistance of *A. baumannii* strains. Resistance was determined as the percentage of survival in 40% non-heated serum relative to survival in heated serum. Values represent the mean (± SD) of five independent experiments. (B) Resistance to desiccation of *A. baumannii* strains: AYE (squares), ACICU (circles), ATCC 17978 (triangles) and SDF (diamonds). Strains were inoculated onto 13-mm diameter rounded glass coverslips and incubated at 22°C and 31% relative humidity. A starting bacterial inoculum of 2×10^7 CFU per coverslip was used. Values represent the mean (± SD) of three independent experiments. The lower detection limit of the assay is 10 CFU per coverslip. ** $P<0.01$ (ANOVA).
doi:10.1371/journal.pone.0022674.g007

other hand, SDF showed hemolytic, phospholipase and protease activities comparable to the average values obtained for the clinical strains (Figs. 3 and 4), suggesting that the reduced virulence of SDF in the *G. mellonella* model of infection cannot be ascribed to any of these factors. It should be pointed out that SDF showed limited metabolic capabilities, as inferred by its lower growth kinetics and biomass yields in the majority of culture media tested, as compared to the clinical *A. baumannii* strains (Fig. 1; data not shown). The genome of SDF is much smaller than that of the other *A. baumannii* genomes sequenced to date [5], presumably as a result of extensive insertion sequence-mediated deletion events [27]. Given that strain SDF was isolated from a human body louse, its adaptation to such a restricted host might provide an explanation for the reductive evolution of its genome and, consequently, for its metabolic restrictions, as documented for other pathogens restricted to a narrow ecological niche [reviewed in ref. 46]. Therefore, the virulence defect of SDF in *G. mellonella* can more likely be ascribed to a reduced ability to grow and persist in this model host than to impaired production of any virulence factor among those analyzed in the present study.

Some interesting differences were observed among the strains with respect to the multifactorial phenotypes related to pathogenesis, such as biofilm formation, motility and resistance to desiccation. The non-human isolate SDF was strongly impaired in its ability to survive on dry surfaces compared to the clinical isolates (Fig. 7B), suggesting that the ability to persist under dry conditions may represent a factor accounting for *A. baumannii* survival in the hospital setting and, ultimately, for its ability to cause outbreaks of infection.

A remarkable difference was observed between the representative CC1 and CC2 strains with regard to surface motility. While AYE displayed both twitching and swarming motilities, ACICU was apparently non-motile (Fig. 6), despite carrying the genetic potential to encode functional type IV pili (Table S2). Additional studies are required to assess whether the lack of motility is a specific feature of strain ACICU or a common trait of CC2 members.

Finally, it is worth noting that strain SDF is endowed with a surprisingly high capability to adhere to abiotic surfaces and to form biofilm. Very recently, de Breij and coworkers showed that no evident correlation exists in *A. baumannii* strains between biofilm formation capability and clinical impact [44]. The results obtained with SDF are in agreement with this conclusion. Intriguingly, the genome of SDF lacks most of the factors which have been implicated in *A. baumannii* biofilm formation, namely Csu pili, the quorum sensing signal synthase AbaI and exopolysaccharide PNAG synthesis enzymes (http://www.genome.jp/kegg/), suggesting either that these systems are not essential for biofilm development or that strain SDF possesses alternative compensatory function(s). However, a search for gene clusters exclusive to the genome of SDF did not reveal any obvious candidate(s), but a number of genomic regions of prophage origin with unpredictable function were identified. Whether these regions provide SDF with additional functions related to biofilm formation remains to be assessed.

In summary, the present work confirms the multifactorial nature of *A. baumannii* virulence, with no unique virulence factor being identified that individually accounts for the pathogenic success of this bacterium. Moreover, the results indicate that metabolic capabilities and resistance to environmental stresses might be more important for *A. baumannii* pathogenicity than the production of specific virulence factors. In support of this, it is noteworthy that genes coding for the only factors demonstrated to affect *A. baumannii* pathogenicity *in vivo* (OmpA, phospholipase D and penicillin-binding protein 7/8) are present in all annotated *A. baumannii* genomes, including the avirulent strain SDF, as well as in the genome of the related soil bacterium *Acinetobacter baylyi* (http://www.genome.jp/kegg/). The present investigation strengthens the view that the epidemic potential of *A. baumannii* is more likely related to the MDR phenotype than to the production of specific virulence factor(s) [1,5], as shown here by the overall similarity of the virulence-related phenotype between epidemic MDR strains AYE and ACICU and the sporadic isolate ATCC 17978.

A comparative-genomics analysis recently demonstrated that the SDF genome is highly divergent from the genomes of clinical *A. baumannii* strains [5]. This work shows that such diversity reflects upon the atypical phenotype of SDF with regard to growth rate, iron uptake, biofilm formation and resistance to stress, compared with the clinical strains. Furthermore, the attenuated virulence in the insect model of infection argues against any potential role of SDF as a human pathogen. Further studies are mandatory to understand the actual distribution of such aberrant *A. baumannii* strains in reservoirs other than the hospital setting, which could possibly help to reconstruct the evolution of *A. baumannii* toward human pathogenicity.

Supporting Information

Table S1 *A. baumannii* genomic ORFs predicted to encode hemolysin-, phospholipase- and exoprotease-related proteins.
(DOC)

Table S2 *A. baumannii* genomic ORFs predicted to encode proteins related to type IV pilus biogenesis and functioning.
(DOC)

Figure S1 Kaplan-Meier survival plots of *G. mellonella* larvae infected with the different *A. baumannii* strains. Time-kill results from a representative experiment are shown, which were obtained by inoculating 10^4 (A), 10^5 (B), 10^6 (C) or 10^7 (D) bacterial cells per larva. Strains are: AYE (dashed red lines), ACICU (straight green lines), ATCC 17978 (dashed blue lines) and SDF (straight black lines). Statistically significant differences ($P<0.05$ calculated by the log-rank test option of GraphPad) were only observed between SDF and the three clinical strains, but not between clinical strains.
(PPT)

Figure S2 Swarming-like motility on the air-agarose interface of ATCC 17978 on TSBD plates (A) and AYE on CAA plates (B) after 24 h of growth at 37°C. The plates are representative of three independent experiments giving similar results.
(PPT)

Acknowledgments

The authors are grateful to Dr. K. J. Towner (Department of Clinical Microbiology, Nottingham University Hospitals, Nottingham, UK) for critical reading of the manuscript, and to Prof. P. Nordmann (Hôpital de Bicêtre, le Kremlin–Bicêtre, France) for kindly providing us with the AYE and SDF strains.

Author Contributions

Conceived and designed the experiments: LCSA FI PV. Performed the experiments: LCSA FI. Analyzed the data: LCSA FI AC PV. Contributed reagents/materials/analysis tools: PV. Wrote the paper: LCSA FI AC PV.

References

1. Dijkshoorn L, Nemec A, Seifert H (2007) An increasing threat in hospitals: multidrug-resistant *Acinetobacter baumannii*. Nat Rev Microbiol 5: 939–951.
2. Joly-Guillou ML (2005) Clinical impact and pathogenicity of *Acinetobacter*. Clin Microbiol Infect 11: 868–873.
3. Peleg AY, Seifert H, Paterson DL (2008) *Acinetobacter baumannii*: emergence of a successful pathogen. Clin Microbiol Rev 21: 538–582.
4. Diancourt L, Passet V, Nemec A, Dijkshoorn L, Brisse S (2010) The population structure of *Acinetobacter baumannii*: expanding multiresistant clones from an ancestral susceptible genetic pool. PLoS One 7: e10034.
5. Imperi F, Antunes LCS, Blom J, Villa L, Iacono M, et al. (2011) The genomics of *Acinetobacter baumannii*: insights into genome plasticity, antimicrobial resistance and pathogenicity. IUBMB Life 63: xxx–xxx (in press).
6. Landman D, Quale JM, Mayorga D, Adedeji A, Vangala K, et al. (2002) Citywide clonal outbreak of multiresistant *Acinetobacter baumannii* and *Pseudomonas aeruginosa* in Brooklyn, NY: the preantibiotic era has returned. Arch Intern Med 8: 1515–20.
7. Towner KJ (2009) Acinetobacter: an old friend, but a new enemy. J Hosp Infect 73: 355–363.
8. Falagas M, Rafailidis P (2007) Attributable mortality of *Acinetobacter baumannii*: no longer a controversial issue. Crit Care 11: 134.
9. Choi C, Lee E, Lee Y, Park T, Kim H, et al. (2005) Outer membrane protein 38 of *Acinetobacter baumannii* localizes to the mitochondria and induces apoptosis of epithelial cells. Cell Microbiol 7: 1127–1138.
10. Gaddy J, Actis L (2009) Regulation of *Acinetobacter baumannii* biofilm formation. Future Microbiol 4: 273–278.
11. Kim S, Choi C, Moon D, Jin J, Lee J, et al. (2009) Serum resistance of *Acinetobacter baumannii* through the binding of factor H to outer membrane proteins. FEMS Microbiol Lett 301: 224–231.
12. Jacobs A, Hood I, Boyd K, Olson P, Morrison J, et al. (2010) Inactivation of phospholipase D diminishes *Acinetobacter baumannii* pathogenesis. Infect Immun 78: 1952–1962.
13. Camarena L, Bruno V, Euskirchen G, Poggio S, Snyder M (2010) Molecular mechanisms of ethanol-induced pathogenesis revealed by RNA-sequencing. PLoS Pathog 6: e1000834.
14. Russo TA, MacDonald U, Beanan JM, Olson R, MacDonald IJ, et al. (2009) Penicillin-binding protein 7/8 contributes to the survival of *Acinetobacter baumannii* in vitro and in vivo. J Infect Dis 199: 513–21.
15. Russo TA, Luke NR, Beanan JM, Olson R, Sauberan SL, et al. (2010) The K1 capsular polysaccharide of *Acinetobacter baumannii* strain 307-0294 is a major virulence factor. Infect Immun 78: 3993–4000.
16. Choi A, Slamti L, Avci F, Pier G, Maira-Litran T (2009) The *pgaABCD* locus of *Acinetobacter baumannii* encodes the production of poly-β-1-6-N-acetyl glucosamine PNAG that is critical for biofilm formation. J Bacteriol 191: 5953–5963.
17. Tomaras AP, Dorsey CW, Edelmann RE, Actis L (2003) Attachment to and biofilm formation on abiotic surfaces by *Acinetobacter baumannii*: involvement of a novel chaperone-usher pili assembly system. Microbiology 149: 3473–3484.
18. Loehfelm T, Luke N, Campagnari A (2008) Identification and characterization of an *Acinetobacter baumannii* biofilm-associated protein. J Bacteriol 190: 1036–1044.
19. Niu C, Clemmer K, Bonomo R, Rather P (2008) Isolation and characterization of an autoinducer synthase from *Acinetobacter baumannii*. J Bacteriol 190: 3386–3392.
20. Peleg A, Jara S, Monga D, Eliopoulos G, Moellering R, et al. (2009) *Galleria mellonella* as a model system to study *Acinetobacter baumannii* pathogenesis and therapeutics. Antimicrob Agents Chemother 53: 2605–2609.
21. Cevahir N, Demir M, Kaleli I, Gurbuz M, Tikvesli S (2008) Evaluation of biofilm production, gelatinase activity, and mannose-resistant hemagglutination in *Acinetobacter baumannii* strains. J Microbiol Immunol *Infect* 41: 513–518.
22. Jawad A, Seifert H, Snelling A, Heritage J, Hawkey P (1998) Survival of *Acinetobacter baumannii* on dry surfaces: comparison of outbreak and sporadic isolates. J Clin Microbiol 36: 1938–1941.
23. Braun V (2001) Iron uptake mechanisms and their regulation in pathogenic bacteria. Int J Med Microbiol 291: 67–79.
24. Yamamoto S, Okujo N, Sakakibara Y (1994) Isolation and structure elucidation of acinetobactin, a novel siderophore from *Acinetobacter baumannii*. Arch Microbiol 162: 249–254.
25. Antunes LCS, Imperi F, Towner KJ, Visca P (2011) Genome-assisted identification of putative iron-utilization genes in *Acinetobacter baumannii* and their distribution among a genotypically diverse collection of clinical isolates. Res Microbiol 162: 279–284.
26. Zimbler DL, Penwell WF, Gaddy J, Menke SM, Tomaras AP, et al. (2009) Iron acquisition functions expressed by the human pathogen *Acinetobacter baumannii*. Biometals 22: 23–32.
27. Vallenet D, Nordmann P, Barbe V, Poirel L, Mangenot S, et al. (2008) Comparative analysis of Acinetobacters: three genomes for three lifestyles. PLoS ONE 3: e1805.
28. Iacono M, Villa L, Fortini D, Bordoni R, Imperi F, et al. (2008) Whole-genome pyrosequencing of an epidemic multidrug-resistant *Acinetobacter baumannii* strain belonging to the European clone II group. Antimicrob Agents Chemother 52: 2616–2625.
29. Smith M, Gianoulis T, Pukatzki S, Mekalanos J, Ornston L, et al. (2007) New insights into *Acinetobacter baumannii* pathogenesis revealed by high-density pyrosequencing and transposon mutagenesis. Genes Dev 21: 601–614.
30. La Scola B, Raoult D (2004) *Acinetobacter baumannii* in human body louse. Emerg Infect Dis 10: 1671–1673.
31. Sambrook J, Fitsch EF, Maniatis T (1989) Molecular Cloning: A Laboratory Manual. Cold Spring Harbor: Cold Spring Harbor Press. 2344 p.
32. Ohman D, Sadoff J, Iglewski B (1980) Toxin A-deficient mutants of *Pseudomonas aeruginosa* PA103: isolation and characterization. Infect Immun 28: 899–908.
33. Visca P, Chiarini F, Mansi A, Vetriani C, Serino L, et al. (1992) Virulence determinants in *Pseudomonas aeruginosa* strains from urinary tract infections. Epidemiol Infect 108: 323–336.
34. Jander G, Rahme L, Ausubel F (2000) Positive correlation between virulence of *Pseudomonas aeruginosa* mutants in mice and insects. J Bacteriol 182: 3843–3845.
35. Hunt D, Sandham H (1969) : Improved agar gradient-plate technique. App Environ Microb 17: 329–330.
36. Schwyn B, Neilands JB (1987) Universal chemical assay for the detection and determination of siderophores. Anal Biochem 160: 47–56.
37. Gillam A, Lewis A, Andersen R (1981) Quantitative determination of hydroxamic acids. Anal Chem 53: 841–844.
38. Arnow L (1937) Colorimetric determination of the components of 3, 4-dihydroxyphenylalaninetyrosine mixtures. J Biol Chem 118: 531–537.
39. Blocker A, Gounon P, Larquet E, Niebuhr K, Cabiaux V, et al. (1999) The tripartite type III secreton of *Shigella flexneri* inserts IpaB and IpaC into host membranes. J Cell Biol 147: 683–693.
40. Berka R, Gray G, Vasil M (1981) Studies of phospholipase C (heat-labile hemolysin) in *Pseudomonas aeruginosa*. Infect Immun 34: 1071–1074.
41. Phillips P, Prior D, Dawes B (1984) A modified azoalbumin technique for the assay of proteolytic enzymes for use in blood group serology. J Clin Pathol 37: 329–331.
42. Merritt JH, Kadouri DE, O'Toole GA (2005) Growing and analyzing static biofilms. In: Coico R, Kowalik T, Quarles JM, Stevenson B, Taylor RK, eds. Curr Protoc Microbiol, John Wiley & Sons. 1B.1.1.
43. Bouvet P, Grimont P (1986) Taxonomy of the genus *Acinetobacter* with the recognition of *Acinetobacter baumannii* sp. nov., *Acinetobacter haemolyticus* sp. nov., *Acinetobacter johnsonii* sp. nov., and *Acinetobacter junii* sp. nov. and emended descriptions of *Acinetobacter calcoaceticus* and *Acinetobacter lwoffii*. Int J Syst Evol Microbiol 36: 228–240.

44. de Breij A, Dijkshoorn L, Lagendijk E, van der Meer J, Koster A, et al. (2010) Do biofilm formation and interactions with human cells explain the clinical success of *Acinetobacter baumannii*? PLoS ONE 5: e10732.
45. Mattick JS (2002) Type IV pili and twitching motility. Annu Rev Microbiol 56: 289–314.
46. Moran NA (2002) Microbial minimalism: genome reduction in bacterial pathogens. Cell 108: 583–586.

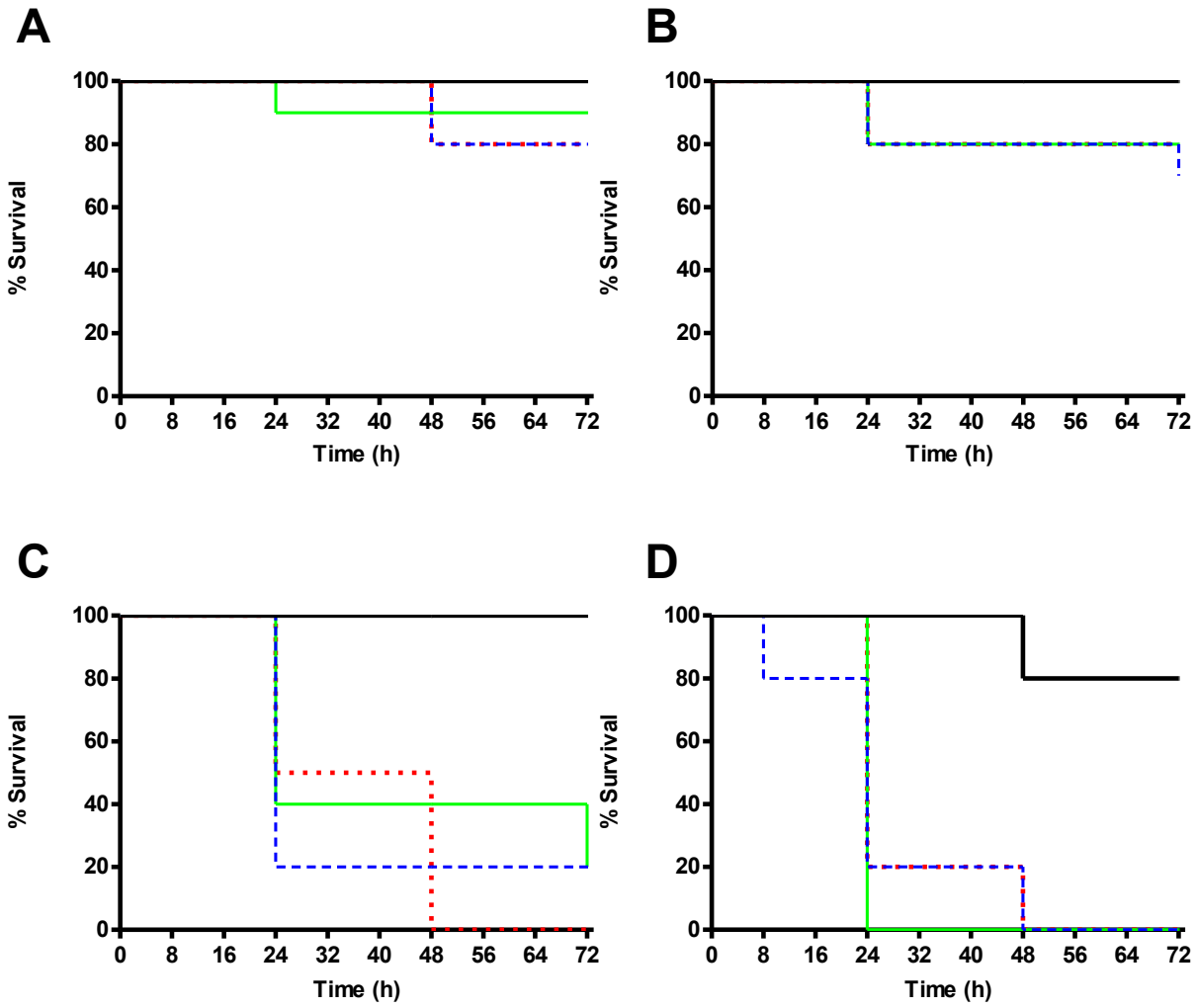

Figure S1. Kaplan-Meier survival plots of *G. mellonella* larvae infected with the different *A. baumannii* strains. Time-kill results from a representative experiment are shown, which were obtained by inoculating 10^4 (A), 10^5 (B), 10^6 (C) or 10^7 (D) bacterial cells per larva. Strains are: AYE (dashed red lines), ACICU (straight green lines), ATCC 17978 (dashed blue lines) and SDF (straight black lines). Statistically significant differences ($P < 0.05$ calculated by the log-rank test option of GraphPad) were only observed between SDF and the three clinical strains, but not between clinical strains.

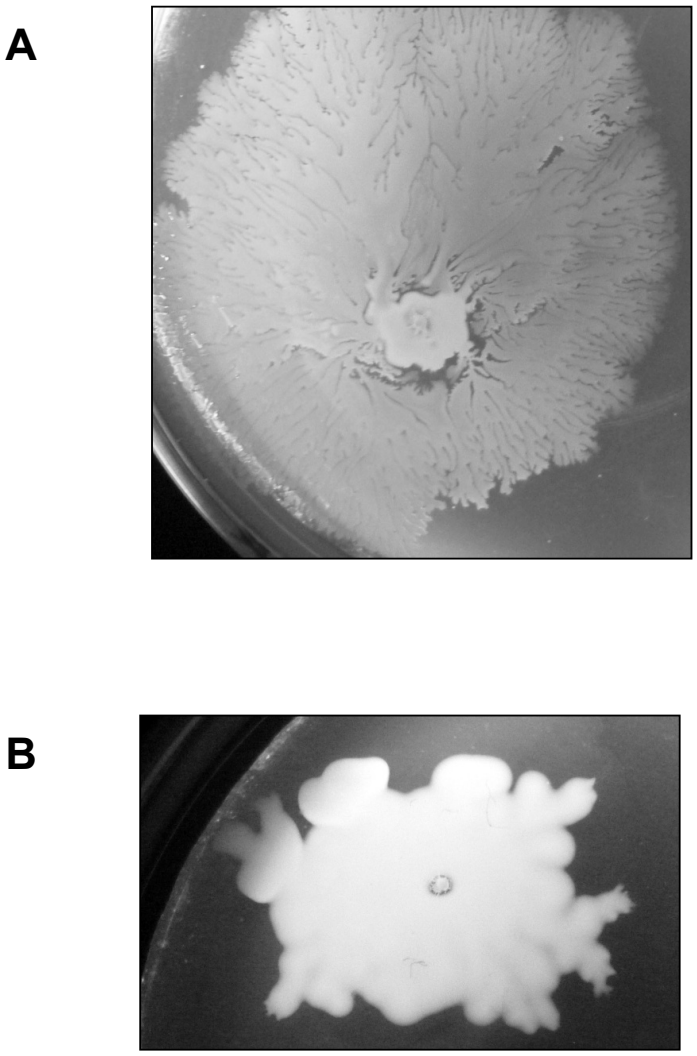

Figure S2. Swarming-like motility on the air-agarose interface of ATCC 17978 on TSBD plates (A) and AYE on CAA plates (B) after 24 h of growth at 37°C. The plates are representative of three independent experiments giving similar results.

Table S1. *A. baumannii* genomic ORFs predicted to encode hemolysin-, phospholipase- and exoprotease-related proteins.

Predicted function(s)[a]	Strain[b]			
	AYE	ACICU	ATCC 17978	SDF
Putative hemagglutinin/hemolysin-related protein (no signal peptide, OM)	-	-	-	3544
Putative hemolysin (no signal peptide, unknown)	2926	0840	0889	2547
Putative hemolysin-related protein (no signal peptide, IM)	2786	0966	1005	2385
Hemolysin-type calcium-binding region (no signal peptide, extracellular)	-	-	1073	-
Putative hemolysin (signal peptide, extracytoplasmic)	2389	1322	1321	-
Hemagglutinin/hemolysin-related protein (no signal peptide, OM)	-	1911	-	-
Putative hemolysin-type calcium-binding region (no signal peptide, extracellular)	-	-	2413	-
Putative calcium binding hemolysin protein (no signal peptide, extracellular)	-	-	2414	-
Hemolysin-type calcium-binding protein with a RTX N-terminal domain (no signal peptide, OM or extracellular)	-	2938	2696	-
Putative hemolysin III (no signal peptide, IM)	0623	3107	2859	0585
Phospolipase C (signal peptide, extracellular)	3825	0064	0043	0054
Phospolipase C (signal peptide, extracellular)	1520	2247	2055	2207
Serine protease (signal peptide, extracellular)	1602	2073	1954	-
Putative aminopeptidase N (signal peptide, extracellular)	1122	2554	2356	1167
Putative zinc protease (signal peptide, OM)	990	2679	2470	1071
Serine protease (signal peptide, OM)	359	3327	3126	363

[a] The presence of a signal peptide for protein export into the periplasm and the subcellular localization of each protein have been predicted by the PSORTb program (http://www.psort.org/), and are shown in brackets. Abbreviations; OM, outer membrane; IM, inner membrane.

[b] Number of genes refers to the annotation of each genome sequence (Kyoto Encyclopedia of Genes and Genomes; http://www.genome.jp/kegg/).

Table S2. *A. baumannii* genomic ORFs predicted to encode proteins related to type IV pilus biogenesis and functioning.

Gene	Predicted function	Strain[a]			
		AYE	ACICU	ATCC 17978	SDF
pilR	Type 4 fimbriae expression regulatory protein	3535	0257	0234	-
pilS	Sensor protein	3536	0258	0235	-
pilD	Type 4 prepilin-like proteins leader peptide processing enzyme	3446	0343	0327	3194
pilC	Type 4 fimbrial assembly protein	3445	0344	0328	-
pilB	Type 4 fimbrial biogenesis protein	3444	0345	0329	-
pilF	Type 4 fimbrial biogenesis protein	3265	0509	0500	-
pilU	Twitching motility protein	2919	0847	0896	-
pilT	Twitching motility protein	2918	0848	0897	-
pilZ	Type 4 fimbrial biogenesis protein	2074	1606	1559	1726
pilJ	Type IV pilus biogenesis protein	0670	3060	2812	0641
pilI	Twitching motility protein	0669	3061	2813	0640
pilH	Twitching motility two-component system response regulator	0668	3062	2814	0639
pilG	Twitching motility two-component system response regulator	0667	3063	2815	0638
fimT	Type IV pilus assembly protein	0639	3090	2841	0604
pilE	Type IV pilus assembly protein	0320	3364	3165	0325
pilE	Pilin like competence factor	0319	3365	3166	-
pilY1	Type IV pilus assembly protein	0318	3366	3167	-
pilX	Putative type IV fimbrial biogenesis protein	0317	3367	-	-
pilW	Type IV pilus assembly protein	0316	3368	3168	-
pilV	Type IV fimbrial biogenesis protein	0315	3369	-	-
pilT	Putative type IV fimbrial biogenesis protein	0314	3370	-	-
pilA	Major pilin	0304	3380	3177	-
pilQ	Type IV pilus assembly protein	0294	3390	3191	-
pilp	Type IV pilus assembly protein	0293	3391	3192	0297
pilO	Type IV pilus assembly protein	0292	3392	3193	0296
pilN	Type IV pilus assembly protein	0291	3393	3194	-
pilM	Type IV pilus assembly protein	0290	3394	3195	0293

[a] Number of genes refers to the annotation of each genome sequence (Kyoto Encyclopedia of Genes and Genomes; http://www.genome.jp/kegg/).

Chapter 4

Genome-assisted identification of putative iron-utilisation genes in *Acinetobacter baumannii* and their distribution among a genotypically diverse collection of clinical isolates

Luísa C. S. Antunes[1], Francesco Imperi[1], Kevin J. Towner[2], Paolo Visca[1]

[1]Department of Biology, University Roma Tre, Rome, Italy

[2]Department of Clinical Microbiology, Nottingham University Hospitals NHS Trust, Queen's Medical Centre, Nottingham, UK

Research in Microbiology 162 (2011): 279-284

Abstract

Acinetobacter baumannii survival and persistence in the human host is dependent upon its capacity to acquire iron, and hence on the expression of iron-acquisition systems. A single iron-acquisition system had been characterised in this bacterium, the mixed catechol-hydroxamate siderophore acinetobactin. Previously, genomic analysis identified the capacity in this species for the production of alternative iron-acquisition systems (**Chapter 2**). In addition, all strains showed haemolytic activity *in vitro* (**Chapter 3**).

In the present chapter, the distribution of iron uptake/utilisation genes was investigated in a genotypically diverse collection of 50 clinical *A. baumannii* isolates using PCR and Southern blot assays. Results showed the conservation of two endogenous siderophores (including acinetobactin), a haem and a ferrous iron uptake system. Two thirds of isolates also had the potential to use a second haem uptake system.

The conservation of iron-acquisition systems among genotypically diverse strains demonstrates the importance of such systems for *A. baumannii* pathogenicity. In addition, the presence of multiple iron-acquisition strategies in this species could be indicative of a wide adaptation to different habitats (human, haematophage gut, anoxic environments).

ELSEVIER

INSTITUT PASTEUR

Research in Microbiology 162 (2011) 279–284

www.elsevier.com/locate/resmic

Genome-assisted identification of putative iron-utilization genes in *Acinetobacter baumannii* and their distribution among a genotypically diverse collection of clinical isolates

Luísa C.S. Antunes [a], Francesco Imperi [a], Kevin J. Towner [b], Paolo Visca [a,*]

[a] *Department of Biology, University "Roma Tre", Viale G. Marconi 446, 00146 Roma, Italy*
[b] *Department of Clinical Microbiology, Nottingham University Hospitals NHS Trust, Queen's Medical Centre, Nottingham NG7 2UH, UK*

Received 2 July 2010; accepted 21 October 2010
Available online 7 December 2010

Abstract

New putative iron-uptake genes were identified in published genomes of the opportunistic human pathogen *Acinetobacter baumannii*, and their occurrence was determined in a genotypically distinct collection of 50 clinical isolates by PCR and Southern blot assays. The results demonstrated that all *A. baumannii* isolates tested share the coding potential for two endogenous siderophores, a heme-acquisition and a ferrous iron-uptake system. A second heme-uptake cluster was detected in almost two thirds of isolates, without any apparent correlation with the clonal lineage of the strains. The wide distribution of multiple iron-acquisition systems among diverse *A. baumannii* clinical isolates argues for a contribution of iron uptake to the pathogenicity of this species.

Keywords: Acinetobactin; Feo system; Heme uptake; Siderophore

1. Introduction

Acinetobacter baumannii is the most clinically important species of the *Acinetobacter* genus and is generally found only in the hospital environment (Towner, 2009). *A. baumannii* has been widely studied for its ability to steadily acquire multiple antibiotic resistance genes (Dijkshoorn et al., 2007). However, the mechanisms which enable *A. baumannii* to colonize the human host and establish infection deserve further investigation.

One of the major challenges pathogenic bacteria face in their host is the scarcity of freely available iron. In mammals, iron is virtually unavailable to invading bacteria, being mainly incorporated into iron transport and storage proteins. The host's iron withholding capacity substantially reduces the bioavailability of iron to infecting bacteria and constitutes an important component of innate immunity (Guerinot, 1994). This is particularly important for *A. baumannii* opportunism, since this organism has to combat the iron-binding capacity of lactoferrin and transferrin during mucosal and bloodstream infections, respectively.

While iron withholding by the host resists establishment of an infection, pathogens respond by exploiting a number of strategies for high-affinity iron acquisition, including production of ferric [Fe(III)] iron chelators (siderophores), uptake of exogenous chelators, such as heme and heterologous siderophores, and acquisition of ferrous [Fe(II)] iron. Bacterial cells acquire Fe(III)-loaded siderophores and heme by means of specific receptor proteins. In Gram-negative bacteria, these receptors are localized on the outer membrane, where internalization of the siderophore-Fe(III) complex or heme is coupled to dissipation of the proton gradient on the inner membrane. Energy transduction from the inner to the outer membrane is mediated by the TonB protein complex in the periplasmic space (Miethke and Marahiel, 2007). Another major route for bacterial iron assimilation is the direct uptake

* Corresponding author. Tel.: +39 6 5517 6347; fax: +39 6 5517 6321.
E-mail addresses: lantunes@uniroma3.it (L.C.S. Antunes), imperi@uniroma3.it (F. Imperi), kevin.towner@btinternet.com (K.J. Towner), visca@uniroma3.it (P. Visca).

0923-2508/$ - see front matter © 2010 Institut Pasteur. Published by Elsevier Masson SAS. All rights reserved.
doi:10.1016/j.resmic.2010.10.010

of Fe(II) by the Feo system which, in γ-proteobacteria, consists of the cytosolic FeoA protein, the inner membrane Fe(II) permease FeoB, and the putative transcriptional repressor FeoC (Cartron et al., 2006).

The first iron-uptake molecule characterized in *A. baumannii* was a mixed catechol–hydroxamate siderophore termed acinetobactin (Yamamoto et al., 1994; Dorsey et al., 2004; Mihara et al., 2004). The recent publication of the complete genome sequences of six *A. baumannii* strains, namely ATCC 17978, AYE, SDF, ACICU, AB0057 and AB307-294, revealed that an acinetobactin gene cluster is present in all but one of the sequenced strains, being absent in the non-clinical isolate SDF (Adams et al., 2008; Iacono et al., 2008; Smith et al., 2007; Vallenet et al., 2008).

The aim of this study was to analyze the available *A. baumannii* genome sequences for additional gene clusters putatively involved in iron acquisition, and to establish the distribution of identified iron-uptake genes in a genotypically diverse collection of 50 clinical *A. baumannii* isolates, comprising representatives of the major epidemic worldwide lineages.

2. Materials and methods

2.1. Bacterial strains and growth media

The collection of *A. baumannii* strains used in this study includes the type strain ATCC 19606^T, the sequenced strains ACICU, ATCC 17978, AYE and SDF, and 50 genotypically diverse clinical isolates (see list in Fig. 1) collected as part of the EU-funded Antibiotic Resistance; Prevention and Control (ARPAC) project (MacKenzie et al., 2005; Towner et al.,

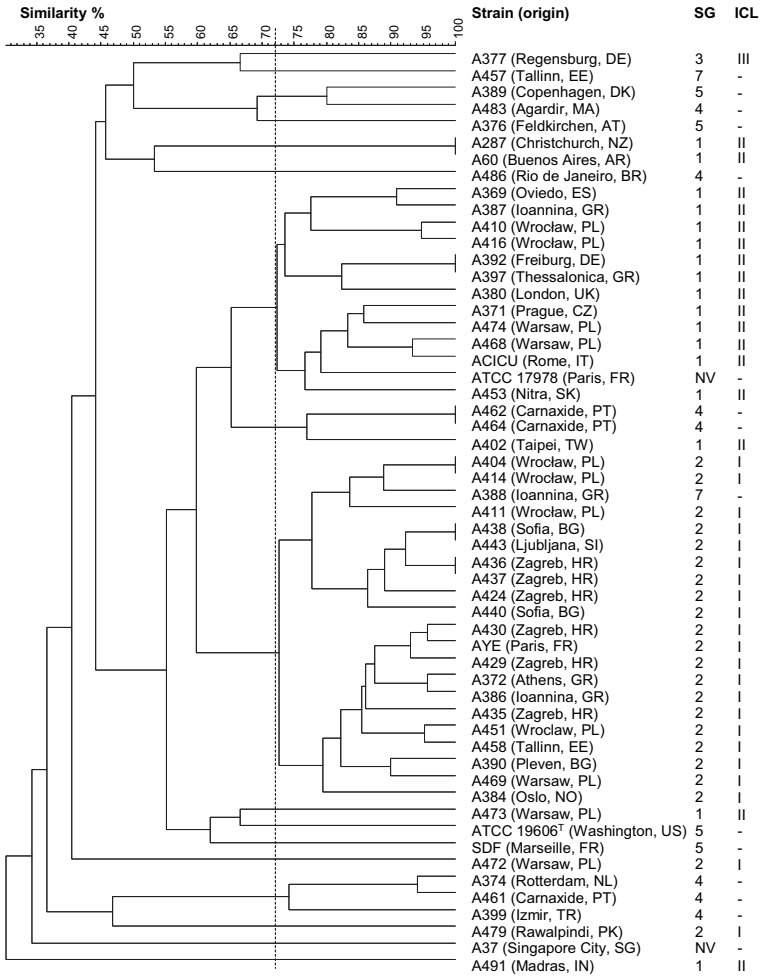

Fig. 1. Clustering relationships of the 50 clinical isolates, the type strain ATCC 19606^T and the four sequenced strains used in this study. RAPD analysis was performed with primer DAF-4. The dendrogram was generated with Bionumerics v.5.1 software (Applied Maths) using the Dice coefficient and the UPGMA method. The dotted vertical line defines the 72% cut-off level used previously to group isolates into the major epidemic lineages/clones. The sequence group (SG) and the origin of each strain are also shown. NV, new variant SG. As reported in figure, SG1, SG2 and SG3 correspond to the International clonal lineages (ICL) 2, 1 and 3, respectively (Turton et al., 2007). Two-letters country codes are according to the ISO standard ISO 3166-1 alpha-2: AR, Argentina; AT, Austria; BG, Bulgaria; BR, Brazil; CZ, Czech Republic; DE, Germany; DK, Denmark; EE, Estonia; ES, Spain; FR, France; GR, Greece; HR, Croatia; IN, India; IT, Italy; MA, Morocco; NL, The Netherlands; NO, Norway; NZ, New Zealand; PK, Pakistan; PL, Poland; PT, Portugal; SG, Singapore; SI, Slovenia; SK, Slovakia; TR, Turkey; TW, Taiwan; UK, United Kingdom; US, United States.

2008). Identification of these isolates as members of the species *A. baumannii* was confirmed as part of the present study by demonstrating the presence of an intrinsic $bla_{\text{OXA-51-like}}$ gene, found only in *A. baumannii* (see below). *P. aeruginosa* PAO1 (ATCC 15692) was used as negative control where indicated. Unless otherwise stated, strains were grown in Tryptic Soy Broth (Acumedia).

2.2. Identification of putative iron-acquisition gene clusters

The complete genome sequences of *A. baumannii* strains ATCC 17978, ACICU, AYE, SDF, AB0057, AB307-294 (GenBank accession nos. CP000521, CP000863, CU459141, CU468230, CP001182 and CP001172, respectively) and the draft genome sequence of the type strain ATCC 19606^T (ACQB00000000) were screened for putative TonB-dependent outer membrane receptor genes and for homolog(s) of the *Escherichia coli feoB* gene. Only TonB-dependent receptor genes flanked by genes that were predicted to encode proteins involved in siderophore synthesis or heme utilization were further analyzed. Putative TonB-dependent receptor genes that did not cluster with any putative iron-related gene were discarded since their specific substrate and, therefore, their actual function can be predicted with low confidence only on the basis of the encoded amino acid sequence (Schauer et al., 2008).

2.3. Genomic DNA extraction, PCR and Southern blot assays

Genomic DNA was extracted with the Wizard® Genomic DNA Purification Kit (Promega). PCRs were performed using puReTaq Ready-To-Go PCR Beads (GE Healthcare). Southern blot assays were performed according to standard procedures (Sambrook et al., 1989). Digoxygenin-labeled probes were PCR-generated and detected using the DIG DNA Labeling and Detection Kit (Roche). Primers for PCR and probe generation (Table S1) were designed on the basis of the six annotated *A. baumannii* genome sequences using the CLC Main Workbench 5.0 software (CLC Bio).

2.4. A. baumannii genotyping

The overall genotypic diversity of the 50 *A. baumannii* clinical isolates was confirmed by randomly amplified polymorphic DNA (RAPD) analysis using primer DAF-4 and a cut-off value of 72% to differentiate particular epidemic lineages/clones (Grundmann et al., 1997). Membership of the major *A. baumannii* sequence groups (SGs) was determined by PCR using primers for *ompA*, *csuE* and $bla_{\text{OXA-51-like}}$ genes (Turton et al., 2007) and interpretation of amplicon profiles according to Turton et al. (2007) and Towner et al. (2008).

2.5. Assays for siderophore production

Selected strains were grown for 18 h at 37 °C in 0.5% Casamino Acids (Difco) medium (CAA) supplemented with 0.4 mM $MgCl_2$ and either 100 μM 2,2-dipyridyl or 100 μM $FeCl_3$ (low and high iron conditions, respectively). The total iron-chelating activity and the amounts of catechol and hydroxamate groups in culture supernatants were determined by the chromo azurol S (CAS) liquid assay (Schwyn and Neilands, 1987), the Arnow assay (Arnow, 1937), and the modified Csáky test (Gillam et al., 1981), respectively.

3. Results and discussion

The number of putative TonB-dependent outer membrane receptor genes identified in the seven analyzed *A. baumannii* genomes ranged from 8 in SDF to 21 in ACICU, ATCC 17978 and AB0057 (data not shown). Of these, five were found to be flanked by genes putatively involved in siderophore synthesis or heme utilization (Fig. 2).

Two clusters encoding functions related to heme uptake were identified. One of these was common to all the *A. baumannii* strains sequenced to date and encodes an outer membrane receptor, a TonB-like system also including *exb* homologs, periplasmic heme-binding proteins, and an inner membrane ATP-binding cassette (ABC) importer. The second cluster, present only in ACICU, AB0057 and SDF, includes an outer membrane receptor gene, the *hemO* gene involved in oxidative cleavage of heme to release iron, a *tonB* gene and genes encoding an extra-cytoplasmic function (ECF) sigma and its cognate antisigma factor.

Two siderophore synthesis/transport gene clusters other than the acinetobactin cluster were identified, both of which include genes for putative ω-amino acid monooxygenase (or hydroxylase) and acetyltransferase enzymes, suggestive of the synthesis of hydroxamate-type siderophores. One of these clusters was exclusive to ATCC 17978 and corresponded to that described previously by Zimbler et al. (2009), while the other was common to all the sequenced strains except SDF (Fig. 2). Notably, the outer membrane receptor of this second siderophore cluster (ACICU_01679 in Fig. 2) was recently found among proteins expressed under conditions of limiting iron by strain ATCC 19606^T (Nwugo et al., 2010), supporting the prediction that this cluster plays a role in iron uptake.

In addition, a homolog of the *E. coli feoB* gene was present in all the sequenced *A. baumannii* strains. This gene was always found in association with *feoA* and *feoC* homolog genes (Fig. 2), suggestive of the presence of the typical ferrous iron-uptake (Feo) system of γ-proteobacteria (Cartron et al., 2006).

A. baumannii possesses a single homolog of the ferric uptake regulator Fur (Vallenet et al., 2008), which is the master transcriptional regulator of iron uptake in bacteria. A bioinformatics search for Fur-binding sites (Fur boxes) revealed that putative Fur boxes were present in several intergenic regions of the gene clusters described above (Fig. 2), corroborating the proposed role of these clusters in iron acquisition.

To verify the distribution of the putative iron-uptake systems in the *A. baumannii* population, 50 genotypically diverse *A. baumannii* clinical isolates collected over several

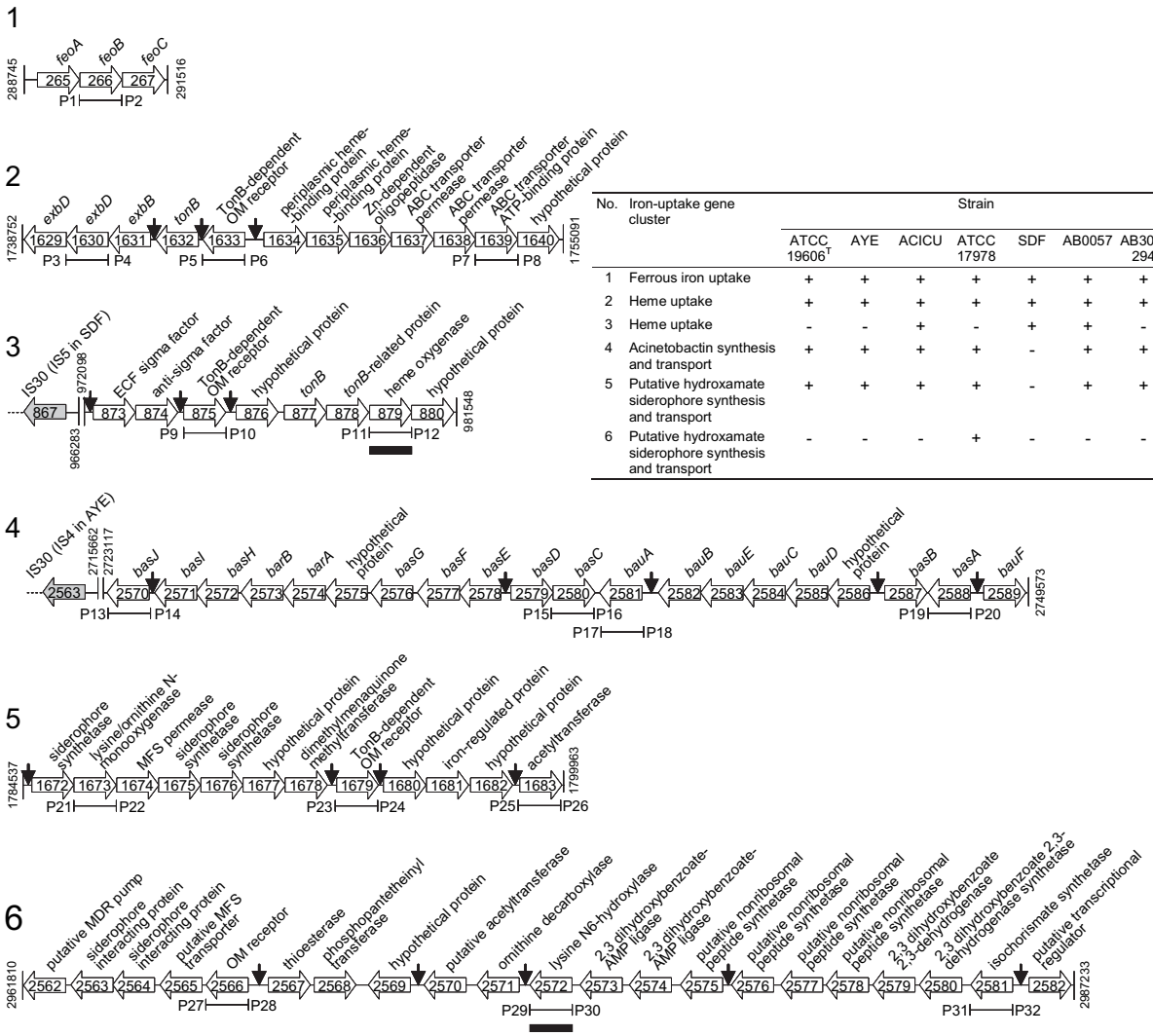

No.	Iron-uptake gene cluster	Strain						
		ATCC 19606^T	AYE	ACICU	ATCC 17978	SDF	AB0057	AB307-294
1	Ferrous iron uptake	+	+	+	+	+	+	+
2	Heme uptake	+	+	+	+	+	+	+
3	Heme uptake	-	-	+	-	+	+	-
4	Acinetobactin synthesis and transport	+	+	+	+	-	+	+
5	Putative hydroxamate siderophore synthesis and transport	+	+	+	+	-	+	+
6	Putative hydroxamate siderophore synthesis and transport	-	-	-	+	-	-	-

Fig. 2. Schematic representation of the iron-acquisition gene clusters identified in the six sequenced strains of *A. baumannii*. The table shows the presence (+) or absence (−) of each cluster in the reference strains. Unless otherwise stated, gene numbers, annotations and positions refer to the genome of ACICU (gene clusters 1 to 5) or ATCC 17978 (gene cluster 6). Coding sequences are shown as arrows (not to scale) oriented according to the direction of transcription. Putative Fur boxes are shown as vertical black arrows. P1 to P32 refer to the position of primers (Table S1). Probes used for Southern dot blot are shown as black rectangles.

decades from different worldwide sources were selected for further study (Fig. 1). The overall genotypic diversity among these isolates was initially confirmed by RAPD analysis (Fig. 1), followed by allocation to SGs. The sequenced strains ACICU, AYE, ATCC 17978 and SDF, and the type strain ATCC 19606^T, were included as reference strains. Forty-four isolates formed six RAPD clusters, while 11 did not cluster with any other isolate at the cut-off level of 72% used by Grundmann et al. (1997) to recognize the major epidemic lineages/clones (Fig. 1). Significant genetic diversity within the major epidemic lineages/clones was also apparent (Fig. 1). Six of the seven SGs described previously in *A. baumannii* (Turton et al., 2007; Towner et al., 2008) were identified (SG1-5 and 7) in addition to two new variant SGs.

The distribution of 16 individual genes belonging to the six different putative iron-acquisition clusters in the collection of *A. baumannii* isolates was determined by PCR and, where needed, confirmed by Southern blot hybridization. The results indicated that genes belonging to two putative siderophore gene clusters, coding for the acinetobactin system and for a putative hydroxamate-type siderophore (no. 5 in Fig. 2), are conserved among clinical isolates of *A. baumannii*, while a third siderophore cluster (no. 6 in Fig. 2) appeared to be exclusive to ATCC 17978 (Table S2). This result was confirmed by Southern blot analysis with a probe matching the gene for the essential enzyme lysine N^6-hydroxylase (Fig. S1). Genes belonging to a putative heme-utilization cluster (no. 2 in Fig. 2) were present in all *A. baumannii* isolates, while those

belonging to a second heme-uptake cluster (no. 3 in Fig. 2) were found in approximately 60% of strains (Table S2). Three isolates showed discordant results, giving amplification of the receptor gene but not of *hemO* (Table S2). However, Southern blot analysis with a specific probe detected the *hemO* gene in the genome of these isolates (Fig. S1), indicating that false-negative results were obtained during the PCR screening. For all other strains, PCR and Southern blot results were fully concordant (Table S2). Finally, the *feoB* gene, encoding the ferrous iron permease of the Feo system, was amplified from all isolates.

Overall, the screening results showed that clinical *A. baumannii* isolates share the potential to utilize at least two endogenous siderophores, one heme-uptake system and the Feo system for ferrous iron acquisition. A second heme-uptake cluster is present in about two thirds of isolates, and no apparent correlation exists between presence/absence of this cluster and the SG. This cluster is located in a putative alien island (Iacono et al., 2008) and is flanked by an insertion sequence in two of the three sequenced strains harboring this cluster (IS30 and IS5 in ACICU and SDF, respectively; Fig. 2). It is possible that these mobile elements played a role in the horizontal transfer of this heme-uptake system, causing its variable occurrence in the *A. baumannii* population. Notably, the additional siderophore cluster identified previously in the genome of ATCC 17978 (Zimbler et al., 2009; Fig. 2) seems to be exclusive to this strain. The function of this gene cluster remains elusive, but its absence in *A. baumannii* clinical isolates belonging to the most widespread clonal lineages suggests that it is not essential for the success of *A. baumannii* as a pathogen. Thus, by combining comparative genomics with genetic screening, it was possible to identify three novel iron-acquisition clusters (nos. 1, 3 and 5 in Fig. 2) which appear to be widely distributed in a genetically diverse collection of clinical *A. baumannii* isolates.

The presence in all isolates except SDF of a second siderophore cluster, in addition to the previously characterized cluster for acinetobactin (Mihara et al., 2004), corroborates previous reports which suggested that this species produces more than one siderophore (Dorsey et al., 2003; Zimbler et al., 2009). In a preliminary attempt to verify this hypothesis, the total iron-chelating activity and the amounts of iron-regulated catechol and hydroxamate groups secreted by the selected clinical isolates and reference strains were determined. Consistent with the genetic evidence, all *A. baumannii* isolates secreted iron-chelating compounds when grown in CAA supplemented with the iron-chelator 2,2-dipyridyl (Fig. 3A and Table S2). However, the ratio between iron-regulated catechol- and hydroxamate-type groups was highly variable among strains, ranging from 0.02 to 12.75 (Fig. 3B and Table S2). Considering that acinetobactin is characterized by a 1:1 catechol:hydroxamate ratio (Yamamoto et al., 1994), the observed variability in the catechol:hydroxamate ratios is suggestive of the production of iron-chelating molecule(s) additional to acinetobactin. Reverse genetics and regulatory studies are mandatory to verify whether such molecule(s) correspond to that synthesized by the genetic cluster here identified (no. 5 in Fig. 2) and to what extent regulation of these systems may differ among strains.

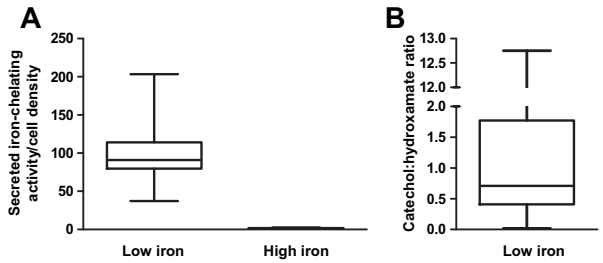

Fig. 3. Siderophore production by a selection of *A. baumannii* strains. Boxplots showing (A) the iron-chelating activity and (B) the ratio between catechol and hydroxamate groups in the supernatant of *A. baumannii* cultures (n = 15). Low and high iron represent iron-chelated and iron-repleted growth conditions, respectively. Boxes represent medians and second and third interquartiles, while whiskers represent the range of the 15 strains analyzed. Iron-chelating activity is expressed as the percentage of siderophore units normalized to the culture cell density (OD_{600}) (see Table S2 for details).

In conclusion, this study predicts the existence of multiple iron-acquisition systems in *A. baumannii*. The wide distribution of these systems among genotypically diverse clinical *A. baumannii* isolates argues for a possible role in pathogenicity. *A. baumannii* seems to be a very adaptable pathogen, and the existence of several different iron-acquisition systems would give this organism the opportunity to utilize different iron sources, ultimately enhancing its capability to colonize and prosper in the human host.

Acknowledgements

The authors gratefully acknowledge the use of strains originally obtained by K.J.T. from the many participants in the EU ARPAC project (MacKenzie et al., 2005). L.C.S.A. was supported by a PhD fellowship from the Portuguese Fundação para a Ciência e a Tecnologia (FCT) (grant SFRH/BD/43420/2008). Work in K. J. T.'s laboratory was supported, in part, by the UK Medical Research Council (grant RA0119). The authors otherwise declare that they have no conflicting or dual interests in relation to this work.

Appendix. Supplementary data

Supplementary data associated with this article can be found in the online version, at doi:10.1016/j.resmic.2010.10.010.

References

Adams, M.D., Goglin, K., Molyneaux, N., Hujer, K.M., Lavender, H., Jamison, J.J., MacDonald, I.J., Martin, K.M., Russo, T., Campagnari, A.A., Hujer, A.M., Bonomo, R.A., Gill, S.R., 2008. Comparative genome sequence analysis of multidrug-resistant *Acinetobacter baumannii*. J. Bacteriol. 190, 8053–8064.

Arnow, L.E., 1937. Colorimetric determination of the components of 3, 4-dihydroxyphenylalanine-tyrosine mixtures. J. Biol. Chem. 118, 531–537.

Cartron, M.L., Maddocks, S., Gillingham, P., Craven, C.J., Andrews, S.C., 2006. Feo–transport of ferrous iron into bacteria. Biometals 19, 143–157.

Dijkshoorn, L., Nemec, A., Seifert, H., 2007. An increasing threat in hospitals: multidrug-resistant *Acinetobacter baumannii*. Nat. Rev. Microbiol. 5, 939–951.

Dorsey, C.W., Beglin, M.S., Actis, L.A., 2003. Detection and analysis of iron uptake components expressed by *Acinetobacter baumannii* clinical isolates. J. Clin. Microbiol. 41, 4188–4193.

Dorsey, C.W., Tomaras, A.P., Connerly, P.L., Tolmasky, M.E., Crosa, J.H., Actis, L.A., 2004. The siderophore-mediated iron acquisition systems of *Acinetobacter baumannii* ATCC 19606 and *Vibrio anguillarum* 775 are structurally and functionally related. Microbiology 150, 3657–3667.

Gillam, A.H., Lewis, A.G., Andersen, R.J., 1981. Quantitative determination of hydroxamic acids. Anal. Chem. 53, 841–844.

Grundmann, H.J., Towner, K.J., Dijkshoorn, L., Gerner-Smidt, P., Maher, M., Seifert, H., Vaneechoutte, M., 1997. Multicenter study using standardized protocols and reagents for evaluation of reproducibility of PCR-based fingerprinting of *Acinetobacter* spp. J. Clin. Microbiol. 35, 3071–3077.

Guerinot, M.L., 1994. Microbial iron transport. Annu. Rev. Microbiol. 48, 743–772.

Iacono, M., Villa, L., Fortini, D., Bordoni, R., Imperi, F., Bonnal, R.J., Sicheritz-Ponten, T., De Bellis, G., Visca, P., Cassone, A., Carattoli, A., 2008. Whole-genome pyrosequencing of an epidemic multidrug-resistant *Acinetobacter baumannii* strain belonging to the European clone II group. Antimicrob. Agents Chemother. 52, 2616–2625.

MacKenzie, F.M., Struelens, M.J., Towner, K.J., Gould, I.M.on behalf of the ARPAC Steering group and the ARPAC Consensus Conference Participants, 2005. Report of the Consensus Conference on antibiotic resistance; Prevention and control (ARPAC). Clin. Microbiol. Infect. 11, 937–954.

Miethke, M., Marahiel, M.A., 2007. Siderophore-based iron acquisition and pathogen control. Microbiol. Mol. Biol. Rev. 71, 413–451.

Mihara, K., Tanabe, T., Yamakawa, Y., Funahashi, T., Nakao, H., Narimatsu, S., Yamamoto, S., 2004. Identification and transcriptional organization of a gene cluster involved in biosynthesis and transport of acinetobactin, a siderophore produced by *Acinetobacter baumannii* ATCC 19606^{T}. Microbiology 150, 2587–2597.

Nwugo, C.C., Gaddy, J.A., Zimbler, D.L., Actis, L.A., 2010. Deciphering the iron response in *Acinetobacter baumannii*: a proteomics approach. J. Proteomics 74, 44–58.

Sambrook, J., Fritsch, E.F., Maniatis, T., 1989. Molecular Cloning: A Laboratory Manual, second ed.. Cold Spring Harbor Laboratory, Cold Spring Harbor New York.

Schauer, K., Rodionov, D.A., de Reuse, H., 2008. New substrates for TonB-dependent transport: do we only see the 'tip of the iceberg'? Trends Biochem. Sci. 33, 330–338.

Smith, M.G., Gianoulis, T.A., Pukatzki, S., Mekalanos, J.J., Ornston, L.N., Gerstein, M., Snyder, M., 2007. New insights into *Acinetobacter baumannii* pathogenesis revealed by high-density pyrosequencing and transposon mutagenesis. Genes Dev. 21, 601–614.

Schwyn, B., Neilands, J.B., 1987. Universal chemical assay for the detection and determination of siderophores. Anal. Biochem. 160, 46–56.

Towner, K.J., Levi, K., Vlassiadi, M.on behalf of the ARPAC Steering Group, 2008. Genetic diversity of carbapenem-resistant isolates of *Acinetobacter baumannii* in Europe. Clin. Microbiol. Infect. 14, 161–167.

Towner, K.J., 2009. Acinetobacter: an old friend, but a new enemy. J. Hosp. Infect. 73, 355–363.

Turton, J.F., Gabriel, S.N., Valderrey, C., Kaufmann, M.E., Pitt, T.L., 2007. Use of sequence-based typing and multiplex PCR to identify clonal lineages of outbreak strains of *Acinetobacter baumannii*. Clin. Microbiol. Infect. 13, 807–815.

Vallenet, D., Nordmann, P., Barbe, V., Poirel, L., Mangenot, S., Bataille, E., Dossat, C., Gas, S., Kreimeyer, A., Lenoble, P., Oztas, S., Poulain, J., Segurens, B., Robert, C., Abergel, C., Claverie, J.M., Raoult, D., Médigue, C., Weissenbach, J., Cruveiller, S., 2008. Comparative analysis of Acinetobacters: three genomes for three lifestyles. PLoS One 3, e1805.

Yamamoto, S., Okujo, N., Sakakibara, Y., 1994. Isolation and structure elucidation of acinetobactin, a novel siderophore from *Acinetobacter baumannii*. Arch. Microbiol. 162, 249–254.

Zimbler, D.L., Penwell, W.F., Gaddy, J.A., Menke, S.M., Tomaras, A.P., Connerly, P.L., Actis, L.A., 2009. Iron acquisition functions expressed by the human pathogen *Acinetobacter baumannii*. Biometals 22, 23–32.

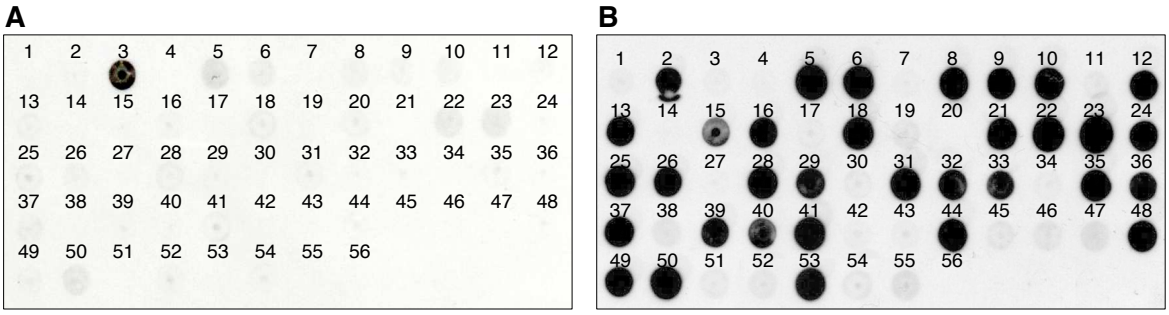

1. AYE	6. A37	11. A372	16. A384	21. A390	26. A404	31. A424	36. A437	41. A453	46. A464	51. A474
2. ACICU	7. A60	12. A374	17. A386	22. A392	27. A410	32. A429	37. A438	42. A457	47. A468	52. A479
3. ATCC 17978	8. A287	13. A376	18. A387	23. A397	28. A411	33. A430	38. A440	43. A458	48. A469	53. A483
4. ATCC 19606^T	9. A369	14. A377	19. A388	24. A399	29. A414	34. A435	39. A443	44. A461	49. A472	54. A486
5. SDF	10. A371	15. A380	20. A389	25. A402	30. A416	35. A436	40. A451	45. A462	50. A473	55. A491

Fig. S1. Southern dot blot analysis of (A) the gene for lysine N^6-hydroxylase of cluster no. 6 and (B) the *hemO* gene of cluster no. 3 (see Fig. 2 for details). *A. baumannii* isolate numbers are given below the dots. DNA from *P. aeruginosa* PAO1 (No. 56) was included as the negative control.

Table S1. Primers used in this study

Primer[1]	ORF[2]	Gene product	Cluster[3]	Sequence	Annealing T (°C)[4]	Position[2]	Amplicon length (bp)[2]	Application
P1	00266	FeoB	1. Ferrous iron uptake	GGAAGAGGGGCAACAAGA	65	289642	742	PCR screening
P2				GCTTGAAAGTAACGGAATGA		290364		
P3	01629	ExbD	2. Heme uptake	ACTCACAATCCCAATTTTAG	65	1738761	398	PCR screening
P4				TGAATGTTGGCTCAAATAATG		1739138		
P5	01633	Heme outer membrane receptor	2. Heme uptake	GGTAATAHTCCTCCRCG	55	1743281	611	PCR screening
P6				AAAGTCGTAAAAGTTGCC		1743874		
P7	01639	Inner membrane ATPase	2. Heme uptake	GATTTGGCTTTGGTTGGTG	68	1753260	459	PCR screening
P8				TTGATGTAAGCGCATGAGY		1753700		
P9	00875	Heme outer membrane receptor	3. Heme uptake	TTGGATCGACATGAACGG	68	974776	785	PCR screening
P10				GATAGAGCGAATAACTTGGG		975541		
P11	00879	Heme oxygenase (HemO)	3. Heme uptake	GAAACTGCTGCTGAACAC	68	981035	513	PCR screening and Southern dot blot
P12				CGCCTGACCAAAATATCC		980540		
P13	02570	BasJ	4. Acinetobactin synthesis/transport	CTACCCACTCACCATTACC	60	2723272	560	PCR screening
P14				TAACCGTCATCAAGAGCC		2723814		
P15	02580	BasC	4. Acinetobactin synthesis/transport	GTAAAACATTCAGCGGAG	65	2736877	530	PCR screening
P16				GGCCAATCATGAACATAG		2737389		
P17	02581	Acinetobactin outer membrane receptor (BauA)	4. Acinetobactin synthesis/transport	CCACGAATAKMATARYTTTC	60	2739523	338	PCR screening
P18				CTATGTGCATCAAAYACC		2739843		
P19	02588	BasA	4. Acinetobactin synthesis/transport	TTGAGTTTCAGTCGTTGG	60	2746962	624	PCR screening
P20				TGCAAGGTTACGATTTGG		2747568		
P21	01673	Monooxygenase	5. Hydroxamate siderophore synthesis/transport	TGATGTGGAGGTAGTGTG	65	1786891	595	PCR screening
P22				CTTATTTTGCTGACGGTG		1787468		
P23	01679	Siderophore outer membrane receptor	5. Hydroxamate siderophore synthesis/transport	TCCTAGCCGAGAGACAAC	65	1796107	538	PCR screening
P24				AACACGAACACCATACCC		1796627		
P25	01683	Acetyltransferase	5. Hydroxamate siderophore synthesis/transport	CCACACGTTATTCCTCAG	65	1799466	411	PCR screening
P26				CAACATTGCCGTTTTTTCC		1799858		
P27	2566[5]	Siderophore outer membrane receptor	6. Hydroxamate siderophore synthesis/transport	CTGCCCAATGTTTTTTATC	65	2964327[5]	577[5]	PCR screening
P28				GAAGGTTTATCGCAAGG		2964887[5]		
P29	2572[5]	Lysine hydroxylase	6. Hydroxamate siderophore synthesis/transport	TGATGGCATTGCGATAAC	68	2971379[5]	604[5]	PCR screening and Southern dot blot
P30				GGTGCCGAAATTTATTATGAC		2971962[5]		
P31	2581[5]	Isochorismate synthetase	6. Hydroxamate siderophore synthesis/transport	GCCCATTCACCATTACC	65	29849122[5]	400[5]	PCR screening
P32				CTTTAGCAGGGTCTCGG		29852952[5]		

[1] Primer designations correspond to those reported in Fig. 2
[2] Unless otherwise stated, numbers refer to the annotated genome sequence of strain ACICU
[3] Numbering of clusters refers to Fig. 2
[4] The lowest temperature which did not result in appearance of unspecific product(s) with the genome of ATCC 17978 or ACICU or SDF as template was used as annealing temperature
[5] Numbers refer to the annotated genome sequence of strain ATCC 17978

Table S2. Results of the PCR screening and of phenotypic tests to assess the production of iron-chelating compounds

Strain	PCR[1]																Southern dot blot[1]		Iron-chelating activity ($\%/OD_{600}$)[2]		Catechol groups ($\mu M/OD_{600}$)[3]		Hydroxamate groups ($\mu M/OD_{600}$)[4]		Cathecol/hydroxamate ratio[5]	Sequence group (SG)
	1[6]	2[6]			3[6]		4[6]			5[6]			6[6]				3[6]	6[6]								
	feoB	*exbD*	receptor gene	ATPase gene	receptor gene	*hemO*	*basJ*	*basC*	receptor gene	monooxygenase gene	receptor gene	acetyltransferase gene	receptor gene	hydroxylase gene	isochorismate synthetase gene		*hemO*	hydroxylase gene	low iron[7]	high iron[7]	low iron[7]	high iron[7]	low iron[7]	high iron[7]		
AYE	+	+	+	+	-	-	+	+	+	+	+	+	-	-	-		-	-	101,5	0,8	3,8	1,9	111,7	0	0,02	2
ACICU	+	+	+	+	+	+	+	+	+	+	+	+	-	-	-		+	-	128,8	2,1	73,4	1,7	149,0	0	0,48	1
ATCC 17978	+	+	+	+	-	-	+	+	+	+	+	+	+	+	+		-	+	83,6	1,9	62,6	1,7	157,9	0	0,39	NV[9]
ATCC 19606^T	+	+	+	+	-	-	+	+	+	+	+	+	-	-	-		-	-	45,3	0,6	109,8	1,9	57,0	0	1,89	5
SDF	+	+	+	+	+	+	-	-	-	-	-	+	-	-	-		+	-	NT[8]	NT	NT	NT	NT	NT	ND[8]	5
A37	+	+	+	+	+	+	+	+	+	+	+	+	-	-	-		+	-	NT	NT	NT	NT	NT	NT	ND	NV
A60	+	+	+	+	-	-	+	+	+	+	+	+	-	-	-		-	-	NT	NT	NT	NT	NT	NT	ND	1
A287	+	+	+	+	+	+	+	+	+	+	+	+	-	-	-		+	-	106,9	1,4	63,0	1,7	159,8	0	0,38	1
A369	+	+	+	+	+	+	+	+	+	+	+	+	-	-	-		+	-	203,4	0,0	125,7	2,1	204,0	0	0,61	1
A371	+	+	+	+	+	+	+	+	+	+	+	+	-	-	-		+	-	126,5	0,0	57,0	1,9	192,5	0	0,29	1
A372	+	+	+	+	-	-	+	+	+	+	+	+	-	-	-		-	-	NT	NT	NT	NT	NT	NT	ND	2
A374	+	+	+	+	+	+	+	+	+	+	+	+	-	-	-		+	-	NT	NT	NT	NT	NT	NT	ND	4
A376	+	+	+	+	+	+	+	+	+	+	+	+	-	-	-		+	-	NT	NT	NT	NT	NT	NT	ND	5
A377	+	+	+	+	-	-	+	+	+	+	+	+	-	-	-		-	-	116,5	0,0	117,2	2,0	143,8	0	0,80	3
A380	+	+	+	+	+	+	+	+	+	+	+	+	-	-	-		+	-	NT	NT	NT	NT	NT	NT	ND	1
A384	+	+	+	+	+	+	+	+	+	+	+	+	-	-	-		+	-	NT	NT	NT	NT	NT	NT	ND	2
A386	+	+	+	+	-	-	+	+	+	+	+	+	-	-	-		-	-	NT	NT	NT	NT	NT	NT	ND	2
A387	+	+	+	+	+	+	+	+	+	+	+	+	-	-	-		+	-	NT	NT	NT	NT	NT	NT	ND	1
A388	+	+	+	+	-	-	+	+	+	+	+	+	-	-	-		-	-	NT	NT	NT	NT	NT	NT	ND	7
A389	+	+	+	+	-	-	+	+	+	+	+	+	-	-	-		-	-	78,4	1,8	101,2	1,7	108,0	0	0,92	5
A390	+	+	+	+	+	+	+	+	+	+	+	+	-	-	-		+	-	NT	NT	NT	NT	NT	NT	ND	2
A392	+	+	+	+	+	+	+	+	+	+	+	+	-	-	-		+	-	NT	NT	NT	NT	NT	NT	ND	1
A397	+	+	+	+	+	+	+	+	+	+	+	+	-	-	-		+	-	NT	NT	NT	NT	NT	NT	ND	1
A399	+	+	+	+	+	+	+	+	+	+	+	+	-	-	-		+	-	107,2	2,5	98,0	2,4	155,8	0	0,61	4
A402	+	+	+	+	+	+	+	+	+	+	+	+	-	-	-		+	-	NT	NT	NT	NT	NT	NT	ND	1
A404	+	+	+	+	+	+	+	+	+	+	+	+	-	-	-		+	-	NT	NT	NT	NT	NT	NT	ND	2
A410	+	+	+	+	-	-	+	+	+	+	+	+	-	-	-		-	-	72,2	0,4	327,3	1,7	100,7	0	3,23	1
A411	+	+	+	+	+	+	+	+	+	+	+	+	-	-	-		+	-	NT	NT	NT	NT	NT	NT	ND	2
A414	+	+	+	+	+	+	+	+	+	+	+	+	-	-	-		+	-	86,2	1,3	71,3	2,0	126,1	0	0,55	2
A416	+	+	+	+	-	-	+	+	+	+	+	+	-	-	-		-	-	NT	NT	NT	NT	NT	NT	ND	1
A424	+	+	+	+	+	+	+	+	+	+	+	+	-	-	-		+	-	NT	NT	NT	NT	NT	NT	ND	2
A429	+	+	+	+	+	+	+	+	+	+	+	+	-	-	-		+	-	NT	NT	NT	NT	NT	NT	ND	2
A430	+	+	+	+	+	+	+	+	+	+	+	+	-	-	-		+	-	NT	NT	NT	NT	NT	NT	ND	2
A435	+	+	+	+	-	-	+	+	+	+	+	+	-	-	-		-	-	89,2	0,0	114,4	1,7	80,1	0	1,41	2
A436	+	+	+	+	+	+	+	+	+	+	+	+	-	-	-		+	-	NT	NT	NT	NT	NT	NT	ND	2
A437	+	+	+	+	+	+	+	+	+	+	+	+	-	-	-		+	-	NT	NT	NT	NT	NT	NT	ND	2
A438	+	+	+	+	+	+	+	+	+	+	+	+	-	-	-		+	-	NT	NT	NT	NT	NT	NT	ND	2
A440	+	+	+	+	-	-	+	+	+	+	+	+	-	-	-		-	-	NT	NT	NT	NT	NT	NT	ND	2
A443	+	+	+	+	+	+	+	+	+	+	+	+	-	-	-		+	-	NT	NT	NT	NT	NT	NT	ND	2
A451	+	+	+	+	+	+	+	+	+	+	+	+	-	-	-		+	-	NT	NT	NT	NT	NT	NT	ND	2
A453	+	+	+	+	+	-	+	+	+	+	+	+	-	-	-		+	-	37,1	NT	50,1	0,0	3,9	0	12,75	1
A457	+	+	+	+	-	-	+	+	+	+	+	+	-	-	-		-	-	NT	NT	NT	NT	NT	NT	ND	7
A458	+	+	+	+	-	-	+	+	+	+	+	+	-	-	-		-	-	85,8	0,0	125,9	2,2	63,4	0	1,95	2
A461	+	+	+	+	+	+	+	+	+	+	+	+	-	-	-		+	-	NT	NT	NT	NT	NT	NT	ND	4
A462	+	+	+	+	-	-	+	+	+	+	+	+	-	-	-		-	-	NT	NT	NT	NT	NT	NT	ND	4
A464	+	+	+	+	-	-	+	+	+	+	+	+	-	-	-		-	-	NT	NT	NT	NT	NT	NT	ND	4
A468	+	+	+	+	-	-	+	+	+	+	+	+	-	-	-		-	-	NT	NT	NT	NT	NT	NT	ND	1
A469	+	+	+	+	+	+	+	+	+	+	+	+	-	-	-		+	-	NT	NT	NT	NT	NT	NT	ND	2
A472	+	+	+	+	+	+	+	+	+	+	+	+	-	-	-		+	-	92,8	1,7	112,6	1,8	123,4	0	0,90	2
A473	+	+	+	+	+	+	+	+	+	+	+	+	-	-	-		+	-	NT	NT	NT	NT	NT	NT	ND	1
A474	+	+	+	+	-	-	+	+	+	+	+	+	-	-	-		-	-	NT	NT	NT	NT	NT	NT	ND	1
A479	+	+	+	+	-	-	+	+	+	+	+	+	-	-	-		-	-	NT	NT	NT	NT	NT	NT	ND	2
A483	+	+	+	+	+	-	+	+	+	+	+	+	-	-	-		+	-	NT	NT	NT	NT	NT	NT	ND	4
A486	+	+	+	+	-	-	+	+	+	+	+	+	-	-	-		-	-	NT	NT	NT	NT	NT	NT	ND	4
A491	+	+	+	+	-	-	+	+	+	+	+	+	-	-	-		-	-	NT	NT	NT	NT	NT	NT	ND	1

[1] Results are shown as presence (+) or absence (-) of the corresponding amplicon

[2] Total iron-iron chelating activity in the supernatant of bacterial cultures grown for 18 h in CAA medium was determined by the CAS liquid assay (Schwyn and Neilands, 1987), and expressed as the percentage of siderophore units normalized to the cell density (OD_{xxx}) of the culture

[3] The amount of catechol groups in the supernatant of bacterial cultures grown for 18 h in CAA medium was determined by the Arnow test (Arnow, 1937), and normalized to the cell density (OD_{600}) of the culture

[4] The amount of hydroxamate groups in the supernatant of bacterial cultures grown for 18 h in CAA medium was determined by the Csáky test as modified by Gilliam et al. (1981), and normalized to the cell density (OD_{600}) of the culture

[5] The catechol and hydroxamate values obtained under iron-chelated conditions (low iron) were subtracted by the corresponding values obtained under iron-repleted conditions (high iron). The reported values represent the ratio between catchol and hydroxamate groups produced under iron depletion

[6] Numbers refer to the genetic clusters shown in Fig. 2 (1. ferrous iron uptake; 2. heme uptake; 3. heme uptake; 4. acinetobactin synthesis/transport; 5. putative hydroxamate syderophore synthesis/transport; 6 putative hydroxamate syderophore synthesis/transport)

[7] Low iron and high iron stand for iron-chelated (CAA medium plus 100 μM 2,2-dipyridyl) and iron-repleted (CAA medium plus 100 μM $FeCl_3$) growth conditions, respectively

[8] NT, not tested; ND, not determined

[9] NV, new variant SG. The strains ATCC 17978 and A37 showed allelic profiles which differ from each other and from those previously described (Towner, 2009)

Chapter 5

Evidence of diversity among epidemiologically related carbapenemase-producing *Acinetobacter baumannii* strains belonging to international clonal lineage II

Fabrizia Minandri[1], Silvia D'Arezzo[2], Luísa C. S. Antunes[1], Christine Pourcel[3], Luigi Principe[2], Nicola Petrosillo[2], and Paolo Visca[1]

[1]Department of Biology, University Roma Tre, Rome, Italy

[2]National Institute for Infectious Diseases Lazzaro Spallanzani, IRCCS, Rome, Italy

[3]Institute of Genetics and Microbiology, CNRS, University Paris-Sud, Orsay, France

J Clin Microbiol 50 (2012): 590-597

Abstract

Acinetobacter baumannii is the most important pathogenic species of genus *Acinetobacter*, but it is often phenotypically indistinguishable from related, less dangerous, *A. calcoaceticus*, *A. pittii* and *A. nosocomialis*. In addition, *A. baumannii* isolates can be phenotypically similar but have different origin and pathogenic potential. Therefore, there is a need to develop fast and cost-restrained strain differentiation systems in the hospital practice. Other organisms that are endowed with multiple iron uptake capabilities, such as *Pseudomonas spp.*, can be differentiated at species- and strain- levels by siderophore-based typing (siderotyping) based on the structural diversity of pyoverdine siderophores they produce.

Previously, multiple gene clusters for putative or confirmed *A. baumannii* iron uptake systems were identified (**Chapter 4**). In this study, siderotyping based on the genetic potential to produce siderophores or use exogenous iron sources was used as an attempt to discriminate a very homogenous population of isolates. All isolates belonged to the international clone II and could not be distinguished by PFGE, RAPD or MLST, but only by MLVA. The results of this study indicated that the whole panel of strains shared the same profile of iron-utilisation genes, and therefore the same siderotype.

Therefore, it can be concluded that siderotyping should not be used for the fine-typing of very homogenous *A. baumannii* isolates. Additionally, the broad iron uptake capability of the strains investigated indicates the importance of iron uptake to the nosocomial success of the international clone II.

JCM
Journals.ASM.org

Evidence of Diversity among Epidemiologically Related Carbapenemase-Producing *Acinetobacter baumannii* Strains Belonging to International Clonal Lineage II

Fabrizia Minandri,[a] Silvia D'Arezzo,[b] Luísa C. S. Antunes,[a] Christine Pourcel,[c] Luigi Principe,[b] Nicola Petrosillo,[b] and Paolo Visca[a]

Dipartimento di Biologia, Università Roma Tre,[a] and Istituto Nazionale per le Malattie Infettive Lazzaro Spallanzani IRCCS,[b] Rome, Italy, and Université Paris-Sud, Institut de Génétique et Microbiologie, CNRS, Orsay, France[c]

Carbapenem-resistant *Acinetobacter baumannii* strains belonging to international clonal lineage II (ICL-II) have become predominant in intensive care units (ICUs) throughout Italy. Between 2005 and 2009, the carbapenem-hydrolyzing class D β-lactamase (CHDL) bla_{OXA-23} gene became more prevalent than bla_{OXA-58} among epidemic ICL-II strains showing extensive genetic similarity. These findings posed the question of whether CHDL gene replacement occurred in the homogeneous ICL-II population or a new OXA-23 clone(s) emerged and spread in ICUs. In this study, the changes in the ICL-II *A. baumannii* population and CHDL gene carriage were investigated in 30 genetically related isolates collected during the bla_{OXA-58}-to-bla_{OXA-23} transition period. Pulsotyping, randomly amplified polymorphic DNA (RAPD) analysis, and multilocus sequence typing (MLST) results were combined with multilocus variable-number tandem-repeat (VNTR) analysis (MLVA-8), siderotyping, and plasmid profiling to improve genotype-based discrimination between isolates. Pulsotyping, RAPD analysis, and MLST clustered isolates into a single type. MLVA-8 identified 19 types that clustered into three complexes. All OXA-23-producing isolates formed a single complex, while OXA-58 producers were split into two complexes. Southern blot analysis of the physical localization and genetic context of the CHDL genes showed that bla_{OXA-58} was invariably located on plasmids, while bla_{OXA-23} was present within Tn*2006* on the chromosome or both the chromosome and plasmids. These data indicate that the apparently homogeneous population of CHDL-producing ICL-II strains was composed of several independent strains and that, between 2005 and 2009, distinct OXA-23 producers displaced the preexisting OXA-58 producers. Thus, MLVA-8 appears to be a suitable tool not only for investigating *A. baumannii* population structure but also for high-resolution epidemiological typing.

The Gram-negative coccobacillus *Acinetobacter baumannii* has emerged as a leading cause of nosocomial infections, particularly among critically ill patients in intensive care units (ICUs) (22, 38). Features contributing to *A. baumannii* pathogenicity are resistance to a broad range of antimicrobial agents and to environmental stresses, persistence in the hospital setting, and the tendency for epidemic spread (9, 38, 45). Carbapenems have been used widely to treat serious infections associated with multidrug-resistant (MDR) *A. baumannii*, but a trend of increasing resistance to these drugs, associated with the production of acquired carbapenem-hydrolyzing OXA-type class D β-lactamases (CHDLs), has been reported worldwide in the past decade (23, 47). Four main families of CHDL genes have been described for *A. baumannii*, namely, the intrinsic chromosomally and/or plasmid-located $bla_{OXA-51-like}$ gene family (4) and the acquired $bla_{OXA-23-like}$, $bla_{OXA-24/40-like}$, and $bla_{OXA-58-like}$ gene families (23). The $bla_{OXA-58-like}$ genes are found mostly on plasmids, in association with the insertion sequences IS*Aba1*, IS*Aba2*, IS*Aba3*, and IS*18* (2, 42), whereas $bla_{OXA-23-like}$ genes can be found either on the chromosome or on plasmids, in association with IS*Aba1* within Tn*2006* and Tn*2008* transposons or with IS*Aba4* in Tn*2007* (5, 21).

Three epidemic lineages, referred to as international clonal lineages (ICLs), are responsible for the majority of *A. baumannii* infections worldwide (reviewed in references 9 and 45). Strains belonging to ICL-II are widespread throughout Europe, with a number of epidemiological studies reporting the high frequency of OXA-58 producers and the recent emergence of OXA-23 producers within this lineage (2, 5, 6, 7, 10, 12, 13, 19). In a previous survey, a progressive change from bla_{OXA-58} to bla_{OXA-23} gene carriage was observed between 2005 and 2009 among MDR ICL-II *A. baumannii* isolates responsible for ICU outbreaks in the main hospitals of central Italy (6, 7). All isolates from the transition period were epidemiologically related and disclosed extensive genetic similarity (7). These observations posed the question of whether a genetic mechanism causing CHDL gene slippage within a single clone or replacement of one epidemic clone by another had occurred.

Multiple-locus variable-number tandem-repeat (VNTR) analysis (MLVA) is a molecular typing technique which combines portability, high resolution, and cost-effectiveness (44). An MLVA-8 scheme based on the analysis of eight VNTRs was recently developed for *A. baumannii*, and preliminary assessment using a panel of diverse isolates showed an excellent typing performance and high discriminatory power (25).

In this work, we used MLVA-8 to investigate the structure of a representative panel of CHDL-producing *A. baumannii* isolates belonging to ICL-II that circulated in central Italy during the OXA-58-to-OXA-23 transition period.

Received 24 August 2011 Returned for modification 23 September 2011
Accepted 17 December 2011
Published ahead of print 28 December 2011
Address correspondence to Paolo Visca, visca@uniroma3.it.
Supplemental material for this article may be found at http://jcm.asm.org/.

doi:10.1128/JCM.05555-11

MATERIALS AND METHODS

Bacterial isolates. A panel of 30 nonduplicate MDR *A. baumannii* isolates from various clinical specimens from patients hospitalized in eight ICUs of main hospitals of the Rome urban area (labeled G, C, H, I, L, M, N, and P), including the prototype ICL-II strain ACICU (17), was selected from the well-characterized collection of Gruppo Romano *A. baumannii* (GRAB) (6, 7) (see Table S1 in the supplemental material). All isolates had previously been identified as belonging to ICL-II by PCR-based sequence group (SG) determination, with only one isolate (221M) showing a new SG profile related to that of ICL-II (6, 7, 43). Selection criteria for inclusion of *A. baumannii* isolates in the panel were as follows: (i) an identical or highly similar pulsotype and randomly amplified polymorphic DNA (RAPD) profile; (ii) carriage of either the $bla_{\text{OXA-58}}$ or $bla_{\text{OXA-23}}$ gene, with the exception of two carbapenemase-negative isolates (106H and 136L) that were used as internal controls; and (iii) an isolation date in the transition period between $bla_{\text{OXA-58}}$ and $bla_{\text{OXA-23}}$ gene carriage epidemicity (7). The panel was therefore composed of 15 $bla_{\text{OXA-58}}$-positive isolates, 13 $bla_{\text{OXA-23}}$-positive isolates, and two carbapenemase-negative isolates, collected between June 2005 and October 2008 (see Table S1). IS*Aba1* was present upstream of the $bla_{\text{OXA-23}}$ gene in all OXA-23-producing isolates, whereas it was not found upstream of the $bla_{\text{OXA-58}}$ gene among OXA-58-producing isolates (7). Other relevant characteristics of these isolates, including antibiotic resistance profiles (7) and the presence of the origin of replication of plasmid pACICU1 (*repAci1* gene) (17), are summarized in Table S1.

RAPD analysis, pulsotyping, and MLST. All isolates were typed by RAPD analysis with the DAF4 primer (14) and by macrorestriction analysis of ApaI-digested genomic DNA followed by pulsed-field gel electrophoresis (PFGE) (33). Electropherograms were analyzed using BioNumerics, version 5.1 (Applied Maths, Sint-Martems-Latem, Belgium), as previously described (37, 40). Similarity thresholds of ≥72% and ≥85% were used to define isolates belonging to the same RAPD and PFGE types, respectively (37, 40). Multilocus sequence typing (MLST) was performed by double-stranded DNA sequencing of internal regions of seven housekeeping genes, namely, *cpn60*, *fusA*, *gltA*, *pyrG*, *recA*, *rplB*, and *rpoB* (8), and sequence type (ST) results were retrieved from the database available at the Institut Pasteur (Paris, France) MLST website (http://www.pasteur.fr/mlst).

Siderotyping. PCR amplification of 16 *A. baumannii* genes representative of six previously identified putative iron utilization clusters was performed on genomic DNA as previously described (1). The chrome azurol S (CAS) agar assay for detection of siderophore activity (31) was also performed.

MLVA-8 typing. The occurrence of L-repeat VNTRs (Abaum_1988, Abaum_2240, Abaum_3002, and Abaum_3530) and S-repeat VNTRs (Abaum_0826, Abaum_0845, Abaum_2396, and Abaum_3468) was investigated by PCR amplification of *A. baumannii* genomic DNA by use of oligonucleotide primers targeting the 5′- and 3′-flanking regions of the eight VNTR loci (25). After agarose gel electrophoresis, the sizes of amplicons were determined using BioNumerics software (Applied Maths). The allelic profile, or MLVA-8 type, was defined by the number of repeats estimated at each VNTR locus in the predefined order of the previously established MLVA-8 scheme (25; http://mlva.u-psud.fr/MLVAnet/). MLVA-8 types were analyzed as character data sets by BioNumerics software (Applied Maths), and a dendrogram was created using the categorical coefficient and the unweighted-pair group method using average linkages (UPGMA). A similarity threshold of ≥62.5% was used to define isolates belonging to the same MLVA-8 complex, i.e., groups of related MLVA-8 types (25). The polymorphism index for individual or combined VNTR loci was expressed as the Hunter-Gaston diversity index (HGDI), an application of Simpson's diversity index (16, 34).

Plasmid analysis. Plasmid DNAs were extracted from *A. baumannii* isolates by the alkaline lysis method of Kado and Liu (18), modified by incubating the cells in 1× E buffer (40 mM Tris-acetate, 2 mM EDTA [30], pH 12.6) for 1 h at 65°C during the lysis step. This step optimizes the yield of supercoiled plasmid DNA while minimizing contamination by open circular or linear plasmid isoforms and chromosomal DNA. Plasmids were separated by vertical electrophoresis on a 0.8% agarose gel (Bio-Rad) prepared in 1× E buffer (18) and were visualized under UV illumination upon ethidium bromide staining.

Southern blot hybridization of undigested plasmids was performed under conditions of high stringency (30). DNA was transferred onto a positively charged nylon membrane (Hybond N$^+$; Amersham Pharmacia Biotech, United Kingdom) and hybridized overnight with $bla_{\text{OXA-58}}$- and $bla_{\text{OXA-23}}$-specific gene probes at 44°C and 49°C, respectively. The $bla_{\text{OXA-58}}$- and $bla_{\text{OXA-23}}$-negative isolate 136L was included as a negative control. Probes were generated by PCR digoxigenin (DIG) labeling using a commercial kit (Roche Diagnostics, Monza, Italy). Probes consisted of internal 529-bp and 501-bp fragments of the $bla_{\text{OXA-58}}$ and $bla_{\text{OXA-23}}$ genes, respectively. Primer pairs were OXA58A plus OXA58B (24) for the $bla_{\text{OXA-58}}$ probe and OXA-23A plus OXA-23B (15) for the $bla_{\text{OXA-23}}$ probe. Detection was performed with a DIG DNA detection kit (Roche Diagnostics) according to the manufacturer's instructions.

Determination of the $bla_{\text{OXA-23}}$ gene's surrounding region. Total *A. baumannii* DNA was digested with HindIII, separated by electrophoresis on a 0.8% agarose gel (Bio-Rad) in 1× Tris-borate-EDTA buffer (30) in a vertical apparatus, and then transferred to a Hybond N$^+$ membrane (Amersham Pharmacia Biotech). The membrane was hybridized overnight at 49°C with the $bla_{\text{OXA-23}}$ probe. The $bla_{\text{OXA-58}}$- and $bla_{\text{OXA-23}}$-negative isolate 136L was included as a negative control. The DNA regions flanking the $bla_{\text{OXA-23}}$ gene were identified by PCR and sequence analysis using the following primer pairs: ISAba1F (42) and OXA23B (15), F2 (5′-CCCAATTAGCACATACACAGC-3′) and R2 (5′-CGCTCTAGACGCTCTTCATC-3′), and F3 (5′-TATTACGAGATTCGAAGGCG-3′) and R3 (5′-CTTGGAAATACGCGCTTGAC-3′). Primers were designed to generate overlapping fragments encompassing the Tn*2006* sequence (GenBank accession no. EF127491.1).

RESULTS

RAPD, PFGE, and MLST analyses of CHDL-producing ICL-II *A. baumannii* isolates. All isolates were clustered within a single RAPD or PFGE type according to the predefined similarity threshold of ≥72% (37) or ≥85% (40), respectively (Fig. 1A and B). All isolates belonged to ST2, and all but two were characterized by the MLST allelic profile 2-2-2-2-2-2-2. The ST2 strains 149N and 150N carried a variant *rpoB* locus with a C→T substitution at position 68 (99.78% identity to allele 2).

Better discrimination of isolates was achieved by increasing the similarity threshold for both RAPD analysis and PFGE to ≥90%, resulting in the definition of four and three clusters, respectively. Both RAPD analysis and PFGE clustered the isolates according to hospital of origin, while occasionally failing at grouping isolates according to CHDL gene carriage, irrespective of the similarity threshold used (Fig. 1A and B). For instance, the RAPD profiles of the $bla_{\text{OXA-58}}$-positive isolates 218M and 174P were more related to the profiles of $bla_{\text{OXA-23}}$-positive isolates collected in the corresponding hospitals (82.4% similarity with isolates from hospitals M and P) than to those of other $bla_{\text{OXA-58}}$-positive isolates, which were all characterized by an identical pattern (Fig. 1A). Likewise, the $bla_{\text{OXA-58}}$-positive isolate 174P clustered in the main group of $bla_{\text{OXA-23}}$-positive isolates according to PFGE analysis (Fig. 1B). Intriguingly, the $bla_{\text{OXA-58}}$-positive isolate 174P was indistinguishable from $bla_{\text{OXA-23}}$-positive isolate 175P, which was collected 1 day apart in hospital P (Fig. 1B).

ICL-II *A. baumannii* isolates share a siderotype and a broad iron uptake capability. The presence of 16 genes belonging to putative iron utilization clusters previously identified in *A. baumannii* (1) was assessed by PCR. Five gene clusters, including one

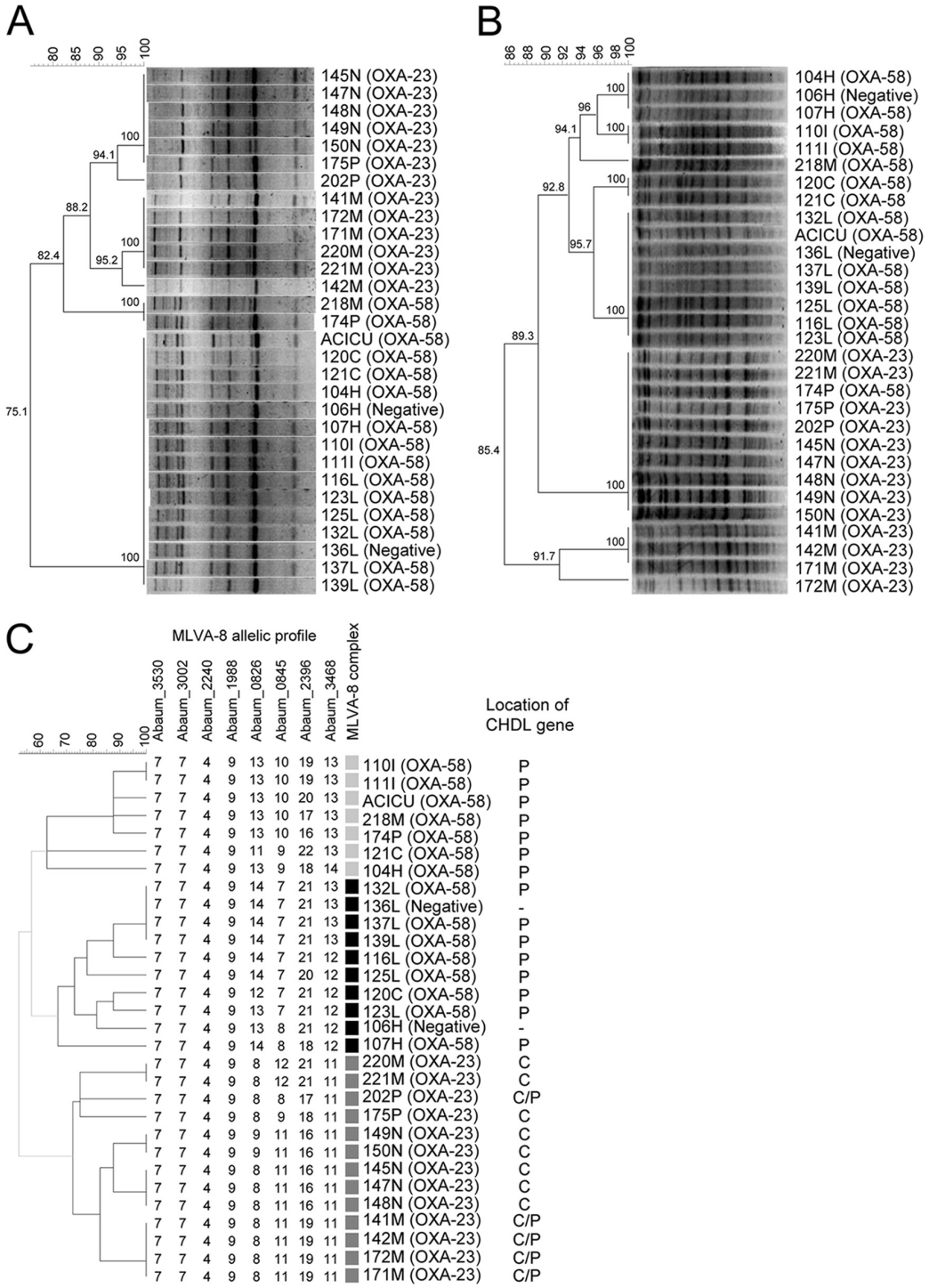

FIG 1 Cluster analysis of 30 *A. baumannii* strains analyzed by RAPD analysis with the primer DAF4 (A), PFGE following ApaI digestion (B), and MLVA-8 (C). Gel images were analyzed with BioNumerics software. Dendrograms A and B were generated using the Dice coefficient and UPGMA clustering, with a 1.5% optimization and 0.5% or 1.5% tolerance limit for RAPD or PFGE analysis, respectively (37, 40). Similarity thresholds of ≥72% and ≥85% were used to define isolates belonging to the same RAPD and PFGE types, respectively (37, 40). MLVA-8 types were analyzed as a character data set by BioNumerics software, using the categorical coefficient and UPGMA clustering. MLVA-8 complexes were defined using a similarity threshold of ≥62.5% (25). The OXA-58-A complex is labeled with light gray, the OXA-58-B complex with black, and the OXA-23 complex with dark gray. The localization of CHDL genes was determined by Southern blotting. P, plasmid; C, chromosome. The CHDL gene carriage of each strain is indicated in parentheses.

for the acinetobactin siderophore (open reading frames [ORFs] ACICU_02570, ACICU_02580, ACICU_02581, and ACICU_02588), one for a hydroxamate-type siderophore (ORFs ACICU_01673, ACICU_01679, and ACICU_01683), one for ferrous iron uptake (Feo; ORF ACICU_00266), and two for putative heme utilization systems (ORFs ACICU_01629, ACICU_01633, and ACICU_01639 and ORFs ACICU_00875 and ACICU_00879), were present in all isolates (data not shown). Notably, one of the putative heme utilization clusters, coding for a heme outer membrane receptor and a heme oxygenase (ORFs ACICU_00875 and ACICU_00879, respectively), which is variably present among ICL-II *A. baumannii* clinical isolates due to the high recombination frequency of the surrounding region (1, 36), was conserved in all isolates of the panel (see Fig. S1 in the supplemental material). Amplification was not observed for a second hydroxamate-type siderophore cluster (ORFs A1S_2566, A1S_2572, and A1S_2581) previously detected in strain ATCC 17978, which does not belong to any ICL (1, 35). Overall, the tested *A. baumannii* isolates shared the coding potential for at least five putative iron utilization clusters, and accordingly, all reacted positively on CAS agar plates for siderophore production (data not shown).

MLVA-8 typing of ICL-II *A. baumannii* defines clonal complexes which correlate with CHDL gene carriage. MLVA-8 genotyping yielded PCR products for L-repeat and S-repeat VNTR loci for all *A. baumannii* isolates. Fragments ranging in size from 154 bp to 826 bp were generated and resolved with sufficient accuracy by agarose gel electrophoresis. No half-sized allelic variants were observed. Identical allelic profiles for L-repeat VNTRs were obtained for all isolates (Fig. 1C), consistent with the low level of polymorphism of these slowly evolving VNTR loci (25). Greater diversity was observed at S-repeat VNTRs (see Fig. S2 in the supplemental material), resulting in HGDI values ranging from 0.68 (Abaum_3468) to 0.82 (Abaum_2396). Isolates were distinguished by 19 different MLVA-8 types, as represented by individual allelic profiles, yielding a combined HGDI value of 0.95 for the MLVA-8 assay. The 19 different MLVA-8 types were grouped into three MLVA-8 complexes, named OXA-58-A, OXA-58-B, and OXA-23, according to a reference similarity threshold of ≥62.5% (25) (Fig. 1C).

The OXA-58-A complex included six MLVA-8 types assigned to seven OXA-58-producing isolates, almost all collected from different hospitals (Fig. 1C). The allelic profiles of this complex differed markedly at the Abaum_2396 S-repeat locus, for a maximum difference of six repeat units (Fig. 1C).

The OXA-58-B complex comprised seven MLVA-8 types assigned to 10 isolates, including 8 $bla_{\text{OXA-58}}$-positive isolates and 2 isolates negative for both CHDL genes, with 4 isolates from hospital L sharing the same allelic profile (Fig. 1C). MLVA-8 allelic profiles within this complex were more similar at the level of S-repeat VNTRs, with a maximum difference of three repeat units at the Abaum_2396 locus (Fig. 1C).

The OXA-23 complex included all 13 OXA-23-producing isolates (Fig. 1C). Isolates from hospitals M and N were distributed into four MLVA-8 types according to hospital of origin, with the exception of isolate 218M, which clustered apart, in the OXA-58-A complex (Fig. 1C). Isolates 202P and 175P from hospital P showed distinct MLVA-8 types within the OXA-23 complex and were clearly distinguishable from the $bla_{\text{OXA-58}}$-positive isolate 174P (Fig. 1C). Overall, MLVA-8 defined complexes that correlate well with both CHDL gene carriage and hospital of origin.

Plasmid profiles and localization of CHDL determinants in ICL-II *A. baumannii* isolates. The OXA-58-producing *A. baumannii* isolates disclosed heterogeneous plasmid profiles, generated by the presence of differently sized plasmids and/or different isoforms of the same plasmid (Fig. 2A). As predicted, two bands were observed for the prototypic ICL-II strain ACICU (Fig. 2A), likely corresponding to plasmids pACICU1 and pACICU2, of 28.2 kb and 64.3 kb, respectively (17). Conversely, OXA-23-producing isolates showed more homogeneous profiles, with a conserved small plasmid in all isolates, with the exception of 202P, for which a larger plasmid band was observed (Fig. 2B). In addition, high-molecular-weight plasmid bands were observed for all OXA-23-producing isolates from hospital M (Fig. 2B). However, a difference in size was noted between the large plasmid band of isolates 141M, 142M, 172M, and 171M and that of isolates 220M and 221M (Fig. 2B). Residual chromosomal DNA was obtained upon alkaline extraction in both experiments (Fig. 2A and B).

Southern blot hybridization with the $bla_{\text{OXA-58}}$ probe yielded several distinct positive signals that could not be associated with the chromosomal DNA, suggesting a plasmid localization of the CHDL determinant and extensive size variability among plasmids harboring the $bla_{\text{OXA-58}}$ gene (Fig. 2C). As expected, a single signal corresponding to the pACICU1 plasmid, which contains two copies of the $bla_{\text{OXA-58}}$ gene (2), was observed for the ACICU strain (Fig. 2C). Hybridization with the $bla_{\text{OXA-23}}$ probe yielded a positive signal corresponding to the chromosomal DNA band for all isolates (Fig. 2D). Additional positive signals were associated with the large plasmid(s) of isolates 141M, 142M, 172M, and 171M and the small plasmid of isolate 202P (Fig. 2D).

The DNA region surrounding the $bla_{\text{OXA-23}}$ gene was investigated by Southern blot hybridization with the $bla_{\text{OXA-23}}$ probe and HindIII-digested total DNA. A single hybridization signal of approximately 2.9 kb was observed for all isolates (Fig. 3A), irrespective of the plasmid or chromosomal localization of the $bla_{\text{OXA-23}}$ gene, consistent with the location of the IS*Aba1*-associated $bla_{\text{OXA-23}}$ gene within a Tn*2006*-like transposon structure (Fig. 3B). This organization was confirmed by sequence analysis of PCR products for regions surrounding the $bla_{\text{OXA-23}}$ gene in all OXA-23-producing *A. baumannii* isolates (Fig. 3B), showing 99% identity to the deposited sequence of Tn*2006* (21).

Lastly, no hybridization signal with either the $bla_{\text{OXA-58}}$- or $bla_{\text{OXA-23}}$-specific probe was observed in both clear lysates and HindIII digests from isolate 136L, used as a negative control (Fig. 2C and D and 3A).

DISCUSSION

Since 2004, an increasing incidence of carbapenem resistance has been reported among MDR ICL-II *A. baumannii* isolates from several ICUs in Italy (6, 7, 10, 12, 13, 19, 20, 28). Between 2005 and 2009, the $bla_{\text{OXA-58}}$ determinant was completely displaced by $bla_{\text{OXA-23}}$ among epidemiologically related ICL-II *A. baumannii* isolates from central Italy (7).

In the present study, the molecular epidemiology of the isolates and the genetic context of CHDL genes were investigated in a representative panel of 30 MDR ICL-II *A. baumannii* isolates collected during the OXA-58-to-OXA-23 transition period. ApaI-PFGE typing and DAF4-RAPD analysis clustered all isolates within a single type by use of standard similarity thresholds, in-

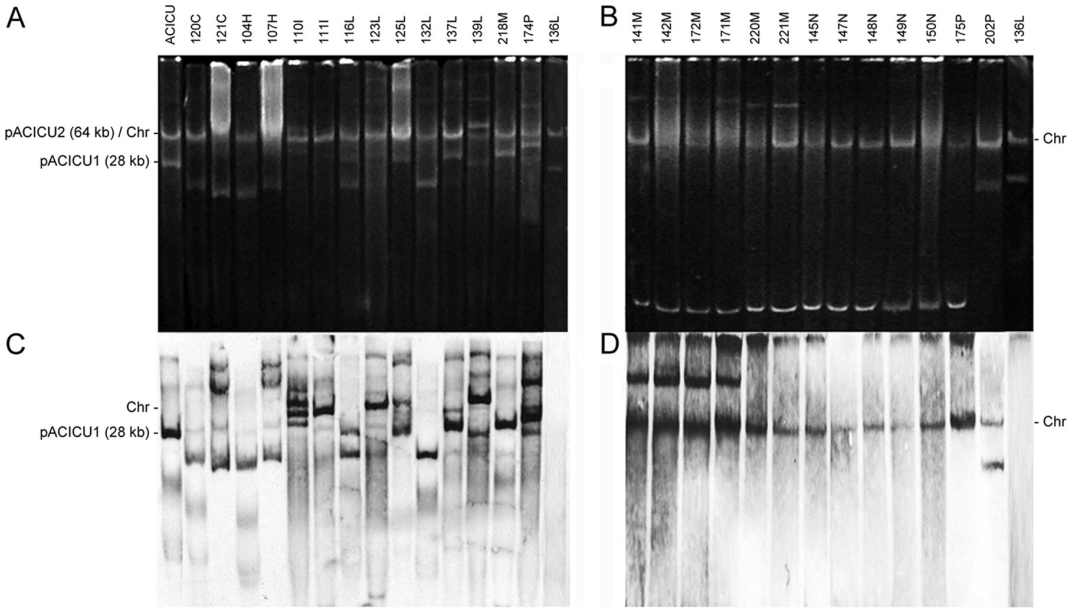

FIG 2 Plasmid profiles and localization of CHDL genes in 15 OXA-58-producing (A and C) and 13 OXA-23-producing (B and D) *A. baumannii* isolates. The images shown are electropherograms on 0.8% agarose gels in 1× E buffer for undigested plasmid DNA preparations stained with ethidium bromide and visualized under UV light. OXA-58- and OXA-23-producing isolates are arranged in hospital order. The bla_{OXA-58}- and bla_{OXA-23}-negative isolate 136L was included as a negative control. Southern blot hybridizations were performed with specific probes for the bla_{OXA-58} (C) and bla_{OXA-23} (D) genes. The sizes of the pACICU1 and pACICU2 plasmids are indicated on the left. Chr, residual chromosomal DNA.

cluding both OXA-58 and OXA-23 producers as well as two carbapenem-susceptible isolates (Fig. 1A and B), with some isolates showing identical fingerprints in spite of their differences in CHDL gene carriage. Consistent with the genetic homogeneity of the selected isolates, MLST showed that all isolates belonged to ST2 and had identical or slightly variant allelic profiles. Siderotyping was used in an attempt to differentiate isolates according to their genetic potential to produce siderophores or utilize exogenous iron sources. This typing approach is suited for bacterial species endowed with multiple iron uptake capabilities and has been applied successfully to *Pseudomonas* typing (3). The whole panel of ICL-II *A. baumannii* isolates showed the same siderotype and released iron-chelating activity in low-iron medium. All isolates carried a complete repertoire of iron uptake genes, particularly those in the locus from ACICU_00875 to ACICU_00879, which is variably present among ICL-II *A. baumannii* strains due to excision events in a region of high recombination frequency (see Fig. S1 in the supplemental material) (1, 36). Overall, such broad iron uptake capability likely contributes to the ecological success of ICL-II both in the environment and in the infected host.

Altogether, the typing results argued for the existence of a highly conserved genetic background in our collection of ICL-II *A. baumannii* isolates and did not provide an answer to the question of whether the recently emerged OXA-23-producing strains originated from the previous population of OXA-58 producers. MLVA was used here to address this question.

MLVA is recognized as the reference typing method for several bacterial species, with applications for evolutionary studies (26, 27, 46) and for subspecies identification (11, 29, 41). The previously developed MLVA-8 scheme (25) was validated here for the purpose of fine typing of the *A. baumannii* panel, in combination with plasmid profiling and CHDL gene localization. Nineteen different MLVA-8 types were assigned to 30 isolates (Fig. 1C), yielding excellent discrimination (HGDI = 0.95). All of the isolates, including the prototypic ICL-II strain ACICU, shared the same allelic profile at L-repeat VNTRs (Fig. 1C), which was also identical to the L-repeat profile previously determined for ICL-II strains (profile 7,7,4,9) (25). This observation corroborates our previous suggestion that L-repeat loci are suitable for establishing phylogenetic relationships among strains evolving over a long period and make it possible to cluster *A. baumannii* strains into clonal complexes that correlate well with ICLs (25). Conversely, S-repeat VNTRs provided greater discrimination and more subtle diversification of isolates. An in-depth analysis of the MLVA-8 allelic profiles showed that changes were often limited to the addition or deletion of one repeat unit at S-repeat VNTRs, in particular at the most polymorphic VNTR locus, Abaum_2396 (Fig. 1C).

Three major groups were recognized according to MLVA-8 allelic profiles (Fig. 1C). The 15 OXA-58-producing isolates were distributed in 12 MLVA-8 types within two complexes, OXA-58-A and OXA-58-B (Fig. 1C). Such diversity was also apparent at the extrachromosomal DNA level, as testified by the diverse plasmid profiles observed among OXA-58 producers (Fig. 2A) and by the variable electrophoretic mobility of plasmids carrying the bla_{OXA-58} gene (Fig. 2C). Remarkably, some epidemiologically related bla_{OXA-58}-positive isolates endowed with identical RAPD, PFGE, and MLVA-8 types were clearly differentiated according to their plasmid content. This held true for isolates 110I and 111I from the OXA-58-A complex and for isolates 132L, 137L, and 139L from the OXA-58-B complex (Fig. 2A). These findings are consistent with the notion that differences exist in the accessory

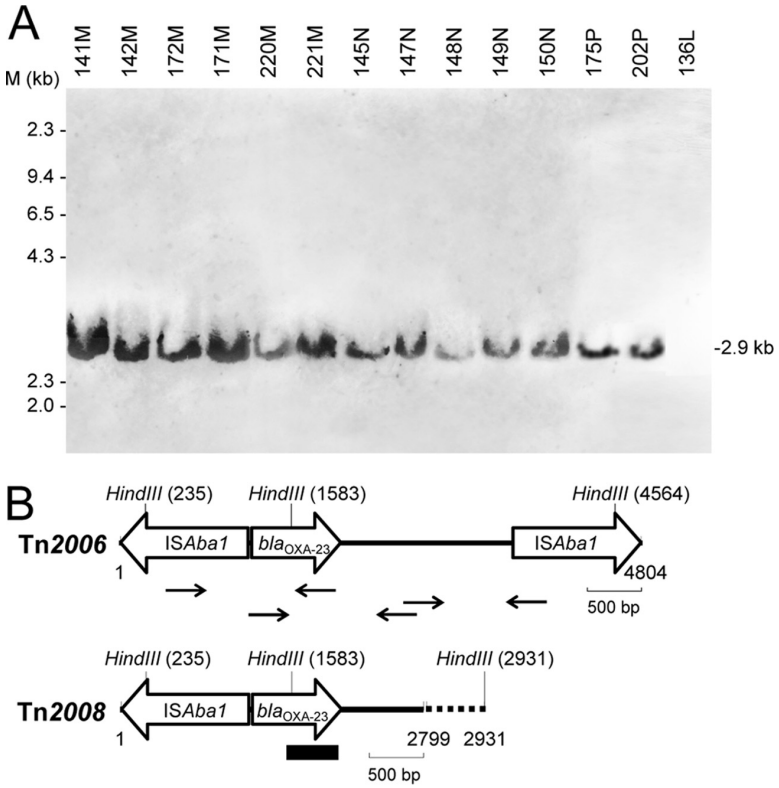

FIG 3 (A) Southern blot hybridization with the bla_{OXA-23} probe of HindIII-digested chromosomal DNAs from OXA-23-producing *A. baumannii* isolates. M, HindIII-digested lambda DNA molecular mass marker (Invitrogen). The bla_{OXA-58}- and bla_{OXA-23}-negative isolate 136L was included as a negative control. (B) Comparison of known transposon structures harboring the IS*Aba1*-associated bla_{OXA-23} gene in ICL-II *A. baumannii* isolates. Coding sequences are indicated by large open arrows. Restriction sites for HindIII, with their positions, are indicated. Primer pairs used for amplification and sequence analysis of the DNA regions flanking the bla_{OXA-23} gene are shown as black arrows. The bla_{OXA-23} gene-specific probe used for Southern blot hybridization is shown as a black rectangle.

genome, including plasmids, among highly related *A. baumannii* strains (32, 39).

The 13 OXA-23-producing isolates were distinguished by six MLVA-8 types within the single OXA-23 complex (Fig. 1C). Identical plasmid profiles were observed for isolates assigned to the same MLVA-8 type (Fig. 2B). Southern blotting revealed a chromosomal location of the bla_{OXA-23} gene in all OXA-23 producers, with five isolates showing an additional plasmid location of the gene (Fig. 2D). The IS*Aba1*-associated bla_{OXA-23} gene was invariably present in a Tn*2006*-like arrangement (Fig. 3A), irrespective of the chromosomal or plasmid localization. Overall, plasmid profiles of OXA-23-producing isolates were congruent with their MLVA-8 type. Isolate 202P, which carried the bla_{OXA-23} gene on a typical low-molecular-mass plasmid (Fig. 2D), was classified as a distinct type by MLVA-8 (Fig. 1C) and showed a distinct plasmid profile compared with the other OXA-23 producers (Fig. 2B). Isolates 141M, 142M, 171M, and 172M, all carrying the bla_{OXA-23} gene on both the chromosome and a large plasmid (Fig. 2D), shared a typical MLVA-8 allelic profile that was clearly distinct from that of other OXA-23 producers (Fig. 1C), particularly isolates 220M and 221M (from the same hospital). It is tempting to hypothesize that the OXA-23 producers 141M, 142M, 171M, and 172M represent a clonal variant in which plasmid amplification of the bla_{OXA-23} determinant occurred, likely driven by Tn*2006*-mediated recombination (21).

MLVA-8 provided a meaningful tool for establishing epidemiological correlations between isolates and helped to resolve some ambiguities generated by PFGE and/or RAPD analysis. As an example, MLVA-8 provided evidence that 174P and 175P, obtained 1 day apart from different patients during an outbreak in hospital P, are unrelated isolates, since they belong to distinct complexes and, accordingly, carry different CHDL genes and differently sized plasmids (Fig. 1C and 2).

In conclusion, the data presented here provide evidence that ICL-II *A. baumannii* isolates endowed with a high level of genetic similarity and showing extensive epidemiological correlations can be resolved into several types by means of MLVA-8. The identification within a hospital of isolates belonging to the same MLVA-8 complex but characterized by different allelic profiles at S-repeat VNTRs suggests that evolution could take place from an outbreak strain into independent variants, likely as the result of local selective pressure. Therefore, the increased circulation of bla_{OXA-23}-positive isolates in central Italy can be attributed to the emergence of different clones (corresponding to six MLVA-8 types) within the OXA-23 complex, which displaced the preexisting bla_{OXA-58}-positive populations. MLVA-8 can therefore be regarded as a suitable method

not only for large population studies but also for fine typing of *A. baumannii* during outbreak investigations and hospital surveillance studies.

ACKNOWLEDGMENTS

We thank GRAB members (A. Capone, M. Ballardini, S. Bartolini, E. Bordi, A. Di Stefano, M. Galiè, R. Minniti, M. Meledandri, L. Pacciani, G. Parisi, G. Prignano, C. Santini, M. Valmarin, M. Venditti, and S. Ziantoni) for providing *A. baumannii* isolates and K. J. Towner for a critical reading of the manuscript.

REFERENCES

1. **Antunes LC, Imperi F, Towner KJ, Visca P.** 2011. Genome-assisted identification of putative iron-utilization genes in *Acinetobacter baumannii* and their distribution among a genotypically diverse collection of clinical isolates. Res. Microbiol. **162**:279–284.
2. **Bertini A, et al.** 2007. Multicopy bla_{OXA-58} gene as a source of high-level resistance to carbapenems in *Acinetobacter baumannii*. Antimicrob. Agents Chemother. **51**:2324–2328.
3. **Bodilis J, et al.** 2009. Distribution and evolution of ferripyoverdine receptors in *Pseudomonas aeruginosa*. Environ. Microbiol. **11**:2123–2135.
4. **Chen TL, et al.** 2010. Emergence and distribution of plasmids bearing the bla_{OXA-51}-like gene with an upstream IS*Aba1* in carbapenem-resistant *Acinetobacter baumannii* isolates in Taiwan. Antimicrob. Agents Chemother. **54**:4575–4581.
5. **Corvec S, Poirel L, Naas T, Drugeon H, Nordmann P.** 2007. Genetics and expression of the carbapenem-hydrolyzing oxacillinase gene bla_{OXA-23} in *Acinetobacter baumannii*. Antimicrob. Agents Chemother. **51**:1530–1533.
6. **D'Arezzo S, et al.** 2009. Epidemic multidrug-resistant *Acinetobacter baumannii* related to European clonal types I and II in Rome (Italy). Clin. Microbiol. Infect. **15**:347–357.
7. **D'Arezzo S, et al.** 2011. Changing carbapenemase gene pattern in an epidemic multidrug-resistant *Acinetobacter baumannii* lineage causing multiple outbreaks in central Italy. J. Antimicrob. Chemother. **66**:54–61.
8. **Diancourt L, Passet V, Nemec A, Dijkshoorn L, Brisse S.** 2010. The population structure of *Acinetobacter baumannii*: expanding multiresistant clones from an ancestral susceptible genetic pool. PLoS One **4**:e10034.
9. **Dijkshoorn L, Nemec A, Seifert H.** 2007. An increasing threat in hospitals: multidrug-resistant *Acinetobacter baumannii*. Nat. Rev. Microbiol. **5**:939–951.
10. **Di Popolo A, Giannouli M, Triassi M, Brisse S, Zarrilli R.** 2011. Molecular epidemiology of multidrug-resistant *Acinetobacter baumannii* strains in four Mediterranean countries using a multilocus sequence typing scheme. Clin. Microbiol. Infect. **17**:197–201.
11. **Elberse KE, Nunes S, Sá-Leão R, van der Heide HG, Schouls LM.** 2011. Multiple-locus variable number tandem repeat analysis for *Streptococcus pneumoniae*: comparison with PFGE and MLST. PLoS One **6**:e19668.
12. **Giannouli M, et al.** 2010. Molecular epidemiology of multidrug-resistant *Acinetobacter baumannii* in a tertiary care hospital in Naples, Italy, shows the emergence of a novel epidemic clone. J. Clin. Microbiol. **48**:1223–1230.
13. **Giordano A, et al.** 2007. Outbreak of *Acinetobacter baumannii* producing the carbapenem-hydrolyzing oxacillinase OXA-58 in Rome, Italy. Microb. Drug Resist. **13**:37–43.
14. **Grundmann HJ, et al.** 1997. Multicenter study using standardized protocols and reagents for evaluation of reproducibility of PCR-based fingerprinting of *Acinetobacter* spp. J. Clin. Microbiol. **35**:3071–3077.
15. **Héritier C, et al.** 2005. Characterization of the naturally occurring oxacillinase of *Acinetobacter baumannii*. Antimicrob. Agents Chemother. **49**:4174–4179.
16. **Hunter PR, Gaston MA.** 1988. Numerical index of the discriminatory ability of typing systems: an application of Simpson's index of diversity. J. Clin. Microbiol. **26**:2465–2466.
17. **Iacono M, et al.** 2008. Whole-genome pyrosequencing of an epidemic multidrug-resistant *Acinetobacter baumannii* strain belonging to the European clone II group. Antimicrob. Agents Chemother. **52**:2616–2625.
18. **Kado CI, Liu ST.** 1981. Rapid procedure for detection and isolation of large and small plasmids. J. Bacteriol. **145**:1365–1373.
19. **Mendes RE, et al.** 2009. Clonal dissemination of two clusters of *Acinetobacter baumannii* producing OXA-23 or OXA-58 in Rome, Italy. Clin. Microbiol. Infect. **15**:588–592.
20. **Mezzatesta ML, et al.** 2011. Epidemiological characterization and distribution of carbapenem-resistant *Acinetobacter baumannii* clinical isolates in Italy. Clin. Microbiol. Infect. doi:10.1111/j.1469-0691.2011.03527.x.
21. **Mugnier PD, Poirel L, Naas T, Nordmann P.** 2010. Worldwide dissemination of the bla_{OXA-23} carbapenemase gene of *Acinetobacter baumannii*. Emerg. Infect. Dis. **16**:35–40.
22. **Peleg AY, Seifert H, Paterson DL.** 2008. *Acinetobacter baumannii*: emergence of a successful pathogen. Clin. Microbiol. Rev. **21**:538–582.
23. **Poirel L, Nordmann P.** 2006. Carbapenem resistance in *Acinetobacter baumannii*: mechanisms and epidemiology. Clin. Microbiol. Infect. **12**:826–836.
24. **Poirel L, et al.** 2005. OXA-58, a novel class D β-lactamase involved in resistance to carbapenems in *Acinetobacter baumannii*. Antimicrob. Agents Chemother. **49**:202–208.
25. **Pourcel C, et al.** 2011. Identification of variable-number tandem-repeat (VNTR) sequences in *Acinetobacter baumannii* and interlaboratory validation of an optimized multiple-locus VNTR analysis typing scheme. J. Clin. Microbiol. **49**:539–548.
26. **Pourcel C, et al.** 2009. Improved multiple-locus variable-number tandem-repeat assay for *Staphylococcus aureus* genotyping, providing a highly informative technique together with strong phylogenetic value. J. Clin. Microbiol. **10**:3121–3128.
27. **Pourcel C, et al.** 2007. Identification of variable-number tandem-repeat (VNTR) sequences in *Legionella pneumophila* and development of an optimized multiple-locus VNTR analysis typing scheme. J. Clin. Microbiol. **45**:1190–1199.
28. **Pournaras S, et al.** 2006. Outbreak of multiple clones of imipenem-resistant *Acinetobacter baumannii* isolates expressing OXA-58 carbapenemase in an intensive care unit. J. Antimicrob. Chemother. **57**:557–561.
29. **Ramisse V, et al.** 2004. Variable number of tandem repeats in *Salmonella enterica subsp. enterica* for typing purposes. J. Clin. Microbiol. **42**:5722–5730.
30. **Sambrook J, Fritsch EF, Maniatis T.** 1989. Molecular cloning: a laboratory manual, 2nd ed. Cold Spring Harbor Laboratory, Cold Spring Harbor, NY.
31. **Schwyn B, Neilands JB.** 1987. Universal chemical assay for the detection and determination of siderophores. Anal. Biochem. **160**:46–56.
32. **Seifert H, Boullion B, Schulze A, Pulverer G.** 1994. Plasmid DNA profiles of *Acinetobacter baumannii*: clinical application in a complex endemic setting. Infect. Control Hosp. Epidemiol. **15**:520–528.
33. **Seifert H, et al.** 2005. Standardization and interlaboratory reproducibility assessment of pulsed-field gel electrophoresis-generated fingerprints of *Acinetobacter baumannii*. J. Clin. Microbiol. **43**:4328–4335.
34. **Simpson EH.** 1949. Measurement of diversity. Nature **163**:688.
35. **Smith MG, et al.** 2007. New insights into *Acinetobacter baumannii* pathogenesis revealed by high-density pyrosequencing and transposon mutagenesis. Genes Dev. **5**:601–614.
36. **Snitkin ES, et al.** 2011. Genome-wide recombination drives diversification of epidemic strains of *Acinetobacter baumannii*. Proc. Natl. Acad. Sci. U. S. A. **108**:13758–13763.
37. **Spence RP, et al.** 2002. Population structure and antibiotic resistance of *Acinetobacter* DNA group 2 and 13TU isolates from hospitals in the UK. J. Med. Microbiol. **51**:1107–1112.
38. **Towner KJ.** 2009. *Acinetobacter*: an old friend, but a new enemy. J. Hosp. Infect. **4**:355–363.
39. **Towner KJ, et al.** 2011. Distribution of intrinsic plasmid replicase genes and their association with carbapenem-hydrolyzing class D β-lactamase genes in European clinical isolates of *Acinetobacter baumannii*. Antimicrob. Agents Chemother. **55**:2154–2159.
40. **Towner KJ, Levi K, Vlassiadi M, Steering Group ARPAC.** 2008. Genetic diversity of carbapenem-resistant isolates of *Acinetobacter baumannii* in Europe. Clin. Microbiol. Infect. **14**:161–167.
41. **Turton JF, Matos J, Kaufmann ME, Pitt TL.** 2009. Variable number tandem repeat loci providing discrimination within widespread genotypes of *Acinetobacter baumannii*. Eur. J. Clin. Microbiol. Infect. Dis. **5**:499–507.
42. **Turton JF, et al.** 2006. The role of IS*Aba1* in expression of OXA carbapenemase genes in *Acinetobacter baumannii*. FEMS Microbiol. Lett. **258**:72–77.
43. **Turton JF, Gabriel SN, Valderrey C, Kaufmann ME, Pitt TL.** 2007. Use of sequence-based typing and multiplex PCR to identify clonal lineages of outbreak strains of *Acinetobacter baumannii*. Clin. Microbiol. Infect. **8**:807–815.

44. **Vergnaud G, Pourcel C.** 2006. Multiple locus VNTR (variable number of tandem repeat) analysis (MLVA), p 83–104. *In* Stackebrandt E (ed), Molecular identification, systematics and population structure of prokaryotes. Springer-Verlag, Berlin, Germany.
45. **Visca P, Seifert H, Towner KJ.** 2011. *Acinetobacter* infection, an emerging threat to human health. IUBMB Life doi:10.1002/iub.534.
46. **Visca P, et al.** 2011. Investigation of the *Legionella pneumophila* population structure by analysis of tandem repeat copy number and internal sequence variation. Microbiology **157**:2582–2594.
47. **Zarrilli R, Giannouli M, Tomasone F, Triassi M, Tsakris A.** 2009. Carbapenem resistance in *Acinetobacter baumannii*: the molecular epidemic features of an emerging problem in health care facilities. J. Infect. Dev. Ctries. **3**:335–341.

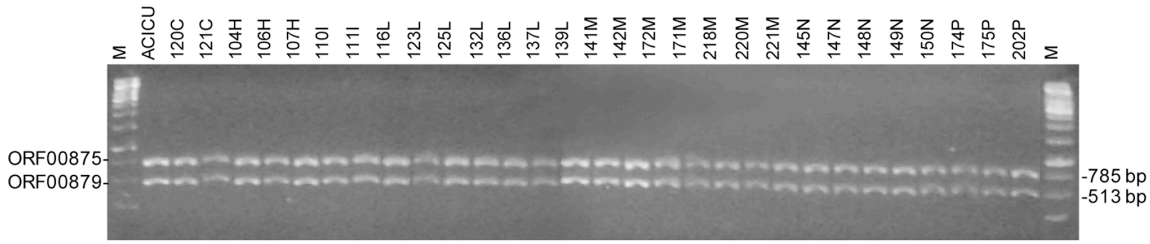

FIG. S1. PCR-based detection of the putative heme outer membrane receptor (ORF ACICU_00875; expected amplicon size 785 bp) and heme oxygenase (ORF ACICU_00879; expected amplicon size 513 bp) genes in thirty *A. baumannii* isolates. Strain designation is indicated above each lane and isolates are ordered according to the hospital. Lane M shows the 1-kb ladder.

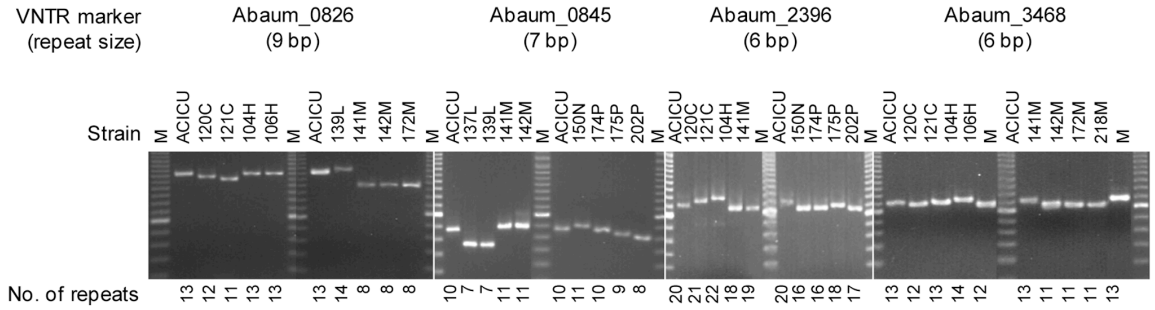

FIG. S2. Electropherograms representing allele polymorphisms at S-repeat VNTR loci in selected isolates. The size of the repeat unit is reported for each VNTR marker. The PCR products were analyzed in 3% agarose gels. The amplicon from the reference strain ACICU was loaded after each DNA size marker, and used as an internal control for band size optimization. Isolate designation and number of repeats are indicated above and below each lane, respectively. Lanes M show the 20-bp ladder.

TABLE S1. Molecular and phenotypic characteristics of selected MDR *A. baumannii* isolates[a]

Hospital	Strain code	Isolation date (mo/day/yr)	Source	Antibiotic resistance profile[b]	Antibiotic susceptibility profile[b]	CHDL content	*repAci1*
G	ACICU	06/10/05	Cerebrospinal fluid	PIP TZP SAM CAZ FEP ATM IPM MEM CIP LVX AMK GEN SXT	CS TIG	OXA-58	+
H	104H	06/23/05	Respiratory secretions	PIP TZP SAM CAZ FEP ATM IPM MEM CIP LVX AMK GEN SXT	CS TIG	OXA-58	+
H	106H	07/27/05	Respiratory secretions	PIP TZP CAZ FEP ATM CIP LVX AMK SXT	SAM IPM MEM GEN CS TIG	Negative	-
H	107H	12/27/05	Respiratory secretions	PIP TZP SAM CAZ FEP ATM IPM MEM CIP LVX AMK GEN SXT	CS TIG	OXA-58	+
I	110I	11/28/06	Respiratory secretions	PIP TZP CAZ FEP ATM IPM MEM CIP LVX AMK SXT	SAM GEN CS TIG	OXA-58	+
I	111I	11/28/06	Respiratory secretions	PIP TZP CAZ FEP ATM IPM CIP LVX AMK SXT	SAM MEM GEN CS TIG	OXA-58	+
L	116L	01/30/07	Blood culture	PIP TZP CAZ FEP ATM IPM CIP LVX AMK SXT	SAM MEM GEN CS TIG	OXA-58	+
C	120C	02/23/07	Respiratory secretions	PIP TZP SAM CAZ FEP ATM IPM MEM CIP LVX AMK GEN SXT	CS TIG	OXA-58	+
C	121C	02/26/07	Blood culture	PIP TZP SAM CAZ FEP ATM IPM MEM CIP LVX AMK GEN SXT	CS TIG	OXA-58	+
L	123L	04/02/07	Respiratory secretions	PIP TZP SAM CAZ FEP ATM IPM MEM CIP LVX AMK SXT	GEN CS TIG	OXA-58	+
L	125L	04/23/07	Respiratory secretions	PIP TZP CAZ FEP ATM IPM MEM CIP LVX AMK GEN SXT	SAM CS TIG	OXA-58	+
N	145N	04/27/07	Respiratory secretions	PIP TZP CAZ FEP ATM IPM MEM CIP LVX AMK GEN SXT	SAM CS TIG	OXA-23	+
L	132L	05/15/07	Respiratory secretions	PIP TZP CAZ FEP ATM IPM MEM CIP LVX AMK GEN SXT	SAM CS TIG	OXA-58	+
N	147N	05/23/07	Urine	PIP TZP CAZ FEP ATM IPM MEM CIP LVX AMK GEN SXT	SAM CS TIG	OXA-23	+
N	148N	06/26/07	Respiratory secretions	PIP TZP CAZ FEP ATM IPM MEM CIP LVX AMK GEN SXT	SAM CS TIG	OXA-23	+
L	136L	06/27/07	Cerebrospinal fluid	PIP CAZ FEP ATM CIP LVX AMK SXT	TZP SAM IPM MEM GEN CS TIG	Negative	+
L	137L	06/27/07	Central venous catheter	PIP TZP CAZ FEP ATM IPM CIP LVX AMK SXT	SAM MEM GEN CS TIG	OXA-58	+
L	139L	07/27/07	Respiratory secretions	PIP TZP CAZ FEP ATM IPM MEM CIP LVX AMK SXT	SAM GEN CS TIG	OXA-58	+
N	149N	10/06/07	Wound swab	PIP TZP CAZ FEP ATM IPM MEM CIP LVX AMK GEN SXT	SAM CS TIG	OXA-23	+
N	150N	11/02/07	Respiratory secretions	PIP TZP CAZ FEP ATM IPM MEM CIP LVX AMK GEN SXT	SAM CS TIG	OXA-23	+
M	141M	12/29/07	Respiratory secretions	PIP TZP SAM CAZ FEP ATM IPM MEM CIP LVX AMK GEN SXT	CS TIG	OXA-23	+
M	142M	01/12/08	Respiratory secretions	PIP TZP SAM CAZ FEP ATM IPM MEM CIP LVX AMK GEN SXT	CS TIG	OXA-23	+
M	172M	02/20/08	Urine	PIP TZP SAM CAZ FEP ATM IPM MEM CIP LVX AMK GEN SXT	CS TIG	OXA-23	+
P	174P	04/28/08	Wound swab	PIP TZP CAZ FEP ATM IPM MEM CIP LVX AMK SXT	SAM GEN CS TIG	OXA-58	+
P	175P	04/29/08	Wound swab	PIP TZP CAZ FEP ATM IPM MEM CIP LVX AMK GEN SXT	SAM CS TIG	OXA-23	+
P	202P	06/04/08	Respiratory secretions	PIP TZP CAZ FEP ATM IPM MEM CIP LVX AMK GEN SXT	SAM CS TIG	OXA-23	+
M	171M	10/01/08	Respiratory secretions	PIP TZP SAM CAZ FEP ATM IPM MEM CIP LVX AMK GEN SXT	CS TIG	OXA-23	+
M	218M	10/09/08	Urine	PIP TZP CAZ FEP ATM IPM MEM CIP LVX AMK SXT	SAM GEN CS TIG	OXA-58	+
M	220M	10/21/08	Respiratory secretions	PIP TZP SAM CAZ FEP ATM IPM MEM CIP LVX AMK GEN SXT	CS TIG	OXA-23	+
M	221M	10/24/08	Respiratory secretions	PIP TZP SAM CAZ FEP ATM IPM MEM CIP LVX AMK GEN SXT	CS TIG	OXA-23	+

[a] Previously determined by D'Arezzo *et al*. (7).

[b] Isolates showing an intermediate level of susceptibility were classified as resistant. Abbreviations: PIP, piperacillin; TZP, piperacillin-tazobactam; SAM, ampicillin-sulbactam; CAZ, ceftazidime; FEP, cefepime; ATM, aztreonam; IPM, imipenem; MEM, meropenem; CIP, ciprofloxacin; LVX, levofloxacin; AMK, amikacin; GEN, gentamicin; SXT, trimethoprim-sulfamethoxazole; CS, colistin; TIG, tigecycline

Chapter 6

Virulence-related traits of *Acinetobacter baumannii* epidemic strains assigned to distinct genotypes

Maria Giannouli[1], Luísa C. S. Antunes[2], Veronica Marchetti[1], Maria Triassi[1], Paolo Visca[2], Raffaele Zarrilli[1]

[1]Department of Preventive Medical Sciences, University of Naples Federico II, Naples, Italy
[2]Department of Biology, University Roma Tre, Rome, Italy

Submitted

Abstract

The combination of genomic and phenotypic analyses (**Chapters 2 and 3**) led to the identification of phenotypic traits likely contributing to *Acinetobacter baumannii* pathogenicity and ecological success, and evidenced the multifactorial and combinatorial nature of *A. baumannii* pathogenicity.

Here, the occurrence of traits contributing to *A. baumannii* pathogenicity and ecological success was determined in a collection of drug-resistant epidemic *A. baumannii* isolates assigned to distinct PFGE and MLST genotypes. Phenotypic traits analysed were resistance to desiccation, biofilm formation on abiotic surfaces, and adhesion and invasion of A459 epithelial cells. In addition, the lethality of isolates was compared in the *Galleria mellonella* insect infection model.

Biofilm formation was more abundant for strains assigned to MLST sequence types ST2 (belonging to the international clone II), ST25 and ST78. Exposure to sub-inhibitory imipenem concentrations enhanced biofilm formation in the majority of strains irrespective of their genotype. All strains survived on dry surfaces for long periods of time (at least three weeks), with strains assigned to ST1 (belonging to the international clone I) and ST78 genotypes surviving for over two months. Adhesion to A549 epithelial cells was higher for strains assigned to the ST2, ST25 and ST78 genotypes, and positively correlated with biofilm formation. Strains assigned to ST78 also showed significantly higher ability to invade A549 cells. However, no significant differences in the killing of *G. mellonella* worms were found among isolates assigned to distinct genotypes, and all epidemic isolates showed relatively low lethal doses in this model system.

This work confirmed the multifactorial and combinatorial nature of *A. baumannii* pathogenicity and suggests that certain virulence-related traits might account for the higher predominance in the nosocomial environment of a few *A. baumannii* genotypes, including the international clones I and II and genotypes ST25 and ST78.

Introduction

Acinetobacter baumannii is an emerging bacterial pathogen responsible for widespread and persistent outbreaks among hospitalized patients. *A. baumannii* infections, are difficult to control since many epidemic strains can resist several classes of antibiotics and disinfectants and are able to colonize abiotic surfaces of the contaminated hospital environment, including the medical equipment [1,2]. Mounting evidence indicates that *A. baumannii* epidemics are caused worldwide by a limited number of strains which have been assigned by different genotypic methods, including multilocus sequence typing (MLST), to international clonal lineages (IC) I, II and II [3-5], and to additional genotypes, such as the closely related ST15 and ST84 genotypes from Europe [3,4], the ST25 genotype from Eurasia [4,6] and genotype ST78 isolated in several Italian hospitals [4,7]. Since the majority of epidemic strains are multi-drug-resistant (MDR) or extensively-drug-resistant (XDR) [8], many studies have investigated the genetic and functional basis of antimicrobial resistance [1-7]. In contrast, few studies are available on the virulence traits and pathogenic potential of *A. baumannii*. It has been reported that *A. baumannii* can form biofilms on several abiotic surfaces, including polystyrene, polypropylene, polytetrafluoroethylene and glass [9], and ca. 70% of strains are biofilm-formers [10]. While no difference in biofilm formation was observed between outbreak and sporadic strains, IC-II strains seem to form larger biofilms than IC-I strains [11]. Biofilm formation appeared to be positively correlated with multidrug resistance [10], as well as with the expression of several virulence factors, including the outer membrane protein OmpA, the extracellular polysaccharide poly-β-(1,6)-N-acetyl glucosamine (PNAG), type I pili, a homologue of the staphylococcal biofilm-associated protein (Bap), the outer membrane protein CarO, a quorum sensing system and proteins involved in histidine metabolism, such as urocanase [9,12-17]. The ability of *A. baumannii* strains to survive for a long time on dry surfaces is likely to contribute to persistence in hospitals [18]. In this respect, it has been recently reported that RecA protein is involved in general stress response and resistance to heat shock and desiccation in *A. baumannii* [19]. In addition, the ability of *A. baumannii* to adhere and invade epithelial cells has been investigated [20]. Among the virulence factors that may contribute to these processes, the biofilm-associated protein Bap has been demonstrated to play a role during adhesion [21], OmpA and phospholipase D have been shown to contribute to invasion of epithelial cells [13,22].

The majority of these studies, however, have been performed using a limited number of strains, often ATCC 19606^T and/or ATCC 17978 reference strains [12,13,15,23]. Only a few studies have compared the virulence traits of ICs I-III and no studies have analyzed the virulence features of additional epidemic lineages identified so far [11,23,24]. Although comparative genome analysis of epidemic strains assigned to distinct genotypes has demonstrated that the genes encoding putative *A. baumannii* virulence factors are mostly conserved [25,26], their expression levels may vary among strains [23].

The objective of the present study was to identify virulence-related traits of epidemic strains assigned to distinct genotypes of *A. baumannii* that could contribute to their ability to colonize and infect the human host and persist in the hospital environment. Biofilm formation, resistance to desiccation, adhesion and invasion of A549 human bronchial cells, and killing of *Galleria mellonella* caterpillars were evaluated in a diverse collection of MDR or XDR *A. baumannii* strains isolated during outbreaks in European hospitals, and in the reference strains ATCC 19606^T and ATCC 17978.

Materials and Methods

Bacterial strains, cell line and culture conditions

Twenty-three *A. baumannii* strains were included in this study that had previously been assigned to 10 different MLST sequence types (STs), according to Institute Pasteur's MLST scheme, and to 17 different major PFGE types (Table 1). The collection included 23 strains representative of outbreaks that occurred in several hospitals in France, Greece, Italy, Lebanon, Netherlands and Turkey [4,27-30], plus *A. baumannii* ATCC19606^T and ATCC17978 reference strains [31,32]. MDR and XDR phenotypes were designed according to ref [8]. Seventeen strains exhibited an imipenem minimum inhibitory concentration (MIC) ≥16 mg/L and were considered to be carbapenem-resistant and XDR; four strains were classified as MDR (Table 1).

Bacteria were routinely cultured in Luria-Bertani broth (LB). The M9 minimal broth supplemented with magnesium sulphate and glucose as carbon source (M9) and Mueller Hinton broth [Oxoid, Milan, Italy] were used for biofilm growth [33] and pellicle formation [34], respectively. A549 human alveolar epithelial cells were maintained at 37°C in the presence of 5% CO_2 using Dulbecco modified Eagle medium (DMEM) [Sigma-Aldrich, Milan, Italy] supplemented with 10% heat-inactivated foetal bovine serum [Sigma-Aldrich, Milan, Italy]. Monolayers were cultured to 70-80% confluence before use in bacterial attachment and invasion assays [13].

Measurement of biofilm formation

The ability of *A. baumannii* strains to form biofilm was measured using a microtiter plate assay [35]. Overnight cultures grown in M9 were diluted to an optical density at 600 nm (OD_{600}) of ~ 1.0. One hundred microliter aliquots were deposited in 96-well polystyrene microtiter plates and incubated for 24 h at 37°C. Plates were then washed three times with 200 µl phosphate-buffer saline solution (PBS) and air-dried. Biofilm was stained with 0.1% crystal violet solution for 15 min. After washing with distilled water, the biofilm-associated dye was solubilised with 200 µl of 95 % ethanol. The dye solutions from three wells were pooled and the OD_{540} was measured. In order to assay the induction of biofilm formation, the bacteria were grown for 24 h in microtiter plates in the presence of imipenem (Merck Research Laboratories, Rahway, N.J., USA) at sub-inhibitory concentrations as previously described [33]. Sub-inhibitory concentrations of imipenem were 0.5 mg/L for strains AYE, 700, 2979, LUH 5875, ATCC 19606^T, and ATCC 17978, and of 4 mg/L for all other strains, which corresponded to 1/4 and 1/4-1/16 the MIC, respectively (Table 1). Three independent experiments, each one performed in triplicate, were conducted for each strain. For the pellicle formation at air-liquid interface assay, bacteria were grown for 72 h at 37°C without shaking, as previously described [34].

Desiccation survival assay

The desiccation assay was performed according to the protocol of Jawad *et al.* [18]. One ml aliquots of overnight LB cultures were centrifuged at 11,600 × g for 5 min in a microcentrifuge. The cell pellet was washed twice with PBS and suspended in distilled water to an OD_{600} of 1.0. Twenty microliters of each suspension were deposited onto a glass cover slip to produce an inoculum of ~2×10^7 colony-forming units (CFU). The coverslip was kept at 31% relative humidity by the presence of a saturated $CaCl_2\times6H_2O$ in an uncovered Petri dish, and stored at room temperature in an airtight transparent plastic box (17×11×5.5 cm) for up to 16 weeks. Strain viable counts were determined once a week.

Adhesion to and invasion of A549 cells

Adhesion of *A. baumannii* strains to A549 cells (human type 2 pneumocytes) was determined as described previously, with minor modifications [13]. In brief, ~ 10^5 A549 cells in 12-well tissue culture plates were infected with ~ 10^7 bacterial CFU and incubated for 60 min at 37°C in a CO_2 5% (v/v) atmosphere. Non-adherent bacterial cells were removed by washing three times with PBS. Infected cells were lysed by the addition of 1 ml distilled water and serial 10-fold dilutions were plated on LB agar to determine the number of CFU of adherent bacteria per well. To determine bacterial invasion, A549 cells were infected with *A. baumannii* strains as described above. The monolayers were then treated with 1 ml of fresh culture medium containing 5 mg/L of colistin sulfate (Sigma-Aldrich, Milan, Italy) for further 30 min, the shortest time point that resulted in the killing of all bacteria added to the monolayers. Afterwards, the cells were washed three times with PBS, harvested with trypsin, lysed with sterile distilled water, and plated as described above. Dilutions from harvested samples were inoculated on LB agar plates and bacterial colony counts (CFU/ml) were estimated after overnight incubation. Each experiment was performed in triplicate.

G. mellonella killing assay

A. baumannii lethality was assessed using the *Galleria mellonella* insect model of infection [23], with minor modifications. Ten *G. mellonella* caterpillars (average weight 500±60 mg) were injected with 10 µl of serial ten-fold dilutions in PBS of *A. baumannii* cells grown overnight at 37°C in LB. Bacterial colony counts (CFU/ml) on LB agar plates were used to estimate the number of viable cells in each inoculum. Ten larvae that received no injection and ten larvae injected with 10 µl PBS were used as negative controls of each experiment. Two independent experiments, each one performed in triplicate, were conducted for each strain. Larvae were incubated at 37°C in Petri dishes (ten larvae per dish) and monitored every 12 h for a total of 72 h. Survival curves were plotted using the Kaplan-Meier estimator and expressed in percentage. Lethal dose 50% (LD_{50}) values were calculated using GraphPad Prism v.5.04 (GraphPad Software, La Jolla California USA) according to the following equation: $Y=A+(1-A)/(1+e^{(B-G\times\ln X)})$, where X is the number of viable bacterial cells injected, Y the fraction of larvae killed by a given bacterial inoculum, A is the fraction of larvae killed by the control solution, and B and G are curve-fitting constants automatically calculated by GraphPad Prism [23]. LD_{50} values were calculated as the value of X that corresponds to Y= 0.5.

Statistical analysis

Data were analysed using Statistical Package for the Social Sciences Version 13.0 (SPSS Inc., Chicago, IL, USA). The significance of the induction of biofilm formation in the presence of imipenem was analyzed with the Student's *t* test and induction was considered significant when the P value was <0.05. The variability of strains assigned to the same ST was investigated using the One-Way Analysis of Variance (ANOVA), in which strains were grouped according to ST and differences were considered significant when the P value was <0.05. Correlations were evaluated by regression analysis using the Pearson's correlation coefficient (r).

Results

Biofilm formation

The ability to form biofilm on polystyrene microtiter plates was evaluated for a collection of outbreak *A. baumannii* strains assigned to different PFGE genotypes and STs (Table 1). Strains assigned to the four major PFGE types E-H (ST2, corresponding to IC-II), PFGE types L-N (ST25), and PFGE type Q (ST78) formed significantly higher biofilm levels than strains assigned to other PFGE types (including ST1, ST20, ST3, ST15, ST84, ST52, and ST77) ($p < 0.05$) (Fig. 1A). In addition, *A. baumannii* strains assigned to ST2, ST25 and ST78 formed a robust biofilm pellicle at the air-liquid interface when grown at 37°C for 72 h without shaking (data not shown).

Since exposure of *A. baumannii* to sub-inhibitory concentrations of imipenem has been demonstrated to stimulate biofilm growth [33], biofilm formation was evaluated in the presence of sub-inhibitory concentrations of the antibiotic (Fig. 1B). Growth yields were not affected by imipenem at the used concentrations for all strains tested. Compared with the untreated control, significantly higher biofilm formation was observed after exposure to imipenem for strains assigned to ST2 (except strain 3889), and ST78, which already produced high biofilm levels before treatment, and for strains assigned to ST1 and its single locus variant ST20 (IC-I), to ST3 (IC-III) and to ST52 (ATCC 19606^T) ($p < 0.05$) which, conversely, were weak producers when grown in the absence of antibiotic. On the other hand, no significant differences in biofilm formation were observed for the strains assigned to ST15, ST84 ST25 and ST77 (Fig. 1A and 1B).

Resistance to desiccation

Strains showed an overall ability to resist desiccation, though survival times ranged from 16-96 days depending on the strain (Fig. 2 and Table S1). In particular, strains assigned to ST1 and ST78 showed extremely high resistance to desiccation, with survival times of 75 to 89 days and 68 to 96 days, respectively. Strains assigned to ST15, strain 4025 (ST3) and strain 3890 (ST25) showed a comparable trend of high resistance to desiccation, with survival times of 75 to 89 days. Strains assigned to ST2 and ST20, strains 4190 and 3865 (assigned to ST25) and strain ATCC 17978 were moderately resistant to desiccation with survival times of 33 to 54 days. Finally, strains 3871 (assigned to ST84), LUH 5875 (assigned to ST3) and ATCC 19606^T were less resistant to dry conditions, and survived for < 29 days (Fig. 2 and Table S1).

Adhesion and invasion of A549 human bronchial cells

Different steps of the interaction between *A. baumannii* and A549 human alveolar epithelial cells investigated, including cell adhesion and subsequent invasion [13]. *A. baumannii* strains displayed different ability to adhere to epithelial cells (Fig. 3A). In particular, all strains assigned to ST2, ST25, ST78 and strain ATCC 17978 adhered to epithelial cells at significantly higher levels than other strains ($p < 0.05$). Moreover, a highly significant correlation was found between adhesiveness of *A. baumannii* to A549 human alveolar epithelial cells and biofilm formation for all strains, except ATCC 19606^T and ATCC 17978 ($r = 0.832$, $p < 0.01$).

Strains assigned to ST1, ST20, ST2, ST25 and ST78 and reference strain ATCC 19606^T were all invasive, although only strains assigned to ST78 showed significantly high levels of invasiveness when compared with other genotypes ($p < 0.05$) (Fig. 3B). A similar number of bacteria adhered to A549 cells when the monolayers were incubated with *A. baumannii* strains for 60 min at 4°C, i.e. under conditions that do not allow for tissue invasion (data not shown). Since invasive bacteria at 37°C represented approximately 5% and no more than 10% of adherent bacteria to A549 cells for all strains (Fig. 3B), the counts of adherent bacteria were contributed for less than 10% by bacteria which invaded the epithelial cells (Fig. 3A).

G. mellonella killing assays

The LD_{50} values were calculated for each strain at 24, 48 and 72 h post-infection (Table 2). For all strains, the LD_{50} decreased with post-infection time, attaining the final value at 72 h (Fig. S1), after which no relevant difference was observed in larval death (data not shown). Differences in LD_{50} between 24 h and 72 h provide a trend of the killing rapidity for individual strains (Table 2 and Fig. S1). The LD_{50} at 72 h were comprised between 8.1×10^4 and 4.7×10^6 CFU/larva, with the average LD_{50} being $5.8(\pm9.5)\times10^5$ CFU/larva. These values are in the range of those determined in a previous study on clinical *A. baumannii* isolates [23]. Strain-specific differences between LD_{50} calculated at 72 h were significant ($p < 0.001$). In particular, strains ATCC 19606^T (ST52) and 3868 (ST15) had significantly ($p < 0.001$) higher LD_{50} than all the other strains tested. In contrast, ST-specific differences between LD_{50} calculated at 72 h were not significant ($p \geq 0.05$).

Discussion

Antibiotic resistance and long-term persistence in the hospital environment are two factors that most likely contribute to the success of *A. baumannii* as an opportunistic pathogen [1,2,5]. However, it is possible that the emergence of some epidemic strains or clones over others is the result of an improved ability to colonize patients and cause disease. In the present study, biofilm formation, resistance to desiccation, adhesion to and invasion of human epithelial cells and lethality to *G. mellonella* catterpilars were investigated as possible virulence-related phenotypes [10,13,18,23]. A collection of 21 *A. baumannii* strains assigned to the three main lineages circulating worldwide, i.e. IC-I-III, as well as to distinct genotypes recently identified as responsible for outbreaks, and two reference *A. baumannii* strains ATCC19606^T and ATCC17978 were analysed (Table 1).

Results demonstrate that epidemic *A. baumannii* clonal lineages differ in the ability to form biofilm on abiotic surfaces. In particular, strains assigned to genotypes ST2, ST25 and ST78 produce biofilm more efficiently and are able to form a robust biofilm pellicle at the air-liquid interface of the culture medium. In keeping with this result, it has been shown that strains belonging to the *A. baumannii-calcoaceticus* complex form higher biofilm pellicle than other *Acinetobacter* species [34] and that *A. baumannii* strains assigned to the IC-II form more biofilm than *A. baumannii* strains assigned to the IC-I [11]. It is also worth mentioning that the *A. baumannii* strain SMAL, responsible for two outbreaks in Northern Italy and shown to be an efficient biofilm producer [33], has recently been assigned to ST78 [7]. Biofilm could therefore be regarded as an important virulence feature for *A. baumannii* strains belonging to ST2, ST78 and also ST25. In consistence with previous findings [33], this study showed that exposure to sub-inhibitory concentrations of imipenem stimulated biofilm formation in *A. baumannii* epidemic strains assigned to ST2 and ST78, which already produced high levels of biofilm before antibiotic treatment, as well as in epidemic strains assigned to ST1, ST3 and ST20, which were weak producers when grown in the absence of this antibiotic. This suggests that regulation of biofilm formation can differ within *A. baumannii* lineages, as strains belonging to the same sequence type or clonal complex, endowed with substantially similar genetic background, showed variability in biofilm yields. Nevertheless, exposure to sub-inhibitory imipenem concentrations caused an overall increase of biofilm formation in the majority of the strains and STs tested. It is plausible that transition from planktonic to biofilm lifestyle upon imipenem exposure represents a defensive response of *A. baumannii* to the threat posed by the antibiotic challenge.

In accordance with previous findings [18,23,36], *A. baumannii* outbreak strains analyzed herein showed the ability to survive on dry surfaces for impressively long time periods, although great strain variation was found (16-96 days). In particular, strains assigned to ST1 and ST78, as well as one strain assigned to ST25, showed extremely high resistance to desiccation. Moreover, strains assigned to ST20, which belong to the same clonal complex as ST1, all ST2 strains, and two of three strains assigned to ST25 were moderately resistant to desiccation. In contrast, six other strains, including ATCC 19606^T, were less resistant to drought. It has recently been reported that the survival times on dry surfaces of *A. baumannii* biofilm-forming strains are longer than those of non-biofilm-forming ones [36]. However, the collection analysed in this study did not reveal a strong correlation between biofilm formation and survival to desiccation, except for strains assigned to ST78 and two out of three strains assigned to ST25. A possible explanation for this discrepancy is that this correlation depends on the strains and/or culture conditions used.

The data obtained in this study also indicate that *A. baumannii* clonal lineages differ in the ability to adhere to bronchial epithelial cells. In particular, adhesion to A549 cells was higher for strains assigned to ST2, ST25 and ST78, and correlated positively with biofilm formation in these strains. This is consistent with a previous report showing a positive association between biofilm production and adhesiveness to epithelial cells in MDR clinical isolates of *A. baumannii* [20]. Therefore, it can be speculated that common or partly overlapping cellular mechanisms might control biofilm growth on abiotic surfaces and adhesion to epithelial cells. In partial support of this hypothesis, it was recently shown that the biofilm-associated protein Bap plays a role in both biofilm formation and adherence to human epithelial cells [21]. Our study also demonstrated that *A. baumannii* strains assigned to ST78 have a higher ability to invade A549 human bronchial epithelial cells than other genotypes. However, since the three strains assigned to ST78 belong to the same major PFGE type, it cannot be excluded that differences in the capacity to invade epithelial cells are strain-specific rather than lineage-specific.

No significant differences in the killing of *G. mellonella* larvae, measured as the LD_{50} at the 72 h post-infection time point, were found among strains assigned to the distinct genotypes, with the exception of strains ATCC 19606^T (ST52) and 3868 (ST15), which showed significantly lower lethality. In contrast, strain-specific differences were observed in the rate of killing, expressed as the ratio between LD_{50} values determined at 24 and 72 h. Killing was delayed for strains AYE (ST1) and 3990 (ST2) and, to a lesser extent, 3865, 4190 (both ST25) and 3911 (ST78) (LD_{50} ratio 5.3-12.2; Table 2 and Fig. S1). Overall, the LD_{50} values determined for our collection of isolates is in the same order of magnitude as that previously reported for prototypic *A. baumannii* strains of clinical origin (AYE, ACICU and ATCC 17978) [23].

In conclusion, although equally virulent in an insect infection model, epidemic *A. baumannii* clonal lineages show differences in virulence traits. In particular, resistance to desiccation, biofilm growth on abiotic surfaces and adhesion and invasion of bronchial epithelial cells could have favoured the spread and persistence in the hospital environment of *A. baumannii* strains assigned to ST1, ST2, ST25 and ST78. On a second note, ST1 and ST2 seem to differ in the expression of virulence-associated phenotypes. Whereas ST1 showed higher resistance to desiccation, ST2 showed higher adhesion to both biotic and abiotic surfaces, providing further evidence that the virulence of the two main *A. baumannii* ICs might be multifactorial and combinatorial [23]. It remains to be investigated whether the differential expression of virulence traits between these two clones could reflect a specialisation in the colonisation of nosocomial niches or different pathogenic strategies between the two. Lastly, to the best of our knowledge, this is the first study to identify common *A. baumannii* virulence-associated phenotypes (resistance to desiccation, adhesion to biotic and abiotic surfaces and bronchial epithelial cell invasion) in genotypes other than the three main ICs.

Acknowledgments

The Authors thank all colleagues who generously provided strains included in the study: Antonella Agodi, Matteo Bassetti, Susanna Cuccurullo, Ziad Daoud, Patrice Nordmann, Athanassios Tsakris, and Haluk Vahaboglu. The Authors also thank Elvira Crescenzi for kindly providing the A549 human alveolar epithelial cells. LA was supported by a PhD fellowship from the Portuguese Fundação para a Ciência e a Tecnologia (FCT) (grant SFRH/BD/43420/2008).

Authors' contributions

Conceived and designed the experiments: MG, LA, MT, PV, RZ. Performed the experiments: MG, LA, VM. Analyzed the data: MG, LA, PV, RZ. Wrote the paper: MG, LA, PV, RZ. All authors read and approved the final manuscript.

Transparency declaration

The authors declare no conflicts of interest.

References

1. Durante-Mangoni E and Zarrilli R. Global spread of drug-resistant *Acinetobacter baumannii*: molecular epidemiology and management of antimicrobial resistance. *Future Microbiol* 2011; **6:** 407-422.
2. Peleg AY, Seifert H, Paterson DL. *Acinetobacter baumannii*: emergence of a successful pathogen. *Clin Microbiol Rev* 2008; **21:** 538-582.
3. Diancourt L, Passet V, Nemec A, Dijkshoorn L, Brisse S. The population structure of *Acinetobacter baumannii*: expanding multiresistant clones from an ancestral susceptible genetic pool. *PLoS One* 2010; **5:** e10034.
4. Di Popolo A, Giannouli M, Triassi M, Brisse S, Zarrilli R. Molecular epidemiology of multidrug-resistant *Acinetobacter baumannii* strains in four Mediterranean countries using a multilocus sequence typing scheme. *Clin Microbiol Infect* 2011; **17:** 197-201.
5. Zarrilli R, Pournaras S, Giannouli M, Tsakris A. Global evolution of multidrug-resistant *Acinetobacter baumannii* clonal lineages. *Int J Antimicrob Agents* 2012 Nov 2. doi: 10.1016/j.ijantimicag.2012.09.008. [Epub ahead of print].
6. Karah N, Giske CG, Sundsfjord A, Samuelsen O. A diversity of OXA-carbapenemases and class 1 integrons among carbapenem-resistant *Acinetobacter baumannii* clinical isolates from Sweden belonging to different international clonal lineages. *Microbial Drug* Resistance 2011; **17:** 545–549.
7. Carretto E, Barbarini D, Dijkshoorn L *et al*. Widespread carbapenem resistant *Acinetobacter baumannii* clones in Italian hospitals revealed by a multicenter study. *Infect Genet Evol* 2011; **11:** 1319-1326.
8. Magiorakos AP, Srinivasan A, Carey RB *et al*. Multidrug-resistant, extensively drug-resistant and pandrug-resistant bacteria: an international expert proposal for interim standard definitions for acquired resistance. *Clin Microbiol Infect* 2012; **18:** 268-281.
9. Tomaras AP, Dorsey CW, Edelmann RE, Actis L. Attachment to and biofilm formation on abiotic surfaces by *Acinetobacter baumannii*: involvement of a novel chaperone-usher pili assembly system. *Microbiology* 2003; **149:** 3473-3484.
10. Rodríguez-Baño J, Martí S, Soto S *et al*. Biofilm formation in *Acinetobacter baumannii*: associated features and clinical implications. *Clin Microbiol Infect* 2008; **14:** 276-278.
11. de Breij A, Dijkshoorn L, Lagendijk E *et al*. Do biofilm formation and interactions with human cells explain the clinical success of *Acinetobacter baumannii*? *PLoS One* 2010; **5:** e10732.

12. Choi C, Lee E, Lee Y *et al*. Outer membrane protein 38 of *Acinetobacter baumannii* localizes to the mitochondria and induces apoptosis of epithelial cells. *Cell Microbiol* 2005; **7:** 1127-1138.
13. Gaddy JA, Tomaras AP, Actis LA. The *Acinetobacter baumannii* 19606 OmpA protein plays a role in biofilm formation on abiotic surfaces and in the interaction of this pathogen with eukaryotic cells. *Infect Immun* 2009; **77:** 3150-3160
14. Kim S, Choi C, Moon D *et al*. Serum resistance of *Acinetobacter baumannii* through the binding of factor H to outer membrane proteins. *FEMS Microbiol Lett* 2009; **301:** 224-231.
15. Cabral MP, Soares NC, Aranda J *et al*. Proteomic and functional analyses reveal a unique lifestyle for *Acinetobacter baumannii* biofilms and a key role for histidine metabolism. *J Proteome Res* 2011; **10:** 3399-417.
16. Choi A, Slamti L, Avci F, Pier G, Maira-Litran T. The *pgaABCD* locus of *Acinetobacter baumannii* encodes the production of poly-β-1-6-N-acetyl glucosamine PNAG that is critical for biofilm formation. *J Bacteriol* 2009; **191:** 5953-5963.
17. Loehfelm T, Luke N, Campagnari A. Identification and characterization of an *Acinetobacter baumannii* biofilm-associated protein. *J Bacteriol* 2008; **190:** 1036-1044.
18. Jawad A, Seifert H, Snelling A, Heritage J, Hawkey P. Survival of *Acinetobacter baumannii* on dry surfaces: comparison of outbreak and sporadic isolates. *J Clin Microbiol* 1998; **36:** 1938-1941.
19. Aranda J, Bardina C, Beceiro A, Rumbo S, Cabral MP, Barbé J, Bou G. *Acinetobacter baumannii* RecA protein in repair of DNA damage, antimicrobial resistance, general stress response, and virulence. *J Bacteriol* 2011;**193:**3740-3747.
20. Lee H-W, Koh YM, Kim J *et al*. Capacity of multidrug-resistant clinical isolates of *Acinetobacter baumannii* to form biofilm and adhere to epithelial cell surfaces. *Clin Microbiol Infect* 2008; **14:** 49-54.
21. Brossard KA, Campagnari AA. The *Acinetobacter baumannii* biofilm-associated protein plays a role in adherence to human epithelial cells. *Infect Immun* 2012; **80:** 228-233.
22. Jacobs AC, Hood I, Boyd KL, Olson PD, Morrison JM, Carson S, Sayood K, Iwen PC, Skaar EP, Dunman PM. Inactivation of phospholipase D diminishes *Acinetobacter baumannii* pathogenesis. *Infect Immun* 2010;**78:**1952-1962.
23. Antunes LC, Imperi F, Carattoli A, Visca P. Deciphering the multifactorial nature of *Acinetobacter baumannii* pathogenicity. *PLoS One* 2011; **6:** e22674.
24. de Breij A, Eveillard M, Dijkshoorn L *et al*. Differences in *Acinetobacter baumannii* strains and host innate immune response determine morbidity and mortality in experimental pneumonia. *PLoS One* 2012; **7:** e30673
25. Di Nocera PP, Rocco F, Giannouli M, Triassi M, Zarrilli R. Genome organization of epidemic *Acinetobacter baumannii* strains. *BMC Microbiology* 2011; 11: 224.
26. Imperi F, Antunes LC, Blom J *et al*. The genomics of *Acinetobacter baumannii*: insights into genome plasticity, antimicrobial resistance and pathogenicity. *IUBMB Life* 2011; **63:** 1068-1074.
27. Giannouli M, Cuccurullo S, Crivaro V *et al*. Molecular epidemiology of multi-drug resistant *Acinetobacter baumannii* in a tertiary care hospital in Naples, Italy, shows the emergence of a novel epidemic clone. *J Clin Microbiol* 2010; **48:** 1223-1230
28. Poirel L, Manuteau O, Agoli N, Cattoen C, Nordmann P. Outbreak of Extended-Spectrum β-Lactamase VEB-1-Producing Isolates of *Acinetobacter baumannii* in a French Hospital. *J Clin Microbiol* 2003; **41:** 3542-3547.
29. Iacono M, Villa L, Fortini D *et al*. Whole-Genome Pyrosequencing of an Epidemic Multidrug-Resistant *Acinetobacter baumannii* Strain Belonging to the European Clone II Group. Antimicrob *Agents Chemother* 2008; **52:** 2616-2625.
30. van Dessel H, Dijkshoorn L, van der Reijden T *et al*. Identification of a new geographically widespread multiresistant *Acinetobacter baumannii* clone from European hospitals. *Res Microbiol* 2004; **155:** 105-112.
31. Janssen P, Maquelin K, Coopman R *et al*. Discrimination of *Acinetobacter* Genomic Species by AFLP Fingerprinting. *Int J Syst Bacteriol* 1997; **47:** 1179-1187.
32. Smith MG, Gianoulis TA, Pukatzki S *et al*. New insights into *Acinetobacter baumannii* pathogenesis revealed by high-density pyrosequencing and transposon mutagenesis. *Genes Dev* 2007; **21:** 601-614.
33. Nucleo E, Steffanoni L, Fugazza G *et al*. Growth in glucose-based medium and exposure to subinhibitory concentrations of imipenem induce biofilm formation in a inmultidrug-resistant clinical isolate of *Acinetobacter baumannii. BMC Microbiol* 2009; **9:** 270.
34. Martì S, Rodriguez-Bano J, Catel-Ferreira M *et al*. Biofilm formation at the solid-liquid and air-liquid interfaces by *Acinetobacter* species. *BMC Research Notes* 2011; **4:** 5
35. Merritt JH, Kadouri DE, and O'Toole GA. Growing and Analyzing Static Biofilms. *Current Protocols in Microbiology* 2005; 00: 1B.1.1–1B.1.17.

36. Espinal P, Martì S, Vila J. Effect of biofilm formation on the survival of *Acinetobacter baumannii* on dry surfaces. *J Hosp Infect* 2012; **80:** 56-60.

Table 1. Epidemiological, phenotypic and genotypic data of the *Acinetobacter baumannii* isolates included in the study.

Strain	Hospital	Year	PFGE type[a]	ST type[b]	IMP MIC µg/ml	Reference
AYE	Kremlin-Bicetre/FR	2001	A	ST1	2	[28]
700	F-Naples/IT	1999	B	ST1	2	[4]
2979	Agrigento/IT	2002	C	ST20	2	[4]
3130	SG-Beirut /LB	2004	D	ST20	16	[4]
2105	F-Naples /IT	2002	E	ST2	16	[4]
3990	M-Naples /IT	2006	E	ST2	32	[27]
ACICU	Rome/IT	2005	E1	ST2	32	[29]
2735	M-Naples /IT	2004	E2	ST2	64	[4]
3889	Athens/GR	2005	F	ST2	16	[4]
4026	SJ-Beirut /LB	2007	G	ST2	16	[4]
4009	Genoa/IT	2007	H	ST2	32	[4]
4025	SG-Beirut /LB	2005	I	ST3	16	[4]
LUH 5875	Utrecht/NL,	1997	J	ST3	2	[30]
3868	Izmir/TK	2003	K	ST15	16	[4]
3871	Istanbul/TK	2003	K1	ST84	16	[4]
3890	Thessaloniki/GR	2003	L	ST25	16	[4]
3865	Kocaeli/TK	2005	M	ST25	64	[4]
4190	M-Naples /IT	2009	N	ST25	64	[4]
ATCC 19606^T	Unknown	Before 1949	O	ST52	2	[31]
ATCC 17978	Unknown	1951	P	ST77	2	[32]
3909	M-Naples /IT	2007	Q	ST78	16	[27]
3957	M-Naples /IT	2007	Q	ST78	16	[27]
3911	M-Naples /IT	2007	Q1	ST78	16	[27]

Abbreviations: F-Naples, Federico II University Hospital, Naples; M-Naples, Monaldi Hospital, Naples; SG-Beirut, Saint Gorge Hospital, Beirut; SJ-Beirut, Saint Joseph Hospital, Beirut; GR, Greece; IT, Italy; LB, Lebanon; TK, Turkey; ST, sequence type; IMP, imipenem; MIC, Minimum inhibitory concentration.
[a] PFGE types according to reference [27].
[b] ST determined according to the Institute Pasteur's MLST scheme [3].

Table 2. *G. mellonella* killing (LD_{50}, expressed as CFU/larva) by *A. baumannii* strains.

Strain	ST type	LD_{50}			Ratio 24/72 h
		24 h	48 h	72 h	
AYE	ST1	$2.8 (\pm0.3)\times10^{6}$	$5.4 (\pm0.3)\times10^{5}$	$2.3 (\pm0.1)\times10^{5}$	12.2
700	ST1	$7.2 (\pm4.2)\times10^{5}$	$2.7 (\pm0.5)\times10^{5}$	$2.3 (\pm0.4)\times10^{5}$	3.1
2979	ST20	$1.0 (\pm0.2)\times10^{6}$	$6.6 (\pm0.2)\times10^{5}$	$4.2 (\pm0.6)\times10^{5}$	2.4
3130	ST20	$7.3 (\pm0.3)\times10^{5}$	$5.8 (\pm0.6)\times10^{5}$	$5.8 (\pm0.6)\times10^{5}$	1.3
2105	ST2	$9.2 (\pm0.6)\times10^{5}$	$8.2 (\pm0.5)\times10^{5}$	$7.4 (\pm0.7)\times10^{5}$	1.2
3990	ST2	$6.6 (\pm0.7)\times10^{5}$	$1.1 (\pm0.2)\times10^{5}$	$8.1 (\pm0.5)\times10^{4}$	8.1
ACICU	ST2	$1.3 (\pm0.4)\times10^{6}$	$7.4 (\pm0.3)\times10^{5}$	$6.4 (\pm0.9)\times10^{5}$	2.0
2735	ST2	$2.2 (\pm0.3)\times10^{5}$	$2.0 (\pm0.1)\times10^{5}$	$1.3 (\pm0.7)\times10^{5}$	1.7
3889	ST2	$4.2 (\pm0.4)\times10^{5}$	$2.4 (\pm0.1)\times10^{5}$	$1.8 (\pm0.2)\times10^{5}$	2.3
4026	ST2	$4.5 (\pm0.6)\times10^{5}$	$2.7 (\pm0.5)\times10^{5}$	$2.7 (\pm0.5)\times10^{5}$	1.7
4009	ST2	$3.7 (\pm0.2)\times10^{5}$	$3.2 (\pm0.7)\times10^{5}$	$3.0 (\pm0.7)\times10^{5}$	1.2
4025	ST3	$9.4 (\pm0.2)\times10^{5}$	$2.7 (\pm0.9)\times10^{5}$	$2.2 (\pm0.8)\times10^{5}$	4.3
LUH 5875	ST3	$3.8 (\pm1.2)\times10^{5}$	$2.8 (\pm0.2)\times10^{5}$	$2.3 (\pm0.1)\times10^{5}$	1.7
3868	ST15	$2.3 (\pm0.5)\times10^{6}$	$2.3 (\pm0.6)\times10^{6}$	$1.6 (\pm0.1)\times10^{6}$	1.4
3871	ST84	$5.8 (\pm0.3)\times10^{5}$	$3.9 (\pm0.5)\times10^{5}$	$3.5 (\pm0.3)\times10^{5}$	1.7
3890	ST25	$6.6 (\pm0.8)\times10^{5}$	$4.6 (\pm0.3)\times10^{5}$	$2.4 (\pm0.4)\times10^{5}$	2.8
3865	ST25	$1.6 (\pm0.4)\times10^{6}$	$1.3 (\pm0.1)\times10^{6}$	$3.0 (\pm0.3)\times10^{5}$	5.3
4190	ST25	$3.1 (\pm0.5)\times10^{6}$	$2.1 (\pm0.3)\times10^{6}$	$5.0 (\pm0.9)\times10^{5}$	6.0
ATCC 19606^{T}	ST52	$9.1 (\pm3.4)\times10^{6}$	$6.7 (\pm0.7)\times10^{6}$	$4.7 (\pm0.2)\times10^{6}$	1.9
ATCC 17978	ST77	$6.7 (\pm0.1)\times10^{5}$	$4.5 (\pm0.7)\times10^{5}$	$3.1 (\pm0.6)\times10^{5}$	2.2
3909	ST78	$2.0 (\pm0.4)\times10^{6}$	$6.4 (\pm0.7)\times10^{5}$	$6.4 (\pm0.7)\times10^{5}$	3.1
3957	ST78	$3.3 (\pm1.2)\times10^{5}$	$2.8 (\pm0.4)\times10^{5}$	$2.5 (\pm0.6)\times10^{5}$	1.3
3911	ST78	$7.8 (\pm1.9)\times10^{5}$	$5.6 (\pm0.6)\times10^{5}$	$1.4 (\pm0.6)\times10^{5}$	5.6

Figure legends

Figure 1. Biofilm formation. Biofilm formation on 96-well polystyrene microtiter plates by *A. baumannii* grown statically in M9 medium for 24 hours in the absence (panel A) or presence (panel B) of imipenem concentrations 0.5 mg/L (strains AYE, 700, LUH 5875, 2979, ATCC 19606^T and ATCC 17978), or 4 mg/L (all other strains). Strain and ST types are indicated on the bottom of the figure. Error bars represent standard deviations based on three independent experiments. Asterisks indicate statistically significant differences in biofilm formation among different STs (panel A) ($p < 0.05$) and statistically significant induction in biofilm formation upon exposure to sub-MIC imipenem concentrations (panel B) ($p < 0.05$).

Figure 2. Resistance to desiccation. Resistance to desiccation of *A. baumannii* strains. Strains were inoculated onto rounded glass cover slips and incubated at 31% relative humidity and room temperature. A starting bacterial inoculum of ~ 2×10^7 per cover slip was used. Values represent the mean of three independent experiments.

Figure 3. Bacterial adhesion and invasion of A549 bronchial epithelial cells. (A) Cell surface-associated bacteria after 60 min incubation at 37°C. Statistically significant differences ($p < 0.05$) among different STs are indicated with asterisks. (B) Intracellular bacterial counts (CFU/ml) obtained after 60 min incubation of A549 cells with bacterial strains and subsequent treatment for 30 min at 37°C with colistin (5mg/L). Statistically significant differences among different STs ($p < 0.05$) are indicated with asterisks. Each value represents the mean ± standard deviation (error bar) of three independent experiments performed in duplicate.

Supporting information

Figure S1. Kaplan-Meier survival plots of *G. mellonella* larvae infected with the different *A. baumannii* strains.

Table S1. Resistance to desiccation of *A. baumannii* strains. Values are means ± standard deviations of three independent experiments done in duplicate.

A

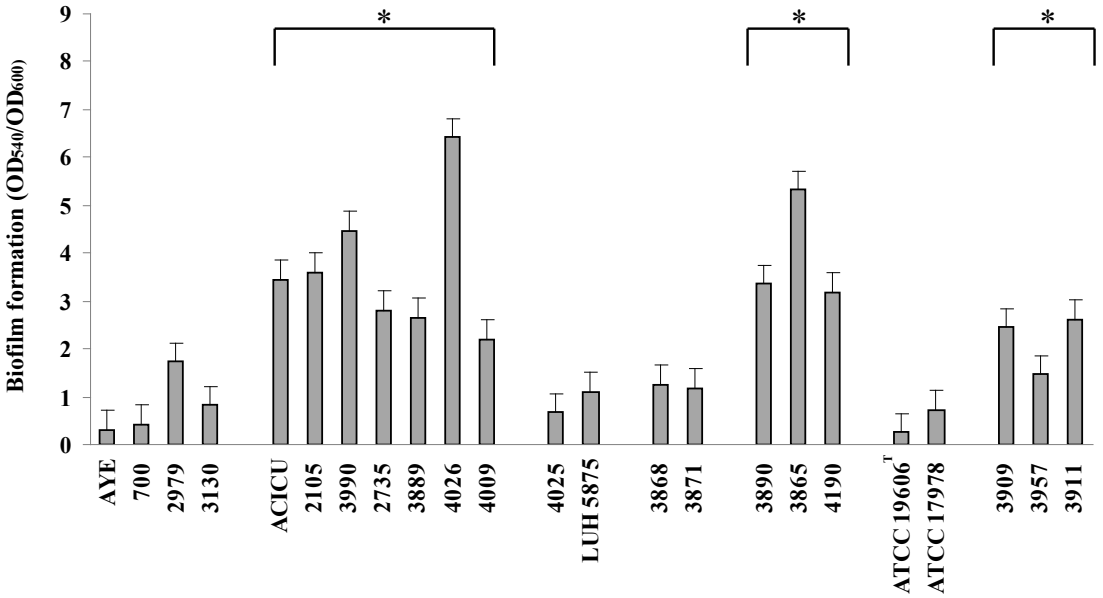
Biofilm formation (OD540/OD600)
0
1
2
3
4
5
6
7
8
9
*
*
*
AYE
700
2979
3130
ACICU
2105
3990
2735
3889
4026
4009
4025
LUH 5875
3868
3871
3890
3865
4190
ATCC 19606T
ATCC 17978
3909
3957
3911

B

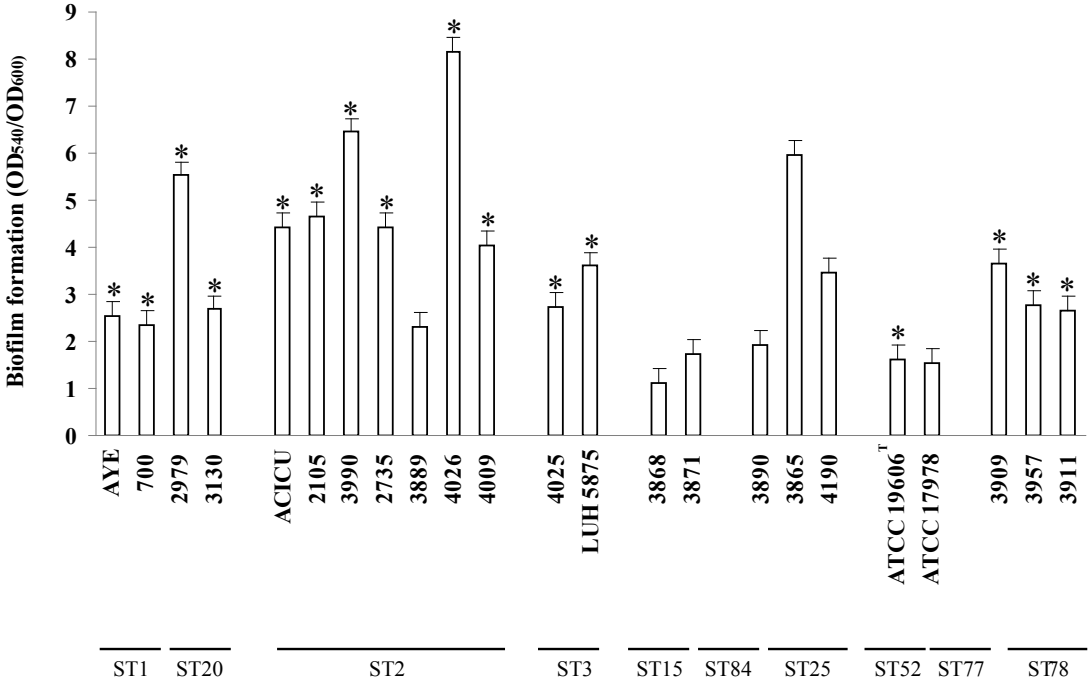
Biofilm formation (OD540/OD600)
0
1
2
3
4
5
6
7
8
9
AYE
700
2979
3130
ACICU
2105
3990
2735
3889
4026
4009
4025
LUH 5875
3868
3871
3890
3865
4190
ATCC 19606T
ATCC 17978
3909
3957
3911
ST1
ST20
ST2
ST3
ST15
ST84
ST25
ST52
ST77
ST78

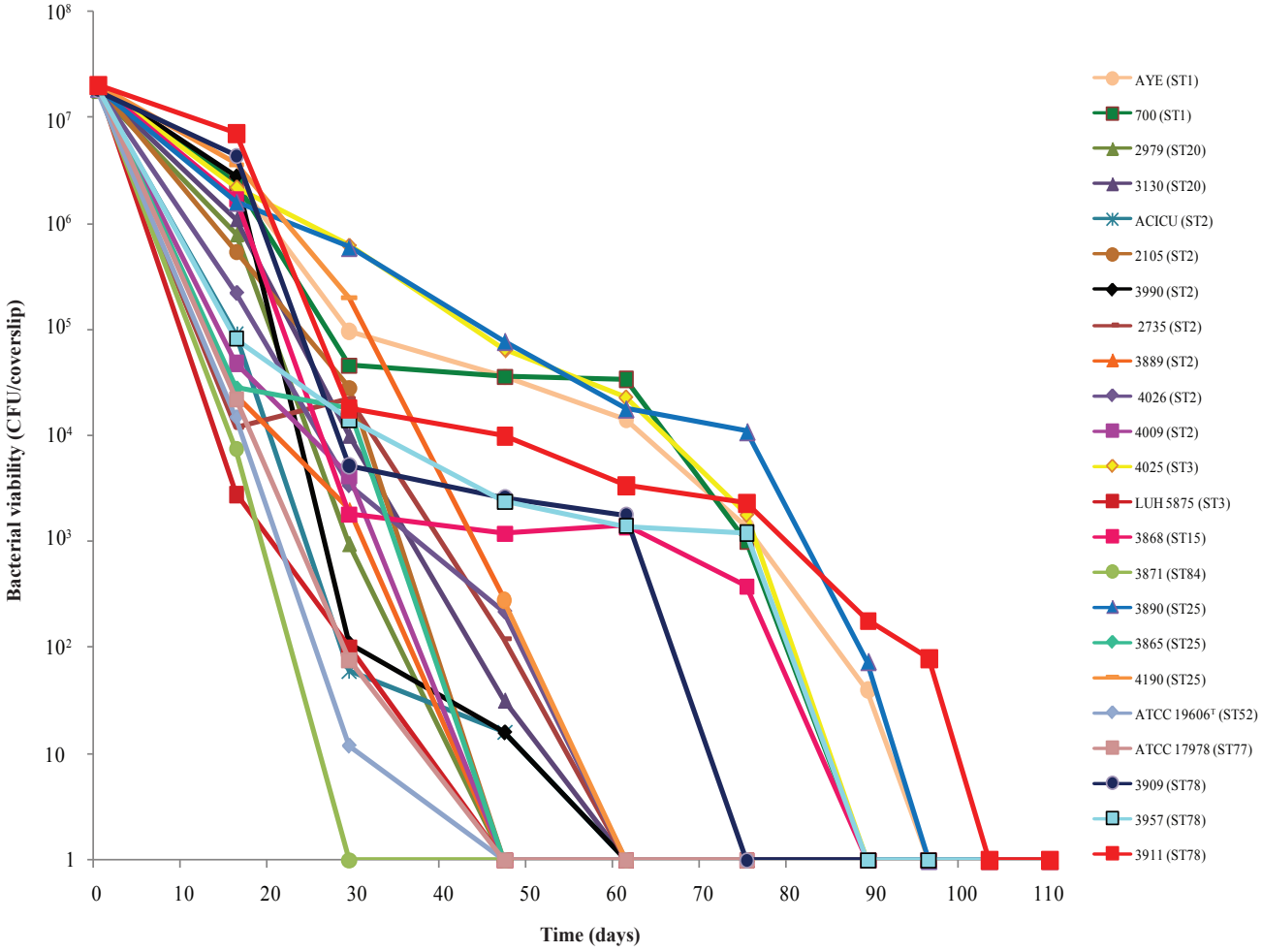
Bacterial viability (CFU/coverslip)
10^8
10^7
10^6
10^5
10^4
10^3
10^2
10
1
0
10
20
30
40
50
60
70
80
90
100
110
Time (days)
AYE (ST1)
700 (ST1)
2979 (ST20)
3130 (ST20)
ACICU (ST2)
2105 (ST2)
3990 (ST2)
2735 (ST2)
3889 (ST2)
4026 (ST2)
4009 (ST2)
4025 (ST3)
LUH 5875 (ST3)
3868 (ST15)
3871 (ST84)
3890 (ST25)
3865 (ST25)
4190 (ST25)
ATCC 19606^T (ST52)
ATCC 17978 (ST77)
3909 (ST78)
3957 (ST78)
3911 (ST78)

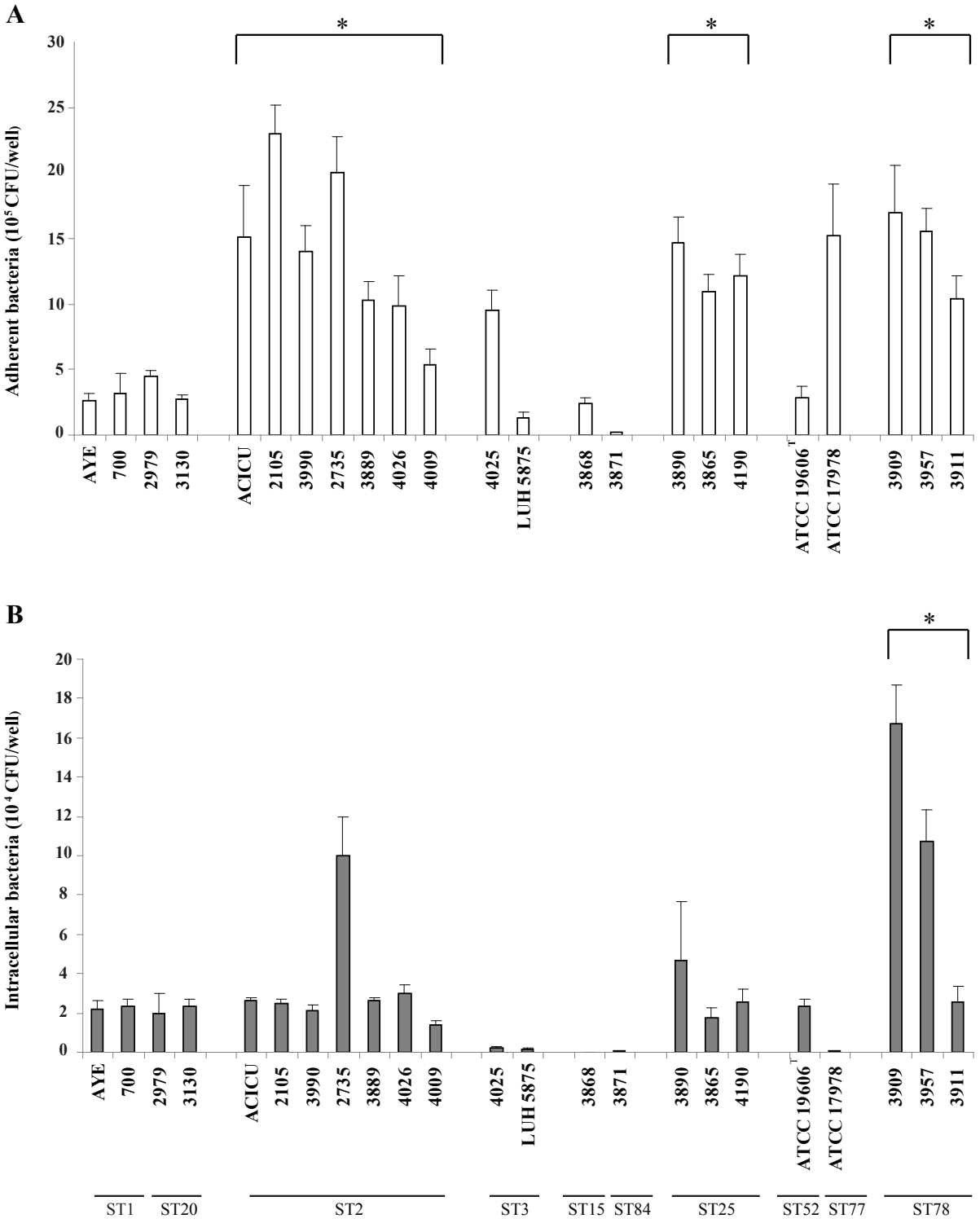
A
Adherent bacteria (10^5 CFU/well)
30
25
20
15
10
5
0
*
*
*
AYE
700
2979
3130
ACICU
2105
3990
2735
3889
4026
4009
4025
LUH 5875
3868
3871
3890
3865
4190
ATCC 19606T
ATCC 17978
3909
3957
3911
B
Intracellular bacteria (10^4 CFU/well)
20
18
16
14
12
10
8
6
4
2
0
*
AYE
700
2979
3130
ACICU
2105
3990
2735
3889
4026
4009
4025
LUH 5875
3868
3871
3890
3865
4190
ATCC 19606T
ATCC 17978
3909
3957
3911
ST1
ST20
ST2
ST3
ST15
ST84
ST25
ST52
ST77
ST78

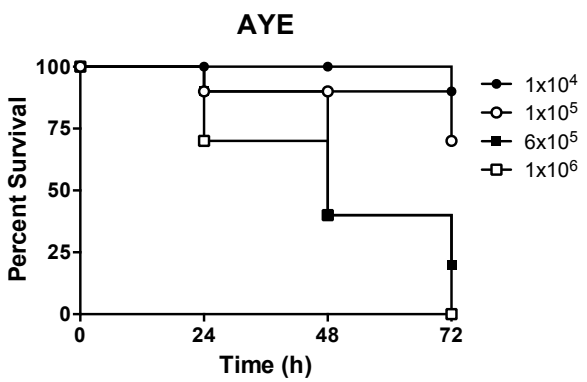
AYE
Percent Survival
100
75
50
25
0
0
24
48
72
Time (h)
1x10^4
1x10^5
6x10^5
1x10^6

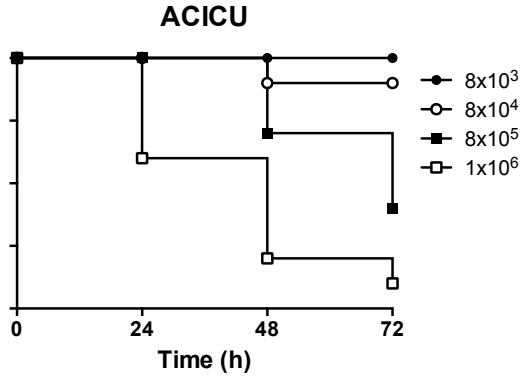
ACICU
0
24
48
72
Time (h)
8x10^3
8x10^4
8x10^5
1x10^6

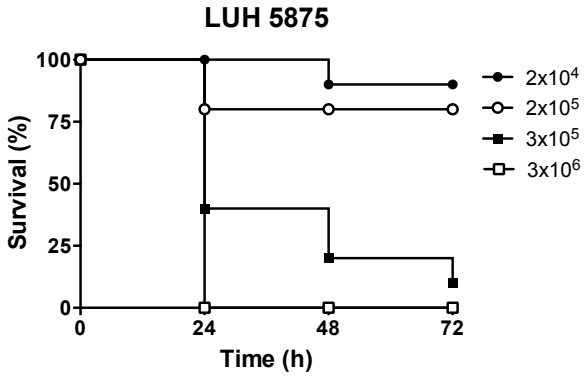
LUH 5875
Survival (%)
100
75
50
25
0
0
24
48
72
Time (h)
2x10^4
2x10^5
3x10^5
3x10^6

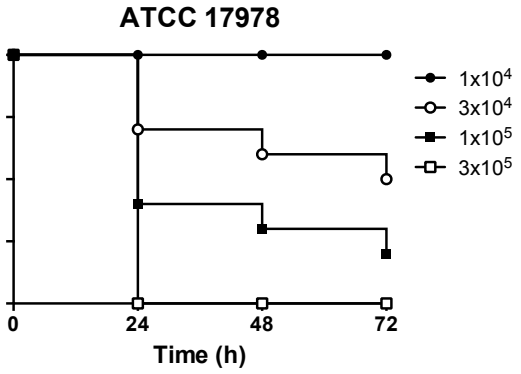
ATCC 17978
0
24
48
72
Time (h)
1x10^4
3x10^4
1x10^5
3x10^5

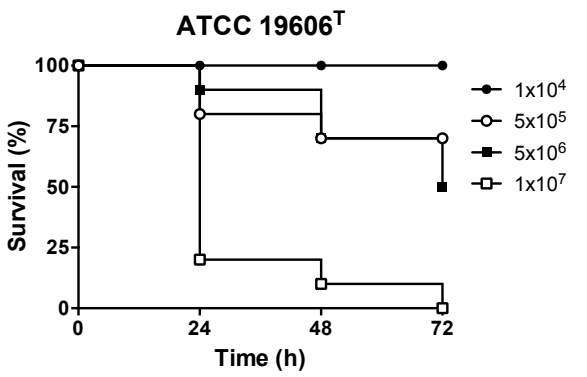
ATCC 19606^T
Survival (%)
100
75
50
25
0
0
24
48
72
Time (h)
1x10^4
5x10^5
5x10^6
1x10^7

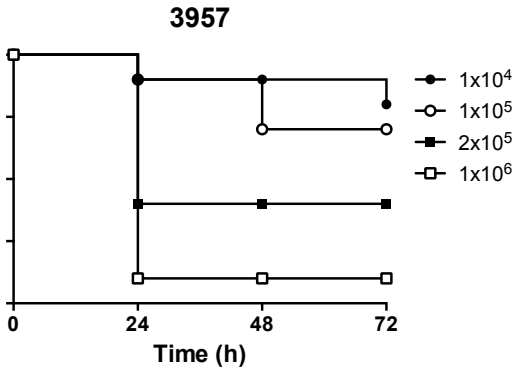
3957
0
24
48
72
Time (h)
1x10^4
1x10^5
2x10^5
1x10^6

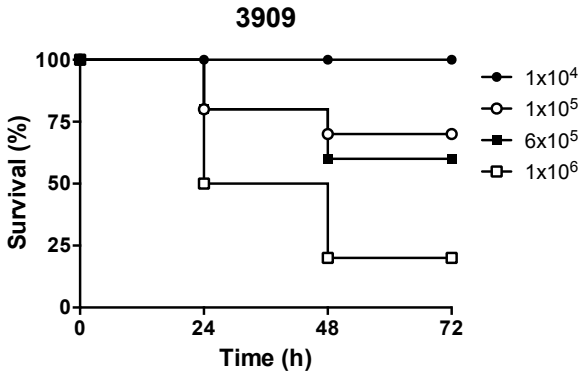
3909
Survival (%)
100
75
50
25
0
0
24
48
72
Time (h)
1x10^4
1x10^5
6x10^5
1x10^6

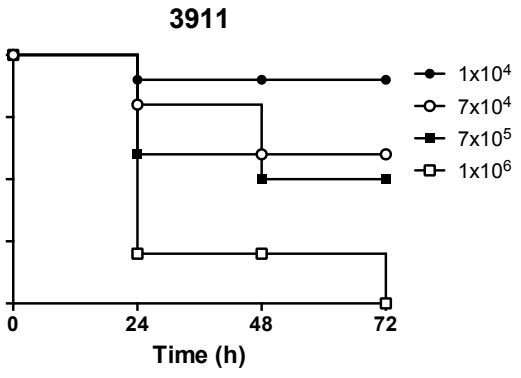
3911
0
24
48
72
Time (h)
1x10^4
7x10^4
7x10^5
1x10^6

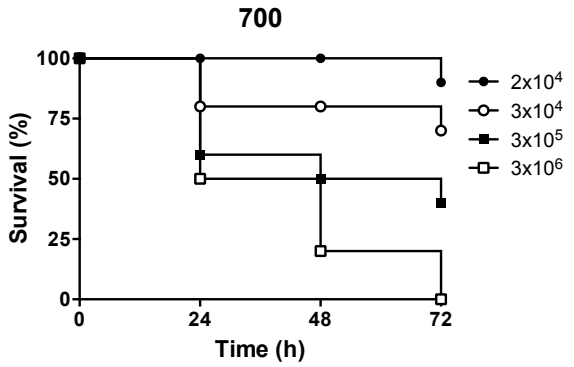
700
Survival (%)
100
75
50
25
0
0
24
48
72
Time (h)
2x10^4
3x10^4
3x10^5
3x10^6

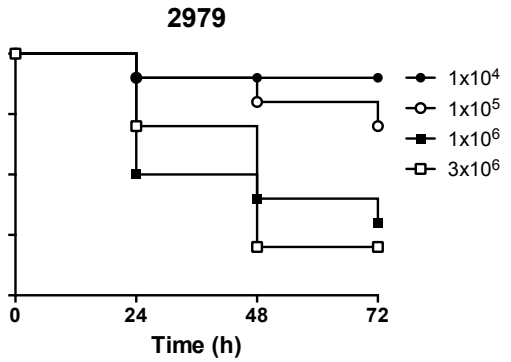
2979
0
24
48
72
Time (h)
1x10^4
1x10^5
1x10^6
3x10^6

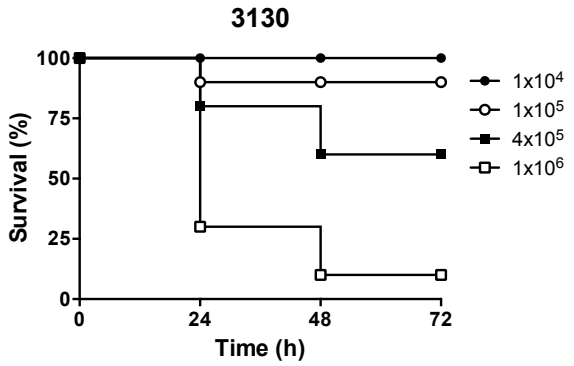
3130
Survival (%)
100
75
50
25
0
0
24
48
72
Time (h)
1x10^4
1x10^5
4x10^5
1x10^6

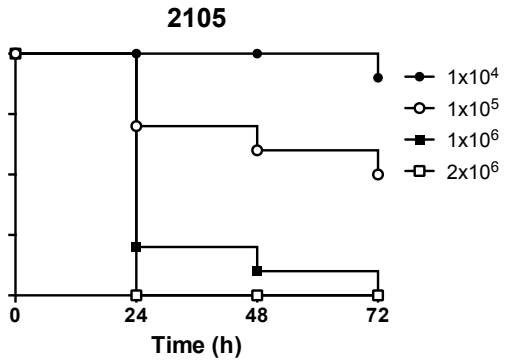
2105
0
24
48
72
Time (h)
1x10^4
1x10^5
1x10^6
2x10^6

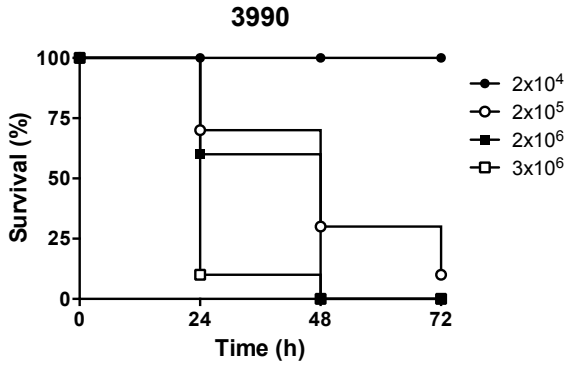
3990
Survival (%)
100
75
50
25
0
0
24
48
72
Time (h)
2x10^4
2x10^5
2x10^6
3x10^6

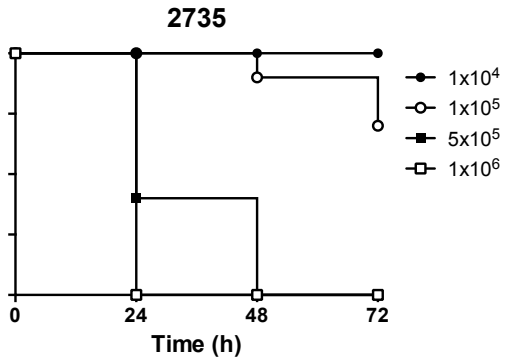
2735
0
24
48
72
Time (h)
1x10^4
1x10^5
5x10^5
1x10^6

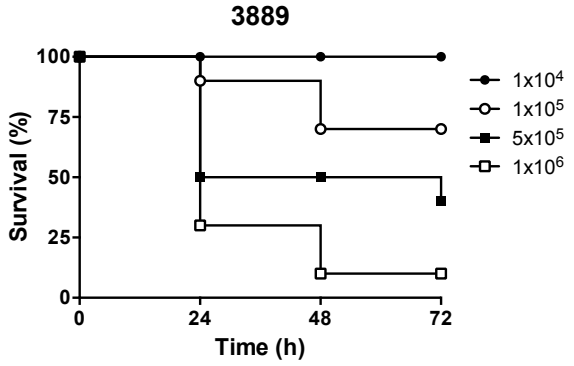
3889
Survival (%)
100
75
50
25
0
0
24
48
72
Time (h)
1x10^4
1x10^5
5x10^5
1x10^6

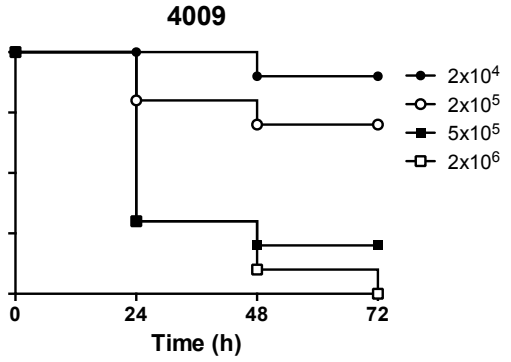
4009
0
24
48
72
Time (h)
2x10^4
2x10^5
5x10^5
2x10^6

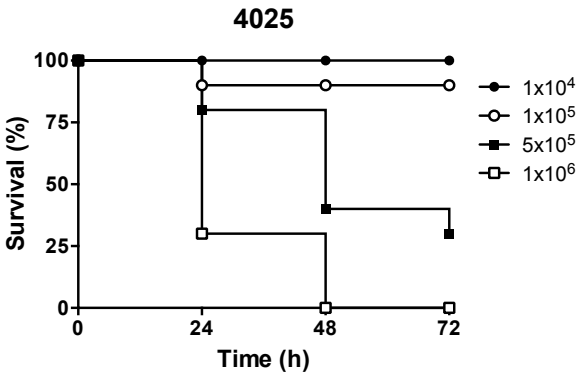
4025
Survival (%)
100
75
50
25
0
0
24
48
72
Time (h)
1x10^4
1x10^5
5x10^5
1x10^6

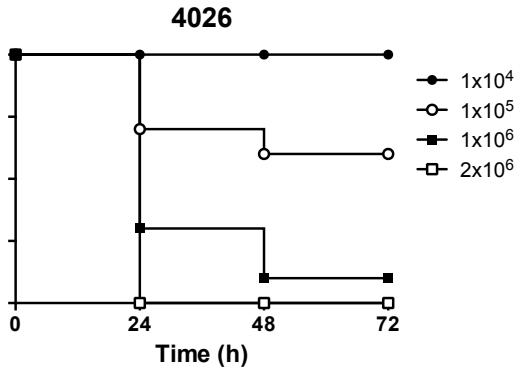
4026
0
24
48
72
Time (h)
1x10^4
1x10^5
1x10^6
2x10^6

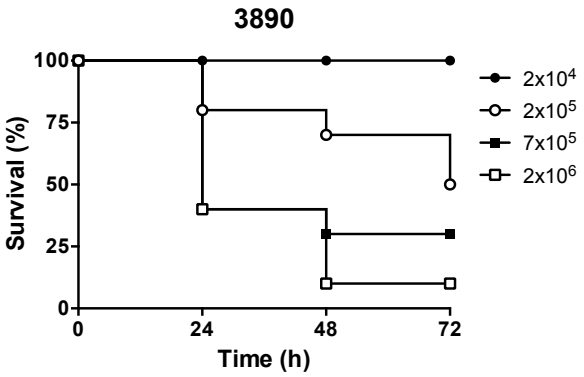
3890
Survival (%)
100
75
50
25
0
0
24
48
72
Time (h)
2x10^4
2x10^5
7x10^5
2x10^6

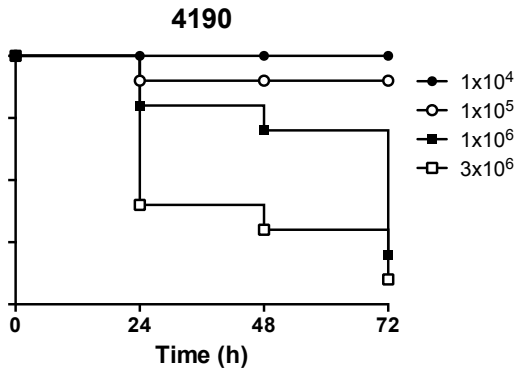
4190
0
24
48
72
Time (h)
1x10^4
1x10^5
1x10^6
3x10^6

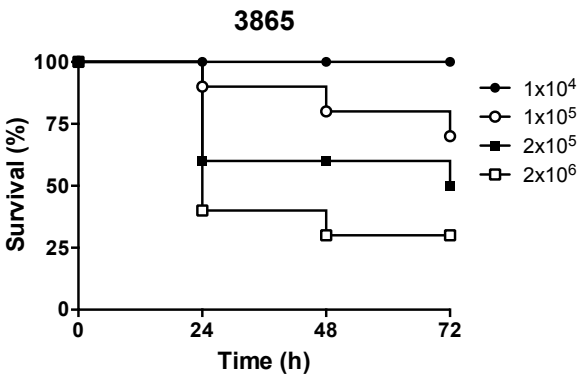
3865
Survival (%)
100
75
50
25
0
0
24
48
72
Time (h)
1x10^4
1x10^5
2x10^5
2x10^6

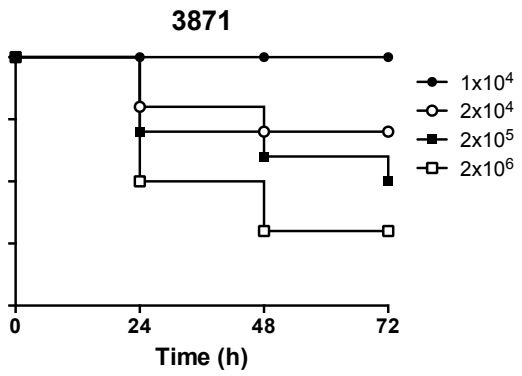
3871
0
24
48
72
Time (h)
1x10^4
2x10^4
2x10^5
2x10^6

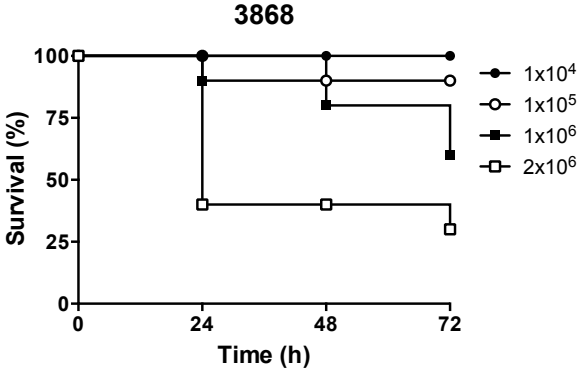
3868
Survival (%)
100
75
50
25
0
0
24
48
72
Time (h)
1x10^4
1x10^5
1x10^6
2x10^6

Strain	ST type	Time (days)															
		0	9	16	23	29	33	40	47	54	61	68	75	82	89	96	103
AYE	ST1	$1.9(\pm0.0)\times10^{7}$	$8.6(\pm0.8)\times10^{6}$	$2.6(\pm0.3)\times10^{6}$	$7.6(\pm0.5)\times10^{5}$	$9.6(\pm3.3)\times10^{4}$	$7.6(\pm1.7)\times10^{4}$	$4.0(\pm0.4)\times10^{4}$	$3.6(\pm0.5)\times10^{4}$	$1.8(\pm0.3)\times10^{4}$	$1.4(\pm0.3)\times10^{4}$	$3.6(\pm0.5)\times10^{3}$	$1.4(\pm0.3)\times10^{3}$	$3.8(\pm0.3)\times10^{2}$	$4.0(\pm0.0)\times10^{1}$	0.0(±0.0)	0.0(±0.0)
700	ST1	$2.0(\pm0.0)\times10^{7}$	$7.6(\pm1.1)\times10^{6}$	$2.4(\pm1.6)\times10^{6}$	$6.0(\pm0.0)\times10^{5}$	$4.6(\pm0.3)\times10^{4}$	$5.2(\pm1.1)\times10^{4}$	$3.6(\pm0.3)\times10^{4}$	$3.6(\pm0.3)\times10^{4}$	$3.4(\pm0.3)\times10^{4}$	$3.4(\pm0.3)\times10^{4}$	$1.2(\pm0.3)\times10^{3}$	$1.0(\pm0.3)\times10^{3}$	0.0(±0.0)	0.0(±0.0)	0.0(±0.0)	0.0(±0.0)
2979	ST20	$1.8(\pm0.1)\times10^{7}$	$3.8(\pm0.3)\times10^{6}$	$8.0(\pm1.1)\times10^{5}$	$3.4(\pm0.3)\times10^{4}$	$9.6(\pm1.1)\times10^{2}$	$6.6(\pm0.1)\times10^{2}$	8.0(±0.0)	0.0(±0.0)	0.0(±0.0)	0.0(±0.0)	0.0(±0.0)	0.0(±0.0)	0.0(±0.0)	0.0(±0.0)	0.0(±0.0)	0.0(±0.0)
3130	ST20	$1.9(\pm0.2)\times10^{7}$	$2.8(\pm1.1)\times10^{6}$	$1.1(\pm0.1)\times10^{6}$	$1.6(\pm0.5)\times10^{4}$	$1.0(\pm0.3)\times10^{4}$	$1.4(\pm0.3)\times10^{3}$	$7.0(\pm1.4)\times10^{2}$	$3.2(\pm5.0)\times10^{1}$	0.0(±0.0)	0.0(±0.0)	0.0(±0.0)	0.0(±0.0)	0.0(±0.0)	0.0(±0.0)	0.0(±0.0)	0.0(±0.0)
ACICU	ST2	$1.8(\pm0.2)\times10^{7}$	$1.2(\pm0.6)\times10^{6}$	$9.0(\pm1.9)\times10^{4}$	$1.1(\pm0.0)\times10^{3}$	$6.0(\pm5.0)\times10^{2}$	$5.2(\pm1.6)\times10^{1}$	$1.8(\pm0.2)\times10^{1}$	$1.6(\pm0.0)\times10^{1}$	0.0(±0.0)	0.0(±0.0)	0.0(±0.0)	0.0(±0.0)	0.0(±0.0)	0.0(±0.0)	0.0(±0.0)	0.0(±0.0)
2105	ST2	$2.0(\pm0.0)\times10^{7}$	$4.6(\pm1.9)\times10^{6}$	$5.4(\pm1.4)\times10^{5}$	$5.4(\pm0.8)\times10^{5}$	$2.8(\pm0.0)\times10^{4}$	$1.6(\pm0.5)\times10^{4}$	$2.0(\pm0.5)\times10^{2}$	0.0(±0.0)	0.0(±0.0)	0.0(±0.0)	0.0(±0.0)	0.0(±0.0)	0.0(±0.0)	0.0(±0.0)	0.0(±0.0)	0.0(±0.0)
3990	ST2	$2.0(\pm0.0)\times10^{7}$	$1.3(\pm0.4)\times10^{7}$	$2.8(\pm0.5)\times10^{6}$	$1.0(\pm0.3)\times10^{6}$	$1.1(\pm0.3)\times10^{2}$	$1.0(\pm0.1)\times10^{2}$	$1.0(\pm0.1)\times10^{2}$	$1.6(\pm0.0)\times10^{1}$	0.0(±0.0)	0.0(±0.0)	0.0(±0.0)	0.0(±0.0)	0.0(±0.0)	0.0(±0.0)	0.0(±0.0)	0.0(±0.0)
2735	ST2	$1.9(\pm0.0)\times10^{7}$	$1.6(\pm0.0)\times10^{5}$	$1.2(\pm0.2)\times10^{4}$	$1.3(\pm0.1)\times10^{4}$	$2.2(\pm1.4)\times10^{4}$	$2.0(\pm0.5)\times10^{3}$	$3.2(\pm0.5)\times10^{2}$	$1.2(\pm0.0)\times10^{2}$	$6.0(\pm2.8)\times10^{1}$	0.0(±0.0)	0.0(±0.0)	0.0(±0.0)	0.0(±0.0)	0.0(±0.0)	0.0(±0.0)	0.0(±0.0)
3889	ST2	$2.0(\pm0.0)\times10^{7}$	$2.0(\pm0.5)\times10^{5}$	$2.4(\pm0.5)\times10^{4}$	$2.6(\pm0.8)\times10^{4}$	$2.0(\pm0.5)\times10^{3}$	$1.0(\pm0.3)\times10^{3}$	$1.4(\pm0.2)\times10^{2}$	0.0(±0.0)	0.0(±0.0)	0.0(±0.0)	0.0(±0.0)	0.0(±0.0)	0.0(±0.0)	0.0(±0.0)	0.0(±0.0)	0.0(±0.0)
4026	ST2	$1.9(\pm0.1)\times10^{7}$	$1.0(\pm0.3)\times10^{7}$	$2.2(\pm0.8)\times10^{5}$	$1.4(\pm0.8)\times10^{5}$	$3.4(\pm0.3)\times10^{3}$	$1.8(\pm0.3)\times10^{3}$	$3.2(\pm0.1)\times10^{2}$	$2.2(\pm0.3)\times10^{2}$	$1.4(\pm0.3)\times10^{2}$	0.0(±0.0)	0.0(±0.0)	0.0(±0.0)	0.0(±0.0)	0.0(±0.0)	0.0(±0.0)	0.0(±0.0)
4009	ST2	$1.9(\pm0.1)\times10^{7}$	$3.8(\pm0.8)\times10^{6}$	$4.8(\pm0.5)\times10^{4}$	$1.9(\pm0.2)\times10^{4}$	$4.2(\pm1.4)\times10^{3}$	$3.0(\pm0.8)\times10^{3}$	0.0(±0.0)	0.0(±0.0)	0.0(±0.0)	0.0(±0.0)	0.0(±0.0)	0.0(±0.0)	0.0(±0.0)	0.0(±0.0)	0.0(±0.0)	0.0(±0.0)
4025	ST3	$2.0(\pm0.1)\times10^{7}$	$2.1(\pm0.5)\times10^{7}$	$2.2(\pm0.2)\times10^{6}$	$1.0(\pm0.4)\times10^{6}$	$6.2(\pm0.7)\times10^{5}$	$4.4(\pm0.5)\times10^{5}$	$1.6(\pm0.3)\times10^{5}$	$6.6(\pm0.3)\times10^{4}$	$4.3(\pm0.9)\times10^{4}$	$2.3(\pm0.9)\times10^{4}$	$1.8(\pm0.3)\times10^{4}$	$1.8(\pm0.3)\times10^{3}$	$5.0(\pm0.0)\times10^{1}$	0.0(±0.0)	0.0(±0.0)	0.0(±0.0)
LUH 5875	ST3	$2.0(\pm0.0)\times10^{7}$	$1.1(\pm0.2)\times10^{5}$	$2.8(\pm0.5)\times10^{3}$	$1.0(\pm0.1)\times10^{2}$	$1.0(\pm0.1)\times10^{2}$	0.0(±0.0)	0.0(±0.0)	0.0(±0.0)	0.0(±0.0)	0.0(±0.0)	0.0(±0.0)	0.0(±0.0)	0.0(±0.0)	0.0(±0.0)	0.0(±0.0)	0.0(±0.0)
3868	ST15	$2.0(\pm0.0)\times10^{7}$	$1.4(\pm0.2)\times10^{7}$	$1.7(\pm0.1)\times10^{6}$	$6.2(\pm0.8)\times10^{4}$	$1.8(\pm0.1)\times10^{3}$	$1.6(\pm0.1)\times10^{3}$	$1.3(\pm0.1)\times10^{3}$	$1.2(\pm0.1)\times10^{3}$	$1.1(\pm0.1)\times10^{3}$	$1.4(\pm0.3)\times10^{3}$	$9.0(\pm1.4)\times10^{2}$	$3.8(\pm0.3)\times10^{2}$	0.0(±0.0)	0.0(±0.0)	0.0(±0.0)	0.0(±0.0)
3871	ST84	$1.9(\pm0.0)\times10^{7}$	$4.2(\pm0.8)\times10^{6}$	$7.4(\pm1.4)\times10^{3}$	0.0(±0.0)	0.0(±0.0)	0.0(±0.0)	0.0(±0.0)	0.0(±0.0)	0.0(±0.0)	0.0(±0.0)	0.0(±0.0)	0.0(±0.0)	0.0(±0.0)	0.0(±0.0)	0.0(±0.0)	0.0(±0.0)
3890	ST25	$1.9(\pm0.1)\times10^{7}$	$1.8(\pm0.8)\times10^{7}$	$1.6(\pm0.5)\times10^{6}$	$1.0(\pm0.1)\times10^{6}$	$6.0(\pm0.1)\times10^{5}$	$5.1(\pm0.5)\times10^{5}$	$4.8(\pm0.5)\times10^{5}$	$7.8(\pm0.5)\times10^{4}$	$2.8(\pm0.0)\times10^{4}$	$1.8(\pm0.0)\times10^{4}$	$1.2(\pm0.0)\times10^{4}$	$1.1(\pm0.3)\times10^{4}$	$4.8(\pm0.0)\times10^{2}$	$7.5(\pm0.0)\times10^{1}$	0.0(±0.0)	0.0(±0.0)
3865	ST25	$2.0(\pm0.1)\times10^{7}$	$2.9(\pm0.5)\times10^{4}$	$2.8(\pm0.5)\times10^{4}$	$2.3(\pm0.2)\times10^{4}$	$1.8(\pm0.3)\times10^{4}$	$1.6(\pm0.2)\times10^{4}$	0.0(±0.0)	0.0(±0.0)	0.0(±0.0)	0.0(±0.0)	0.0(±0.0)	0.0(±0.0)	0.0(±0.0)	0.0(±0.0)	0.0(±0.0)	0.0(±0.0)
4190	ST25	$2.0(\pm0.0)\times10^{7}$	$9.6(\pm1.1)\times10^{6}$	$3.6(\pm0.5)\times10^{6}$	$2.0(\pm0.4)\times10^{6}$	$2.0(\pm0.5)\times10^{5}$	$1.2(\pm0.2)\times10^{5}$	$1.1(\pm0.1)\times10^{5}$	$2.8(\pm0.0)\times10^{2}$	0.0(±0.0)	0.0(±0.0)	0.0(±0.0)	0.0(±0.0)	0.0(±0.0)	0.0(±0.0)	0.0(±0.0)	0.0(±0.0)
ATCC 19606^{T}	ST52	$1.8(\pm0.2)\times10^{7}$	$8.0(\pm2.2)\times10^{4}$	$1.5(\pm0.1)\times10^{4}$	$1.1(\pm0.2)\times10^{3}$	$1.2(\pm5.0)\times10^{1}$	0.0(±0.0)	0.0(±0.0)	0.0(±0.0)	0.0(±0.0)	0.0(±0.0)	0.0(±0.0)	0.0(±0.0)	0.0(±0.0)	0.0(±0.0)	0.0(±0.0)	0.0(±0.0)
ATCC 17978	ST77	$2.0(\pm0.1)\times10^{7}$	$5.5(\pm0.6)\times10^{4}$	$2.2(\pm0.6)\times10^{4}$	$1.9(\pm0.3)\times10^{4}$	$7.6(\pm1.6)\times10^{1}$	$1.6(\pm0.0)\times10^{1}$	$1.6(\pm0.0)\times10^{1}$	0.0(±0.0)	0.0(±0.0)	0.0(±0.0)	0.0(±0.0)	0.0(±0.0)	0.0(±0.0)	0.0(±0.0)	0.0(±0.0)	0.0(±0.0)
3909	ST78	$1.8(\pm0.1)\times10^{7}$	$7.6(\pm0.6)\times10^{6}$	$4.4(\pm0.5)\times10^{6}$	$5.4(\pm0.3)\times10^{4}$	$5.2(\pm1.6)\times10^{3}$	$3.4(\pm0.3)\times10^{3}$	$2.8(\pm0.5)\times10^{3}$	$2.6(\pm0.3)\times10^{3}$	$2.0(\pm0.5)\times10^{3}$	$1.8(\pm0.3)\times10^{3}$	$1.3(\pm0.4)\times10^{3}$	0.0(±0.0)	0.0(±0.0)	0.0(±0.0)	0.0(±0.0)	0.0(±0.0)
3957	ST78	$1.9(\pm0.0)\times10^{7}$	$6.8(\pm1.6)\times10^{6}$	$8.2(\pm0.8)\times10^{4}$	$5.0(\pm1.4)\times10^{4}$	$1.4(\pm0.3)\times10^{4}$	$7.6(\pm0.5)\times10^{4}$	$1.8(\pm0.2)\times10^{3}$	$2.4(\pm0.5)\times10^{3}$	$2.0(\pm0.5)\times10^{3}$	$1.4(\pm0.3)\times10^{3}$	$1.4(\pm0.2)\times10^{3}$	$1.2(\pm0.2)\times10^{3}$	0.0(±0.0)	0.0(±0.0)	0.0(±0.0)	0.0(±0.0)
3911	ST78	$2.0(\pm0.0)\times10^{7}$	$8.2(\pm0.3)\times10^{6}$	$7.0(\pm0.3)\times10^{6}$	$1.4(\pm0.3)\times10^{6}$	$1.8(\pm0.5)\times10^{4}$	$1.3(\pm0.1)\times10^{4}$	$1.1(\pm0.0)\times10^{4}$	$1.0(\pm0.0)\times10^{4}$	$3.6(\pm0.5)\times10^{3}$	$3.4(\pm0.3)\times10^{3}$	$2.6(\pm0.3)\times10^{3}$	$2.3(\pm0.4)\times10^{3}$	$6.0(\pm0.0)\times10^{2}$	$1.8(\pm0.0)\times10^{2}$	$8.0(\pm0.0)\times10^{1}$	0.0(±0.0)

Chapter 7

In vitro and *in vivo* antimicrobial activity of gallium nitrate against multidrug resistant *Acinetobacter baumannii*

Luísa C. S. Antunes[1], Francesco Imperi[2], Fabrizia Minandri[1], and Paolo Visca[1]

[1]Department of Biology, University Roma Tre, Rome, Italy

[2]Department of Biology and Biotechnology Charles Darwin, Sapienza University of Rome, Rome, Italy

Antimicrob Agents Chemother 56 (2012): 5961-5970

Abstract

Acinetobacter baumannii is a paradigmatic example of a multidrug resistant bacterium. The scarcity of effective antimicrobials against *A. baumannii* warrants the development of alternative therapeutic strategies that possibly have lower associated resistance rates. The species conservation of iron-acquisition systems and their importance for *A. baumannii* pathogenicity indicates that iron metabolism could be an optimal target for new antimicrobial strategies.

In this study, an innovative antimicrobial strategy based on gallium, an iron mimetic metal, was devised. Results showed that therapeutic concentrations of the FDA-approved drug gallium nitrate (Ganite®) could effectively inhibit the growth of *A. baumannii* in a chemically-defined medium and in human serum. In addition, gallium nitrate protected *Galleria mellonella* larvae from lethal *A. baumannii* infection. Lastly, gallium nitrate showed synergism with colistin, suggesting that this combination could be used against colistin-resistant *A. baumannii*.

Therefore, gallium nitrate shows promising therapeutic potential in the treatment of bloodstream *A. baumannii* infections. Further clinical studies using mammalian models are needed to confirm the promising potential of this drug against multidrug resistant *A. baumannii*.

AAC
Journals.ASM.org

In Vitro and *In Vivo* Antimicrobial Activities of Gallium Nitrate against Multidrug-Resistant *Acinetobacter baumannii*

Luísa C. S. Antunes,[a] Francesco Imperi,[b] Fabrizia Minandri,[a] and Paolo Visca[a]

Department of Biology, University Roma Tre, Rome, Italy,[a] and Department of Biology and Biotechnology Charles Darwin, Sapienza University of Rome, Rome, Italy[b]

Multidrug-resistant *Acinetobacter baumannii* poses a tremendous challenge to traditional antibiotic therapy. Due to the crucial role of iron in bacterial physiology and pathogenicity, we investigated iron metabolism as a possible target for anti-*A. baumannii* chemotherapy using gallium as an iron mimetic. Due to chemical similarity, gallium competes with iron for binding to several redox enzymes, thereby interfering with a number of essential biological reactions. We found that $Ga(NO_3)_3$, the active component of an FDA-approved drug (Ganite), inhibits the growth of a collection of 58 *A. baumannii* strains in both chemically defined medium and human serum, at concentrations ranging from 2 to 80 μM and from 4 to 64 μM, respectively. $Ga(NO_3)_3$ delayed the entry of *A. baumannii* into the exponential phase and drastically reduced bacterial growth rates. $Ga(NO_3)_3$ activity was strongly dependent on iron availability in the culture medium, though the mechanism of growth inhibition was independent of dysregulation of gene expression controlled by the ferric uptake regulator Fur. $Ga(NO_3)_3$ also protected *Galleria mellonella* larvae from lethal *A. baumannii* infection, with survival rates of ≥75%. At therapeutic concentrations for humans (28 μM plasma levels), $Ga(NO_3)_3$ inhibited the growth in human serum of 76% of the multidrug-resistant *A. baumannii* isolates tested by ≥90%, raising expectations on the therapeutic potential of gallium for the treatment of *A. baumannii* bloodstream infections. $Ga(NO_3)_3$ also showed strong synergism with colistin, suggesting that a colistin-gallium combination holds promise as a last-resort therapy for infections caused by pan-resistant *A. baumannii*.

The threat to public health posed by multidrug-resistant (MDR) bacteria has become a pressing problem on a global scale. In this scenario, the Gram-negative bacterium *Acinetobacter baumannii* provides a paradigmatic example of the impressively fast acquisition and accumulation of antibiotic resistance (32, 45, 61). *A. baumannii* is a versatile pathogen implicated in a wide range of hospital infections, particularly among critically ill patients in intensive care units (ICUs), and certain worldwide epidemic lineages are responsible for large citywide and even nationwide outbreaks (19, 45, 61).

During the 1970s, *A. baumannii* infections could be treated successfully with gentamicin, minocycline, nalidixic acid, ampicillin, or carbenicillin, but high proportions of strains rapidly became resistant to most antimicrobials, including carbapenems (7, 32, 45). Colistin (CST) and tigecycline retain activity against most *A. baumannii* isolates (49), though infections sustained by resistant strains have already been documented in several countries (12, 15, 36), and such infections are untreatable with any commercially available antibiotic.

The paucity of effective drugs for the treatment of MDR infections has highlighted the overwhelming need for research and development programs aimed at identifying new therapeutic options. The siderophore-mimetic BAL30072 is a new monosulfactam containing a dihydropyridone siderophore-like moiety which is believed to accelerate its flux across the Gram-negative cell envelope (27). Gallium [Ga(III)] is an iron-mimetic metal that exerts a significant antimicrobial activity against a number of bacteria, also including the reference *A. baumannii* strain ATCC 17978 (5, 13, 18, 23, 31, 39, 40, 41). Ga(III), in the form of citrate-buffered $Ga(NO_3)_3$ solution (Ganite; Genta), is an FDA-approved drug for intravenous (i.v.) treatment of hypercalcemia associated with malignancy (14). Ga(III) activity is due to its chemical resemblance to Fe(III). Both metals show similarities in nuclear radius and coordination chemistry so that Ga(III) can efficiently compete with Fe(III) for binding to iron-containing enzymes, as well as to transferrin, lactoferrin, and microbial iron chelators (siderophores). However, Ga(III) cannot be physiologically reduced, and when it replaces Fe(III) in redox enzymes, a number of essential biological reactions are inhibited, including those responsible for DNA and protein synthesis and energy production (8). Given the competitive nature of Ga(III)-dependent inhibition of bacterial metabolism, the antibacterial activity of Ga(III) is reversed by Fe(III), influenced by ligand complexation, and strongly reduced in iron-rich media (5, 6, 18, 31, 50).

Invading pathogens are faced with an extreme iron limitation during infection as a means of host defense and must gain access to Fe(III) retained by chelating proteins such as transferrin and lactoferrin (64). To accomplish this essential function, microorganisms have evolved different strategies, including the expression of high-affinity, siderophore-mediated iron uptake systems (11). Production of siderophores is stimulated under iron-limiting conditions [Fe(III) ≤ 1 to 5 μM] and repressed when sufficient iron is available. The Fur (ferric uptake regulator) repressor protein acts as the master regulator of iron homeostasis in bacteria. In cells containing sufficient iron levels, the Fur-Fe(II) complex blocks transcription arising from Fur-controlled promoters, which in turn are transcribed under conditions of iron starvation

Received 24 July 2012 **Returned for modification** 26 August 2012
Accepted 3 September 2012
Published ahead of print 10 September 2012
Address correspondence to Paolo Visca, visca@uniroma3.it.
All authors contributed equally to this article.
Supplemental material for this article may be found at http://aac.asm.org/.

doi:10.1128/AAC.01519-12

(33). Iron acquisition from the human host appears to be crucial for *A. baumannii* pathogenicity, as inferred by the presence in this species of multiple iron-uptake systems (3, 24) and the reduced lethality of mutants impaired in acinetobactin siderophore synthesis (25). The importance of iron in host-pathogen interactions led us to investigate the effect of Ga(III) on *A. baumannii* growth, iron regulation, and virulence. Here we demonstrate that $Ga(NO_3)_3$ exerts potent growth inhibition of clinical *A. baumannii* strains in both chemically defined medium and human serum. While the inhibitory mechanism of $Ga(NO_3)_3$ appears to involve interference with iron metabolism, $Ga(NO_3)_3$ did not affect iron-dependent regulation of gene expression mediated by the Fur protein. $Ga(NO_3)_3$ also caused a dramatic reduction of *A. baumannii* lethality in the *Galleria mellonella* insect model of infection and showed significant *in vitro* synergism with CST.

MATERIALS AND METHODS

Bacterial strains and culture conditions. The 58 *A. baumannii* strains used in this study are listed in Table S1 in the supplemental material. The collection includes the following strains: type strain ATCC 19606^T, representative strains for the international clonal lineages (ICL) I, II, and III, RUH 875, RUH 134, and RUH 5875, respectively (38, 59), strains AYE (ICL I), ACICU (ICL II), and ATCC 17978, for which the annotated genome sequence is available (28, 53, 58), CST-resistant clinical isolate 50C (15, 16), and 50 genotypically diverse, previously described clinical isolates collected as part of the European Union-funded Antibiotic Resistance, Prevention and Control (ARPAC) project (3, 35). All strains, except ATCC 19606^T, ATCC 17978, RUH 875, and RUH 134, showed an MDR phenotype (16, 28, 57, 58).

Culture media were as follows: M9 minimal medium (51) supplemented with 20 mM sodium succinate as the carbon source (hereby called M9) and, when indicated, 100 μM 2,2′-dipyridyl (DIP) to reduce iron availability (M9-DIP), 1% and 10% tryptic soy broth (TSB; Neogen Co., Lansing, MI) (31), iron-depleted Bacto Casamino Acids (Becton, Dickinson, Sparks, MD) medium (DCAA) (60); BBL Mueller-Hinton broth (MH; Becton, Dickinson). When needed, media were supplemented with $FeCl_3$ or $FeSO_4$ at appropriate concentrations to increase iron availability.

Human serum collected from 50 healthy donors was pooled, filtered, and inactivated (30 min, 56°C) as described previously (2). Serum chemistry was as follows: total iron, 0.89 μg/ml; ferritin, 0.17 μg/ml; transferrin, 2.53 mg/ml; and total iron binding capacity, 3.16 μg/ml (28% transferrin saturation, equivalent to 46.7 μM unsaturated iron binding sites). To achieve complete transferrin saturation, an excess of $FeCl_3$ (200 μM) was added to human serum when indicated.

Isolates were grown overnight at 37°C in the above media and then diluted to an optical density at 600 nm (OD_{600}) of 0.01 in the same medium with or without $FeCl_3$. For growth in human serum, inocula were obtained upon dilution to the OD_{600} of 0.01 of an overnight culture at 37°C in M9. Two hundred microliters of bacterial suspensions were dispensed in 96-well microtiter plates, and growth (OD_{600}) was periodically monitored for up to 48 h in a Wallac 1420 Victor3 V multilabel plate reader (Perkin Elmer). Large-scale cultures were performed in flasks containing 25 ml of medium, and growth (OD_{600}) was monitored spectrophotometrically for up to 48 h. All cultures were incubated at 37°C with vigorous shaking (200 rpm). Each strain was tested at least twice in independent experiments.

Assays for siderophore production. The total iron-chelating activity in culture supernatants was determined by the chromoazurol S (CAS) liquid assay (52). The assay was preliminarily performed on 24- and 48-h large-scale cultures of strain ATCC 17978 and then extended to the whole collection in microtiter scale. For this purpose, 24- and 48-h cultures were centrifuged for 10 min at 3,000 × *g* in a microtiter plate centrifuge (Eppendorf model no. 5810r), and 100 μl of supernatant was mixed with an equal volume of the CAS solution. Iron-chelating activity was expressed as siderophore units (U) normalized to the cell density (OD_{600}) of the bacterial culture. Siderophore units are defined as $[(OD_{630\ reference} - OD_{630\ sample})/OD_{630\ reference}] \times 100$ (42).

Generation of the Fur-regulated *basA*::*lacZ* promoter fusion and β-galactosidase activity assay. The 596-bp DNA fragment encompassing the Fur box within the *basA* (A1S_2391) promoter region was obtained by PCR amplification with primers P*basA*_FW (CGGAATTCGCCATATTC TTGTTTCGAT) and P*basA*_RV (TTATGCTGAGGTAGGGACTCTAG ACG) and cloned at the EcoRI-XbaI restriction sites (underlined) of the pMP220 broad-host-range promoter probe plasmid upstream of the reporter *lacZ* gene (54) to yield pMP220::P*basA*. The Fur titration assay (FURTA) (55) was used to confirm the presence of a functional Fur box in the promoter region of the *A. baumannii* ATCC 17978 *basA* gene. Briefly, the 596-bp DNA fragment encompassing the *basA* promoter was cloned in pBluescript II SK vector (Stratagene) to yield pBS::P*basA* and introduced in *Escherichia coli* H1717 to assess the FURTA phenotype as described previously (55).

The pMP220::P*basA* transcriptional fusion was introduced in *A. baumannii* strain ATCC 17978 by electroporation, and transformants were selected on 10-μg/ml tetracycline plates. Plasmid pMP220::P*basA* was used to probe the intracellular iron pool of bacteria, as inferred by Fur and iron regulation of the P*basA* fusion in different growth media and in the presence or absence of $Ga(NO_3)_3$ or $FeSO_4$. For the latter purpose, *A. baumannii* ATCC 17978(pMP220::P*basA*) was grown at 37°C for up to 48 h in M9-DIP with or without $FeSO_4$ (1.25, 2.5, 5, or 10 μM) and/or $Ga(NO_3)_3$ (6.25 or 12.5 μM).

The β-galactosidase (LacZ) activity was determined spectrophotometrically on toluene/SDS-permeabilized cells using *o*-nitrophenyl-β-D-galactopyranoside as the substrate, normalized to the OD_{600} of the bacterial culture, and expressed in Miller units (37). Results are the means of triplicate experiments.

$Ga(NO_3)_3$ susceptibility testing and iron-gallium competition assays. $Ga(NO_3)_3$ activity was tested in 96-well microtiter plates. Briefly, *A. baumannii* isolates were grown overnight at 37°C in M9, diluted in M9-DIP to a final OD_{600} of 0.01, and 200 μl of the bacterial suspensions were dispensed in 96-well microtiter plates containing increasing $Ga(NO_3)_3$ concentrations (0 to 128 μM). Inhibitory concentrations (ICs) of $Ga(NO_3)_3$ in human serum were determined using a protocol similar to that described for M9-DIP, except that bacteria were diluted in inactivated pooled human serum supplemented with increasing $Ga(NO_3)_3$ concentrations (0 to 128 μM). For Fe(III)-Ga(III) competition experiments, the same procedure was performed, except that $FeCl_3$ was added in a range of 0.4 to 50.0 μM. Microtiter plates were incubated for up to 48 h at 37°C and growth (OD_{600}) was measured in a Wallac 1420 Victor3 V multilabel plate reader. For each strain, the $Ga(NO_3)_3$ concentrations that inhibited growth by 50% and 90% (IC_{50} and IC_{90}, respectively) in M9-DIP and human serum were calculated at 24 and/or 48 h using GraphPad Prism software (version 5.0; GraphPad Software, San Diego, CA). The effect of Fe(III) on Ga(III) activity was expressed as a percentage relative to bacterial growth at 48 h in M9-DIP without Fe(III) and Ga(III).

For large-scale cultures, a subset of representative *A. baumannii* isolates with IC values comparable to the median values of the bacterial collection (see Tables S2 and S3 in the supplemental material), including ACICU, A376, A399, and A451, were grown overnight at 37°C in M9, diluted to an OD_{600} of 0.01 in flasks containing 25 ml of M9-DIP and different $Ga(NO_3)_3$ concentrations (0, 4, 16, 64, and 128 μM), and grown at 37°C for up to 48 h.

***G. mellonella* killing assays and *in vivo* Ga(III) treatments.** The *A. baumannii* virulence assay in *G. mellonella* was performed as described previously (2), with few alterations. In order to establish the *A. baumannii* inoculum required to kill *G. mellonella* (580 mg ± 60 mg weight), 10 caterpillars were injected with 10 μl of three serial 10-fold dilutions in saline solution of bacteria grown in M9 to an OD_{600} of 1.0 (late exponential phase, predicted to contain ~1×10^9 CFU/ml). A panel of seven strains showing different levels of $Ga(NO_3)_3$ resistance *in vitro* (see Tables

S2 and S3 in the supplemental material), including ATCC 19606^T, ATCC 17978, RUH 5875, AYE, ACICU, 50C, and A371, was used. Bacterial colony counts on TSB agar plates were used to estimate the number of viable cells in each inoculum. Ten larvae that received no injection and 10 larvae injected with 10 μl of sterile saline solution were used as negative controls for each experiment. Two independent experiments were performed for each strain. Larvae were incubated at 37°C in petri dishes and monitored for up to 96 h. Survival curves were plotted using the Kaplan-Meier estimator and expressed in percentages.

In preliminary toxicology assays, *G. mellonella* caterpillars were injected with 10 μl of $Ga(NO_3)_3$ (0 to 3 M corresponding to 0 to 52 mmol/kg of body weight) or sodium nitrate ($NaNO_3$) (0 to 6 M corresponding to 0 to 102 mmol/kg) solutions. At least 10 larvae were inoculated per condition, incubated at 37°C in petri dishes, and monitored daily for up to 96 h. Caterpillars were considered dead when they did not react to gentle prodding (2).

The $Ga(NO_3)_3$ dosage for treatment of *A. baumannii* infections in *G. mellonella* (1.2 mmol/kg) was extrapolated from the human therapeutic dose (~47 μM) by allometric scaling based on body surface area (BSA), as recommended by the FDA. Normalization to BSA is preferable to simple weight conversion since it takes into consideration metabolic rates and corrects for problems of overdosing (48). Human and larval BSAs were thus calculated using the formula described by DuBois and DuBois (20), and dose translation was performed using the formula described by Reagan-Shaw et al. (48).

The effect of $Ga(NO_3)_3$ on *A. baumannii*-infected caterpillars was assessed by injecting the right proleg of 16 *G. mellonella* caterpillars with a lethal dose of each *A. baumannii* strain, followed by injection into the left proleg with 1.2 mmol/kg of $Ga(NO_3)_3$ after 15 min. Ten larvae that received 10 μl of sterile saline solution in place of $Ga(NO_3)_3$ were used as a Ga(III)-untreated control, and 10 larvae injected twice with 10 μl of sterile saline solution were used as negative controls for $Ga(NO_3)_3$ protection experiments.

Checkerboard assay for Ga(III)-CST interactions. The interaction between Ga(III) and CST (purchased from Sigma-Aldrich as sulfate salt) was determined in MH broth and M9-DIP, using the checkerboard assay as described previously (46). A panel of nine *A. baumannii* strains showing levels of $Ga(NO_3)_3$ resistance representative of the range observed for the whole bacterial collection (see Tables S2 and S3 in the supplemental material) was selected, including the reference strains ATCC 19606^T, ATCC 17978, RUH 875, RUH 134, RUH 5875, AYE, and ACICU and the clinical isolates A371 and 50C, the latter one being CST resistant (15, 16). The MIC of CST was determined in 96-well microtiter plates as described previously (46). The criteria proposed by Gales et al. (26) were used for interpretation of CST susceptibility. For the checkerboard assay, microtiter plates were inoculated with each *A. baumannii* isolate to yield ~5 × 10^5 CFU/ml in a 100-μl final volume of MH broth or, alternatively, OD_{600} of 0.01 in a 200-μl final volume of M9-DIP and incubated at 37°C. Two independent experiments were performed per isolate. Results were recorded after 18 h for MH plates and after 48 h for M9-DIP plates. The CST concentration range tested was from 0.0625 to 256 μg/ml. The MIC was defined as the lowest drug concentration that completely inhibited the growth of the organism, as detected by visual inspection. The fractional inhibitory concentration index (FICI) was calculated for each combination using the following formula: $FICI = FIC_{Ga(III)} + FIC_{CST}$, where $FIC_{Ga(III)}$ represents the MIC of Ga(III) in combination/the MIC of Ga(III) alone and FIC_{CST} represents the MIC of CST in combination/the MIC of CST alone. The FICI was interpreted as follows: synergy, $FICI \leq 0.5$; indifference, $0.5 < FICI \leq 4$; and antagonism, $FICI > 4$ (46).

Statistical analysis. All statistical analyses, including inhibition and survival curve analyses, were performed using GraphPad Prism software. Since a large variation in growth yields and response to Ga(III) was observed among strains, results were reported in boxplots showing medians rather than means.

RESULTS

Assessment of growth media for $Ga(NO_3)_3$ susceptibility testing. The antibacterial properties of gallium are attributable to its ability to substitute for iron in bacterial metabolism, and a number of previous reports have demonstrated that an iron surplus abrogates gallium activity (18, 31, 43). Moreover, invading pathogens are generally faced with an extreme iron limitation during growth *in vivo* as the result of the host innate defense against infection (64). To mimic the iron-poor environment of the host and define suitable conditions for Ga(III) activity testing, a preliminary investigation of siderophore production and intracellular iron levels was performed in the *A. baumannii* prototype strain ATCC 17978, grown in a set of chemically defined (M9, M9-DIP, and DCAA) and undefined (1% TSB, 10% TSB, and MH broth) media. As a trend, growth of ATCC 17978 was poor in DCAA and 1% TSB, moderate in 10% TSB and M9 with or without DIP, and abundant in MH broth (Fig. 1A). Addition of 100 μM $FeCl_3$ strongly increased growth yields in DCAA and, to a lesser extent, in M9 and M9-DIP, suggesting that iron is a limiting nutrient in these media (Fig. 1A). Accordingly, high siderophore production was observed in M9 and M9-DIP but not in 1% TSB, 10% TSB, and MH broth (Fig. 1B). Siderophore production was moderate in DCAA, plausibly due to the very poor growth (Fig. 1A and B). Expression of the Fur-Fe(II)-controlled *basA*::*lacZ* transcriptional fusion was then measured in *A. baumannii* ATCC 17978 carrying plasmid pMP220::P*basA*. The presence of a functional Fur box in the promoter region of the *A. baumannii* ATCC 17978 *basA* gene was confirmed through the FURTA (see Fig. S1 in the supplemental material). Since the Fur repressor protein acts as an iron sensor, the activity of the Fur-controlled *basA* promoter provides an indirect estimate of the intracellular iron levels of bacteria grown in the different media. Consistent with siderophore production, iron repressible β-galactosidase expression was high in M9 and M9-DIP but low or null in DCAA, 1% TSB, 10% TSB, and MH broth (Fig. 1C). Based on the above results, it was concluded that M9-DIP could be used as an easily reproducible, chemically defined, iron-deplete medium for Ga(III) susceptibility testing. Addition of 100 μM DIP to M9 would ensure an iron-deficient medium in the event that iron traces were present as contaminants of the M9 basal salt solution.

Growth and siderophore production was then evaluated for the whole collection of 58 *A. baumannii* strains in M9-DIP using a microtiter plate assay. All strains showed sufficient growth and produced detectable siderophore levels in M9-DIP (Fig. 2; see also Table S4 in the supplemental material). As expected, addition of 100 μM $FeCl_3$ to M9-DIP increased growth yields and abrogated siderophore production (Fig. 2; see also Table S4).

Ga(III) inhibits *A. baumannii* growth in a chemically defined medium. The effect of Ga(III) on *A. baumannii* growth in M9-DIP was determined for all strains in a microtiter plate assay and expressed as IC_{50} and IC_{90} after 24 and 48 h growth (see Table S2 in the supplemental material). Ga(III) inhibited *A. baumannii* growth in a dose- and strain-dependent manner. In general, the IC values were lower at 24 than 48 h (Fig. 3; see also Table S2). At 48 h, the IC_{50} and IC_{90} values varied in the ranges of 1 to 28 μM and 2 to 80 μM $Ga(NO_3)_3$, respectively, with median values of 8.5 ± 5.0 and 23.8 ± 12.0 μM $Ga(NO_3)_3$, respectively (Fig. 3). Growth inhibition was also assessed in flask cultures using a representative subset of strains, namely, ACICU, A376, A399, and A451, en-

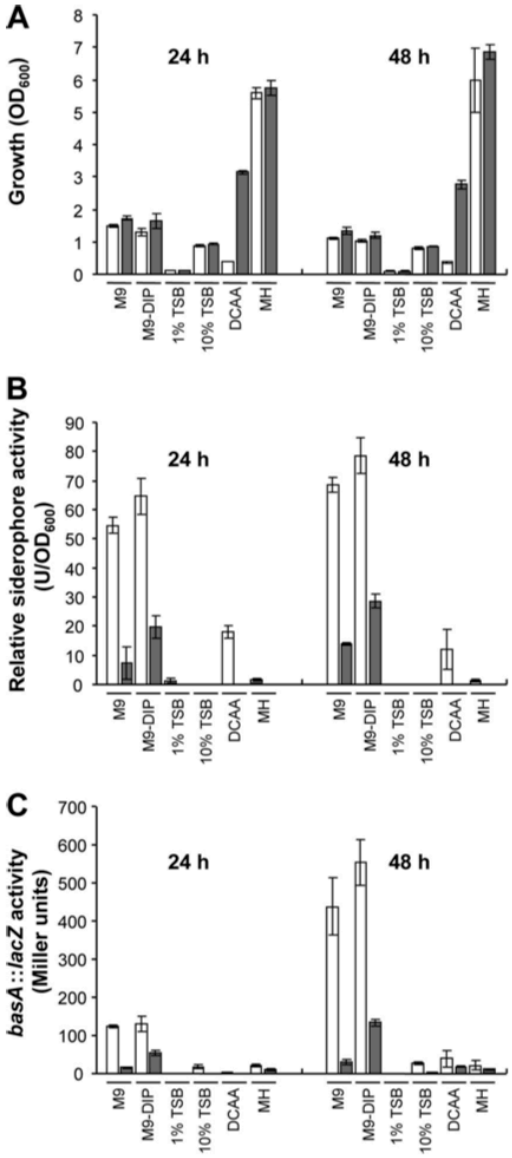

FIG 1 *A. baumannii* ATCC 17978 growth (A), siderophore production (B), and activity of the *basA*::*lacZ* iron-regulated fusion (C). Bacteria were grown in different media for 24 or 48 h, in the absence (white bars) or presence (gray bars) of 100 μM $FeCl_3$. Data are the means (± standard deviations [SD]) of triplicate experiments.

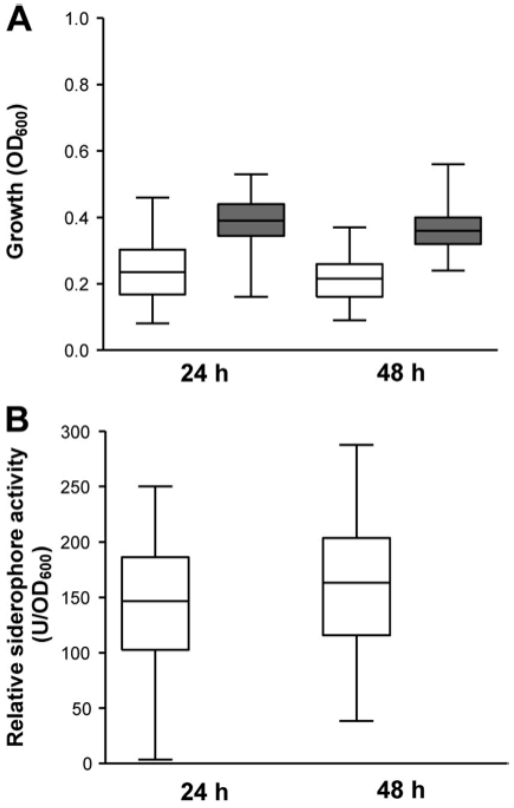

FIG 2 Growth (A) and siderophore production (B) in a collection of 58 *A. baumannii* strains grown for 24 and 48 h in M9-DIP. Boxes represent medians and second and third interquartiles; whiskers represent range of 58 strains. White boxes, M9-DIP without added iron; gray boxes, M9-DIP supplemented with 100 μM $FeCl_3$. For each strain, the mean value of two independent microtiter plate assays was considered.

dowed with Ga(III) susceptibility levels close to the median values determined for the whole collection. The IC_{50}s of $Ga(NO_3)_3$ did not differ substantially between strains grown in flasks or in microtiter plates, while IC_{90} values were 1.02- to 1.74-fold higher for strains grown in flasks (see Fig. S2 in the supplemental material; also data not shown), suggesting that Ga(III) activity is slightly influenced by culture scale and conditions.

The anti-*A. baumannii* activity of Ga(III) is reversed by Fe(III). Since Ga(III) exerts its inhibiting activity by interfering with bacterial iron metabolism, the effect of Fe(III) on Ga(III)-dependent growth inhibition was investigated using the subset of *A. baumannii* strains described above. As expected, Ga(III)-dependent growth inhibition was reversed with increasing Fe(III) concentrations (Fig. 4). For all strains tested, Fe(III) concentrations from 0.4 to 2 μM were sufficient to double the IC_{50}s, while 2 μM Fe(III) caused a 2- to 4-fold increase of the IC_{90} values after 48 h (Fig. 4). The addition of 2 μM Fe(III) was sufficient to increase $Ga(NO_3)_3$ IC_{50} and IC_{90} values from 13 and 36 μM to 29 and 128 μM, respectively, as exemplified by *A. baumannii* strain ACICU (Fig. 4). In general, addition of 50 μM Fe(III) completely abrogated the activity of 128 μM $Ga(NO_3)_3$ (Fig. 4), indicating that an Fe(III)/Ga(III) molar ratio of ~1:2.5 is sufficient to reverse the effect of Ga(III).

Effect of Ga(III) on iron-regulated gene expression and siderophore production. Since Ga(III) cannot be reduced by the cell, it could not substitute for Fe(II) in Fur binding and consequent repression of Fur-controlled promoters. To verify this hypothesis, the effect of Ga(III) on iron homeostasis was investigated in the prototype isolate *A. baumannii* ATCC 17978 by using the Fur-controlled *basA* promoter (see above; see also Fig. S1 in the supplemental material) as a probe for the intracellular iron level. $FeSO_4$ was used in place of $FeCl_3$ since Fe(II) is more soluble and readily available for Fur binding. Addition of up to 2.5 μM $FeSO_4$

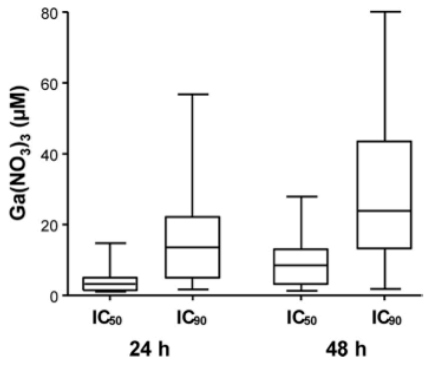

FIG 3 Inhibitory activity of $Ga(NO_3)_3$ on a collection of 58 *A. baumannii* strains grown in chemically defined medium. Plots show the $Ga(NO_3)_3$ concentrations (μM) required to inhibit the growth of each isolate by 50% (IC_{50}) and 90% (IC_{90}) at 24 and 48 h in M9-DIP. Boxes represent medians and second and third interquartiles; whiskers represent range of 58 strains. For each strain, the mean value of two independent microtiter plate assays was considered.

resulted in a dose-dependent reduction of P*basA*::*lacZ* expression, while complete repression was observed at >5 μM $FeSO_4$ (Fig. 5). In contrast, addition of 6.25 and 12.5 μM $Ga(NO_3)_3$ did not influence the level of β-galactosidase activity (Fig. 5). The expression profile of *basA*::*lacZ* in the presence of both $Ga(NO_3)_3$ and $FeSO_4$ was comparable to that observed with $FeSO_4$ alone (Fig. 5). These results suggest that Ga(III) does not interfere with iron homeostasis and Fur-dependent iron regulation in *A. baumannii*. To confirm this conclusion, the effect of Ga(III) on siderophore production, which is a typical response to iron starvation, was investigated. Siderophore production by the subset of *A. baumannii* strains described above was measured after 48 h growth in M9-DIP supplemented with subinhibitory $Ga(NO_3)_3$ concentrations (0, 2, 4, and 8 μM). Overall, addition of $Ga(NO_3)_3$ up to 8 μM did not repress siderophore production (see Fig. S3 in the supplemental material), further supporting the hypothesis that Ga(III) does not interfere with the bacterial response to iron starvation. Higher $Ga(NO_3)_3$ concentrations could not be tested due to strong inhibition of bacterial growth.

Ga(III) inhibits *A. baumannii* growth in human serum. The spread of bacteria into the bloodstream is a frequent complication of primary *A. baumannii* infection. Therefore, the inhibitory activity of Ga(III) in complement-inactivated human serum was investigated. Initially, the growth of strain ACICU in serum with or without $FeCl_3$ was monitored for 56 h using both flask and microtiter plate conditions. Irrespective of the culture mode, *A. baumannii* ACICU growth yields in serum without exogenously added iron were always lower than in iron-replete serum (see Fig. S4 in the supplemental material), confirming that (apo-)transferrin confers to human serum the characteristics of an iron-deplete medium. Since growth yields in microtiter plates were lower than in flasks and the stationary phase was delayed (see Fig. S4), $Ga(NO_3)_3$ inhibitory concentrations for the whole collection could only be calculated at 48 h. At this time point, the IC_{50} and IC_{90} values of $Ga(NO_3)_3$ varied in the range of 2 to 35 μM and 4 to 64 μM, respectively, with median values of 6.0 ± 1.7 and 14.5 ± 0.7 μM, respectively (Fig. 6; see also Table S3 in the supplemental material). Growth of strain ATCC 19606^T was very poor in serum, so the inhibitory effect of Ga(III) could not be assessed even after 48 h of growth (see Table S3). The Ga(III) inhibitory effect in serum was completely abrogated by the addition of 200 μM $FeCl_3$ (data not shown), i.e., an excess of Fe(III) over the transferrin Fe(III) binding capacity (~47 μM).

No statistically significant difference in Ga(III) susceptibility between *A. baumannii* sequence groups (Welch's *t* test, $P > 0.05$) and no correlation between IC values of Ga(III) in M9-DIP and

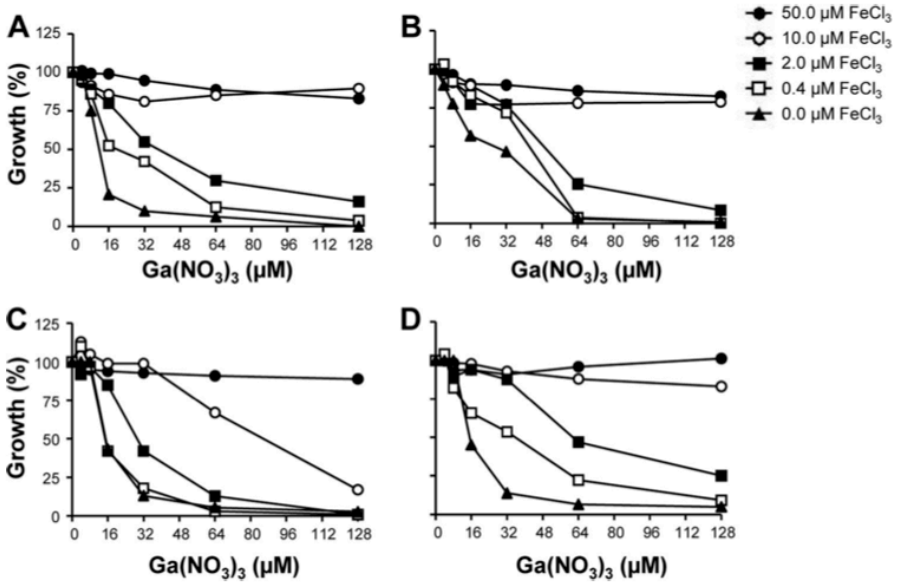

FIG 4 Effect of iron on the inhibitory activity of $Ga(NO_3)_3$. *A. baumannii* strains ACICU (A), A376 (B), A399 (C), and A451 (D) were grown for 48 h in M9-DIP supplemented with increasing $FeCl_3$ (0 to 50 μM) and $Ga(NO_3)_3$ (0 to 128 μM) concentrations. Growth is expressed as percentage relative to growth (OD_{600}) of control cultures in M9-DIP.

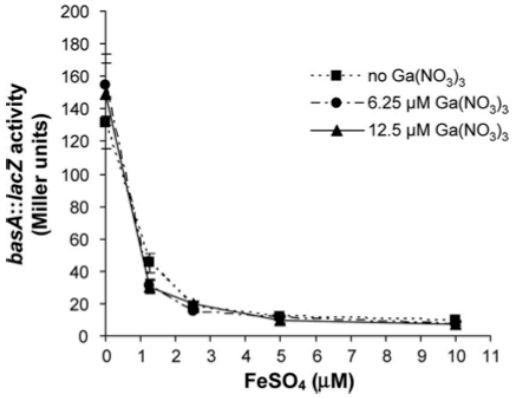

FIG 5 Effect of $Ga(NO_3)_3$ on the activity of the Fur-Fe(II)-regulated *basA*::*lacZ* transcriptional fusion. *A. baumannii* ATCC 17978 carrying plasmid pMP220::P*basA* was grown in M9-DIP supplemented or not supplemented with increasing $FeSO_4$ (1.25, 2.5, 5, or 10 μM) and/or $Ga(NO_3)_3$ (6.25 or 12.5 μM) concentrations. LacZ activity was measured at 48 h and expressed in Miller units (37). Data are the means (±SD) of triplicate experiments.

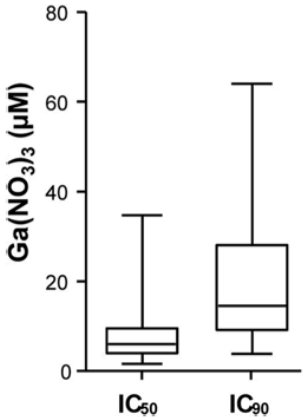

FIG 6 Inhibitory activity of $Ga(NO_3)_3$ on a collection of 57 *A. baumannii* strains grown in human serum. Strains were grown for 48 h in serum supplemented with increasing $Ga(NO_3)_3$ concentrations (0 to 128 μM). Plots show the $Ga(NO_3)_3$ concentrations (μM) required to inhibit the growth of each isolate by 50% (IC_{50}) and 90% (IC_{90}) at 48 h. Boxes represent medians and second and third interquartiles; whiskers represent range of 57 strains. For each strain, the mean value of two independent microtiter plate assays was considered.

human serum (Pearson correlation coefficient, $P > 0.05$) were observed.

Ga(III) promotes the survival of *G. mellonella* larvae infected with *A. baumannii*. The promising results obtained *in vitro* prompted an investigation of the ability of Ga(III) to inhibit *A. baumannii* pathogenicity *in vivo*. To this aim, an infection model based on the larvae of the greater wax moth *G. mellonella* was used. This model has previously been used successfully in the study of *A. baumannii* pathogenesis and therapeutics (2, 44).

$Ga(NO_3)_3$ toxicity to *G. mellonella* was initially tested by injecting larvae with 10 μl of water solutions containing $Ga(NO_3)_3$ up to 3 M, i.e., the maximum experimental solubility of $Ga(NO_3)_3$ in water, and by monitoring the survival of larvae for 96 h. At this time point, killing was only observed for larvae injected with >4.2-mmol/kg $Ga(NO_3)_3$, with lethal doses 50% (LD_{50}) and 90% (LD_{90}) corresponding to 10.0 and 17.8 mmol/kg of $Ga(NO_3)_3$, respectively (see Fig. S5A in the supplemental material). At high $Ga(NO_3)_3$ concentrations (>LD_{90}), nearly all larvae died within 24 h (see Fig. S5A). Injecting *G. mellonella* with $NaNO_3$ as a control for the effect of nitrate resulted, at 96 h, in an LD_{50} and an LD_{90} of 25.4 and 51.7 mmol/kg, respectively (see Fig. S5B). These values are comparable to those observed for $Ga(NO_3)_3$, so it can be argued that the observed mortality of larvae can primarily be attributed to nitrate toxicity. However, the *G. mellonella* equivalent of the therapeutic $Ga(NO_3)_3$ dosage used in humans is 1.2 mmol/kg (see Materials and Methods) (14, 48), corresponding to ~1/10 of the LD_{50} predetermined for Ga(III) and nitrate in *G. mellonella*. At this $Ga(NO_3)_3$ dosage, no larvae were killed at any time (see Fig. S5).

A. baumannii lethal doses for *G. mellonella* were then calculated for strains ATCC 19606^T, ATCC 17978, RUH 5875, AYE, ACICU, 50C, and A371. At 96 h postinfection, all strains but ATCC 19606^T showed LD_{50}s between 1×10^5 and 2×10^6 CFU/larva and LD_{90}s between 3×10^5 and 8×10^6 CFU/larva (see Table S5 in the supplemental material). The LD_{50} of ATCC 19606^T for *G. mellonella* was very high (~ 4×10^7 CFU/larva) (see Table S5), typical of nonpathogenic species (2, 4). For this reason, and considering the extreme susceptibility of ATCC 19606^T to Ga(III) *in vitro*, this strain was excluded from subsequent Ga(III) protection experiments.

To test Ga(III) efficacy *in vivo*, a lethal dose of *A. baumannii* (~10^6 to ~10^7 CFU/larva, depending on the strain) (Fig. 7) was administered to *G. mellonella* larvae, followed by the administration of 1.2 mmol/kg of $Ga(NO_3)_3$ to mimic the therapeutic dose used in humans (see Materials and Methods for details). Administration of $Ga(NO_3)_3$ protected *G. mellonella* from *A. baumannii*-mediated killing, with survival rates of ≥75% for all strains at 96 h postinoculation (Fig. 7). Conversely, rapid killing and <20% survival rates were observed for Ga(III)-untreated larvae (Fig. 7).

Ga(III) interacts synergistically with CST. Synergistic effects of the Ga(III)-CST combination were determined using a panel of nine *A. baumannii* strains endowed with different levels of susceptibility to $Ga(NO_3)_3$ and CST. Checkerboard assays in MH broth only allowed inhibition by CST to be determined, since $Ga(NO_3)_3$ concentrations as high as 128 μM had no apparent effect on bacterial growth, likely due to the high iron concentration in this medium (Fig. 1). However, MIC values of CST were substantially lower in the presence of $Ga(NO_3)_3$. Strains ATCC 19606^T, ACICU, A371, and 50C showed a 4-fold reduction of the CST MIC in the presence of 2 μM $Ga(NO_3)_3$, while strains ATCC 17978, AYE, ACICU, RUH 875, RUH 134, and RUH 5875 showed an 8-fold reduction of the CST MIC in a $Ga(NO_3)_3$ range of 2 to 16 μM (Table 1). Notably, the synergistic effect of the tested combinations was also evident for the CST-resistant isolate 50C, even if $Ga(NO_3)_3$ did not lower the CST MIC below the susceptibility threshold (Table 1). Strong synergistic effects were evident in M9-DIP, with FICI values ranging from 0.13 to 0.50 (Table 1). Overall, synergism resulted in a 4- to 32-fold reduction in the MIC of $Ga(NO_3)_3$ and a 2- to 16-fold reduction in the MIC of CST for all but one of the strains tested (Table 1). Noteworthy, the CST-resistant isolate 50C showed an impressive synergism, with a 128-fold reduction of the CST MIC in the presence of 8 μM $Ga(NO_3)_3$ (Table 1).

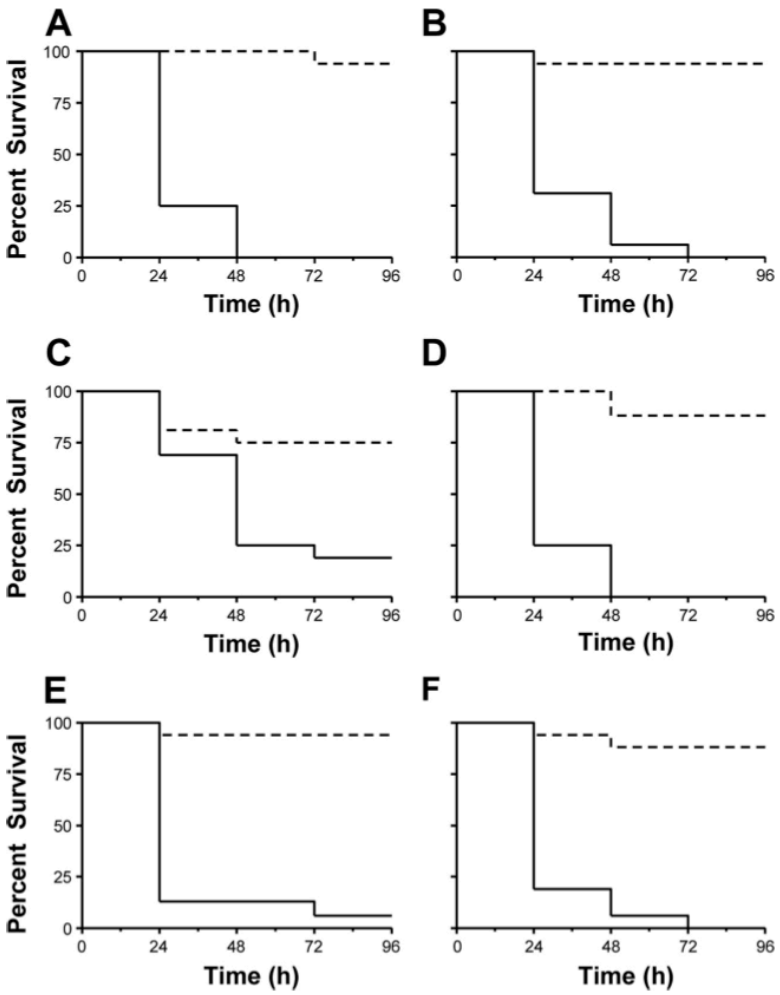

FIG 7 Effect of $Ga(NO_3)_3$ on the viability of *G. mellonella* caterpillars infected with a lethal dose of the following *A. baumannii* strains: ATCC 17978 (~ 5×10^6 CFU/larva) (A), RUH 5875 (~ 1×10^7 CFU/larva) (B), AYE (~ 5×10^6 CFU/larva) (C), ACICU (~ 7×10^6 CFU/larva) (D), 50C (~ 1×10^6 CFU/larva) (E), and A371 (~ 6×10^5 CFU/larva) (F). Solid lines, Ga(III)-untreated larvae; dotted lines, Ga(III)-treated larvae.

DISCUSSION

To face the challenge of progressively expanding resistance in *A. baumannii*, novel microbial targets must be identified and alternative therapeutic approaches developed. Here, we exploited iron metabolism as a possible target for antibacterial chemotherapy. *A. baumannii* possesses several iron uptake systems (3, 24), and almost all of these are encoded by genes belonging to the core genome of nosocomial strains (29). Acinetobactin, the most extensively studied *A. baumannii* siderophore, has the ability to withhold iron from transferrin and lactoferrin (65) and appears to be crucial for *A. baumannii* to establish infection and kill both *G. mellonella* and mice (25). These features reflect an exceptional adaptability to growth in iron-limiting environments and highlight the essential role of iron metabolism in *A. baumannii* pathogenicity. For this reason, a variety of chelating agents have recently been tested for suppression of *A. baumannii* growth (18, 56).

In the present study, the iron-mimetic metal gallium was used to interfere with *A. baumannii* iron metabolism. The results demonstrated that Ga(III), the active component of an FDA-approved drug, exerts a strong anti-*A. baumannii* activity both *in vitro* and *in vivo*. We showed that Ga(III) suppresses the growth of genotypically diverse MDR *A. baumannii* strains, representative of the major sequence groups encountered worldwide (see Table S1 in the supplemental material). The inhibitory activity of Ga(III) was counteracted by iron, confirming that the mechanism of action of Ga(III) in *A. baumannii* involves the disruption of iron metabolism. Consistent with previous findings (18), the anti-*A. baumannii* activity of Ga(III) *in vitro* was strongly dependent on iron availability, being higher in iron-poor, chemically defined media and lower, or even absent, in iron-rich, complex media (Table 1; also data not shown). At present, neither standard protocols nor reference media for Ga(III) susceptibility testing have been defined. MH broth, the standard medium for antibiotic susceptibility testing, appears inappropriate for assessment of Ga(III) activity due to the high iron content (Fig. 1) (5). By comparing bacterial growth and expression of iron-uptake genes in a variety of growth

TABLE 1 Checkerboard assay for CST-Ga(III) interactions in MH broth and M9-DIP with a selected panel of *A. baumannii* strains[a]

	MH broth				M9-DIP			
		MIC				MIC		
Strain	Effect (FICI value) of combination[b]	CST (μg/ml)[c]	$Ga(NO_3)_3$ (μM)	CST (μg/ml)-$Ga(NO_3)_3$ (μM)	Effect (FICI value) of combination	CST (μg/ml)	$Ga(NO_3)_3$ (μM)	CST (μg/ml)-$Ga(NO_3)_3$ (μM)
ATCC 19606^T	Sy (≤0.26)	0.5	≥256	0.125–2	Sy (0.31)	2	8	0.125–2
ATCC 17978	Sy (≤0.13)	1	≥256	0.125–2	Sy (0.28)	4	64	1–2
RUH 875	Sy (≤0.19)	1	≥256	0.125–16	Sy (0.25)	4	64	0.5–8
RUH 134	Sy (≤0.16)	2	≥256	0.25–8	Sy (0.16)	4	64	0.5–2
RUH 5875	Sy (≤0.14)	1	≥256	0.125–4	Sy (0.50)	4	16	1–4
AYE	Sy (≤0.14)	1	≥256	0.125–4	Sy (0.25)	4	16	0.5–2
ACICU	Sy (≤0.26)	1	≥256	0.25–2	Sy (0.37)	8	32	1–4
50C	Sy (≤0.26)	16	≥256	4–2	Sy (0.13)	256	64	2–8
A371	Sy (≤0.26)	1	≥256	0.25–2	Sy (0.25)	4	64	0.5–8

[a] MICs for drug(s) alone and in effective synergistic combination, measured after 18 h growth in MH or 48 h growth in M9-DIP.
[b] In order to calculate the FICI, the MIC of $Ga(NO_3)_3$ in MH broth was assumed to be ≥256 μM for all strains.
[c] Breakpoint criteria for CST in MH broth were susceptible, ≤2 mg/liter, and resistant, ≥4 mg/liter (26).

media (Fig. 1), we selected an iron-depleted minimal salt medium (M9-DIP) in which Ga(III) activity could be determined in microtiter plate assays (Fig. 3). M9-DIP is an easily reproducible, chemically defined medium that can be recommended for future interlaboratory assessment of the *in vitro* antibacterial activity of Ga(III). In this medium, Ga(III) inhibited *A. baumannii* growth in a dose-, strain-, and time-dependent manner (Fig. 2 and 3; see also Fig. S2 and Table S2 in the supplemental material).

To gain insight into the mechanism of action of Ga(III), the effect of $Ga(NO_3)_3$ on iron-regulated gene expression and siderophore production was then investigated. No effect of Ga(III) on Fur-Fe(II)-dependent regulation of gene expression in *A. baumannii* was observed (Fig. 5), and accordingly, siderophore production by *A. baumannii* was not repressed in the presence of subinhibitory concentrations of $Ga(NO_3)_3$ (see Fig. S3 in the supplemental material). This is consistent with the notion that Ga(III) cannot be reduced under physiological conditions and hence cannot act as cofactor in the repression of Fur-regulated genes, including those encoding iron uptake functions. We therefore hypothesize that Ga(III) exerts its negative effect on *A. baumannii* growth by interfering with iron-containing essential enzymes, including those participating in the electron transport chain, resulting in a deleterious effect for *A. baumannii* because of its obligate aerobic metabolism.

Since the two most severe types of *A. baumannii* infection (meningitis and bloodstream infections) involve systemic dissemination of the organism via the circulatory system, the activity of Ga(III) was also assessed in human serum. Evidence has recently been provided that expression of iron acquisition systems in *A. baumannii* is induced during growth in human serum (30), due to the presence of transferrin. Thus, growth inhibition assays in human serum provide a more realistic assessment of $Ga(NO_3)_3$ therapeutic potential when supplied *in vivo*. The IC_{90} values of $Ga(NO_3)_3$ calculated at 48 h in human serum for the collection of *A. baumannii* strains were in the range of 4 to 64 μM, which was similar to the range determined in M9-DIP (2 to 80 μM). Overall, the *in vitro* activity of Ga(III) against *A. baumannii* appears to be comparable to or higher than that reported for other Gram-negative pathogens endowed with high resistance to antibiotics, such as *Pseudomonas aeruginosa* and the *Burkholderia cepacia* complex (31, 43), although data comparison between different studies can only be speculative because of the medium-dependent variability of Ga(III) activity. Moreover, the IC_{90} for the reference strain ATCC 17978 in human serum (3.8 μM) was very similar to that recently determined for this strain in RPMI 1640 supplemented with 10% calf serum (3.1 μM) (18). It is worth noting that 90% of isolates showed IC_{90} values of <47 μM, corresponding to the transferrin iron binding capacity of the serum sample used. Below this concentration, Ga(III) is expected to be completely bound by transferrin due to the high stability constant of the transferrin-$Ga(III)_2$ complex ($\sim 10^{20}\ M^{-1}$) (1). Since Ga(III) must enter the cell to exert its activity, it can be hypothesized that the antibacterial effect of Ga(III) in serum is attributable to gallium removal from transferrin and subsequent acquisition by the bacterial cell via either a siderophore-dependent mechanism or proteolytic cleavage of transferrin. Of note, Ga(III) transport as a siderophore complex has been reported in some bacterial species (9, 10, 22, 63), and extracellular proteolytic activity has previously been documented in *A. baumannii* (2).

Not only was Ga(III) effective in inhibiting bacterial growth *in vitro*, but it also provided a powerful protection against *A. baumannii* infection *in vivo*. Experiments in the *G. mellonella* model demonstrated that Ga(III) is also active in preventing lethal infection by different *A. baumannii* strains (Fig. 7). *G. mellonella* hemolymph contains both iron transport and storage proteins (transferrin and ferritin, respectively), and iron has been shown to be essential to an early antimicrobial response of the insect, where hemocytes limit iron availability to invading pathogens (21). Considering that iron concentration in *G. mellonella* hemolymph is ca. 1.7 μg/ml, i.e., the upper normal range of human serum iron (ca. 0.5 to 1.8 μg/ml), the protective effect of Ga(III) in this insect model could somehow mirror its activity in vertebrate models. In fact, a protective effect of Ga(III) has previously been documented in two mouse models of infection, in which local or systemic administration of different gallium formulations significantly reduced *A. baumannii* growth (17, 18).

The currently recommended dosing regimens for the treatment of cancer-related hypercalcemia (200 to 300 mg/m^2 BSA, i.v.) ensure a peak serum concentration of $Ga(NO_3)_3$ of ca. 28 μM (8, 14). This concentration is higher than the observed IC_{50} and IC_{90} values of $Ga(NO_3)_3$ in human serum for about 98% and 76% of the MDR *A. baumannii* isolates tested in this study, respectively,

suggesting that $Ga(NO_3)_3$ therapy could be effective in reducing the ability of *A. baumannii* to cause bacteremia and spread in the human host.

CST is currently used as a last-line antibiotic for otherwise untreatable MDR *A. baumannii* infections, often in combination with other drugs (34). The present study demonstrated that $Ga(NO_3)_3$, besides being active *per se*, also synergizes with CST *in vitro* against both CST-sensitive and -resistant *A. baumannii* isolates (Table 1). CST acts as a cationic polypeptide that perturbs the outer membrane through interaction with lipopolysaccharide (LPS) molecules (34). It can therefore be hypothesized that CST facilitates Ga(III) diffusion into *A. baumannii* cells, thereby promoting growth inhibition. In addition, interference of Ga(III) with *A. baumannii* iron metabolism impairs essential cellular functions, which could potentiate the CST effect. It was observed that CST MICs were higher in M9-DIP than in MH broth (Table 1). This effect can be ascribed to a high content of magnesium and calcium ions (1 and 0.2 mM, respectively), which stabilize the outer membrane and, thus, antagonize CST activity at the bacterial cell surface (47), consequently increasing CST MICs in M9-DIP. In conclusion, the CST-Ga(III) combination could represent a promising therapeutic option against pan-resistant *A. baumannii*, since it would provide the dual benefit of (i) broadening the range of activity of Ga(III) by making it also effective against strains moderately resistant to therapeutic Ga(III) serum concentrations and (ii) reducing the CST dosages required to treat *A. baumannii* infections, ultimately mitigating the adverse effects of CST therapy.

Though $Ga(NO_3)_3$ therapy could potentially be used as a last resort for treating otherwise untreatable *A. baumannii* infections, the nephrotoxicity of $Ga(NO_3)_3$ should be taken into account, especially in patients who are at risk for renal insufficiency (8). Nevertheless, nephrotoxicity only occurs at extremely high Ga(III) serum concentrations (>200 μM), much higher than those required to treat hypercalcemia and suppress the growth of most *A. baumannii* strains in serum (up to 28 μM) (8) (Fig. 6; see Table S3 in the supplemental material). At these serum concentrations of Ga(III), serum creatinine remains in the normal concentration range and there are no adverse reactions (62). Clinical studies are therefore needed to confirm the promising potential of Ga(III) as an antibacterial agent.

ACKNOWLEDGMENTS

We are grateful to K. J. Towner (Department of Clinical Microbiology, Nottingham University Hospitals, Nottingham, United Kingdom) for critical reading of the manuscript and for providing strains collected as part of the European Union ARPAC project and to P. Nordmann (Hôpital de Bicêtre, le Kremlin-Bicêtre, France) for kindly providing the AYE strain.

Luísa C. S. Antunes was supported by a Ph.D. fellowship from the Portuguese Fundação para a Ciência e a Tecnologia (FCT) (grant SFRH/BD/43420/2008).

REFERENCES

1. **Aisen P, Leibman A, Zweier J.** 1978. Stoichiometric and site characteristics of the binding of iron to human transferrin. J. Biol. Chem. **253**: 1930–1937.
2. **Antunes LC, Imperi F, Carattoli A, Visca P.** 2011. Deciphering the multifactorial nature of *Acinetobacter baumannii* pathogenicity. PLoS One **6**:e22674. doi:10.1371/journal.pone.0022674.
3. **Antunes LC, Imperi F, Towner KJ, Visca P.** 2011. Genome-assisted identification of putative iron-utilization genes in *Acinetobacter baumannii* and their distribution among a genotypically diverse collection of clinical isolates. Res. Microbiol. **162**:279–284.
4. **Aperis G, et al.** 2007. *Galleria mellonella* as a model host to study infection by the *Francisella tularensis* live vaccine strain. Microbes Infect. **9**:729–734.
5. **Baldoni D, Steinhuber A, Zimmerli W, Trampuz A.** 2010. *In vitro* activity of gallium maltolate against Staphylococci in logarithmic, stationary, and biofilm growth phases: comparison of conventional and calorimetric susceptibility testing methods. Antimicrob. Agents Chemother. **54**:157–163.
6. **Banin E, et al.** 2008. The potential of desferrioxamine-gallium as an anti-*Pseudomonas* therapeutic agent. Proc. Natl. Acad. Sci. U. S. A. **105**: 16761–16766.
7. **Bergogne-Bérézin E, Towner KJ.** 1996. *Acinetobacter* spp. as nosocomial pathogens: microbiological, clinical, and epidemiological features. Clin. Microbiol. Rev. **9**:148–165.
8. **Bernstein LR.** 1998. Mechanisms of therapeutic activity for gallium. Pharmacol. Rev. **50**:665–682.
9. **Braud A, Hannauer M, Mislin GL, Schalk IJ.** 2009. The *Pseudomonas aeruginosa* pyochelin-iron uptake pathway and its metal specificity. J. Bacteriol. **191**:3517–3525.
10. **Braud A, Hoegy F, Jezequel K, Lebeau T, Schalk IJ.** 2009. New insights into the metal specificity of the *Pseudomonas aeruginosa* pyoverdine-iron uptake pathway. Environ. Microbiol. 11:1079–1091.
11. **Braun V, Hantke K.** 2011. Recent insights into iron import by bacteria. Curr. Opin. Chem. Biol. **15**:328–334.
12. **Capone A, D'Arezzo S, Visca P, Petrosillo N; GRAB.** 2008. *In vitro* activity of tigecycline against multidrug-resistant *Acinetobacter baumannii*. J. Antimicrob. Chemother. **62**:422–423.
13. **Coleman M, et al.** 2010. *In vitro* antimicrobial activity of gallium maltolate against virulent *Rhodococcus equi*. Vet. Microbiol. **146**:175–178.
14. **Collery P, Keppler B, Madoulet C, Desoize B.** 2002. Gallium in cancer treatment. Crit. Rev. Oncol. Hematol. **42**:283–296.
15. **D'Andrea MM, et al.** 2009. Characterization of pABVA01, a plasmid encoding the OXA-24 carbapenemase from Italian isolates of *Acinetobacter baumannii*. Antimicrob. Agents Chemother. **53**:3528–3533.
16. **D'Arezzo S, et al.** 2009. Epidemic multidrug-resistant *Acinetobacter baumannii* related to European clonal types I and II in Rome (Italy). Clin. Microbiol. Infect. **15**:347–357.
17. **DeLeon K, et al.** 2009. Gallium maltolate treatment eradicates *Pseudomonas aeruginosa* infection in thermally injured mice. Antimicrob. Agents Chemother. **53**:1331–1337.
18. **de Léséleuc L, Harris G, Kuolee R, Chen W.** 23 July 2012. *In vitro* and *in vivo* biological activity of iron chelators and gallium nitrate against *Acinetobacter baumannii*. Antimicrob. Agents Chemother. doi: 10.1128/AAC.00778-12.
19. **Dijkshoorn L, Nemec A, Seifert H.** 2007. An increasing threat in hospitals: multidrug-resistant *Acinetobacter baumannii*. Nat. Rev. Microbiol. **5**:939–951.
20. **DuBois D, DuBois EF.** 1916. Clinical calorimetry: formula to estimate approximate surface area if height and weight be known. Arch. Int. Med. 17:863–871.
21. **Dunphy GB, Niven DF, Chadwick JS.** 2002. Iron contributes to the antibacterial functions of the haemolymph of *Galleria mellonella*. J. Insect Physiol. **48**:903–914.
22. **Emery T.** 1986. Exchange of iron by gallium in siderophores. Biochemistry **25**:4629–4633.
23. **Fecteau ME, et al.** 2011. Antimicrobial activity of gallium nitrate against *Mycobacterium avium subsp. paratuberculosis* in neonatal calves. J. Vet. Intern. Med. **25**:1152–1155.
24. **Funahashi T, et al.** 2012. Identification and characterization of an outer membrane receptor gene in *Acinetobacter baumannii* required for utilization of desferricoprogen, rhodotorulic acid, and desferrioxamine B as xenosiderophores. Biol. Pharm. Bull. **35**:753–760.
25. **Gaddy JA, et al.** 2012. Role of acinetobactin-mediated iron acquisition functions in the interaction of *Acinetobacter baumannii* strain ATCC 19606^T with human lung epithelial cells, *Galleria mellonella* caterpillars, and mice. Infect. Immun. **80**:1015–1024.
26. **Gales AC, Reis AO, Jones RN.** 2001. Contemporary assessment of antimicrobial susceptibility testing methods for polymyxin B and colistin: review of available interpretative criteria and quality control guidelines. J. Clin. Microbiol. **39**:183–190.
27. **Higgins PG, Stefanik D, Page MG, Hackel M, Seifert H.** 2012. *In vitro*

activity of the siderophore monosulfactam BAL30072 against meropenem-non-susceptible *Acinetobacter baumannii*. J. Antimicrob. Chemother. **67**:1167–1169.
28. **Iacono M, et al.** 2008. Whole-genome pyrosequencing of an epidemic multidrug-resistant *Acinetobacter baumannii* strain belonging to the European clone II group. Antimicrob. Agents Chemother. **52**:2616–2625.
29. **Imperi F, et al.** 2011. The genomics of *Acinetobacter baumannii*: insights into genome plasticity, antimicrobial resistance and pathogenicity. IUBMB Life **63**:1068–1074.
30. **Jacobs AC, et al.** 2012. Characterization of the *Acinetobacter baumannii* growth phase-dependent and serum responsive transcriptomes. FEMS Immunol. Med. Microbiol. **64**:403–412.
31. **Kaneko Y, Thoendel M, Olakanmi O, Britigan BE, Singh PK.** 2007. The transition metal gallium disrupts *Pseudomonas aeruginosa* iron metabolism and has antimicrobial and antibiofilm activity. J. Clin. Invest. **117**: 877–888.
32. **Kempf M, Rolain JM.** 2012. Emergence of resistance to carbapenems in *Acinetobacter baumannii* in Europe: clinical impact and therapeutic options. Int. J. Antimicrob. Agents **39**:105–114.
33. **Lee JW, Helmann JD.** 2007. Functional specialization within the Fur family of metalloregulators. Biometals **20**:485–499.
34. **Li J, et al.** 2006. Colistin: the re-emerging antibiotic for multidrug-resistant Gram-negative bacterial infections. Lancet Infect. Dis. **6**:589–601.
35. **MacKenzie FM, et al.** 2005. Report of the Consensus Conference on Antibiotic Resistance; Prevention and Control (ARPAC). Clin. Microbiol. Infect. 11:938–954.
36. **Michalopoulos A, Falagas ME.** 2010. Treatment of *Acinetobacter* infections. Expert Opin. Pharmacother. **11**:779–788.
37. **Miller JH.** 1972. Experiments in molecular genetics, p 252–255. Cold Spring Harbor Laboratory, Cold Spring Harbor, NY.
38. **Nemec A, Dijkshoorn L, van der Reijden TJ.** 2004. Long-term predominance of two pan-European clones among multi-resistant *Acinetobacter baumannii* strains in the Czech Republic. J. Med. Microbiol. **53**:147–153.
39. **Nerren JR, et al.** 2011. Evaluation of the effect of gallium maltolate on fecal *Salmonella* shedding in cattle. J. Food Prot. **74**:524–530.
40. **Olakanmi O, Britigan BE, Schlesinger LS.** 2000. Gallium disrupts iron metabolism of mycobacteria residing within human macrophages. Infect. Immun. **68**:5619–5627.
41. **Olakanmi O, et al.** 2010. Gallium disrupts iron uptake by intracellular and extracellular *Francisella* strains and exhibits therapeutic efficacy in a murine pulmonary infection model. Antimicrob. Agents Chemother. **54**: 244–253.
42. **Payne SM.** 1994. Detection, isolation, and characterization of siderophores. Methods Enzymol. **235**:329–344.
43. **Peeters E, Nelis HJ, Coenye T.** 2008. Resistance of planktonic and biofilm-grown *Burkholderia cepacia* complex isolates to the transition metal gallium. J. Antimicrob. Chemother. **61**:1062–1065.
44. **Peleg AY, et al.** 2009. *Galleria mellonella* as a model system to study *Acinetobacter baumannii* pathogenesis and therapeutics. Antimicrob. Agents Chemother. **53**:2605–2609.
45. **Perez F, et al.** 2007. Global challenge of multidrug-resistant *Acinetobacter baumannii*. Antimicrob. Agents Chemother. **51**:3471–3484.
46. **Petersen PJ, Labthavikul P, Jones CH, Bradford PA.** 2006. *In vitro* antibacterial activities of tigecycline in combination with other antimicrobial agents determined by chequerboard and time-kill kinetic analysis. J. Antimicrob. Chemother. **57**:573–576.
47. **Raetz CR, Reynolds CM, Trent MS, Bishop RE.** 2007. Lipid A modification systems in Gram-negative bacteria. Annu. Rev. Biochem. **76**:295–329.
48. **Reagan-Shaw S, Nihal M, Ahmad N.** 2008. Dose translation from animal to human studies revisited. FASEB J. **22**:659–661.
49. **Roca I, Espinal P, Vila-Farrés X, Vila J.** 2012. The *Acinetobacter baumannii* oxymoron: commensal hospital dweller turned pan-drug-resistant menace. Front. Microbiol. **3**:148.
50. **Rzhepishevska O, et al.** 2011. The antibacterial activity of Ga^{3+} is influenced by ligand complexation as well as the bacterial carbon source. Antimicrob. Agents Chemother. **55**:5568–5580.
51. **Sambrook J, Fitsch EF, Maniatis T.** 1989. Molecular cloning: a laboratory manual, p 2344. Cold Spring Harbor Laboratory, Cold Spring Harbor, NY.
52. **Schwyn B, Neilands JB.** 1987. Universal chemical assay for the detection and determination of siderophores. Anal. Biochem. **160**:47–56.
53. **Smith MG, et al.** 2007. New insights into *Acinetobacter baumannii* pathogenesis revealed by high-density pyrosequencing and transposon mutagenesis. Genes Dev. **21**:601–614.
54. **Spaink HP, Okker RJH, Wijffelman CA, Pees E, Lugtenberg BJJ.** 1987. Promoters in the nodulation region of the *Rhizobium leguminosarum* Sym plasmid pRL1J1. Plant Mol. Biol. **9**:27–39.
55. **Stojiljkovic I, Baumler AJ, Hantke K.** 1994. Fur regulon in Gram negative bacteria. Identification and characterization of new iron-regulated *Escherichia coli* genes by a Fur titration assay. J. Mol. Biol. **236**:531–544.
56. **Thompson MG, Corey BW, Si Y, Craft DW, Zurawski DV.** 30 July 2012. Antibacterial activities of iron chelators against common nosocomial pathogens. Antimicrob. Agents Chemother. doi:10.1128/AAC.01197-12.
57. **Towner KJ, et al.** 2011. Distribution of intrinsic plasmid replicase genes and their association with carbapenem-hydrolyzing class D beta-lactamase genes in European clinical isolates of *Acinetobacter baumannii*. Antimicrob. Agents Chemother. **55**:2154–2159.
58. **Vallenet D, et al.** 2008. Comparative analysis of Acinetobacters: three genomes for three lifestyles. PLoS One **3**:e1805. doi:10.1371/journal.pone.0001805.
59. **van Dessel H, et al.** 2004. Identification of a new geographically widespread multiresistant *Acinetobacter baumannii* clone from European hospitals. Res. Microbiol. **2**:105–112.
60. **Visca P, Ciervo A, Sanfilippo V, Orsi N.** 1993. Iron-regulated salicylate synthesis by *Pseudomonas* spp. J. Gen. Microbiol. **139**:1995–2001.
61. **Visca P, Seifert H, Towner KJ.** 2011. *Acinetobacter* infection-an emerging threat to human health. IUBMB Life **63**:1048–1054.
62. **Warrell RP, Jr, Skelos A, Alcock NW, Bockman RS.** 1986. Gallium nitrate for acute treatment of cancer-related hypercalcemia: clinicopharmacological and dose response analysis. Cancer Res. **46**:4208–4212.
63. **Weaver KD, et al.** 2008. Ga^{3+} as a mechanistic probe in Fe^{3+} transport: characterization of Ga^{3+} interaction with FbpA. J. Biol. Inorg. Chem. **13**:887–898.
64. **Weinberg ED.** 2009. Iron availability and infection. Biochim. Biophys. Acta **1790**:600–605.
65. **Yamamoto S, Okujo N, Kataoka H, Narimatsu S.** 1999. Siderophore-mediated utilization of transferrin- and lactoferrin-bound iron by *Acinetobacter baumannii*. J. Health Sci. **45**:297–302.

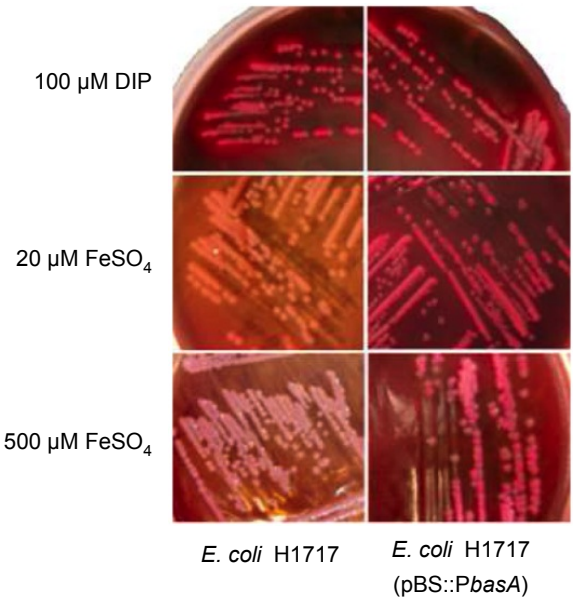

FIG S1 FURTA assay. Introduction of pBSP*basA* into *E. coli* H1717 produced red (Lac^+) colonies on McConkey agar supplemented with ≥ 20 µM $FeSO_4$ concentrations, while *E. coli* H1717 gave white (Lac^-) colonies on McConkey agar at the same $FeSO_4$ concentrations. The addition of 100 µM DIP restored the Lac^+ phenotype both in *E. coli* H1717(pBSP*basA*) and *E. coli* H1717.

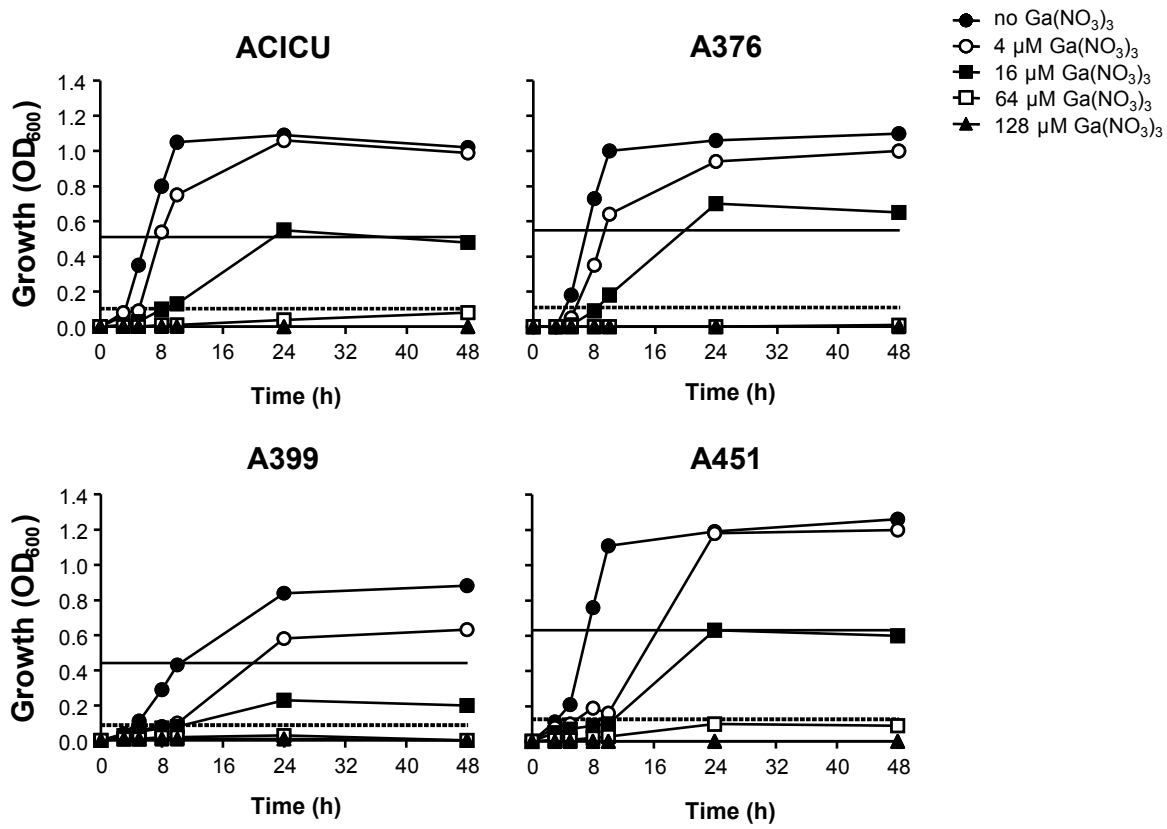

FIG S2 Effect of $Ga(NO_3)_3$ on *A. baumannii* growth in flask culture. Selected strains were grown for up to 48 h in M9-DIP supplemented with increasing $Ga(NO_3)_3$ concentrations (0 to 128 µM). Solid and dotted lines show OD_{600} values corresponding to 50% and 90% growth inhibition at 48 h relative to the untreated controls, respectively.

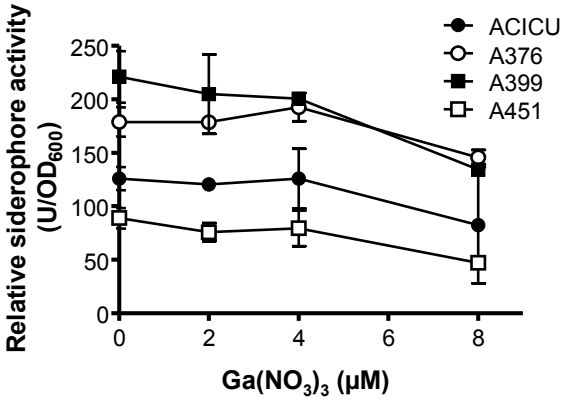

FIG S3 Effect of $Ga(NO_3)_3$ on siderophore production. Siderophore production by *A. baumannii* strains ACICU, A376, A399 and A451 after 48 h growth in M9-DIP supplemented with different $Ga(NO_3)_3$ concentrations (0, 2, 4, and 8 μM).

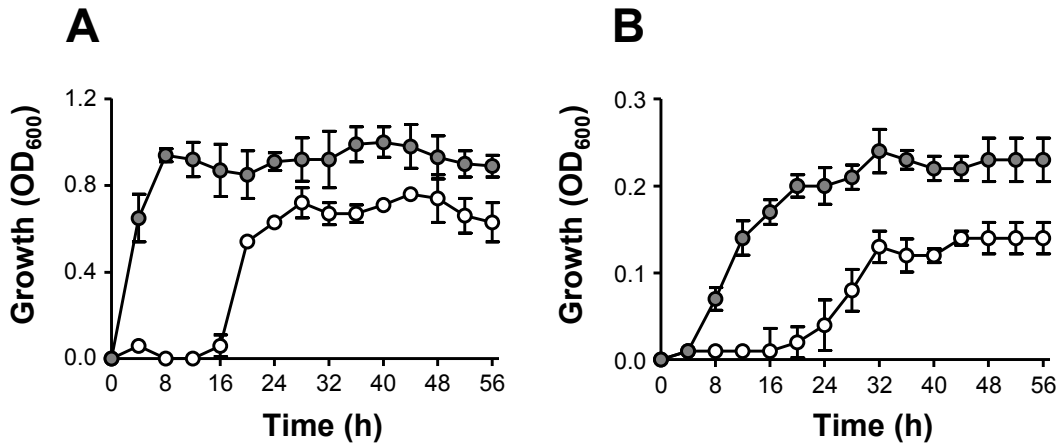

FIG S4 Growth of *A. baumannii* ACICU in human serum in flasks (A) and microtiter plates (B). White symbols: serum without added iron; grey symbols: serum supplemented with 200 μM $FeCl_3$. Data are the means (± SD) of two independent experiments.

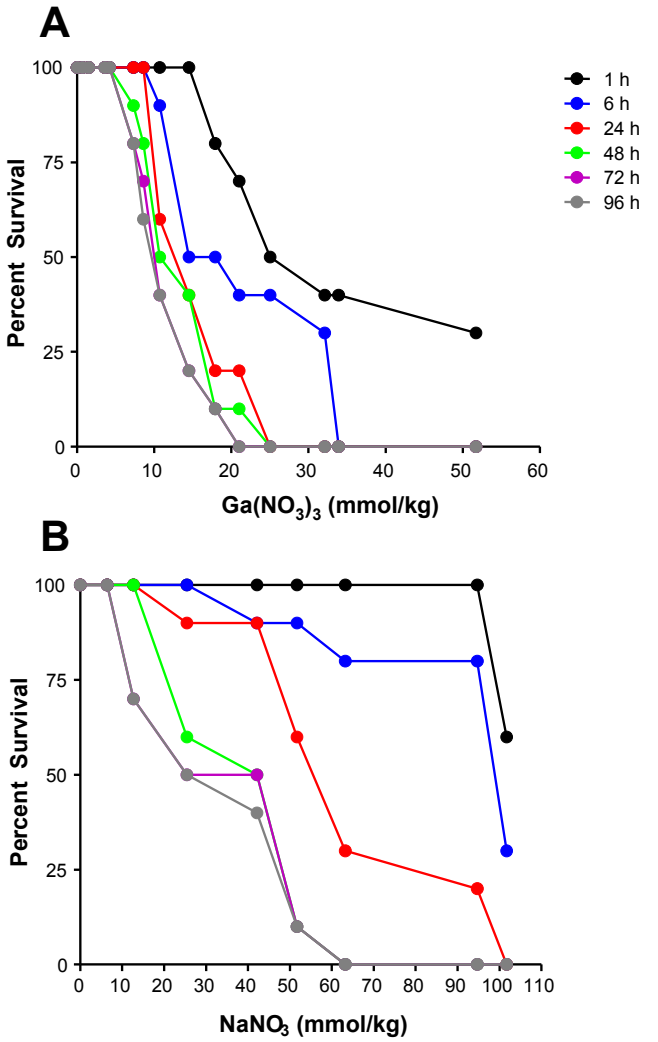

FIG S5 Toxicity of $Ga(NO_3)_3$ (A) and $NaNO_3$ (B) to *G. mellonella* larvae incubated at 37ºC for up to 96 h. Concentrations 0-52 mmol/kg (corresponding to 0-3.0 M) $Ga(NO_3)_3$ and 0-102 mmol/kg (corresponding to 0-6.0 M) $NaNO_3$ were tested.

TABLE S1 Characteristics of *A. baumannii* strains used in this study

Strain	Country of origin	Sequence group (SG)[a] and relevant characteristics	Reference
ATCC 19606^T	United States	SG5; type strain	
ATCC 17978	France	NV[b]; complete genome sequenced	6
RUH 875	The Netherlands	SG2; representative for ICL I	5
RUH 134	The Netherlands	SG1; representative for ICL II	5
RUH 5875	The Netherlands	SG3; representative for ICL III	10
AYE	France	SG2; related to ICL I, complete genome sequenced	9
ACICU	Italy	SG1; related to ICL II, complete genome sequenced	4
50C	Italy	SG4; related to ICL II, colistin resistant	2, 3
A37	Singapore	SG8	1, 7
A60	Argentina	SG1	1, 7
A287	New Zealand	SG1	1, 7
A369	Spain	SG1	1, 7
A371	Czech Republic	SG1	1, 7
A372	Greece	SG2	1, 7
A374	The Netherlands	SG4	1, 7
A376	Austria	SG5	1, 7
A377	Germany	SG3	1, 7
A380	United Kingdom	SG1	1, 7
A384	Sweden	SG2	1, 7
A386	Greece	SG2	1, 7
A387	Greece	SG1	1, 7
A388	Greece	SG7	1, 7
A389	Denmark	SG5	1, 7
A390	Bulgaria	SG2	1, 7
A392	Germany	SG1	1, 7
A397	Greece	SG1	1, 7
A399	Turkey	SG4	1, 7
A402	Taiwan	SG1	1, 7
A404	Poland	SG2	1, 7
A410	Poland	SG1	1, 7
A411	Poland	SG2	1, 7
A414	Poland	SG2	1, 7
A416	Poland	SG1	1, 7
A424	Croatia	SG2	1, 7
A429	Croatia	SG2	1, 7
A430	Croatia	SG2	1, 7
A435	Croatia	SG2	1, 7

A436	Croatia	SG2	1, 7
A437	Croatia	SG2	1, 7
A438	Bulgaria	SG2	1, 7
A440	Bulgaria	SG2	1, 7
A443	Slovenia	SG2	1, 7
A451	Poland	SG2	1, 7
A453	Slovakia	SG1	1, 7
A457	Estonia	SG7	1, 7
A458	Estonia	SG2	1, 7
A461	Portugal	SG4	1, 7
A462	Portugal	SG4	1, 7
A464	Portugal	SG4	1, 7
A468	Poland	SG1	1, 7
A469	Poland	SG2	1, 7
A472	Poland	SG2	1, 7
A473	Poland	SG1	1, 7
A474	Poland	SG1	1, 7
A479	United Kingdom import from Pakistan	SG2	1, 7
A483	United Kingdom import from Malaysia	SG4	1, 7
A486	Brazil	SG4	1, 7
A491	India	SG1	1, 7

[a] SG determination was performed as previously described (Turton *et al*., 2007).

[b] NV, new variant SG (4).

REFERENCES

1. **Antunes LC, Imperi F, Towner KJ, Visca P.** 2011. Genome-assisted identification of putative iron-utilization genes in *Acinetobacter baumannii* and their distribution among a genotypically diverse collection of clinical isolates. Res Microbiol. **162**:279-284.

2. **D'Andrea MM, Giani T, D'Arezzo S, Capone A, Petrosillo N, Visca P, Luzzaro F, Rossolini GM.** 2009. Characterization of pABVA01, a plasmid encoding the OXA-24 carbapenemase from Italian isolates of *Acinetobacter baumannii*. Antimicrob. Agents Chemother. **53:**3528-3533.

3. **D'Arezzo S, Capone A, Petrosillo N, Visca P; GRAB.** 2009. Epidemic multidrug-resistant *Acinetobacter baumannii* related to European clonal types I and II in Rome (Italy). Clin. Microbiol. Infect. **15:**347-357.

4. **Iacono M, Villa L, Fortini D, Bordoni R, Imperi F, Bonnal RJ, Sicheritz-Ponten T, De Bellis G, Visca P, Cassone A, Carattoli A.** 2008. Whole-genome pyrosequencing of an epidemic multidrug-resistant *Acinetobacter baumannii* strain belonging to the European clone II group. Antimicrob. Agents Chemother. **52:**2616-2625.

5. **Nemec A, Dijkshoorn L, van der Reijden TJ.** 2004. Long-term predominance of two pan-European clones among multi-resistant *Acinetobacter baumannii* strains in the Czech Republic. J. Med. Microbiol. **2:**147–153.

6. **Smith MG, Gianoulis TA, Pukatzki S, Mekalanos JJ, Ornston LN, Gerstein M, Snyder M.** 2007. New insights into *Acinetobacter baumannii* pathogenesis revealed by high-density pyrosequencing and transposon mutagenesis. Genes Dev. **21:**601-614.

7. **Towner KJ, Levi K, Vlassiadi M; ARPAC Steering Group.** 2008. Genetic diversity of carbapenem-resistant isolates of *Acinetobacter baumannii* in Europe. Clin. Microbiol. Infect. **14:**161-167.

8. **Turton JF, Gabriel SN, Valderrey C, Kaufmann ME, Pitt TL.** 2007. Use of sequence-based typing and multiplex PCR to identify clonal lineages of outbreak strains of *Acinetobacter baumannii*. Clin. Microbiol. Infect. **8:**807–815.

9. **Vallenet D, Nordmann P, Barbe V, Poirel L, Mangenot S, Bataille E, Dossat C, Gas S, Kreimeyer A, Lenoble P, Oztas S, Poulain J, Segurens B, Robert C, Abergel C, Claverie JM, Raoult D, Médigue C, Weissenbach J, Cruveiller S.** 2008. Comparative analysis of Acinetobacters: three genomes for three lifestyles. PLoS One. **3:**e1805.

10. **van Dessel H, Dijkshoorn L, van der Reijden T, Bakker N, Paauw A, van den Broek P, Verhoef J, Brisse S.** 2004. Identification of a new geographically widespread multiresistant *Acinetobacter baumannii* clone from European hospitals. Res. Microbiol. **2:**105-112.

TABLE S2 $Ga(NO_3)_3$ inhibitory concentrations (IC_{50} and IC_{90}, μM) at 24 and 48 h in a collection of 58 *A. baumannii* strains cultivated in M9-DIP. Results are the means (± SD) of two independent experiments.

Strain	24 h [a]		48 h	
	IC_{50}	IC_{90}	IC_{50}	IC_{90}
ATCC 19606^T	ND	ND	2.8 ± 1.4	5.6 ± 2.2
ATCC 17978	9.8 ± 2.9	47.9 ± 6.4	22.7 ± 3.3	53.2 ± 4.6
RUH 875	5.7 ± 1.5	26.4 ± 1.1	11.6 ± 5.4	58.5 ± 7.4
RUH 134	6.9 ± 0.2	31.6 ± 0.6	20.3 ± 8.3	51.1 ± 2.1
RUH 5875	1.1 ± 0.3	3.1 ± 0.2	3.3 ± 0.4	14.0 ± 3.3
AYE	4.7 ± 0.8	32.4 ± 0.6	1.9 ± 0.1	9.8 ± 3.2
ACICU	4.6 ± 1.8	15.9 ± 1.6	13.0 ± 3.3	35.9 ± 5.4
50C	7.5 ± 0.6	56.8 ± 6.2	22.5 ± 1.3	64.0 ± 0.0
A37	6.4 ± 0.1	21.8 ± 2.5	11.2 ± 1.4	35.2 ± 5.0
A60	3.9 ± 0.0	35.2 ± 6.5	13.2 ± 0.7	49.1 ± 3.5
A287	5.0 ± 1.5	12.1 ± 2.8	8.7 ± 1.6	30.6 ± 1.3
A369	2.6 ± 2.1	5.5 ± 2.5	6.3 ± 0.3	17.7 ± 3.7
A371	3.7 ± 0.2	14.7 ± 1.3	13.3 ± 1.4	45.9 ± 2.7
A372	6.2 ± 0.4	17.4 ± 2.5	11.9 ± 1.3	36.0 ± 5.7
A374	1.2 ± 0.1	2.7 ± 1.3	1.2 ± 0.1	2.6 ± 0.8
A376	14.7 ± 1.6	45.7 ± 3.0	27.9 ± 1.8	57.2 ± 0.6
A377	5.1 ± 2.3	17.7 ± 6.2	14.1 ± 2.3	49.6 ± 6.6
A380	1.3 ± 0.1	3.3 ± 0.2	1.9 ± 0.3	9.0 ± 2.8
A384	4.4 ± 0.9	24.5 ± 0.5	13.5 ± 0.8	31.7 ± 4.9
A386	2.6 ± 0.1	9.4 ± 3.8	8.5 ± 2.1	21.0 ± 8.6
A387	5.0 ± 3.2	17.4 ± 8.3	2.2 ± 1.1	18.0 ± 6.4
A388	2.2 ± 0.3	13.8 ± 2.9	6.5 ± 0.2	25.4 ± 1.3
A389	2.7 ± 0.3	10.2 ± 4.1	6.1 ± 0.4	16.4 ± 2.3
A390	6.0 ± 0.2	15.4 ± 0.6	11.0 ± 0.1	25.9 ± 5.6
A392	3.3 ± 0.8	15.5 ± 6.2	4.2 ± 2.5	13.6 ± 2.0
A397	1.0 ± 0.1	1.7 ± 0.1	1.3 ± 0.0	2.5 ± 0.7
A399	7.8 ± 0.2	34.6 ± 0.5	15.3 ± 0.4	35.2 ± 5.9
A402	1.7 ± 0.1	16.6 ± 4.3	1.4 ± 0.1	12.3 ± 3.0
A404	2.8 ± 0.5	5.6 ± 0.8	12.4 ± 0.5	18.5 ± 3.6
A410	1.3 ± 0.2	4.6 ± 3.0	3.4 ± 0.1	13.2 ± 1.7
A411	7.3 ± 0.3	19.3 ± 5.3	19.9 ± 6.5	56.7 ± 8.8
A414	3.3 ± 0.0	6.4 ± 0.5	8.0 ± 0.5	24.5 ± 4.2
A416	1.2 ± 0.1	8.0 ± 0.2	1.4 ± 0.1	3.7 ± 0.1
A424	3.0 ± 0.7	12.7 ± 2.8	9.0 ± 2.5	21.2 ± 0.9
A429	1.5 ± 0.1	6.4 ± 1.9	9.4 ± 3.9	18.6 ± 5.4
A430	4.9 ± 1.8	14.0 ± 0.6	13.0 ± 0.4	28.9 ± 2.4
A435	1.4 ± 0.1	1.9 ± 0.1	1.3 ± 0.1	3.0 ± 0.6

A436	1.2 ± 0.2	12.5 ± 1.7	10.8 ± 3.0	28.9 ± 4.5
A437	1.3 ± 0.1	2.6 ± 0.8	4.3 ± 1.3	11.8 ± 0.4
A438	1.3 ± 0.1	3.0 ± 1.4	1.5 ± 0.7	4.4 ± 1.7
A440	1.2 ± 0.0	2.0 ± 0.0	1.6 ± 0.3	10.3 ± 3.4
A443	ND	ND	3.9 ± 3.0	15.5 ± 4.9
A451	6.5 ± 0.5	23.1 ± 3.0	15.7 ± 1.1	34.5 ± 2.1
A453	1.4 ± 0.3	4.2 ± 3.0	6.5 ± 0.0	23.8 ± 0.2
A457	1.3 ± 0.1	8.8 ± 1.1	5.4 ± 2.5	24.6 ± 1.7
A458	1.3 ± 0.1	2.1 ± 0.1	1.2 ± 0.3	11.6 ± 6.3
A461	ND	ND	27.5 ± 3.5	80.0 ± 4.2
A462	4.2 ± 0.6	19.9 ± 3.5	13.3 ± 1.3	46.3 ± 1.6
A464	1.5 ± 0.1	7.8 ± 1.7	3.3 ± 0.2	19.3 ± 6.9
A468	2.2 ± 0.9	4.4 ± 0.6	3.3 ± 0.1	13.6 ± 1.2
A469	2.1 ± 1.0	4.8 ± 0.0	2.9 ± 0.4	7.2 ± 1.1
A472	7.6 ± 0.4	41.8 ± 1.5	10.8 ± 0.4	15.7 ± 0.5
A473	ND	ND	3.4 ± 0.6	14.2 ± 1.1
A474	6.2 ± 1.1	25.8 ± 3.7	18.2 ± 4.2	39.0 ± 7.5
A479	4.4 ± 1.2	15.1 ± 1.3	10.7 ± 0.4	27.0 ± 6.2
A483	3.5 ± 0.1	13.1 ± 4.1	11.4 ± 0.5	29.2 ± 0.2
A486	1.3 ± 0.1	2.9 ± 1.6	6.0 ± 4.0	61.5 ± 7.8
A491	3.7 ± 0.1	37.6 ± 8.3	11.5 ± 1.2	63.9 ± 6.1

[d] ND, not determined due to poor growth.

TABLE S3 $Ga(NO_3)_3$ inhibitory concentrations (IC_{50} and IC_{90}, μM) at 48 h in a collection of 58 *A. baumannii* strains cultivated in human serum. Results are the means (± SD) of two independent experiments.

Strain	IC_{50}	IC_{90}
ATCC 19606^T	ND[a]	ND[a]
ATCC 17978	2.2 ± 0.2	3.8 ± 0.0
RUH 875	5.3 ± 0.8	14.6 ± 2.1
RUH 134	7.9 ± 0.2	15.0 ± 0.4
RUH 5875	5.4 ± 0.8	14.5 ± 5.2
AYE	5.9 ± 0.4	10.7 ± 1.3
ACICU	6.2 ± 0.4	14.0 ± 2.1
50C	9.7 ± 0.5	30.4 ± 2.3
A37	12.1 ± 0.4	45.3 ± 8.6
A60	3.9 ± 0.1	7.7 ± 0.1
A287	23.7 ± 1.7	54.5 ± 3.6
A369	26.2 ± 5.5	58.4 ± 3.7
A371	34.7 ± 6.4	64.0 ± 4.5
A372	16.0 ± 0.1	58.0 ± 3.6
A374	2.8 ± 0.4	9.3 ± 3.6
A376	3.0 ± 0.1	7.0 ± 0.2
A377	2.8 ± 0.8	4.0 ± 0.0
A380	6.2 ± 0.8	7.6 ± 0.3
A384	12.7 ± 1.1	37.2 ± 6.9
A386	5.5 ± 1.0	9.4 ± 1.8
A387	5.2 ± 0.3	8.6 ± 0.3
A388	6.8 ± 0.8	15.0 ± 1.5
A389	5.7 ± 2.7	18.7 ± 3.7
A390	5.8 ± 2.5	15.5 ± 0.6
A392	12.4 ± 0.6	26.6 ± 0.2
A397	7.1 ± 1.8	14.4 ± 2.3
A399	21.0 ± 5.7	58.7 ± 5.9
A402	5.0 ± 1.3	17.2 ± 1.6
A404	4.2 ± 0.1	15.4 ± 0.4
A410	2.5 ± 0.1	6.7 ± 0.5
A411	6.3 ± 3.3	13.2 ± 3.4
A414	12.9 ± 2.1	29.1 ± 0.9
A416	3.7 ± 0.4	13.7 ± 0.6
A424	6.0 ± 0.3	15.2 ± 1.2
A429	2.5 ± 0.7	4.0 ± 0.4
A430	6.0 ± 0.3	16.2 ± 2.1
A435	6.0 ± 1.2	27.0 ± 6.2
A436	1.6 ± 0.3	5.3 ± 0.4

A437	7.8 ± 3.2	40.5 ± 14.7
A438	7.4 ± 0.1	20.6 ± 0.4
A440	3.8 ± 0.7	9.0 ± 2.1
A443	9.3 ± 0.4	26.9 ± 2.6
A451	12.2 ± 0.5	48.2 ± 1.1
A453	6.4 ± 0.0	13.3 ± 0.0
A457	4.9 ± 2.5	11.8 ± 5.2
A458	8.9 ± 1.2	21.2 ± 1.7
A461	4.0 ± 0.1	13.2 ± 2.3
A462	3.3 ± 0.3	7.7 ± 0.2
A464	11.0 ± 0.6	31.8 ± 2.1
A468	13.0 ± 3.0	32.5 ± 0.6
A469	24.3 ± 2.6	63.9 ± 9.1
A472	4.0 ± 0.3	7.5 ± 0.4
A473	4.8 ± 0.3	13.2 ± 1.6
A474	2.6 ± 0.2	5.1 ± 1.0
A479	3.0 ± 0.1	7.1 ± 0.4
A483	7.1 ± 0.7	12.5 ± 2.3
A486	5.4 ± 0.3	10.2 ± 0.2
A491	6.7 ± 1.3	14.0 ± 2.3

[a] ND, not determined due to poor growth.

TABLE S4 Growth yields and relative siderophore production at 24 and 48 h in a collection of 58 *A. baumannii* strains cultivated in microtiter plates in M9-DIP supplemented or not with 100 µM $FeCl_3$.

Strain	Growth (OD_{600})				Relative siderophore production (U/OD_{600})[a]			
	24 h		48 h		24 h		48 h	
	M9-DIP	M9-DIP + $FeCl_3$	M9-DIP	M9-DIP + $FeCl_3$	M9-DIP	M9-DIP + $FeCl_3$	M9-DIP	M9-DIP + $FeCl_3$
ATCC 19606^T	0.08 ± 0.01	0.35 ± 0.08	0.09 ± 0.01	0.32 ± 0.01	3.33 ± 2.1	ND	38.3 ± 2.92	ND
ATCC 17978	0.38 ± 0.02	0.41 ± 0.09	0.26 ± 0.03	0.41 ± 0.05	65.30 ± 2.16	ND	75.00 ± 7.0	ND
RUH 875	0.09 ± 0.01	0.28 ± 0.01	0.09 ± 0.01	0.25 ± 0.02	112.90 ± 12.29	ND	129.84 ± 7.3	ND
RUH 134	0.11 ± 0.01	0.47 ± 0.02	0.13 ± 0.01	0.42 ± 0.02	90.80 ± 18.01	ND	104.42 ± 15.4	ND
RUH 5875	0.24 ± 0.03	0.35 ± 0.06	0.22 ± 0.02	0.40 ± 0.02	200.10 ± 15.43	ND	210.10 ± 11.1	ND
AYE	0.24 ± 0.07	0.42 ± 0.01	0.24 ± 0.04	0.34 ± 0.01	155.30 ± 3.45	ND	178.80 ± 5.1	ND
ACICU	0.32 ± 0.01	0.46 ± 0.03	0.31 ± 0.02	0.40 ± 0.05	90.70 ± 2.58	ND	126.00 ± 6.5	ND
50C	0.11 ± 0.01	0.41 ± 0.01	0.13 ± 0.01	0.49 ± 0.01	119.90 ± 5.00	ND	136.00 ± 8.5	ND
A37	0.30 ± 0.09	0.41 ± 0.03	0.21 ± 0.03	0.37 ± 0.03	122.70 ± 6.54	ND	141.11 ± 3.4	ND
A60	0.33 ± 0.01	0.44 ± 0.04	0.31 ± 0.03	0.37 ± 0.01	139.70 ± 11.63	ND	160.66 ± 4.4	ND
A287	0.34 ± 0.07	0.36 ± 0.03	0.33 ± 0.02	0.40 ± 0.03	138.00 ± 7.95	ND	158.70 ± 4.2	ND
A369	0.36 ± 0.01	0.35 ± 0.02	0.28 ± 0.01	0.32 ± 0.02	216.60 ± 3.62	ND	249.09 ± 16.2	ND
A371	0.23 ± 0.04	0.46 ± 0.04	0.16 ± 0.02	0.38 ± 0.03	189.90 ± 5.44	ND	113.00 ± 2.5	ND
A372	0.25 ± 0.04	0.33 ± 0.01	0.22 ± 0.02	0.30 ± 0.07	102.90 ± 4.80	ND	118.30 ± 4.1	ND
A374	0.37 ± 0.05	0.41 ± 0.03	0.27 ± 0.01	0.37 ± 0.03	42.20 ± 9.42	ND	48.50 ± 6.1	ND
A376	0.29 ± 0.02	0.37 ± 0.03	0.24 ± 0.01	0.36 ± 0.06	153.90 ± 2.81	ND	178.90 ± 5.0	ND
A377	0.29 ± 0.01	0.39 ± 0.02	0.25 ± 0.02	0.35 ± 0.02	155.10 ± 3.16	ND	138.10 ± 12.2	ND
A380	0.19 ± 0.05	0.39 ± 0.01	0.19 ± 0.01	0.35 ± 0.03	120.10 ± 4.64	ND	287.60 ± 27.1	ND
A384	0.40 ± 0.01	0.52 ± 0.01	0.36 ± 0.04	0.47 ± 0.03	250.10 ± 18.01	ND	137.20 ± 13.4	ND
A386	0.17 ± 0.03	0.37 ± 0.01	0.15 ± 0.01	0.33 ± 0.02	119.30 ± 1.87	ND	89.80 ± 14.6	ND
A387	0.23 ± 0.07	0.50 ± 0.04	0.21 ± 0.02	0.48 ± 0.03	78.10 ± 2.96	ND	128.90 ± 7.4	ND
A388	0.18 ± 0.02	0.40 ± 0.01	0.18 ± 0.01	0.32 ± 0.02	112.10 ± 6.74	ND	135.00 ± 17.6	ND
A389	0.16 ± 0.03	0.53 ± 0.01	0.16 ± 0.06	0.56 ± 0.05	117.40 ± 3.56	ND	255.50 ± 17.2	ND
A390	0.09 ± 0.01	0.35 ± 0.02	0.15 ± 0.01	0.32 ± 0.03	222.20 ± 13.50	ND	202.10 ± 6.9	ND
A392	0.23 ± 0.01	0.45 ± 0.01	0.16 ± 0.01	0.42 ± 0.01	175.70 ± 20.54	ND	227.10 ± 19.2	ND
A397	0.25 ± 0.06	0.41 ± 0.03	0.31 ± 0.04	0.37 ± 0.02	197.50 ± 12.07	ND	171.50 ± 6.9	ND
A399	0.26 ± 0.01	0.47 ± 0.03	0.24 ± 0.03	0.33 ± 0.02	219.70 ± 12.19	ND	190.80 ± 14.5	ND
A402	0.23 ± 0.01	0.35 ± 0.02	0.17 ± 0.04	0.32 ± 0.02	149.10 ± 8.18	ND	255.50 ± 8.6	ND
A404	0.31 ± 0.02	0.39 ± 0.03	0.22 ± 0.02	0.34 ± 0.03	180.50 ± 12.57	ND	260.70 ± 4.3	ND
A410	0.21 ± 0.01	0.38 ± 0.02	0.22 ± 0.05	0.33 ± 0.03	222.20 ± 13.00	ND	165.40 ± 1.2	ND
A411	0.20 ± 0.02	0.37 ± 0.01	0.16 ± 0.03	0.37 ± 0.02	226.70 ± 5.72	ND	105.70 ± 4.5	ND
A414	0.22 ± 0.03	0.32 ± 0.03	0.17 ± 0.02	0.29 ± 0.06	143.80 ± 13.72	ND	186.10 ± 5.9	ND
A416	0.14 ± 0.02	0.41 ± 0.04	0.16 ± 0.02	0.39 ± 0.04	91.90 ± 5.72	ND	147.50 ± 6.6	ND
A424	0.17 ± 0.01	0.28 ± 0.01	0.23 ± 0.01	0.29 ± 0.02	161.80 ± 16.16	ND	119.70 ± 1.1	ND

A429	0.27	± 0.01	0.39	± 0.01	0.21	± 0.03	0.35	± 0.02		128.30	± 6.13	ND	97.90	± 8.1	ND
A430	0.36	± 0.03	0.33	± 0.02	0.30	± 0.03	0.32	± 0.03		104.10	± 3.24	ND	224.90	± 4.6	ND
A435	0.41	± 0.02	0.42	± 0.03	0.37	± 0.02	0.38	± 0.02		85.10	± 1.35	ND	108.40	± 10.7	ND
A436	0.32	± 0.01	0.40	± 0.04	0.24	± 0.03	0.36	± 0.01		195.60	± 3.24	ND	116.50	± 7.4	ND
A437	0.12	± 0.01	0.28	± 0.02	0.12	± 0.03	0.39	± 0.03		94.30	± 4.89	ND	96.10	± 6.1	ND
A438	0.27	± 0.02	0.37	± 0.02	0.21	± 0.04	0.35	± 0.02		101.30	± 4.73	ND	165.40	± 2.0	ND
A440	0.13	± 0.02	0.29	± 0.03	0.15	± 0.02	0.31	± 0.02		40.10	± 1.27	ND	80.30	± 2.0	ND
A443	0.11	± 0.01	0.30	± 0.05	0.12	± 0.06	0.29	± 0.01		143.80	± 5.77	ND	182.50	± 3.3	ND
A451	0.10	± 0.02	0.47	± 0.01	0.14	± 0.06	0.46	± 0.01		69.80	± 3.82	ND	89.00	± 14.7	ND
A453	0.12	± 0.10	0.16	± 0.02	0.12	± 0.02	0.24	± 0.03		158.70	± 7.65	ND	182.51	± 3.1	ND
A457	0.28	± 0.01	0.44	± 0.03	0.33	± 0.03	0.40	± 0.03		240.0	± 8.27	ND	276.00	± 10.2	ND
A458	0.20	± 0.03	0.41	± 0.01	0.18	± 0.03	0.39	± 0.02		184.9	± 4.59	ND	212.64	± 35.6	ND
A461	0.29	± 0.01	0.44	± 0.01	0.25	± 0.01	0.41	± 0.01		233.8	± 1.70	ND	268.87	± 3.6	ND
A462	0.21	± 0.02	0.30	± 0.01	0.16	± 0.03	0.32	± 0.03		156.3	± 1.46	ND	179.75	± 3.6	ND
A464	0.30	± 0.01	0.33	± 0.01	0.23	± 0.01	0.31	± 0.01		155.8	± 2.94	ND	179.17	± 2.7	ND
A468	0.31	± 0.03	0.33	± 0.03	0.26	± 0.02	0.26	± 0.01		167.0	± 10.47	ND	192.05	± 1.7	ND
A469	0.30	± 0.03	0.44	± 0.03	0.27	± 0.02	0.39	± 0.02		180.3	± 2.61	ND	207.35	± 7.9	ND
A472	0.11	± 0.04	0.42	± 0.01	0.13	± 0.03	0.40	± 0.05		151.4	± 7.31	ND	174.11	± 7.0	ND
A473	0.10	± 0.01	0.37	± 0.03	0.19	± 0.01	0.35	± 0.03		242.0	± 32.02	ND	278.30	± 7.3	ND
A474	0.23	± 0.02	0.33	± 0.01	0.22	± 0.04	0.29	± 0.02		108.9	± 2.55	ND	125.24	± 15.4	ND
A479	0.46	± 0.03	0.47	± 0.01	0.35	± 0.03	0.45	± 0.04		59.6	± 2.73	ND	68.54	± 11.1	ND
A483	0.29	± 0.05	0.49	± 0.02	0.26	± 0.01	0.41	± 0.05		168.3	± 2.44	ND	193.55	± 5.1	ND
A486	0.32	± 0.07	0.33	± 0.01	0.24	± 0.02	0.30	± 0.01		87.1	± 1.44	ND	100.17	± 6.5	ND
A491	0.19	± 0.01	0.45	± 0.02	0.16	± 0.01	0.39	± 0.03		241.1	± 7.15	ND	277.27	± 6.7	ND

[a] ND, not detectable.

TABLE S5 *G. mellonella* killing by selected *A. baumannii* strains at 24, 48, 72 and 96 h after inoculation.

Strain	LD_{50} (CFU/larva)				LD_{90} (CFU/larva)			
	24 h	48 h	72 h	96 h	24 h	48 h	72 h	96 h
ATCC 19606^T	2×10^8	9×10^7	5×10^7	4×10^7	5×10^8	3×10^8	9×10^7	7×10^7
ATCC 17978	4×10^6	2×10^6	2×10^6	2×10^6	3×10^7	7×10^6	5×10^6	5×10^6
RUH 5875	9×10^6	3×10^6	2×10^6	2×10^6	4×10^8	5×10^7	8×10^6	8×10^6
AYE	6×10^6	2×10^6	1×10^6	1×10^6	2×10^7	5×10^6	5×10^6	5×10^6
ACICU	6×10^6	3×10^6	2×10^6	9×10^5	1×10^7	1×10^7	5×10^6	5×10^6
50C	5×10^5	3×10^5	2×10^5	2×10^5	1×10^7	1×10^6	8×10^5	8×10^5
A371	1×10^5	1×10^5	1×10^5	1×10^5	9×10^5	3×10^5	3×10^5	3×10^5

Chapter 8

Discussion and conclusion

Acinetobacter baumannii is one of the most problematic pathogens for patients in ICUs, causing millions of cases of pneumonia and bloodstream infections worldwide each year (Talbot et al., 2006). The pathogenic success of *A. baumannii* most likely arises from its ability to resist adverse environmental conditions in hospitals, including antibiotic and antiseptic treatments, and from its ability to attach to human cells and invade host tissues (Choi et al., 2008; Dijkshoorn et al., 2007). Despite the progress in understanding the genetic and functional basis of multidrug resistance in *A. baumannii* and ongoing studies on its virulence factors, the pathogenic potential of this bacterium remains, in large part, to be elucidated. Deciphering the pathogenicity mechanisms of this pathogen is crucial to understand its pathogenicity and to develop new strategies of infection prevention and control.

The aims of the research described in this thesis were to explore the virulence strategies of *A. baumannii* in order to gain further insight into the mechanism of its pathogenicity and to explore novel therapeutic strategies. In order to elucidate the virulence of *A. baumannii*, we opted for a combinatorial approach of genomic and phenotypic analyses, which are described in **Chapters 3-6**. A novel therapeutic strategy based on metal gallium is proposed in **Chapter 7**.

8.1 *A. baumannii* genomics and population structure

Genomic analyses have allowed the acquisition of essential knowledge on *A. baumannii* population structure and phylogenetic relationships within the *Acinetobacter* genus, as well as on potential virulence and antimicrobial resistance determinants. Previous studies have mostly focused on the structural organisation and acquisition mechanisms of antibiotic-resistance genes.

At the start of this study, two aspects of *A. baumannii* biology were mainly unknown: 1) what virulence factors and mechanisms are associated with its pathogenesis, and 2) what is its natural habitat and how has the species *A. baumannii* evolved to adapt to the nosocomial environment. A genomic approach was used to tentatively answer these questions (**Chapter 2**). The main findings of this initial study were that *A. baumannii* virulence genes are mostly common to all clinical strains analysed, be they involved in outbreaks or sporadic infection, or isolated over 60 years ago or recently. Therefore, it was argued that the acquisition of new virulence traits was not a predominant factor in the recent (post-1980s) nosocomial expansion of *A. baumannii* clones.

Conversely, antimicrobial resistance genes were found either shared by all strains (the core genome of *A. baumannii*) or distributed in one strain or a set of strains (the dispensable genome of *A. baumannii*). Dispensable antimicrobial resistance genes are often found in alien islands and flanked by transposases or phage-related insertion sequences (Fournier et al., 2006; Iacono et al., 2008), indicating their probable acquisition by horizontal gene transfer from other bacteria that colonise the same environment. In fact, previous studies (Iacono et al., 2008; Vallenet et al., 2008) showed that most antimicrobial resistance genes present in alien islands of *A. baumannii* are homologous to genes of other common bacterial pathogens in the hospital setting.

In addition, this initial comparative study evidenced that the *A. baumannii* core genome is quite small, in contrast to a very large dispensable genome. Such a genomic organisation is indicative of a species with a population structure characterised by small intraspecific variability and fast genetic expansion of strains. The same conclusion has recently been achieved by an MLST-based population study (Diancourt et al., 2010), which proposed an evolutionary model involving a population bottleneck followed by a recent expansion of clones. The work described in this thesis complements the model proposed by Diancourt and colleagues in that virulence genes, which are mostly common to all strains, would have been present prior to this population bottleneck, whereas most antimicrobial resistance genes, which are differentially distributed between strains, would have been acquired subsequently, during the period of clonal expansion.

On a positive note, the localisation of the majority of virulence genes in the core genome of the species and the apparent lack of genetic potential for specific toxin(s) are indicative of a species with an intrinsic low pathogenic potential. These observations suggest that *A. baumannii* does not have a specialised niche, but is probably an opportunistic pathogen with broad environmental adaptability. This aspect of multifactorial and combinatorial virulence is explored further in **Chapter 3**.

8.2 Multifactorial and combinatorial virulence

In **Chapter 2**, virulence genes were found to be essentially conserved among *A. baumannii* clinical strains, and clues on the possible evolution and adaptation of this species were collected. To gain further insight into the particular virulence factors expressed by clinical strains and to explain the predominance of particular clonal groups, an integrative approach of genomic and phenotypic analyses was taken to compare the distribution of

virulence factors in strains from different origins and of different pathogenic potential: two multidrug-resistant (MDR) outbreak strains (AYE and ACICU); a clinical, non-MDR, strain isolated over 60 years ago (ATCC 17978), and a strain isolated from a human body louse (SDF).

The first conclusion from this study was that the outbreak strains, representative of the two main *A. baumannii* clonal groups (IC-I and IC-II) and responsible for the majority of recent *A. baumannii* infections, do not express specific virulence factors to which their predominance can be ascribed. For instance, IC-I strain AYE shows more surface motility and higher resistance to desiccation than IC-II strain ACICU, which, in turn, shows higher biofilm formation and proteolytic activity, although both are equally virulent in an insect infection model (**Chapter 3**). Interestingly, the higher adherence and biofilm formation of ACICU and the higher motility of AYE could be a common characteristic of IC-II and IC-I isolates, respectively, and was also documented in a larger collection of clinical isolates (**Chapter 6**, de Breij et al., 2010; Eijkelkamp et al., 2011b, Lee et al., 2006).

Secondly, no clear differences in the genomic conservation and gene expression of virulence factors were observed between the outbreak strains, isolated in the 2000s, and a clinical strain, isolated in the 1950s. This indicates that the recent emergence of these clonal lineages is probably not directly connected to the acquisition of particular virulence factors, but is instead linked to their MDR phenotype, strengthening the conclusions drawn by the genomic comparison of a wider number of strains (**Chapter 2**).

Thirdly, not only is there no particular association between the emergence of the two major clonal groups and the acquisition of particular virulence factors, but there is also not a unique set of conserved virulence factors that might explain the increased virulence of clinical strains in an insect infection model (**Chapter 3**), as many virulence determinants are also produced by the non-human isolate SDF (haemolysis, serum resistance, proteases, phospholipase C, biofilm formation) and can be found in the genome of environmental *Acinetobacter* spp. (Table 4; Tayabali et al., 2012). The difference in virulence potential among clinical and non-clinical strains of *Acinetobacter* spp. seems to be mainly linked to the ability to resist adverse environmental conditions, rather than to the production of specific toxins or other virulence factors, a perspective that is supported by other studies (Diancourt et al., 2010; Peleg et al., 2012): the three clinical strains grow in iron-depleted media, survive fever-associated temperatures and resist longer to conditions of desiccation.

To determine the extent to which the conclusions derived from this study could be applicable to a clinical *A. baumannii* population, a larger collection of epidemic strains with international distribution was analysed for the expression of virulence-associated traits (**Chapter 6**). Several virulence-related traits were identified that were expressed by all strains, including resistance to desiccation, biofilm formation and epithelial cell adhesion and invasion. Overall, these traits were more expressed in strains belonging to international clones I and II and to genotypes ST25 and ST78, and thus could account for their emergence and persistence in the nosocomial environment.

Since *A. baumannii* is not the only clinically successful species in the *Acinetobacter* genus (Doughari et al., 2011), the investigation of virulence factors in other clinical *Acinetobacter* spp. could help to understand specific traits of *A. baumannii* pathogenicity. Previously, no putative virulence factors were found to be unique to *A. baumannii*. In agreement with their status as important human pathogens, it was observed that *A. pittii* and *A. nosocomialis* have a degree of conservation of putative virulence genes similar to that found in *A. baumannii* (>85%, in contrast to an average of 55% amongst non-pathogenic *Acinetobacter* spp.; Table 4). In comparison with environmental *Acinetobacter* spp., the genomes of pathogenic *Acinetobacter* spp. are enriched with genes coding for multiple iron uptake systems, Csu and type IV pili, quorum sensing and biofilm-associated (Bap) proteins, thereby suggesting the possible contribution of these factors to virulence.

In contrast, some putative virulence factors are very widely distributed in *A. baumannii* and other *Acinetobacter* spp., regardless of the species pathogenicity, including the two-component BfmRS system, the outer membrane protein OmpA, the cell wall protein PBP 7/8, phospholipases C and D, and the ferrous iron-uptake system (Table 4). Three possibilities can therefore be envisaged:

1) these factors are not important for *A. baumannii* virulence, although this would be in contrast with their experimentally validated role in *A. baumannii* pathogenicity;

2) these factors are remnants of a common pathogenic ancestor of clinical and non-clinical *Acinetobacter* spp., which are not expressed, or poorly expressed, in the non-pathogenic species. Similar evolutionary profiles are widespread in bacterial pathogens that have changed niche (Pallen and Wren, 2007);

3) the same virulence factor can play different roles in different habitats. For example, high biofilm formation by both the outbreak strain ACICU and the insect isolate SDF could reflect a dual function of biofilm in *A. baumannii* and, in general, indicate a high habitat plasticity for this species, as previously observed for *Bacillus* spp. with different pathogenic potential and origins (humans, the invertebrate gut, the soil) that maintain similar biofilm formation capabilities (Jensen et al., 2003).

To summarise, the combinatorial approach to the study of *A. baumannii* virulence revealed that:

1) outbreak strains do not have unique virulence factors that are absent from sporadic clinical strains thus, at least at present, their predominance cannot be reasonably ascribed to increased virulence potential;

2) clinical strains (either outbreak or sporadic) do not have a set of unique virulence factors that are absent from non-clinical strains;
3) *A. baumannii* does not have unique virulence factors absent from other *Acinetobacter* spp.

Taken together, these results corroborate the view that *A. baumannii* virulence could be multifactorial and combinatorial, a situation which is reminiscent of *P. aeruginosa* virulence (Lee et al., 2006). This hypothesis is supported by the systematic failure of previous studies to identify a particular virulence factor unequivocally responsible for the clinical success of *A. baumannii*, including the inability to identify bona fide virulence genes by a transposon inactivation approach (Smith et al., 2007). This perspective highlights the strong adaptive potential of this species and could indicate an adaptation of *A. baumannii* to different hosts and to different pathogenic strategies, as has been proposed for various other pathogenic species (Pallen and Wren, 2007). *A. baumannii* constitutes a prime example of a species in which a study of pathogenicity should not be limited to an oversimplified view, and points to a more pluralistic general perspective on bacterial pathogenesis which is emerging and which takes into consideration the ecology and evolution of a species, namely an 'eco-evo' perspective.

If the expression of particular virulence factors in *A. baumannii* is dependent on the ecology and evolution of each strain, then it is important to explore strains with different habitats. In this regard, findings from strain SDF could provide important clues towards the understanding of *A. baumannii* biology. Strain SDF was isolated from an insect gut, and shows some characteristics that may be linked to its particular adaptation for survival in this host: extensive biofilm production, serum resistance and haemolytic activity, as well as the genomic capacity for haem uptake (**Chapter 4**). SDF seems to be an example of specialisation to a particular niche or host (Lawrence, 2005), in that its genome is smaller than those of clinical strains and is filled with insertion and prophage sequences, which could indicate a reductive evolution by pseudogenisation and gene loss, and the strain is less resistant to high temperatures, iron starvation and desiccation. Curiously, SDF still shares some of the virulence determinants present in clinical strains (Table 4), suggesting that these determinants have a different function in this strain or are not expressed, and represent a continuing reductive evolutionary process (Pallen and Wren, 2007). Another strain that is reminiscent of SDF is the sequenced strain *Acinetobacter* sp. HA, which was also isolated from a haematophage gut. This strain has a smaller genome than clinical *A. baumannii* strains (3.1 Mb versus ca. 3.9 Mb) and lacks many of the *A. baumannii* putative virulence genes (Table 4; Malhotra et al., 2012).

8.3 Correspondence between genomic and phenotypic analyses

The work described in this thesis reveals that the association of a particular phenotype with the presence of specific virulence determinant(s) in the genome of a strain is not a straightforward exercise.

A clear example involves iron uptake in strain AYE, which has the coding capacity for the acinetobactin cluster, but was found to not produce catechol-type compounds, like acinetobactin (**Chapter 3**). A recent study has clarified this discrepancy: the precursor form of acinetobactin, 2,3-dihydroxybenzoic acid (DHBA), is encoded in a separate cluster from the acinetobactin cluster and AYE lacks the gene for the production of this precursor (Penwell et al., 2012). Another example is that the genomes of the four strains analysed in **Chapter 3** encode different numbers of haemolysins, but similar levels of haemolytic activity were produced. Likewise, the AYE and ACICU strains both have a complete gene cluster for the synthesis of type IV pili, but strain AYE clearly showed higher twitching activity compared to strain ACICU. Therefore, virulence-associated phenotypes cannot be confidently predicted from an analysis of the genome of a species, nor vice-versa. This lack of correspondence has been reported previously (Sahl et al., 2011) and underlines the limitations of genomic comparisons in predicting phenotypic behaviour.

8.4 Distribution of iron-acquisition systems

The combination of genomic and phenotypic analyses led to the identification of a putative core set of virulence and adaptive factors common to most *A. baumannii* isolates, as well as factors that could account for strain-specific phenotypes (**Chapters 2 and 3**). In particular, the genomes of sequenced clinical strains encode multiple putative iron-acquisition systems, including the system for the acquisition of the well-characterised siderophore acinetobactin, two additional siderophore-dependent iron-acquisition systems, two haem-acquisition systems and a ferrous iron-acquisition system. In accordance with this finding, clinical strains grew well under iron-limiting conditions and expressed catechol- and hydroxamate-type siderophores (**Chapter 3**).

In order to assess the potential relevance of iron-acquisition systems in *A. baumannii* pathogenicity, their distribution was determined in the genomes of a large collection of genotyped *A. baumannii* clinical isolates (the ARPAC collection) using PCR and Southern blot analyses (**Chapter 4**). All 50 strains except for

the non-clinical isolate SDF encode the gene cluster responsible for the synthesis of acinetobactin, as well as an additional siderophore-acquisition system, a haem uptake system and a ferrous iron-acquisition system. In addition, nucleotide BLAST searches showed the conservation of these three systems in 50 sequenced *A. baumannnii* genomes (Table 4), as well as the conservation of a cluster encoding the precursor of acinetobactin, DHBA, in all strains but SDF and ATCC 17978 (Table 4; Actis et al., 1993). Acinetobactin has been confirmed as an important virulence factor of *A. baumannii* in both the *G. mellonella* and a sepsis mouse infection models (Gaddy et al. 2012), although the inability of strain AYE to produce this siderophore strongly questions its essentiality for *A. baumannii* to cause infections.

The only conserved cluster for iron uptake in the whole *Acinetobacter* genus is the ferrous iron-acquisition system (Table 4), although the majority of strains also encode the acinetobactin cluster and the second siderophore cluster described above. In contrast, other iron-acquisition systems are not conserved in *A. baumannii*: a cluster coding for a second haem uptake system was present in ca. 40% of *A. baumannii* strains (**Chapter 4**; Table 4) and a cluster coding for an additional hydroxamate siderophore was present in ca. 10% of strains (**Chapter 4**; Table 4). These systems are also found in some, but not the majority, of *Acinetobacter* spp. (Table 4) and could have been acquired by horizontal gene transfer, which is supported by the existence of insertion sequences in the neighbourhood of the corresponding gene cluster (**Chapter 4**). Lastly, strain *A. baumannii* 8399 does not encode acinetobactin (Dorsey et al., 2003), but has a different siderophore system (Echenique et al., 1992) that has not been identified in any other *A. baumannii* strain (Table 4; Eijkelkamp et al., 2011a) and was present in 18% of sequenced strains belonging to *Acinetobacter* spp. other than *A. baumannii* (Table 4).

It seems, therefore, that *A. baumannii* can use multiple iron-acquisition systems, some of which are part of its core genome and can be important for pathogenicity, as is the case of acinetobactin (Gaddy et al., 2012), whereas others are found in one or a few strains and may determine adaptation of individual strains to particular habitats. As an example, strain SDF does not produce siderophores, but has the genomic functions for a haem uptake system and, in accordance, is haemolytic, which could be an important function for a haematophage gut coloniser.

8.5 Siderotyping

Phenotypic differentiation of *A. baumannii* isolates is problematic, since there are no biochemical or metabolic markers able to delineate strains or clonal groups within this species. In addition, epidemiological tracing of *A. baumannii* strains is essential for the prevention, control and treatment of *A. baumannii* infections, so there is a need in clinical practice to develop fast and cost-effective methods that allow typing of individual isolates. As *A. baumannii* isolates possess different iron-acquisition clusters (**Chapter 4**), an attempt was made to discriminate strains on the basis of their genetic potential to produce siderophores or use exogenous iron sources, which the present work defined, in *sensu lato*, 'siderotyping'. Siderotyping has been used previously to differentiate strains endowed with multiple iron uptake capacities, such as the case of *Pseudomonas* spp. (Fuchs et al., 2001).

In a preliminary study, no unequivocal correlation between RAPD type and iron-acquisition profile was found in a large population of *A. baumannii* isolates (**Chapter 4**). Therefore, the work described in this thesis investigated whether siderotyping could discriminate among a collection of strains belonging to IC-II (**Chapter 5**) that could not be distinguished by fine-typing methods such as MLST, PFGE or RAPD, but only by MLVA. However, all isolates showed the same siderotype.

Secondly, since *A. baumannii* is almost phenotypically indistinguishable from the related, nosocomial species *A. calcoaceticus*, *A. pittii* and *A. nosocomialis* (Nemec et al., 2011), the work analysed whether siderotyping could be used to discriminate among *Acinetobacter* spp. (Table 4). Considerable intra-specific siderotype variation was found in *A. pittii* and *A. nosocomialis*, but no consistent differences in siderotype were found among *Acinetobacter* spp. in general, regardless of their origin or pathogenic potential (Table 4). Thus, although *Acinetobacter* spp. have the coding potential for multiple iron uptake systems, siderotyping is not a preferable method when compared to the current genomic fine-typing methods (AFLP, MLST, PFGE, RAPD, MLVA), neither for intra- nor for inter-specific discrimination within the *Acinetobacter* genus. Generally speaking, the overall high conservation of *A. baumannii* virulence factors in this species and in the genus *Acinetobacter* (Table 4) argues against their use in virulence-based typing.

8.6 *Galleria mellonella* as an *A. baumannii* infection model

A. baumannii infection studies often use mouse models, but these have serious limitations, including the low virulence in mice of many *A. baumannii* strains. To circumvent this issue, neutropenic mice are often employed

or porcine mucin is added as an adjuvant (de Breij et al., 2012; Gaddy et al., 2012). Alternatively, non-mammalian models have been used, but these may not adequately mimic human infections. In fact, a study employing the worm *Caenorhabditis elegans* and the amoeba *Dictyostelium discoideum* failed to identify bona fide *A. baumannii* virulence factors (Smith et al., 2007).

In the present study, the *G. mellonella* insect infection model was used to investigate the virulence potential of *A. baumannii* strains (**Chapters 3 and 6**) and to test the efficacy of a new antimicrobial drug (**Chapter 7**). This non-mammalian model is a simple, cost-restrained, expedite and arguably more ethical infection model and, in the case of *P. aeruginosa* infection, showed good correlation to the burn mouse model (Jander et al., 2000).

The *G. mellonella* model was effective in testing *A. baumannii* virulence at reasonably high bacterial concentrations even for isolates of ascertained pathogenicity (10^5-10^6 CFU/larva for epidemic isolates; **Chapters 3, 6 and 7**). In addition, clear differences were detectable between the pathogenic potential of clinical strains and that of the non-human isolate SDF and the type strain ATCC 19606 (**Chapters 6 and 7**). This model was useful in assessing the therapeutic efficacy of antibiotics (Hornsey et al., 2011; Peleg et al., 2009) and gallium nitrate (**Chapter 7**), and could thus provide a good option to test new antimicrobial agents.

Unfortunately, the *G. mellonella* infection model proved to be ineffective in discriminating finer differences in the virulence of clinical strains (**Chapters 3 and 6**). In addition, this model might not be sensitive enough to confirm the contribution of individual gene products to *A. baumannii* virulence. For example, quorum sensing regulates important *A. baumannii* pathogenicity-related phenotypes, such as biofilm formation (Niu et al., 2008) and motility (Clemmer et al., 2011), but no differences in virulence were detected between a wild-type strain and its quorum sensing mutant (Peleg et al., 2009). Likewise, a similar shortcoming has been described with this model for detecting *P. aeruginosa* strains with mutations in genes coding for proteases, pili and flagella (Jarrell and Kropinski, 1982).

Lastly, the low virulence of ATCC 19606^T in the *G. mellonella* infection model (50% lethal dose > 10^7 CFU/larva; **Chapters 6 and 7**) poses some questions regarding its suitability as a model strain to study *A. baumannii* virulence. The results obtained in the present thesis are in accordance with a recent study in which the injection of 10^5 CFU/larva did not reach the 50% lethal dose (LD_{50}) up to the sixth day following infection (Gaddy et al., 2012), and this strain was also unable to survive in a neutropenic mouse pneumonia infection model (de Breij et al., 2012). Since ATCC 19606^T does not have a clear clinical background and, unlike the majority of *A. baumannii* isolates (ca. 55%) (Hauck et al., 2012), does not belong to any of the three main international clones, it could be important to consider more appropriate strains when testing *A. baumannii* virulence.

8.7 Gallium for the treatment of *A. baumannii* infections

A. baumannii is typically an MDR bacterium that has acquired resistance to a vast array of antimicrobials in recent decades. This capacity is partly dependent on the ability of this bacterium to acquire resistance genes, often by horizontal gene transfer (**Chapter 2**). Recent studies, including this PhD thesis, strongly suggest that acquisition of the MDR phenotype is a determinant factor for the success of *A. baumannii* as a nosocomial pathogen (**Chapter 2**). In **Chapter 7**, the knowledge gained on *A. baumannii* pathogenicity was used to investigate new potential antimicrobial agents against MDR clinical isolates. Since iron acquisition is important for *A. baumannii* virulence, it was decided to test an antimicrobial strategy an antimicrobial strategy was tested based on the iron-mimetic metal gallium, which competes with iron in binding to redox enzymes essential for many biological functions.

The work described in this thesis revealed that the FDA-approved drug gallium nitrate (Ganite®) could be used to inhibit the growth of *A. baumannii* both *in vitro*, i.e. in laboratory media and in human serum, and *in vivo*, i.e. the *G. mellonella* infection model. In addition, gallium and colistin showed synergism in repressing bacterial growth. Since colistin acts as a cationic polypeptide that disrupts the outer membrane, it could facilitate the diffusion of gallium inside the cells. Therefore, gallium-colistin might be an effective combination to treat MDR *A. baumannii*.

In a drug discovery perspective, one should consider that the pipeline of new antibiotics is almost dry, and the multifactorial and combinatorial nature of *A. baumannii* virulence (**Chapter 3**) complicates the search for drugs targeting specific virulence genes. On the other hand, a recent study corroborated our findings on the bacteriostatic effect of gallium on *A. baumannii* growth and on its ability to alleviate infection in an animal model (Léséleuc et al., 2012). Therefore, this compound could represent an important antimicrobial drug against *A. baumannii*, as the bacterium would hardly develop resistance to a bacteriostatic compound that targets multiple functions, as is the case of gallium. These two advantages raise hope on the possible application of gallium-based therapies for the treatment of infections sustained by MDR or pan-resistant *A. baumannii* strains.

8.8 Conclusion

Recent years in clinical microbiology have seen the emergence of bacterial pathogens resistant to virtually all drugs available in the market. Thus, a paradigm shift is required, where drugs are not designed to target cell viability, but rather target functions essential for infection, with the advantages of offering less selective pressure and preserving the host microbiome.

In this study, an in-depth investigation of the virulence factors and pathogenicity mechanisms of *A. baumannii* was performed and a new therapeutic strategy was proposed. It was revealed that *A. baumannii* has the potential to express a wide repertoire of virulence factors, which are common to the genomes of most strains, but which can be differentially expressed according to each individual strain. Additionally, it was found that epidemic strains had not acquired any new specific virulence determinant in addition to antibiotic resistance genes. Thirdly, a multiplicity of iron uptake capabilities was identified, indicative of the importance of iron metabolism for *A. baumannii* growth. This evidence ultimately prompted the development of a promising novel anti-*A. baumannii* strategy based on the disruption of iron metabolism.

Overall, the results presented in this thesis revealed that *A. baumannii* is a very adaptable pathogen, with an extraordinary ability to acquire new genetic material. Thus, although *A. baumannii* has long been considered a low-grade pathogen, in the future it could easily acquire new and more powerful virulence genes and become a more significant threat to human health. In recognition of this perspective, the control of multiresistant *A. baumannii* infections will have to involve the development of new therapeutic strategies that target conserved cellular processes. In this respect, the novel therapeutic approach involving gallium, as proposed in this thesis, could provide an important advance in combatting the ready adaptation of this increasingly important Gram-negative pathogen to new challenges from more conventional antibiotics.

Table 4. Genomic distribution of virulence factors in sequenced and annotated *Acinetobacter* strains

Strain (*Acinetobacter baumannii*)	Sequence accession number	MLST profile[a]	Gene(s) for[b]																							
			iron acquisition system									virulence factor														
			1[c]	2[d]	3[e]	4[f]	5[g]	6[h]	7[i]	8[j]	Conservation (%)	Bap	BfmRS	LPS	OmpA	PBP 7+8	Phospholipase C	Phospholipase D	Csu pili	Type IV pili	PNAG	Quorum sensing	Urease	RTX toxin	Conservation (%)
ACICU	NC_010611.1	CC2	+	+	+	+	+	-	-	+	75	+	+	+	+	+	+	+	+	+	+	+	+	+	100
AYE	NC_010410.1	CC1	+	+	-	+	+	-	-	+	63	+	+	+	+	+	+	+	+	+	+	+	+	-	92
ATCC 17978	NC_009085.1	ST77	+	+	-	+	+	+	-	-	63	+	+	+	+	+	+	+	+	+	+	+	+	-	92
SDF	NC_010400.1	ST17	+	+	+	-	-	-	-	-	38	-	+	+	+	+	+	+	-	-	-	+	+	-	62
AB0057	NC_011586.1	CC1	+	+	+	+	+	-	-	+	75	+	+	+	+	+	+	+	+	+	+	+	+	+	100
AB307-0294	NC_011595.1	CC1	+	+	-	+	+	-	-	+	63	+	+	+	+	+	+	+	+	+	+	+	+	-	92
1656-2	NC_017162.1	CC2	+	+	-	+	+	-	-	+	63	+	+	+	+	+	+	+	+	+	+	+	+	+	100
TCDC-AB0715	NC_017387.1	CC2	+	+	+	+	+	-	-	+	75	+	+	+	+	+	+	+	+	+	+	+	+	+	100
MDR-TJ	NC_017847.1	CC2	+	+	-	+	+	-	-	+	63	+	+	+	+	+	+	+	+	+	+	+	+	+	100
MDR-ZJ06	NC_017171.1	CC2	+	+	+	+	+	-	-	+	75	+	+	+	+	+	+	+	-	+	+	+	+	+	92
ATCC 19606[T]	NZ_ACQB00000000.1	ST52	+	+	-	+	+	-	-	+	63	+	+	+	+	+	+	+	+	+	+	+	+	-	92
3909	AEOZ00000000.1	ST78	+	+	-	+	+	-	-	+	63	-	+	+	+	+	+	+	+	+	+	+	+	+	92
3990	AEOY00000000.1	CC2	+	+	+	+	+	-	-	+	75	-	+	+	+	+	+	+	+	+	+	+	+	+	92
4190	AEPA00000000.1	ST25	+	+	+	+	+	-	-	+	75	-	+	+	+	+	+	+	+	+	+	+	+	-	85
6013113	NZ_ACYR02000001.1	ST81	+	+	-	+	+	+	-	+	75	+	+	+	+	+	+	+	+	+	+	+	+	-	92
6013150	NZ_ACYQ00000000.2	ST81	+	+	-	+	+	+	-	+	75	-	+	+	+	+	+	+	+	+	+	+	+	-	85
6014059	NZ_ACYS00000000.2	CC2	+	+	-	+	+	-	-	+	63	-	+	+	+	+	+	+	+	+	+	+	+	+	92
A118	AEOW00000000.1	ND[k]	+	+	-	+	+	-	-	+	63	-	+	+	+	+	+	+	+	+	+	+	+	-	85
AB056	NZ_ADGZ00000000.1	CC1	+	+	+	+	+	-	-	+	75	-	+	+	+	+	+	+	+	+	+	+	+	-	85
AB058	NZ_ADHA00000000.1	ST20	+	+	-	+	+	-	-	+	63	-	+	+	+	+	+	+	+	+	+	+	+	-	85
AB059	NZ_ADHB00000000.1	CC1	+	+	+	+	+	-	-	+	75	-	+	+	+	+	+	+	+	+	+	+	+	-	85
AB210	AEOX00000000.1	CC2	+	+	+	+	+	-	-	+	75	-	+	+	+	+	+	+	+	+	+	+	+	+	92
AB4857	AHAG00000000.1	CC3	+	+	-	+	+	-	-	+	63	+	+	+	+	+	+	+	+	+	+	+	+	+	100
AB5075	AHAH00000000.1	CC1	+	+	+	+	+	-	-	+	75	+	+	+	+	+	+	+	+	+	+	+	+	-	92
AB5256	AHAI00000000.1	ST25	+	+	+	+	+	-	-	+	75	-	+	+	+	+	+	+	+	+	+	+	+	-	85
AB5711	AHAJ00000000.1	CC2	+	+	-	+	+	-	-	+	63	+	+	+	+	+	+	+	+	+	+	+	+	-	92
AB900	NZ_ABXK00000000.1	ST49	+	+	-	+	+	-	-	+	63	-	+	+	+	+	+	+	+	+	+	+	+	-	85
ABNIH1	AFSZ00000000.1	CC2	+	+	+	+	+	-	-	+	75	+	+	+	+	+	+	+	+	+	+	+	+	+	100
ABNIH2	AFTA00000000.1	CC2	+	+	-	+	+	-	-	+	63	+	+	+	+	+	+	+	+	+	+	+	+	-	92
ABNIH3	AFTB00000000.1	CC2	+	+	+	+	+	-	-	+	75	+	+	+	+	+	+	+	+	+	+	+	+	+	100
ABNIH4	AFTC00000000.1	CC2	+	+	+	+	+	-	-	+	75	+	+	+	+	+	+	+	+	+	+	+	+	-	92
AC12	ALAM00000000.1	CC2	+	+	+	+	+	-	-	+	75	+	+	+	+	+	+	+	+	+	+	+	+	-	92
BZICU-2	ALOH00000000.1	ND	+	+	-	+	+	-	-	+	63	-	+	+	+	+	+	+	+	+	+	+	+	-	85
Canada BC-5	AFDN00000000.1	CC1	+	+	+	+	+	-	-	+	75	+	+	+	+	+	+	+	+	+	+	+	+	-	92
D1279779	AERZ00000000.1	ND	+	+	-	+	+	-	-	+	63	-	+	+	+	+	+	+	+	+	+	+	+	+	92
IS-123	ALII00000000.1	CC3	+	+	-	+	+	-	-	+	63	+	+	+	+	+	+	+	+	+	+	+	+	+	100
Naval-17	AFDO00000000.1	CC2	+	+	-	+	+	-	-	+	63	+	+	+	+	+	+	+	+	+	+	+	+	+	100
Naval-18	AFDA00000000.2	ST25	+	+	+	+	+	+	-	+	88	-	+	+	+	+	+	+	+	+	+	+	+	-	85
Naval-81	AFDB00000000.2	CC3	+	+	-	+	+	-	-	+	63	+	+	+	+	+	+	+	+	+	+	+	+	+	100
OIFC032	AFCZ00000000.2	ST32	+	+	-	+	+	-	-	+	63	+	+	+	+	+	+	+	+	+	+	+	+	-	92
OIFC109	ALAL00000000.1	CC3	+	+	-	+	+	-	-	+	63	+	+	+	+	+	+	+	+	+	+	+	+	+	100
OIFC137	AFDK00000000.1	CC3	+	+	-	+	+	-	-	+	63	+	+	+	+	+	+	+	+	+	+	+	+	+	100
OIFC143	AFDL00000000.1	ST25	+	+	+	+	+	-	-	+	75	-	+	+	+	+	+	+	+	+	+	+	+	-	85
OIFC189	AFDM00000000.1	CC2	+	+	-	+	+	-	-	+	63	+	+	+	+	+	+	+	+	+	+	+	+	+	100
UMB001	AEPK00000000.1	CC2	+	+	+	+	+	-	-	+	75	+	+	+	+	+	+	+	+	+	+	+	+	+	100
UMB002	AEPL00000000.1	ST16	+	+	-	+	+	-	-	+	63	+	+	+	+	+	+	+	+	+	+	+	+	-	92
UMB003	AEPM00000000.1	ST25	+	+	+	+	+	-	-	+	75	-	+	+	+	+	+	+	+	+	+	+	+	-	85
W6976	AIEG00000000.1	CC2	+	+	+	+	+	-	-	+	75	+	+	+	+	+	+	+	+	+	+	+	+	+	100
W7282	AIEH00000000.1	CC2	+	+	+	+	+	-	-	+	75	+	+	+	+	+	+	+	+	+	+	+	+	+	100
WM99c	AERY00000000.1	CC2	+	+	-	+	+	-	-	+	63	-	+	+	+	+	+	+	+	+	+	+	+	+	92
Conservation among strains (%)			100	100	46	98	98	8	0	96		62	100	100	100	100	100	100	96	98	98	100	100	48	

Strain (other *Acinetobacter* species)	Sequence accession number	Origin (source)[l]	Gene(s) for[b]																						
			iron acquisition system									virulence factor													
			1[c]	2[d]	3[e]	4[f]	5[g]	6[h]	7[i]	8[j]	Conservation (%)	Bap	BfmRS	LPS	OmpA	PBP 7+8	Phospholipase C	Phospholipase D	Csu pili	Type IV pili	PNAG	Quorum sensing	Urease	RTX toxin	Conservation (%)
A. baylyi ADP1	NC_005966.1	E (soil)	+	-	-	-	-	+	-	-	25	-	+	+	+	+	+	+	-	-	+	-	+	-	62
A. oleivorans DR1	NC_014259.1	E (soil)	+	+	+	-	-	-	+	+	63	+	+	+	+	+	+	+	-	-	+	+	+	-	77
A. calcoaceticus PHEA-2	NC_016603.1	E (wastewater)	+	+	+	+	-	-	-	+	63	+	+	+	+	+	+	+	-	+	+	+	+	-	85
A. calcoaceticus DSM 30006	AIEC00000000.1	E (soil)	+	+	+	-	-	-	+	+	63	-	+	+	+	+	+	+	-	-	+	+	+	-	69
A. calcoaceticus RUH2202	NZ_ACPK00000000.1	C (wound)	+	+	+	-	-	-	+	+	63	-	+	+	+	+	+	+	-	+	+	+	+	-	85
A. pittii D499	AGFH00000000.1	ND[k]	+	+	+	+	-	-	-	+	63	+	+	+	+	+	+	+	+	+	+	+	+	-	92
A. pittii DSM 21653	AIEK00000000.1	C (brain)	+	+	-	+	-	-	-	+	50	+	+	+	+	+	+	+	-	+	+	+	+	-	85
A. pittii DSM 9306	AIEF00000000.1	C (urine)	+	+	-	+	-	-	-	+	50	+	+	+	+	+	+	+	+	+	+	+	+	+	100
A. pittii SH024	NZ_ADCH00000000.1	C	+	+	+	+	-	-	-	+	63	+	+	+	+	+	+	+	+	+	+	+	+	-	92
A. haemolyticus ATCC 19194	NZ_ADMT00000000.1	C (skin)	+	+	-	-	-	-	-	-	25	-	+	+	+	+	+	+	-	-	-	-	+	-	54
A. junii SH205	NZ_ACPM00000000.1	C (perineum)	+	+	-	-	+	-	-	-	38	-	+	+	+	+	+	+	-	-	+	-	+	-	62
A. johnsonii SH046	NZ_ACPL00000000.1	C (perineum)	+	+	-	-	-	-	-	-	25	-	+	+	+	+	+	+	-	-	-	-	-	-	46
A. lwoffii NCTC 5866	AIEL00000000.1	C (urine)	+	+	-	-	-	-	-	-	25	-	+	+	+	+	+	+	-	-	-	-	-	-	46
A. lwoffii SH145	NZ_ACPN00000000.1	C (skin)	+	+	-	-	+	-	-	-	38	-	+	+	+	+	+	+	-	-	-	-	-	-	46
A. lwoffii WJ10621	NZ_AFQY00000000.1	C (urine)	+	+	-	-	-	-	-	-	25	-	+	+	+	+	+	+	-	-	-	-	-	-	46
A. bereziniae LMG 1003	NZ_AIEI00000000.1	C (wound)	+	+	-	+	-	-	-	-	38	-	+	+	+	+	+	+	-	-	+	-	+	-	62
A. radioresistens SK82	NZ_ACVR00000000.1	C (skin)	+	-	-	-	-	-	-	-	13	-	+	+	+	+	+	+	-	-	-	-	+	-	54
A. radioresistens SH164	NZ_ACPO00000000.1	C (skin)	+	-	-	-	-	-	-	-	13	-	+	+	+	+	+	+	-	-	-	-	+	-	54
A. radioresistens DSM 6976	BAGY00000000.1	C (tampon)	+	-	-	-	-	-	-	-	13	-	+	+	+	+	+	+	-	-	-	-	+	-	54
A. radioresistens WC-A-157	ALIR00000000.1	ND	+	-	-	-	-	-	-	-	13	-	+	+	+	+	+	+	-	-	-	-	+	-	54
A. nosocomialis NCTC 8102	AIEJ00000000.1	ND	+	+	-	-	-	-	+	+	50	-	+	+	+	+	+	+	+	+	+	+	-	+	85
A. nosocomialis NCTC 10304	NZ_AIEE00000000.1	C (eye)	+	+	-	+	+	-	-	+	63	+	+	+	+	+	+	+	+	+	+	+	+	+	100
A. nosocomialis RUH2624	NZ_ACQF00000000.1	C (skin)	+	+	-	-	-	-	+	+	50	-	+	+	+	+	+	+	+	-	+	+	+	-	77
A. parvus DSM 16617	NZ_AIEB00000000.1	C (inner ear)	+	-	-	-	-	-	-	-	13	-	+	+	+	+	+	+	-	-	+	-	-	-	54
A. ursingii DSM 16037	NZ_AIEA00000000.1	C (blood)	+	-	-	-	-	-	-	-	13	-	+	+	+	+	+	+	-	-	+	-	+	-	62
A. venetianus RAG-1[1]	AKIQ00000000.1	E (seawater)	+	+	-	-	-	-	-	-	25	-	+	+	+	+	+	+	-	-	+	-	-	-	54
A. venetianus VE-C3	ALIG00000000.1	E (fresh water)	+	+	-	-	+	-	-	-	38	-	+	+	+	+	+	+	-	-	+	-	-	-	54
A. sp. ATCC 27244	NZ_ABYN00000000.1	C (uterus)	+	+	+	+	+	-	-	-	63	-	+	+	+	+	+	+	-	-	-	-	-	-	46
A. sp. GG2	ALOW00000000.1	E (soil)	+	+	-	-	-	-	+	+	50	-	+	+	+	+	+	+	+	-	+	+	+	-	77
A. sp. HA	NZ_AJXD00000000.1	A (insect gut)	+	-	-	-	-	-	-	-	13	-	+	+	+	+	+	+	-	-	-	-	+	-	54
A. sp. NBRC 100985	NZ_BAEB00000000.1	E (seawater)	+	+	-	-	+	-	-	-	38	-	+	+	+	+	+	+	-	-	+	-	-	-	54
A. sp. NCTC 7422	NZ_AIED00000000.1	C (burn)	+	+	+	-	-	-	-	-	50	-	+	+	+	+	+	+	-	-	+	-	+	-	62
A. sp. P8-3-8	NZ_AFIE00000000.1	A (fish)	+	+	-	-	+	-	-	-	38	-	+	+	+	+	+	+	-	-	+	-	-	-	54
Conservation among strains (%)			100	76	24	24	18	3	18	36		21	100	100	100	100	100	100	21	24	67	36	67	9	

[a]Defined according to the Pasteur MLST scheme (http://www.pasteur.fr/recherche/genopole/PF8/mlst/Abaumannii.html).
[b]Criteria for CDS comparison (blastn): >70% identity, >50% coverage, < 1×10^{-50} e-value. The basis for comparison was CDS from annotated *A. baumannii* strains. Only genes present in single copy were considered.
[c]Ferrous iron uptake cluster (ACICU_00265-ACICU_00267)
[d]Haem uptake cluster (ACICU_01629-ACICU_01640)
[e]Haem uptake cluster (ACICU_00873-ACICU_00880)
[f]Acinetobactin synthesis and uptake cluster (ACICU_02570-ACICU_02589)
[g]Putative hydroxamate siderophore synthesis and uptake cluster (ACICU_01672-ACICU_01683)
[h]Putative hydroxamate siderophore synthesis and uptake cluster (A1S_2562-A1S_2582)
[i]Catechol siderophore synthesis and uptake cluster identified in *A. baumannii* strain 8399 (Dorsey et al., 2003; accession number AAN28936.1)
[j]DHBA synthesis cluster identified in *A. baumannii* strain AYE (Penwell et al., 2012; ABAYE1888-ABAYE1889)
[k]ND, no data or not determined
[l]Strains collected from: E, environment; C, clinic, and A, animal sources

8.9 References

- **Actis LA, Tolmasky ME, Crosa LM, Crosa JH.** Effect of iron-limiting conditions on growth of clinical isolates of *Acinetobacter baumannii*. J Clin Microbiol. 1993 31(10):2812-5.
- **Choi CH, Lee JS, Lee YC, Park TI, Lee JC.** *Acinetobacter baumannii* invades epithelial cells and outer membrane protein A mediates interactions with epithelial cells. BMC Microbiol. 2008 8:216.
- **Clemmer KM, Bonomo RA, Rather PN.** Genetic analysis of surface motility in *Acinetobacter baumannii*. Microbiology. 2011 157(Pt 9):2534-44.
- **de Breij A, Dijkshoorn L, Lagendijk E, van der Meer J, Koster A, Bloemberg G, Wolterbeek R, van den Broek P, Nibbering P.** Do biofilm formation and interactions with human cells explain the clinical success of *Acinetobacter baumannii*? PLoS One. 2010 5(5):e10732.
- **de Breij A, Eveillard M, Dijkshoorn L, van den Broek PJ, Nibbering PH, Joly-Guillou ML.** Differences in *Acinetobacter baumannii* strains and host innate immune response determine morbidity and mortality in experimental pneumonia. PLoS One. 2012 7(2):e30673.
- **de Léséleuc L, Harris G, Kuolee R, Chen W.** *In Vitro* and *In Vivo* Biological Activities of Iron Chelators and Gallium Nitrate against *Acinetobacter baumannii*. Antimicrob Agents Chemother. 2012 56(10):5397-400.
- **Diancourt L, Passet V, Nemec A, Dijkshoorn L, Brisse S.** The population structure of *Acinetobacter baumannii*: expanding multiresistant clones from an ancestral susceptible genetic pool. PLoS One. 2010 5(4):e10034.
- **Dijkshoorn L, Nemec A, Seifert H.** An increasing threat in hospitals: multidrug-resistant *Acinetobacter baumannii*. Nat Rev Microbiol. 2007 5(12):939-51.
- **Dorsey CW, Tolmasky ME, Crosa JH, Actis LA.** Genetic organization of an *Acinetobacter baumannii* chromosomal region harbouring genes related to siderophore biosynthesis and transport. Microbiology. 2003 149(Pt 5):1227-38.
- **Doughari HJ, Ndakidemi PA, Human IS, Benade S.** The ecology, biology and pathogenesis of *Acinetobacter* spp.: an overview. Microbes Environ. 2011 26(2):101-12.
- **Echenique JR, Arienti H, Tolmasky ME, Read RR, Staneloni RJ, Crosa JH, Actis LA.** Characterization of a high-affinity iron transport system in *Acinetobacter baumannii*. J Bacteriol. 1992 174(23):7670-9.
- **Eijkelkamp BA, Hassan KA, Paulsen IT, Brown MH.** Investigation of the human pathogen *Acinetobacter baumannii* under iron limiting conditions. BMC Genomics. 2011 12:126.
- **Eijkelkamp BA, Stroeher UH, Hassan KA, Papadimitrious MS, Paulsen IT, Brown MH.** Adherence and motility characteristics of clinical *Acinetobacter baumannii* isolates. FEMS Microbiol Lett. 2011 323(1):44-51.
- **Fournier PE, Vallenet D, Barbe V, Audic S, Ogata H, Poirel L, Richet H, Robert C, Mangenot S, Abergel C, Nordmann P, Weissenbach J, Raoult D, Claverie JM.** Comparative genomics of multidrug resistance in *Acinetobacter baumannii*. PLoS Genet. 2006 2(1):e7.
- **Fuchs R, Schäfer M, Geoffroy V, Meyer JM.** Siderotyping--a powerful tool for the characterization of pyoverdines. Curr Top Med Chem. 2001 1(1):31-57.
- **Gaddy JA, Arivett BA, McConnell MJ, López-Rojas R, Pachón J, Actis LA.** Role of acinetobactin-mediated iron-acquisition functions in the interaction of *Acinetobacter baumannii* strain ATCC 19606^T with human lung epithelial cells, *Galleria mellonella* caterpillars, and mice. Infect Immun. 2012 80(3):1015-24.
- **Hauck Y, Soler C, Jault P, Mérens A, Gérome P, Nab CM, Trueba F, Bargues L, Thien HV, Vergnaud G, Pourcel C.** Diversity of *Acinetobacter baumannii* in Four French Military Hospitals, as Assessed by Multiple Locus Variable Number of Tandem Repeats Analysis. PLoS One. 2012 7(9):e44597.
- **Hornsey M, Wareham DW.** *In vivo* efficacy of glycopeptide-colistin combination therapies in a *Galleria mellonella* model of *Acinetobacter baumannii* infection. Antimicrob Agents Chemother. 2011 55(7):3534-7.
- **Iacono M, Villa L, Fortini D, Bordoni R, Imperi F, Bonnal RJ, Sicheritz-Ponten T, De Bellis G, Visca P, Cassone A, Carattoli A.** Whole-genome pyrosequencing of an epidemic multidrug-resistant *Acinetobacter baumannii* strain belonging to the European clone II group. Antimicrob Agents Chemother. 2008 52(7):2616-25.
- **Jander G, Rahme LG, Ausubel FM.** Positive correlation between virulence of *Pseudomonas aeruginosa* mutants in mice and insects. J Bacteriol. 2000 182(13):3843-45.
- **Jarrell KF, Kropinski AM.** The virulence of protease and cell surface mutants of *Pseudomonas aeruginosa* for the larvae of *Galleria mellonella*. J Invertebr Pathol. 1982 39(3):395-400.
- **Jensen GB, Hansen BM, Eilenberg J, Mahillon J.** The hidden lifestyles of *Bacillus cereus* and relatives. Environ Microbiol. 2003 5(8):631-40.
- **Lawrence JG.** Common themes in the genome strategies of pathogens. Curr Opin Genet Dev. 2005 15(6):584-8.

- **Lee JC, Koerten H, van den Broek P, Beekhuizen H, Wolterbeek R, van den Barselaar M, van der Reijden T, van der Meer J, van de Gevel J, Dijkshoorn L.** Adherence of *Acinetobacter baumannii* strains to human bronchial epithelial cells. Res Microbiol. 2006 157(4):360-6.
- **Malhotra J, Dua A, Saxena A, Sangwan N, Mukherjee U, Pandey N, Rajagopal R, Khurana P, Khurana JP, Lal R.** Genome Sequence of *Acinetobacter* sp. Strain HA, Isolated from the Gut of the Polyphagous Insect Pest Helicoverpa armigera. J Bacteriol. 2012 194(18):5156.
- **Nemec A, Krizova L, Maixnerova M, van der Reijden TJ, Deschaght P, Passet V, Vaneechoutte M, Brisse S, Dijkshoorn L.** Genotypic and phenotypic characterization of the *Acinetobacter calcoaceticus-Acinetobacter baumannii* complex with the proposal of *Acinetobacter pittii* sp. nov. (formerly *Acinetobacter* genomic species 3) and *Acinetobacter nosocomialis* sp. nov. (formerly *Acinetobacter* genomic species 13TU). Res Microbiol. 2011 162(4):393-404.
- **Niu C, Clemmer KM, Bonomo RA, Rather PN.** Isolation and characterization of an autoinducer synthase from *Acinetobacter baumannii*. J Bacteriol. 2008 190(9):3386-92.
- **Pallen MJ, Wren BW.** Bacterial pathogenomics. Nature. 2007 449(7164):835-42.
- **Peleg AY, Jara S, Monga D, Eliopoulos GM, Moellering RC Jr, Mylonakis E.** *Galleria mellonella* as a model system to study *Acinetobacter baumannii* pathogenesis and therapeutics. Antimicrob Agents Chemother. 2009 53(6):2605-9.
- **Penwell WF, Arivett BA, Actis LA.** The *Acinetobacter baumannii entA* gene located outside the acinetobactin cluster is critical for siderophore production, iron-acquisition and virulence. PLoS One. 2012 7(5):e36493.
- **Sahl JW, Johnson JK, Harris AD, Phillippy AM, Hsiao WW, Thom KA, Rasko DA.** Genomic comparison of multi-drug resistant invasive and colonizing *Acinetobacter baumannii* isolated from diverse human body sites reveals genomic plasticity. BMC Genomics. 2011 12:291.
- **Smith MG, Gianoulis TA, Pukatzki S, Mekalanos JJ, Ornston LN, Gerstein M, Snyder M.** New insights into *Acinetobacter baumannii* pathogenesis revealed by high-density pyrosequencing and transposon mutagenesis. Genes Dev. 2007 21(5):601-14.
- **Talbot GH, Bradley J, Edwards JE Jr, Gilbert D, Scheld M, Bartlett JG; Antimicrobial Availability Task Force of the Infectious Diseases Society of America.** Bad bugs need drugs: an update on the development pipeline from the Antimicrobial Availability Task Force of the Infectious Diseases Society of America. Clin Infect Dis. 200642(5):657-68.
- **Tayabali AF, Nguyen KC, Shwed PS, Crosthwait J, Coleman G, Seligy VL.** Comparison of the virulence potential of *Acinetobacter* strains from clinical and environmental sources. PLoS One. 2012 7(5):e37024.
- **Vallenet D, Nordmann P, Barbe V, Poirel L, Mangenot S, Bataille E, Dossat C, Gas S, Kreimeyer A, Lenoble P, Oztas S, Poulain J, Segurens B, Robert C, Abergel C, Claverie JM, Raoult D, Médigue C, Weissenbach J, Cruveiller S.** Comparative analysis of Acinetobacters: three genomes for three lifestyles. PLoS One. 2008 19;3(3):e1805.

List of publications

- **Giannouli M, Antunes LC, Marchetti V, Triassi M, Visca P, Zarrilli R.** Characterization of virulence-related traits of *Acinetobacter baumannii* epidemic strains assigned to distinct genotypes. *Submitted*.

- **Antunes LC, Imperi F, Minandri F, Visca P.** *In vitro* and *in vivo* antimicrobial activity of gallium nitrate against multidrug resistant *Acinetobacter baumannii*. Antimicrob Agents Chemother. 2012 56(11): 5961-70.

- **Minandri F, D'Arezzo S, Antunes LC, Pourcel C, Principe L, Petrosillo N, Visca P.** Evidence of diversity among epidemiologically related carbapenemase-producing *Acinetobacter baumannii* strains belonging to international clonal lineage II. J Clin Microbiol. 2012 50(3):590-7.

- **Imperi F, Antunes LC, Blom J, Villa L, Iacono M, Visca P, Carattoli A.** The genomics of *Acinetobacter baumannii*: insights into genome plasticity, antimicrobial resistance and pathogenicity. IUBMB Life. 2011 63(12):1068-74.

- **Antunes LC, Imperi F, Carattoli A, Visca P.** Deciphering the multifactorial nature of *Acinetobacter baumannii* pathogenicity. PLoS One. 2011;6(8):e22674.

- **Antunes LC, Imperi F, Towner KJ, Visca P.** Genome-assisted identification of putative iron-utilization genes in *Acinetobacter baumannii* and their distribution among a genotypically diverse collection of clinical isolates. Res Microbiol. 2011 162(3):279-84

Acknowledgements

I would like to thank Prof. Paolo Visca, Dr. Francesco Imperi and Prof. Kevin Towner for teaching, guiding, and fruitful discussions over the years, which have resulted in the published articles and in this thesis, and for optimism and strength when things did not work.

I would also like to thank the members of the laboratories of Molecular Microbiology and Microbial Biotechnology of the Department of Biology for assistance and for all the good moments that have made this journey a lot easier and fun. A sincere thank you also to the librarians of the Università Roma Tre.

I am forever thankful to the Fundação para a Ciência e a Tecnologia (FCT), Portugal for funding my PhD, as I am to the teachers and colleagues in Portugal that have sparked my interest and motivation in microbiology and from whom I've learned over the years.

Thank you to all my friends in Rome and abroad with whom I've shared the ups and downs of these unforgettable 4 years. Thank you to Simona for supporting and encouraging me.

Lastly, I'm very thankful to my family, who has always showed their unconditional support in my personal and academic choices and without whom I would never have gone this far.